INTRODUCTION TO THE GAS TURBINE

INTRODUCTION TO THE GAS TURBINE

SECOND EDITION

BY

D. G. SHEPHERD
Professor of Mechanical Engineering, Cornell University

CONSTABLE & COMPANY LTD
10 & 12 ORANGE STREET LONDON WC2

LONDON

PUBLISHED BY

Constable and Company Ltd

•

INDIA

Orient Longmans Private Ltd

BOMBAY CALCUTTA MADRAS

•

WEST PAKISTAN AND AFGHANISTAN

Longmans, Green and Company Ltd

LAHORE

•

CANADA

Longmans, Green and Company

TORONTO

•

SOUTH AND EAST AFRICA

Longmans, Green and Company Ltd

CAPE TOWN NAIROBI

•

AUSTRALIA AND NEW ZEALAND

Thomas C. Lothian Pty Ltd

SYDNEY ADELAIDE MELBOURNE PERTH

BRISBANE AUCKLAND (NZ)

First Published	.	.	.	1949
Second Edition	.	.	.	1960

PRINTED IN GREAT BRITAIN BY THE WHITEFRIARS PRESS LTD.
LONDON AND TONBRIDGE

To G. M. S.

PREFACE TO THE SECOND EDITION

THIS volume, though called the Second Edition and thus bearing the same title as before, is a completely rewritten text. In fact, to borrow from the legend customarily appearing in works of fiction, any resemblance between this and the first edition is purely coincidental. After some effort in endeavouring to revise the first edition, it became apparent that, as ten years had elapsed since the original publication, only a complete rewriting would satisfy the author and, it is hoped, be of some value to possible readers.

A compelling reason was that in the intervening years, the experience of the author as a teacher led him to believe that a somewhat more basic approach would lead to better understanding. Hence, this edition endeavours to impart more principle and less detail than before. Furthermore, the ensuing decade has allowed the subject to be viewed in a wider perspective, although one still cannot say that the gas turbine has achieved more than adolescence. One of the kinder comments on the original text was to the effect that it was " very readable ". It is hoped that academic experience has not blunted this aspect in the effort to achieve a more disciplined approach.

In the present edition, the reader is assumed to have a knowledge of elementary thermodynamics and fluid flow, so that only those topics of particular relevance are treated in detail. Cycle analysis is dealt with more fully than before for several reasons. One is, that for an introduction to the subject, a knowledge of the possible performance, as framed by thermodynamics, is more important than that of detailed design. Furthermore, it is hoped that the several demonstrations of simple, analytical methods will encourage the reader to adopt similar methods to discover performance trends in those problems which befall him. Gas turbine performance is subject to innumerable variations in assumed values of contributing factors, and in these days of computer development it is tempting to allow enormous machine effort to replace a modicum of thought in every instance. This is not to deny the very real benefit of machine computation in much gas turbine work, but often the relative effect of differing variables can be gauged in simple fashion, allowing greater understanding at the same time. Also, cycle performance has been approached through looking for the

optimum cycle, given the recognized gas turbine components, rather than by taking the " simple " gas turbine and adding refinements. It is thought that this method allows a better appreciation of the place of the gas turbine as a prime mover.

An attempt has been made to cater for a wider range of readers by using, in most instances, thermal units based on both Fahrenheit and Centigrade scales. Despite the claims of those adhering to the latter school of thought to scientific logic, the power field often insists on sticking to the degree F and Btu, and it is exclusive in the U.S.A.

The chapters on components are couched in more unified fashion than formerly, attempting to give sufficient knowledge of the main elements to enable assessment and understanding of performance to be made, rather than to impart design methods in detail. There are, however, sufficient data given to allow application of principle and skeleton designs to be made. No attempt has been made to incorporate material on mechanical design or on actual gas turbine materials, the former because it is a subject to itself and the latter because it is largely descriptive and ephemeral.

The final chapter reviews briefly both existing and possible future applications and contains an assessment of potentialities which the reader is hereby warned to read critically, as being the individual opinion of the author. It should be taken as an effort to steer between a mere recital of existing practice and a reading of the crystal ball.

I am again indebted to the great number of workers in the field, both past and present, from whose efforts the material in this text has been compiled. The largest bodies of available information are those of the National Gas Turbine Establishment (NGTE) in Great Britain and of the National Advisory Council on Aeronautics (NACA) in the U.S.A. Their work has been drawn upon freely throughout the text and acknowledged by reference in specific cases. I am grateful to all those who took the trouble to inform me of errors and obscurities in the first edition and will appreciate similar suggestions for the second edition. Finally, my thanks to the publishers for their forbearance during the protracted period between promise of a revised edition and receipt of the final rewritten version.

The following figures are British Crown Copyright and are reproduced with the permission of Her Majesty's Stationery Office: Figs. 6.5, 6.7, 6.10, 6.11, 6.12, 6.13, 6.25, 7.11, 7.12, and 7.18.

D. G. SHEPHERD.

Ithaca, N.Y.

CONTENTS

CHAPTER 1

INTRODUCTION

THE gas turbine in its most common form is a heat engine operating by means of a series of processes consisting of compression of air taken from the atmosphere, increase of gas temperature by the constant-pressure combustion of fuel in the air, expansion of the hot gases and, finally, discharge of the gases to atmosphere, the whole being a continuous flow process. It is thus similar to the gasoline and Diesel engines in its working medium and internal combustion, but is akin to the steam turbine in its aspect of the steady flow of the working medium. The compression and expansion processes are both carried out in turbomachines, that is, by means of rotating elements in which the energy transfer between fluid and rotor is effected by means of kinetic action, rather than by positive displacement as in reciprocating machinery.

As a practical heat engine, the gas turbine is only some twenty years old, and it may be asked why this should be the case when all the separate elements described above have been used successfully for many years. The basic idea is over a century and a half old, usually being credited to John Barber, who patented a device containing the essential gas turbine elements (including water injection for cooling and augmentation) in 1791. The first real attempt at construction in modern times occurred around the turn of the century by Armengaud and Lemale in Paris.

However, there was a lapse of many years, until in 1939, a Brown-Boveri unit for emergency electrical-power supply was put into operation in Neuchâtel, Switzerland, the output being 4,000 kW and the efficiency 18%. Also in 1939, some details of a turbine with heat exchanger, designed by the Hungarian engineer Jendrassik, were made known, but, as it was an experimental unit only and the reported data were meagre, the Neuchâtel plant may be regarded as being the first successful constant-pressure gas turbine.

There are two major reasons why the application of internal combustion to turbine machinery waited so long for exploitation. The first is that the working medium has to be compressed to the maximum pressure level of the cycle as a *gas* and, as this represents a large power input, it must be done efficiently for the cycle to be

effective. Until recent years, turbomachines for compression did not have an efficiency high enough for the purpose and it required the methods and outlook of the science of aerodynamics to come to fruition before this was accomplished.

The second reason is that, given a reasonable compression and expansion efficiency, it still requires a high value of maximum cycle or combustion temperature in order to achieve a useful plant output and efficiency. The development of materials capable of long life at the temperatures required was a result of metallurgical progress in the 1930's of the manufacture of alloy steels for the valves of reciprocating engines for aircraft. The latter represented a firm market, whereas the gas turbine was only a dubious one, for which the expenditure on research was not justified. Once metals for such temperature levels were available, however modest they seem compared with today's values, the gas turbine became a practical possibility.

The gap between 1904 and 1939 was not devoid of interest, in fact quite the reverse. There were many patents granted and many tests of experimental variations of the gas turbine proper or of its components. During this period, the Holzwarth constant-volume gas turbine was developed and several units were put into service. The constant-volume type is intermittent in operation, with maximum pressure being attained by combustion of fuel and air in a closed chamber. Following " explosion ", the gases are expanded through a turbine. The discharge from the chamber is then closed, a fresh charge blown into the chamber, the inlet valve closed and the cycle repeated. Because the constant-volume combustion type has not prospered to date in comparison with the constant-pressure combustion type, it will not be discussed further here.

During this period, the development of the supercharger for the reciprocating aircraft engine was a great stimulus to the gas turbine. Both in the gear-driven form and in the turbo-supercharger type, it led to advances in the centrifugal compressor and, in the turbo-supercharger form, it also demonstrated that a turbine operating at a high peak temperature was possible.

In the 1930's, considerable attention was given to the jet propulsion of aircraft, and some of the proposed schemes utilized the gas turbine as the source of high-velocity gas. The progenitor of today's turbo-jet engine is undoubtedly Whittle, whose British patent of 1930 embodies both axial-flow and centrifugal compressors, constant-pressure combustion, axial-flow turbine and propulsion nozzle. In 1935, von Ohain in Germany patented a unit with centrifugal compressor and radial-outflow turbine. It was the military application

of the turbo-jet during World War II which gave such impetus to the subsequent development of the gas turbine in the post-war years. The research effort sponsored by governmental agencies resulted in a tremendous development of the special metals needed for continuous high-temperature service at a high stress level. In addition, it provided a core of engineers and technicians trained in the aircraft development, who to a considerable extent spread out the design knowledge to industrial applications. Furthermore, although transition from aircraft use to industrial use is not direct, the obvious success of the gas turbine in the air gave acceptance to its application on the ground. The development of the turbo-jet engine in the aspects of invention, research and engineering, together with the human qualities involved in bringing to fruition a new advance in technology, make a fascinating story. For those interested in pursuing the subject, some references are given at the end of the chapter, Refs. 1–5.

Today, the gas turbine is pre-eminent as an aircraft power plant, with outputs ranging from a few hundreds of pounds of thrust to over 20,000 pounds. As a shaft power unit, one of the smallest in regular service is about 5 h.p., while at the other end of the scale is a unit of over 35,000 h.p. While the claims of ubiquity for the gas turbine made by some enthusiasts at the time of its practical inception have not been fulfilled, nor are likely to be, the gas turbine has propagated in application in some remarkable ways and it is expected that this will continue as recognition grows in more conservative areas.

It has been stated that compression and expansion are carried by turbomachine elements. In both cases, two typical forms are used, one *radial* flow, the other *axial* flow. These are shown diagrammatically in Fig. 1.1. The analysis of behaviour of the different types in detail is the subject of later chapters, but some general statements will be made now in order to obtain a framework for the design elements. The main advantage of turbomachine elements as opposed to reciprocating elements, other than the steady-flow principle, is that they are capable of handling very large quantities of fluid in compact structures. Basically, this is due to the fact that, with steady flow, high speeds of both fluid and rotor are possible, as the material stresses are direct and not oscillatory. On the other hand, pressures as high as those in the positive displacement machine are not possible. Thus high net outputs for small physical volume are obtained by using large flow rates of fluid, yielding a relatively low *specific* output (i.e. output per unit of working substance).

The radial-flow turbomachine is capable of giving a higher pressure

(as a compressor) or of utilizing a higher pressure (as a turbine) than the axial-flow machine for a single set of moving blades and thus is often a simpler unit to use. Its flow-handling capacity is limited, however, and thus the largest machines are always axial

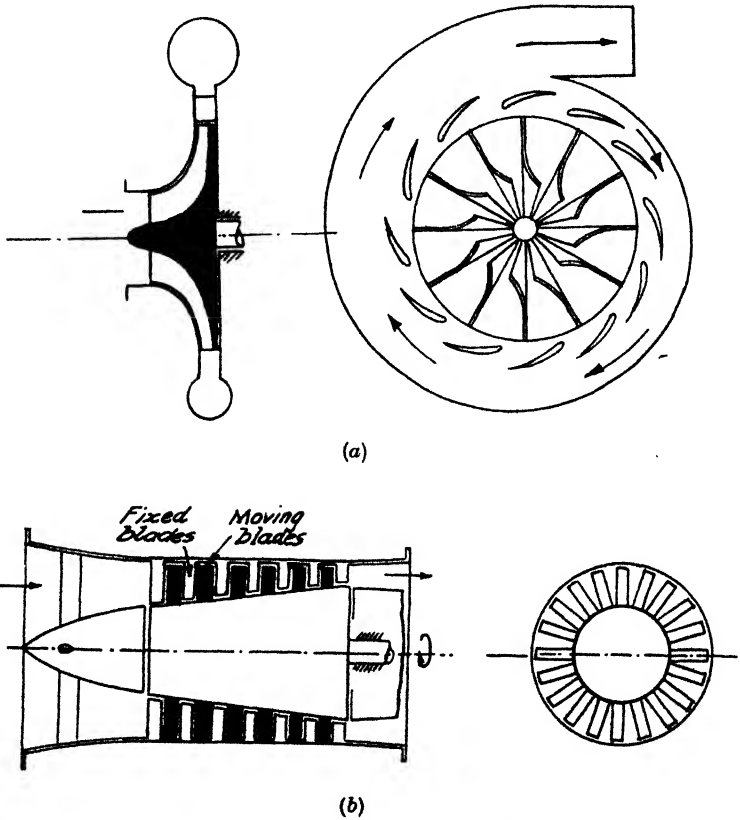

FIG. 1.1. Turbomachine components.

(*a*) Radial-flow compressor (schematic). Radial-flow turbine very similar but with flow and rotor directions reversed.
(*b*) Axial-flow compressor (schematic). Axial-flow turbine similar in principle, but with flow and rotor directions reversed.

flow. For compression, the radial-flow unit is usually called a *centrifugal* compressor and for expansion, a *centripetal* turbine. The performance characteristics and relative merits of these types are discussed in detail in Chapters 5, 6, and 7. These components are not new for the gas turbine and have in fact a relatively long technological history, but it is most certainly true that their development to high performance has been largely stimulated by gas turbine requirements.

Combustion chambers or *combustors*, of which a common type is shown in outline in Fig. 1.2, take a multitude of different forms in detail, although they have the same function, namely of raising the temperature of the air by combustion of fuel, usually internally. Here, although steady-flow combustion is a very old technique, as witness oil- or gas-burning furnaces of all sizes, the requirements of the gas turbine with respect to size and loss of pressure are so stringent that in effect a new technique had to be evolved. Design data and real knowledge of the combustion process were so lacking that a tremendous research programme was put into being and is still being carried on.

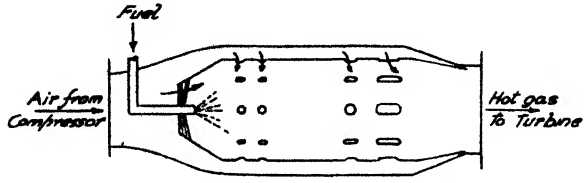

FIG. 1.2. Typical combustor (schematic).

Two components which, while very effective in improving performance but which are not prime necessities, are the *intercooler* and the *heat-exchanger* (or *regenerator*). The former is used to reduce the work of compression by cooling the air through the medium of water during the compression process. The latter is used to reduce the fuel supply for a given required temperature increase by utilizing the heat in the exhaust gases (after they have given up all the energy possible to the turbine) to raise the temperature of the air immediately after compression. Although both intercooling and regeneration raise some special problems in the gas turbine, they are, more than any other process, extensions of a known technique.

The useful power output is obtained by the expansion of the working fluid in the turbine, but as the compression requires a large amount of power (possibly three-fourths of the total expansion power) the compressor is not an auxiliary, but is a main component directly connected to the turbine. Thus a complete gas turbine, in its simplest form, appears as shown diagrammatically in Fig. 1.3.

The problems of the gas turbine are then, firstly, selection of the most suitable cycle from thermodynamic aspects, as even with a minimum of components, performance is not a straightforward matter of the highest pressures and temperatures, and, secondly, the understanding of the component performances in order to achieve the optimum effect, which may be only a single attribute, such as

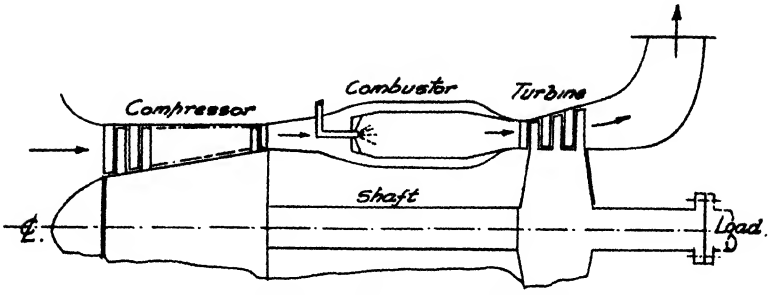

FIG. 1.3. Simple gas turbine (schematic).

high efficiency, high output, small size, range of operation, low cost, etc., or, more usually, a compromise among them. It is the object of the succeeding chapters to lay a foundation for solving some of these problems.

REFERENCES

1. WHITTLE, F. The Early History of the Whittle Jet Propulsion Gas Turbine. *Proc. I. Mech. E.*, **152**, 1945, p. 419.
2. CONSTANT, H. The Early History of the Axial Type of Gas Turbine Engine. *Proc. I. Mech. E.*, **153**, 1945, p. 411.
3. SMITH, G. G. *Gas Turbines and Jet Propulsion*, 6th ed., Iliffe & Sons Ltd., London, 1955.
4. NEVILLE, L. E., and SILSBEE, N. F. *Jet Propulsion Progress*. McGraw-Hill Book Co., Inc., N.Y., 1948.
5. WELSH, R. J. and WALLER, G. *The Gas Turbine Manual*, 2nd ed., Temple Press, Ltd., London, 1955.

CHAPTER 2

IDEAL GAS TURBINE CYCLES

2.1 It has been seen that the gas turbine is a form of power plant which employs turbomachine elements both for compression and for expansion and which, in general, has internal combustion of fuel. Rigorously, a heat engine cycle is composed of a series of thermodynamic processes undergone by a fixed amount of working substance, the latter returning to its original state at the conclusion of the cycle. Cycle analysis allows criteria to be established which will set limits on possible performance and which can be used to assess actual performance. The detailed departure from ideal performance will be examined in the next chapter, but it will be necessary here to keep in mind certain limits of performance, such as pressure ratios obtainable in turbomachines, and temperatures which present-day metals can withstand, in order to allow a reasonable length of working life.

Desirable qualities of a prime mover are the highest possible efficiency, for the sake of operating economy, and the highest possible work output per unit mass of working substance, for the sake of small size and weight and (usually) of initial cost. Thermodynamics tells us that, for given temperature limits, a completely reversible cycle has the highest possible efficiency and specific work output, reversibility being both mechanical and thermal. The former implies a succession of states in mechanical equilibrium, i.e. fluid motion without friction, turbulence, or free expansion, and the latter implies attention to a consequence of the Second Law of thermodynamics, that heat must be added only at the maximum temperature of the cycle and rejected at the minimum temperature. This last-named requirement limits us to *isothermal* heat addition and rejection, and then the other processes in the cycle may be *adiabatic* (isentropic for a reversible process), at *constant volume*, or at *constant pressure*. Three cycles containing such elements are well-known, those of Carnot (1820), Stirling (1820), and Ericsson (1830). These will be discussed in order to examine their possibilities for the gas turbine. For the purpose of comparison, temperature limits of 59° F (15° C) and 1360° F (738° C) will be used, the former because it is the value of the standard atmosphere at sea level and

the latter because it represents a typical value between the present-day variations of 1200° F (670° C) to 1500° F (815° C). A pressure ratio of five will be used where required, again representing an average value for existing practice. The working medium will be taken as air, with the gas constant $R = 53{\cdot}3$ ft lb/lb R (96 ft lb/lb K) or 0·0685 Btu/lb R (Chu/lb K), the constant-pressure specific heat $c_p = 0{\cdot}24$ Btu/lb R (Chu/lb K) and the ratio of specific heats $k = c_p/c_v = 1{\cdot}4$.

2.2 *The Carnot Cycle*

The Carnot cycle is shown in Fig. 2.1, in (a) as a temperature-entropy (T-s) diagram and in (b) as a pressure-volume (p-v) diagram.

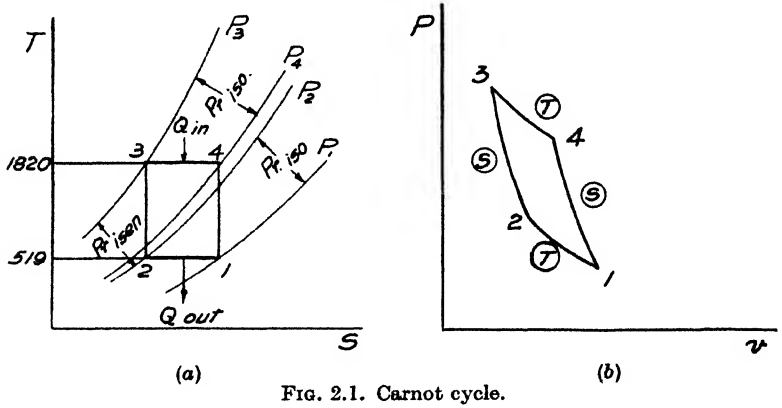

FIG. 2.1. Carnot cycle.

The processes are isothermal compression 1–2, isentropic compression 2–3, isothermal expansion 3–4 and isentropic expansion 4–1. Heat is added during process 3–4 and rejected during process 1–2. The efficiency of all reversible cycles is $(T_{max} - T_{min})/T_{max}$ and thus its value in this case is $(1820 - 519)/1820 \simeq 0{\cdot}715$. The net work or work output of the cycle is most readily obtained in this case as $Q_{in} - Q_{out}$ and since for an isothermal process $Q = W$, then the net work W is

$$R\,T_{max} \ln(P_3/P_4) - R\,T_{min} \ln(P_2/P_1) = R(T_3 - T_1) \ln P_{r_{iso}}$$

since $$P_3/P_4 = P_2/P_1 = P_{r_{iso}}$$

Thus $$W = 0{\cdot}0685\ (1820 - 519) \ln 5 = 143{\cdot}5 \text{ Btu/lb}$$

The temperature rise from T_{min} to T_{max} is obtained by isentropic compression and this pressure ratio $P_{r_{isen}}$ is

$$P_{r_{isen}} = \left(\frac{1820}{519}\right)^{\frac{k}{k-1}} = \left(\frac{1820}{519}\right)^{3{\cdot}5} \simeq 80$$

Isothermal compression and expansion processes are difficult even to approximate directly with turbomachine elements, since the essence of the latter is to provide a large volume flow with small surface. Some attempt can be made with radial-flow machines having a number of stages in series, by means of circulating fluid in jackets surrounding the rotors, but it is next to impossible with axial-flow machines which have many stages in one casing. Also, although cold water is relatively easy to provide during the compression process, the provision of a hot fluid for the expansion process requires a separate system involving combustion of fuel. However, isothermal processes can be approximated by a succession of adiabatic processes through a limited pressure ratio, followed by cooling by heat transfer at constant pressure. These are shown for compression and expansion in Fig. 2.2, in each case with the heat transfer bringing the temperature back to its original value at the start of the adiabatic process. In the limit, of course, an infinite number of such small stage processes renders the overall process isothermal.

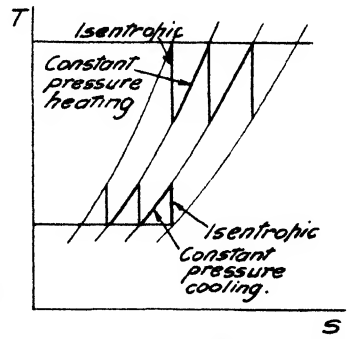

FIG. 2.2. Approximations to isothermal processes.

2.3 *The Stirling Cycle*

The Stirling cycle is shown in Fig. 2.3. The processes are isothermal compression 1–2, increase of temperature at constant volume 2–3, isothermal expansion 3–4, and reduction of temperature

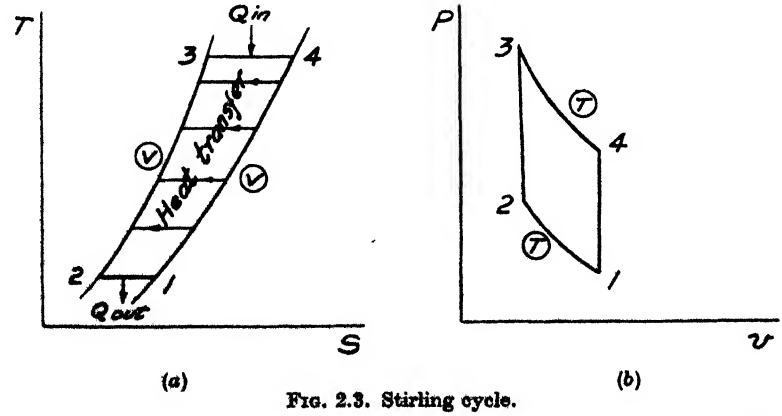

FIG. 2.3. Stirling cycle.

at constant volume 4–1. Again the external heat transfer occurs during the isothermal processes 1–2 and 3–4, the apparent heat transfer during the constant-volume processes taking place *internally* from the hot fluid along 4–1 to the cool fluid along 2–3. The latter process is called *regeneration* and the Stirling cycle is a *regenerative* cycle. As for the Carnot cycle, the efficiency is $(T_{max} - T_{min})/T_{max} = 0{\cdot}715$. The work output is $W_{34} - W_{12} = RT_3 \ln (P_3/P_4) - RT_1 \ln (P_2/P_1) = R(T_{max} - T_{min}) \ln 5 = 143{\cdot}5$ Btu/lb as before. The maximum pressure in the cycle is P_3 and from the constant-volume relationship between 2 and 3, $P_3 = P_2 T_3/T_2 = P_2 T_{max}/T_{min} = (5)\ (14{\cdot}7)\ (1820/519) = 257{\cdot}3$ psia. This pressure, however, requires turbomachine compression of only 5/1, the remainder taking place at constant volume during the regenerative process.

2.4 *The Ericsson Cycle*

The Ericsson cycle is shown in Fig. 2.4 and consists of isothermal compression 1–2 and expansion 3–4, with regenerative processes at

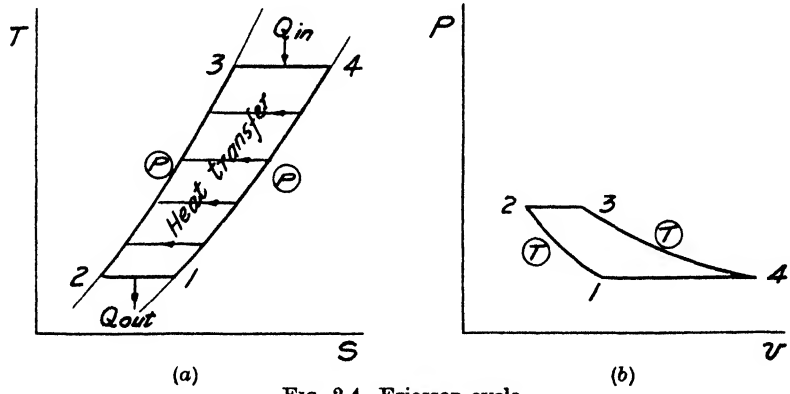

FIG. 2.4. Ericsson cycle.

constant pressure 2–3 and 4–1. In this case, the highest pressure in the cycle is P_2, that reached by the isothermal compression. The efficiency is again 0·715 and the work output is $\int_3^4 v\,dP - \int_1^2 v\,dP$, which for the isothermal processes is $\int_3^4 Pdv - \int_1^2 Pdv = R(T_{max} - T_{min}) \ln 5 = 143{\cdot}5$ Btu/lb as before.

2.5 *Comparison of Reversible Cycles*

All three cycles, Carnot, Stirling and Ericsson, have isothermal compression and expansion and thus are equal in this respect. The Carnot cycle then has isentropic compression and it was seen that a

pressure ratio of about 80/1 is required in order to reach $T_{max.}$ This effectively rules out the Carnot cycle, since although a lower $T_{max.}$ and hence pressure ratio could be used, this would reduce the work output and efficiency so that it would not be competitive. The Stirling and Ericsson cycles both have regeneration, the former at constant volume and the latter at constant pressure. A little reflection will show that a constant-pressure process is much better adapted to turbomachine compression and expansion, because these are essentially continuous steady-flow processes, whereas constant-volume regeneration would be better suited to cyclical reciprocating engine processes. Thus it would seem that the *Ericsson* cycle is the best reversible heat engine cycle on which to base the gas turbine plant, since the maximum pressure is that after isothermal compression and the regenerative process at constant pressure is well suited to known technology in heat transfer.

However, the Ericsson cycle requires isothermal compression and expansion and, in an actual gas turbine plant, these can at best be simulated by a number of adiabatic processes, interspersed with constant-pressure heat transfer processes. Also, although the constant-pressure regenerative process is a known technique, anything approaching 100% regeneration, as ideally postulated, requires a very large area of heat transfer surface and thus the plant becomes somewhat bulky and complex. In view of the advantages of turbomachines in providing compact components of large capacity, then it is as well to look for other heat engine cycles which, while not wholly reversible and hence not having the potentialities of the Ericsson cycle, could act as models for a simple gas turbine plant.

2.6 *Ideal Irreversible Cycles*

The alternatives to isothermal compression and expansion are isentropic compression and expansion and these are ideally suited as model processes for turbomachine components, since the latter essentially perform adiabatic processes. Heat addition and rejection must now be non-isothermal, which is where inevitable irreversibility of the cycles enters, and these may be at constant volume or at constant pressure or with a combination of the two if this has any advantage. Fig. 2.5 shows constant-volume heat addition and rejection, the cycle thus becoming the *Otto* cycle, associated with the spark-ignition engine. It is well-known that the efficiency of the Otto cycle is $(1 - 1/r^{k-1})$, where r is the *compression* ratio, or volume ratio before and after compression. Using *pressure* ratio P_r in place of r, this becomes $1 - 1/(P_r)^{k-1/k}$), giving a cycle efficiency of 0·368, a little over half that of the reversible cycle for a similar pressure

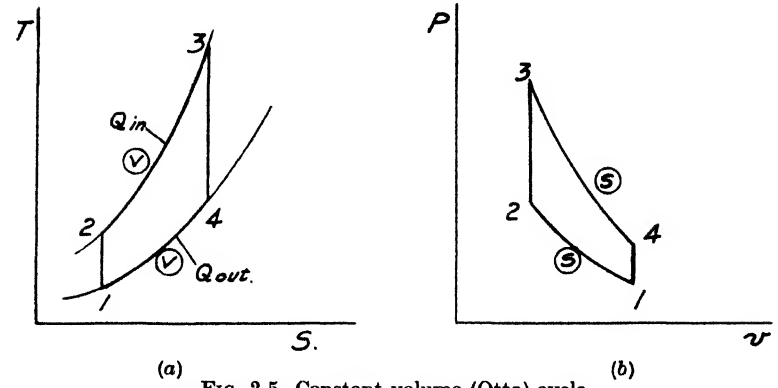

FIG. 2.5. Constant volume (Otto) cycle.

ratio. The Otto cycle efficiency, however, is independent of maximum temperature, although the work output is directly dependent on it. From the T-s diagram, the work output is $Q_{23} - Q_{14}$ and

$$\begin{aligned} Q_{23} - Q_{14} &= c_v (T_3 - T_2) - c_v (T_4 - T_1) \\ &= c_v (T_3 - T_4) - c_v (T_2 - T_1) \\ &= c_v T_3 \left(1 - \frac{T_4}{T_3}\right) - c_v T_1 \left(\frac{T_2}{T_1} - 1\right) \\ &= c_v \left[T_3 \left(1 - \frac{1}{P_r^{\frac{\kappa-1}{\kappa}}}\right) - T_1 \left(P_r^{\frac{\kappa-1}{\kappa}} - 1\right) \right] \end{aligned}$$

For our values of $T_3 = 1820\ R$, $T_1 = 519\ R$, $P_r = 5$ and with $c_v = 0{\cdot}1704$, the work output is 62·5 Btu/lb (34·7 Chu/lb).

Additional work and increased efficiency can be obtained by making the heat rejection at constant pressure, adding the area 451 to the cycle area as shown in Fig. 2.6. The work output is then $Q_{23} - Q_{15}$ and

$$Q_{23} - Q_{15} = c_v (T_3 - T_2) - c_p (T_5 - T_1)$$

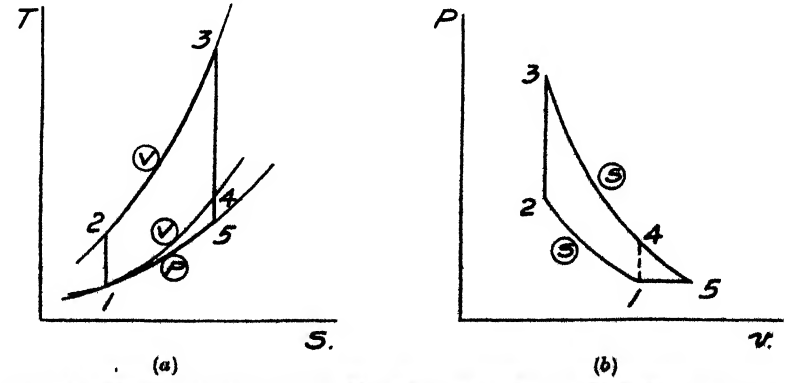

FIG. 2.6. Constant volume combustion with constant pressure heat rejection.

A general expression involving only T_1, T_3 and P_r can be obtained, but it is rather cumbersome and, for the purpose here, it is best to calculate the separate temperatures. If this is done, using the same limit values as for the Otto cycle, the work output is found to be 75 Btu/lb (41·7 Chu/lb), an increase of 20%. Since the heat supplied remains the same, the efficiency is increased by a like amount, to a value of 0·442.

Constant-pressure addition and rejection of heat gives T-s and p-v diagrams as shown in Fig. 2.7. This cycle is known variously as

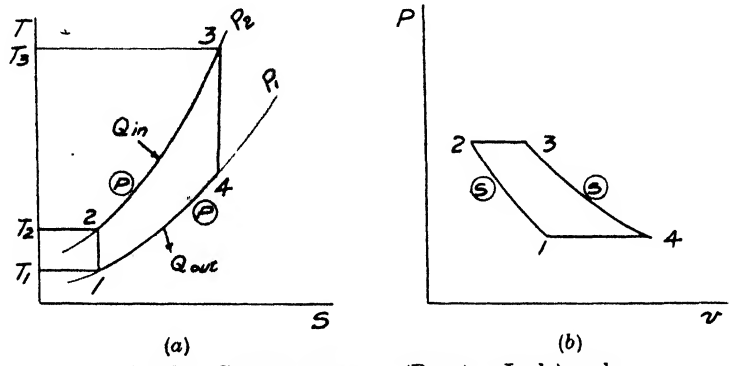

FIG. 2.7. Constant pressure (Brayton-Joule) cycle.

the *Joule* cycle (in Great Britain) and as the *Brayton* cycle in the U.S.A.* As this cycle is not so well known as the Otto cycle, the work output and efficiency will be developed in more detail.

The work output W is given from the T-s diagram as

$$W = Q_{\text{in}} - Q_{\text{out}} = c_p\,(T_3 - T_2) - c_p\,(T_4 - T_1),$$

which may be rearranged or given directly from the p-v diagram as

$$\begin{aligned} W &= c_p(T_3 - T_4) - c_p(T_2 - T_1) \\ &= c_p T_3 \left(1 - \frac{T_4}{T_3}\right) - c_p T_1 \left(\frac{T_2}{T_1} - 1\right) \end{aligned}$$

Now $\dfrac{T_3}{T_4} = \left(\dfrac{P_3}{P_4}\right)^{\frac{k-1}{k}} = P_r^{\epsilon}$, where $\epsilon = \dfrac{k-1}{k}$

* Joule proposed the cycle in 1851 for a hot-air engine consisting of a compression and expansion cylinder, between which were, on one side, an externally fired heat exchanger, and, on the other, an externally cooled heat exchanger. Brayton proposed and constructed a gas engine consisting of a compressor which delivered an air and gas mixture to an expansion cylinder in which the mixture burnt at essentially constant pressure, discharging at constant volume to atmosphere. Neither conceived the gas turbine and even a cursory examination of the literature reveals that the Joule engine was based on earlier suggestions, so that there seems little basis for ascribing the cycle to either Joule or Brayton. However, owing to precedence in time and the fact that the Joule system was a real cycle whereas the Brayton arrangement was for an engine, it will herein be termed the *Joule* cycle.

But $P_3/P_4 = P_2/P_1 = P_r$

Thus $W = c_p(P_r^{\epsilon} - 1)\left(\frac{T_3}{P_r^{\epsilon}} - T_1\right)$

With our standard values, $W = 88{\cdot}3$ Btu/lb (49.1 Chu/lb).

The efficiency, η, is

$$\eta = \frac{Q_{in} - Q_{out}}{Q_{in}} = \frac{c_p(T_3 - T_2) - c_p(T_4 - T_1)}{c_p(T_3 - T_2)}$$

$$= 1 - \frac{T_4 - T_1}{T_3 - T_2}$$

Since $\frac{T_3}{T_4} = \frac{T_2}{T_1}$, then

$$\frac{T_3}{T_2} = \frac{T_4}{T_1}$$

and $$\frac{T_3}{T_2} - 1 = \frac{T_4}{T_1} - 1$$

or $$\frac{T_3 - T_2}{T_2} = \frac{T_4 - T_1}{T_1}$$

and $$\frac{T_4 - T_1}{T_3 - T_2} = \frac{T_1}{T_2}$$

Thus $$\eta = 1 - \frac{T_1}{T_2} = 1 - \frac{1}{T_2/T_1} = 1 - \frac{1}{P_r^{\epsilon}} \qquad (2.1)$$

which is the same as for the Otto cycle and which is independent of either initial or maximum temperature.

2.7 *Discussion of Irreversible Cycles*

From the preceding section, it is seen that the Joule cycle yields the maximum work output for given temperature limits, while the cycle with constant-volume addition of heat and constant-pressure rejection of heat gives the best efficiency. Neither work nor efficiency are so high as those of the reversible cycles, the optimum values both being about 62% of these.

The gas turbine can simulate constant volume heat addition by internal combustion and, in fact, some of the earliest plants constructed (the Holzwarth turbine) were of this type. Expansion down to the original pressure is not only desirable from the point of view of performance, but is more easily accomplished in the gas turbine than is the constant-volume process. However, the constant-volume combustion is difficult to achieve in a satisfactory manner, requiring either a valve arrangement or a pulsating, pressure-generating combustion chamber, and furthermore is liable to engender severe vibration troubles. The Holzwarth turbine was

not developed to any extent following the initial models and while pressure-generating combustion has recently been considered (Reynst, Ref. 1), much work is necessary before it can be considered as suitable for the gas turbine. The overwhelming majority of gas turbines are of the constant-pressure combustion type and in fact the *Joule* cycle is usually called *the* gas turbine cycle. This is because its elements are so well adapted to the simple gas turbine, the turbo-compressor and the turbine both being adapted to adiabatic processes, with constant-pressure combustion being an extension of known techniques of steady-flow combustion and the constant-pressure rejection of heat usually being accomplished by simply discharging the working fluid to atmosphere.

For the rest of the chapter, the Joule cycle will be analysed in more detail, as representing the basic gas turbine cycle, on which improvements are possible at the cost of adding to the complexity.

2.8 *The Basic Joule Cycle*

The efficiency of the Joule cycle was shown to be equal to $1 - (T_1/T_2)$ or $1 - 1/P_r^{\epsilon}$ and thus independent of the temperature limits. It increases with increase of the pressure ratio and in the limit becomes that of the reversible cycle when the limiting maximum temperature is reached by compression alone. This is shown by means of the T-s diagram in Fig. 2.8. In this figure, 1–2–3–4–1 represents a cycle of very low pressure ratio P_2/P_1, having a limiting temperature T_{max}. The area enclosed is very small and, as the heat supplied is represented by the area under 2–3, the efficiency is seen to be very low. Thermodynamically, the efficiency is low because the heat is supplied at a low average temperature, $(T_2 + T_3)/2$, and rejected at a high average temperature, only slightly less than $(T_2 + T_3)/2$. Cycle 1–5–6–7–1 has a higher pressure ratio, P_5/P_1, and a higher efficiency. Cycle 1–8–9–10–1 has a very high pressure ratio, P_8/P_1, and a very high efficiency, because although the area of the diagram is small and hence the work output is small, the heat is supplied at almost the highest temperature of the cycle, T_9, and rejected at the lowest temperature, T_{10}. In the limit, when $\Delta T_{8\text{-}9}$ becomes infinitesimal, cycle 1–8–9–10–1 becomes a Carnot cycle and thus the efficiency is that of a reversible cycle.

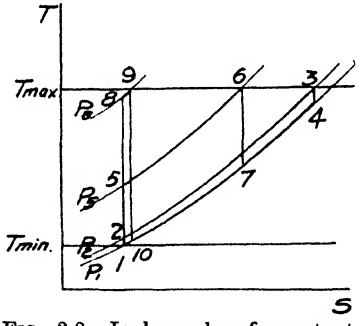

FIG. 2.8. Joule cycle of constant T_{max} with varying pressure ratio.

The diagram also brings out another very important point with respect to work output. At very low pressure ratios and at very high pressure ratios, the work output becomes small, going to zero at the limits of $P_r = 1$ and $P_r = (T_{max}/T_{min})^{\frac{k}{k-1}}$, i.e. no heat addition. Thus in between these limits there must be a maximum, as clearly cycle 1–5–6–7–1 with a moderate pressure ratio has a substantial work output. Since the specific work is an important feature, as it controls the size of the unit for a given output, it is of interest to determine the pressure ratio for maximum work.

Denoting the expansion (turbine) work by W_t and the compression work by W_c, the net or useful work W_n, is equal to the difference. Thus, using the notation of Fig. 2.7,

$$\begin{aligned} W_n &= W_t - W_c \\ &= c_p(T_3 - T_4) - c_p(T_2 - T_1) \\ &= c_p T_3 \left(1 - \frac{T_4}{T_3}\right) - c_p T_1 \left(\frac{T_2}{T_1} - 1\right) \\ &= c_p T_3 \left(1 - \frac{1}{\left(\frac{P_3}{P_4}\right)^{\epsilon}}\right) - c_p T_1 \left(\left(\frac{P_2}{P_1}\right)^{\epsilon} - 1\right) \\ &= c_p T_3 \left[\frac{P_r^{\epsilon} - 1}{P_r^{\epsilon}}\right] - c_p T_1 [P_r^{\epsilon} - 1] \end{aligned} \tag{2.2}$$

For given limiting temperatures T_3 and T_1,

$$\frac{dW_n}{dP_r^{\epsilon}} = c_p T_3 \left[\left(\frac{1}{P_r^{\epsilon}}\right)^2\right] - c_p T_1 = 0$$

and $$P_r^{\epsilon} = \sqrt{\frac{T_3}{T_1}}$$

or $$P_r = \left(\frac{T_3}{T_1}\right)^{\frac{k}{2(k-1)}} \tag{2.3}$$

Thus the pressure ratio for maximum work increases as the ratio of T_{max} to T_{min} increases and for the specimen values used above of 1360° F and 59° F, the optimum pressure ratio is about 8·9. Since the efficiency is given by $[1 - (1/P_r^{\epsilon})]$, then the efficiency at maximum work output is $[1 - 1/(T_3/T_1)^{\frac{1}{2}}]$. The value corresponding to the sample temperatures is 0·465.

The existence of an optimum pressure ratio for maximum work is an important feature, because it shows that high-pressure ratio is not necessarily required. By equating the compression and expansion work outputs, the maximum pressure ratio (giving the

highest efficiency) is seen to be $(T_3/T_1)^{\frac{k}{k-1}}$ or about 80/1 for the sample case. The optimum pressure ratio for maximum work is thus comparatively low compared with the pressure ratio for maximum efficiency. These results are summed up in Fig. 2.9, showing W_n and η plotted against P_r.

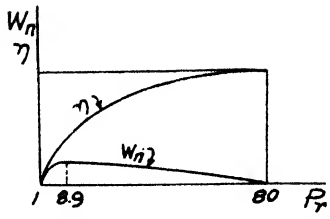

Fig. 2.9. Variation of work output and efficiency with pressure ratio of Joule cycle.

2.9 *Modified Joule Cycle*

It was seen that although the basic Joule cycle is the simplest for the gas turbine plant, the ideal cycle is that of Ericsson. The Joule cycle can be modified so that it approaches the Ericsson cycle, by adding *regeneration* and approaching isothermal compression and expansion by a succession of isentropic and constant-pressure processes (Sec. 2.2). Fig. 2.10 (a) shows a comparison of the basic

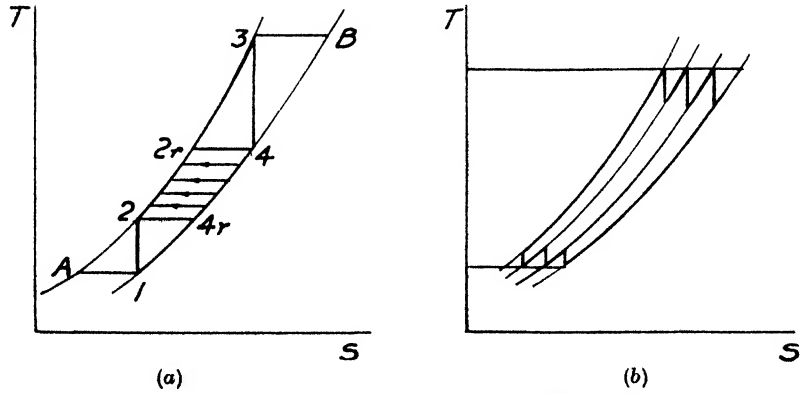

FIG. 2.10 (*a*) Comparison of Joule and Ericsson cycles.
(*b*) Joule cycle with intercooling and reheating.

Joule cycle 1–2–3–4–1 with the corresponding Ericsson cycle 1–A–3–B–1. In this, heat is supplied externally along 2–3 for the Joule cycle and along 3–B for the Ericsson cycle. However, the Joule cycle can be made partly regenerative by internal transfer of heat from 4–4_r to 2–2_r, leaving the external heat addition along 2_r–3 only. Since the area of the diagram is unchanged, the work is the same and therefore the efficiency is increased. In the actual gas turbine plant, the process of regeneration is often called *heat exchange*. This is perhaps a poor term, since it is not explicit, but likewise regeneration is not always exact, since in some terminology, regeneration and recuperation are distinguished as two distinct

methods of heat transfer. In the discussion of cycles, the term regenerative will be used as it is well established for such use, but later on the physical plant for its accomplishment will be called a *heat exchanger*.

Fig. 2.10 (b) shows how compression and expansion may be divided up into small stages, with constant-pressure cooling and heating respectively between the stages. For the actual gas turbine plant, the cooling process is called *intercooling* and the heating process is called *reheating* or simply *reheat*, and these terms will be used in the subsequent discussion of cycles. It will be seen that as the stages become more numerous, the cycle approaches more closely the Ericsson cycle. The gas turbine is often discussed in this manner, that is regarding the gas turbine cycle as the simple Joule cycle, with intercooling, reheat and regeneration being added singly or in combination to yield more efficient cycles. Although the approach here has been to consider the Ericsson cycle as the ideal and the Joule cycle as the simplest possible, it is helpful for a full understanding to take the latter and consider the effect of adding the refinements separately and in combination.

2.10 *Regenerative Joule Cycle*

Fig. 2.11 (a) shows the regenerative Joule cycle, with heat being transferred from the expanded fluid along 4–4_r to the compressed fluid along 2–2_r. The heat added is along 2_r–3 and this is seen to be equal to the expansion work, since $Q_{in} = c_p(T_3 - T_{2_r})$ and $W_t = c_p(T_3 - T_4)$ and $T_{2r} = T_4$.

The work output W_n is $W_t - W_c$ and

$$W_n = c_p(T_3 - T_4) - c_p(T_2 - T_1)$$

$$\text{and } Q_{in} = c_p(T_3 - T_{2_r}) = c_p(T_3 - T_4)$$

$$\therefore \quad \eta = \frac{c_p(T_3 - T_4) - c_p(T_2 - T_1)}{c_p(T_3 - T_4)}$$

$$= 1 - \frac{T_2 - T_1}{T_3 - T_4}$$

Now $T_2 - T_1 = T_1(P_r^{\epsilon} - 1)$

and $T_3 - T_4 = T_3\left(\frac{P_r^{\epsilon} - 1}{P_r^{\epsilon}}\right)$

$$\therefore \eta = 1 - \frac{P_r^{\epsilon}}{T_3/T_1} = 1 - \frac{P_r^{\epsilon}}{T_r}, \text{ where } T_r = T_3/T_1 \qquad (2.4)$$

Eq. 2.4 shows that for a given temperature ratio T_r, the efficiency

decreases as P_r increases, the exact opposite of the basic Joule cycle. The limit case, $P_r = 1$, yields $\eta = 1 - (1/T_r) = (T_r - 1)/T_r = (T_{max} - T_{min})/T_{max}$, which is the ideal reversible cycle efficiency.

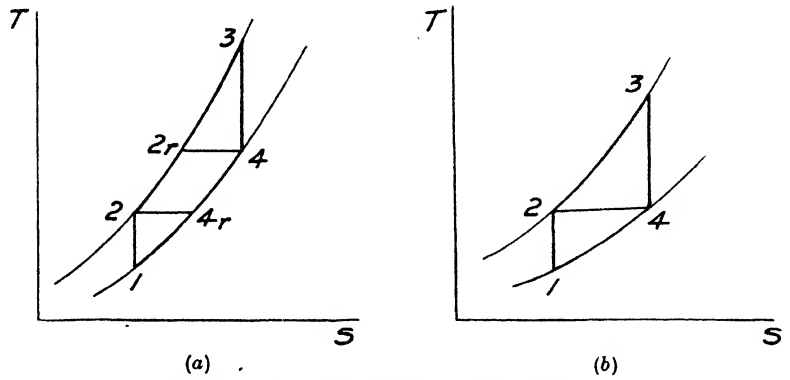

FIG. 2.11. (*a*) Joule cycle with regeneration.
(*b*) Limit of regeneration for Joule cycle.

Fig. 2.11 (b) shows the case where the pressure ratio is such that $T_4 = T_2$ and thus there can be no regeneration, at least no regeneration in the correct direction, as with $T_4 < T_2$, the compressed fluid would be heating the expanded fluid. Under these circumstances,

$$c_p(T_3 - T_4) = c_p(T_3 - T_2)$$

$$T_3\left(\frac{P_r^{\epsilon} - 1}{P_r^{\epsilon}}\right) = T_3\left(1 - \frac{T_2}{T_3}\right) = T_3\left(1 - \frac{T_2}{T_1} \cdot \frac{T_1}{T_3}\right) = T_3\left(1 - \frac{P_r^{\epsilon}}{T_r}\right)$$

$$\therefore \frac{P_r^{\epsilon} - 1}{P_r^{\epsilon}} = 1 - \frac{P_r^{\epsilon}}{T_r}$$

from which $P_r = (T_r)^{\frac{k}{2(k-1)}}$ (2.5)

which is the same value of pressure ratio as that for maximum work of the cycle. These results are summarized in Fig. 2.12, which shows cycle efficiency plotted against P_r for the basic and regenerative Joule cycles. Thus the effect of regeneration is to increase the cycle efficiency, with a low pressure ratio required for high efficiency. Although the

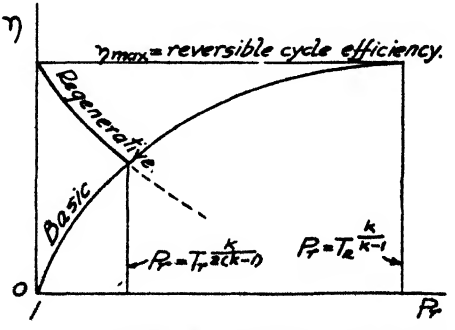

FIG. 2.12. Efficiency of basic and regenerative Joule cycles as a function of pressure ratio.

latter entails a reduced work output, it is advantageous in that, for the actual gas turbine plant, the lower the pressure ratio, the easier it becomes to build a compressor of high internal efficiency.

2.11 *Joule Cycle with Intercooling*

Fig. 2.13 (a) shows a Joule cycle with one stage of intercooling A–B between two isentropic compressions 1–A and B–2. The compression process without intercooling would have been 1–2″ and the

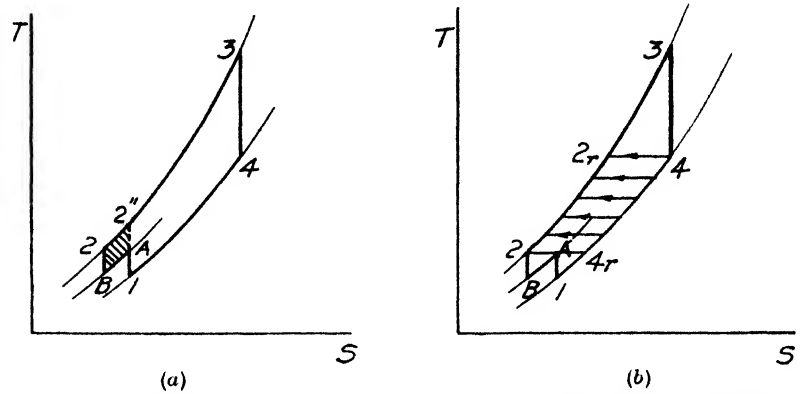

FIG. 2.13. Joule with (*a*) intercooling and (*b*) intercooling with regeneration.

area A–B–2–2″ represents extra work output due tc intercooling. It is important to note that the efficiency is *decreased* however. This may be seen qualitatively without an analytical expression by observing that the heat input $c_p(T_3 - T_2)$ is added at a lower average temperature than it would have been without intercooling, the heat rejection being at the same temperature in both cases. This is contrary to the ideal thermodynamic criterion that, for reversibility, the heat must be added only at the highest temperature of the cycle, and thus because the reversibility is decreased, the cycle efficiency is lowered.

Fig. 2.13 (b) shows regeneration in combination with intercooling. In this case, the heat is added at the same average temperature as that for the basic cycle and the heat is rejected at a lower average temperature. In combination with the additional work output, this raises the efficiency considerably.

2.12 *Joule Cycle with Reheat*

Fig. 2.14 (a) shows a Joule cycle with one stage of reheat AB between two isentropic expansions 3–A and B–4. The expansion process without reheat would have been 3–4″ and the area A–B–4–4″

represents extra work output due to reheat. Similarly to intercooling, the efficiency of the cycle with reheat has a lower efficiency than the basic cycle because the heat is rejected at a higher average temperature. Fig. 2.14 (b) shows regeneration in combination with

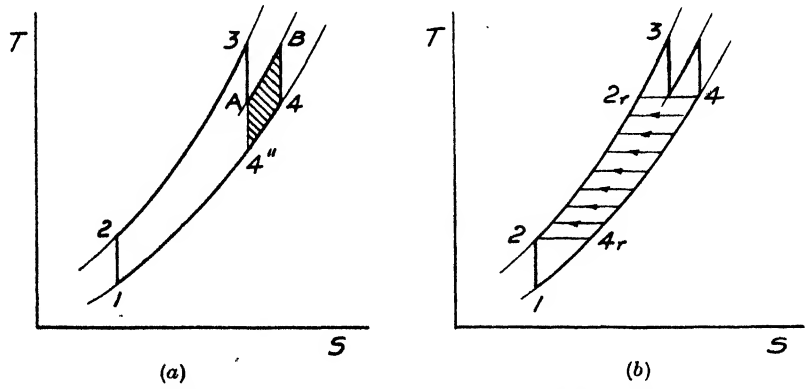

FIG. 2.14. Joule cycle with (*a*) reheat and (*b*) reheat with regeneration.

reheat, which increases the efficiency considerably over that of the basic cycle, because heat is added at a higher average temperature and rejected at the same average temperature, while at the same time, the work output is increased.

2.13 *Complex Joule Cycle*

It will readily be seen from the foregoing that a combination of intercooling and reheat increases the work output, but reduces the cycle efficiency. However, a combination of intercooling, reheat and regeneration, often known as the *complex* cycle, has a very high work output and efficiency which in the limit approaches that of the Ericsson cycle.

2.14 *Graphical Representation*

Some of the major characteristics of the Joule cycle can be demonstrated very clearly in a graphical manner by plotting dimensionless work and heat input quantities against P_r^{ϵ} (rather than P_r). Work and heat are made dimensionless by dividing in all cases by c_pT_1, representing the initial level of enthalpy. Thus for compression work,

$$W_c = c_p(T_2 - T_1) = c_pT_1\left(\frac{T_2}{T_1} - 1\right)$$

and

$$\frac{W_c}{c_pT_1} = P_r^{\epsilon} - 1 \qquad (2.6)$$

Similarly

$$W_t = c_p(T_3 - T_4) = c_p T_3\left(1 - \frac{T_4}{T_3}\right) = c_p T_1 \frac{T_3}{T_1}\left(1 - \frac{1}{P_r^{\epsilon}}\right)$$

and

$$\frac{W_t}{c_p T_1} = T_r\left(\frac{P_r^{\epsilon} - 1}{P_r^{\epsilon}}\right) \tag{2.7}$$

Hence the net work is

$$\frac{W_n}{c_p T_1} = \frac{W_t - W_c}{c_p T_1} = (P_r^{\epsilon} - 1)\left(\frac{T_r}{P_r^{\epsilon}} - 1\right) \tag{2.8}$$

For heat added,

$$Q_{in} = c_p(T_3 - T_2) = c_p T_1\left(\frac{T_3}{T_1} - \frac{T_2}{T_1}\right)$$

and

$$\frac{Q_{in}}{c_p T_1} = T_r - P_r^{\epsilon} \tag{2.9}$$

The efficiency, either as found before or from the above, is

$$\eta = \frac{P_r^{\epsilon} - 1}{P_r^{\epsilon}} \tag{2.10}$$

These relationships are shown in Fig. 2.15 for $T_r = 1820/519 \approx 3{\cdot}5$ and the advantage of using P_r^{ϵ} as abscissa is shown by the

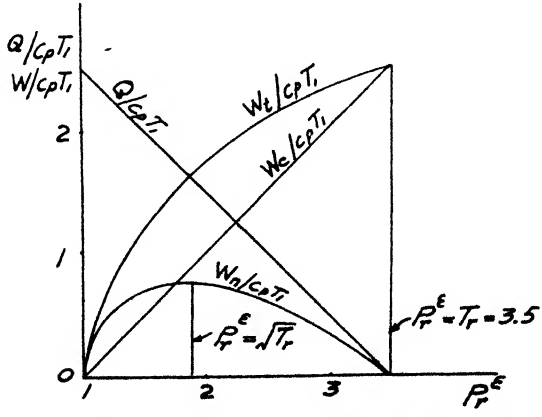

Fig. 2.15. Graphical representation of heat and work quantities—ideal cycle.

linear relationship of W_c and Q_{in}. This diagram is more particularly useful for comparison with a similar one for the cycle with losses, that is, where in particular, compression and expansion are irreversible adiabatic processes.

2.15 *Summary of Ideal Cycle Analysis*

The major results of the foregoing discussion of ideal heat engine cycles on which to base gas turbine plants may be summarized as follows:

(1) The cycle of greatest efficiency and work output is the Ericsson cycle, with isothermal compression and expansion and constant pressure regeneration. The efficiency is $(T_{max} - T_{min})/T_{max}$ and the work output is $R(T_{max} - T_{min}) \ln P_r$. Thus the former is independent of pressure ratio and the latter is dependent on both pressure and temperature ratio.

(2) The simplest cycle is the Joule cycle, with isentropic compression and expansion and constant pressure addition and rejection of heat. The efficiency is $(1 - 1/P_r^{\epsilon})$ and the work output is $c_p T_1 (P_r^{\epsilon} - 1)(T_r/P_r^{\epsilon} - 1)$. Thus the former is independent of temperature ratio and increases with increase of pressure ratio. The latter has a maximum value at a pressure ratio equal to $T_r^{\frac{1}{2}\epsilon}$.

(3) The basic Joule cycle may be modified by (a) regeneration, (b) intercooling and (c) reheat, either singly or in any combination, the addition of all three giving, in the limit, the Ericsson cycle.

(4) Regeneration, added to the Joule cycle, does not affect the work output and improves the efficiency up to the pressure ratio where the temperature after expansion is equal to the temperature after compression. The efficiency is given by $(1 - P_r^{\epsilon}/T_r)$ and is highest at $P_r = 1$ (when $\eta = \eta$ (Ericsson)), decreasing thereafter.

(5) Intercooling alone added to the Joule cycle increases the work output but decreases the efficiency. In combination with regeneration it increases both work output and efficiency.

(6) Reheat has the same effect as intercooling.

(7) Intercooling, reheat and regeneration together modify the Joule cycle to give the highest work output and efficiency.

These results are modified by irreversible processes, in some instances considerably, but it is important to recognize the limits of performance which the gas turbine can attain. As component efficiencies improve, so does the gas turbine approach the cycle performances discussed above.

REFERENCE

1. Reynst, F. H. Pulsating, Pressure Generating Combustion Systems of Gas Turbines. *A.S.M.E.* Paper No. 55-A-56, 1955.

CHAPTER 3

ACTUAL GAS TURBINE CYCLES

It should be recognized at the outset that the vast majority of gas turbines are not heat engines operating in a cycle in the strict thermodynamic sense. They are internal combustion engines, taking in atmospheric air, burning fuel internally, and discharging the products of combustion to the atmosphere. Only in a few actual installations does the working substance go through a complete cycle, with all heat addition and rejection processes taking place by heat transfer, and such plants are said to be operating on a " closed cycle ". The latter term, which is properly speaking tautological, has arisen because of the easy custom of referring to the sequence of processes in internal combustion engines as a " cycle ", with the implication that the sequence is closed by the atmosphere as a vast reservoir of working fluid. Engineering examples of cycles in the proper sense are given by the processes undergone by water in the steam generating unit-turbine-condenser-pump combination, by the refrigerant in the condenser-throttle valve-evaporator-pump combination and by the fluid in the " closed cycle " gas turbine itself. For the " open cycle gas turbine ", in addition to the continual use of fresh working fluid, which obviates the cycle, the heat addition is replaced by internal combustion of fuel, and the heat rejection is replaced by discharge of the products of combustion to atmosphere. Thus the efficiency can no longer be evaluated by the quotient of net work and heat added, but the latter must be replaced by the heating value of the amount of fuel supplied. The use of the term " gas turbine cycle " is so widespread, however, that it will be used here, with the understanding that when applied to the usual gas turbine plant it connotes only that the plant is simulating closely a heat-engine cycle having the same general type of processes.

3.1 *Temperature-entropy Diagram*

Before discussing cycles, it is desirable to analyse the appearance of process lines on a temperature-entropy diagram when the working fluid is a gas. Lines of constant temperature (isothermals), and of constant entropy (isentropics) are apparent, but those of constant pressure and constant volume, together with their relative properties,

may require more explicit analysis, as certain features are important for understanding gas turbine performance.

From thermodynamics, we have the state relationship

$$Tds = c_v dT + Pdv \tag{3.1}$$

From the equation of state for a perfect gas, $Pv = RT$

$$Pdv = RdT - vdP$$

and substituting in eq. (3.1),

$$Tds = c_v dT + RdT - vdP$$

With $R = c_p - c_v$ and $v = RT/P$, this becomes

$$Tds = c_p dT - \frac{RTdP}{P}$$

and

$$ds = c_p \frac{dT}{T} - R \frac{dP}{P} \tag{3.2}$$

For a line of constant pressure, $dP/P = 0$, thus

$$\frac{dT}{ds} = \frac{T}{c_p} \tag{3.3}$$

Hence a line of constant pressure on a T-s diagram has increasing slope as T increases, i.e. it is " concave upward ". The increasing slope is slightly reduced by the increase of c_p as temperature increases.

Integrating Eq. (3.2) between a datum state (subscript 0) and any other state,

$$s - s_0 = \int_{T_0}^{T} c_p \frac{dT}{T} - R \ln P/P_0 \tag{3.4}$$

Thus for making a diagram with arbitrary datum points suitable for the range required, a base pressure P_0 can be selected for which $s = s_0$ at $T = T_0$. The integral represented by the first term on the right hand side of Eq. (3.4) requires a knowledge of c_p as a function of temperature. For many purposes, if the temperature limits between which the integration is made are not too large, an arithmetic average, $\bar{c}_p$ can be used. Thus Eq. (3.4) becomes

$$s - s_0 = \bar{c}_p \ln \frac{T}{T_0} - R \ln P/P_0 \tag{3.5}$$

s_0 may conveniently be taken as zero and with T_0 the lowest temperature required, say $-100°$ F $= 360°$ R, then the base line where $P = P_0$ is calculated from

$$s = \bar{c}_p \ln \left(\frac{T}{360}\right)$$

Since use is made of $\bar{c}_p$, it is best to calculate successive increments of s in intervals of say 100° F, or lower if greater accuracy is required,

rather than to calculate all values from $s_0 = 0$. Other lines of constant pressure are obtained very readily, since for any given temperature, the increment of entropy between $P = P_1$ and $P = P_0$ is

$$\Delta\bar{s} = -R \ln P_1/P_0$$

Lines of constant pressure on a T-s diagram then appear as shown in Fig. 3.1 (a). A feature of importance is that they " diverge "

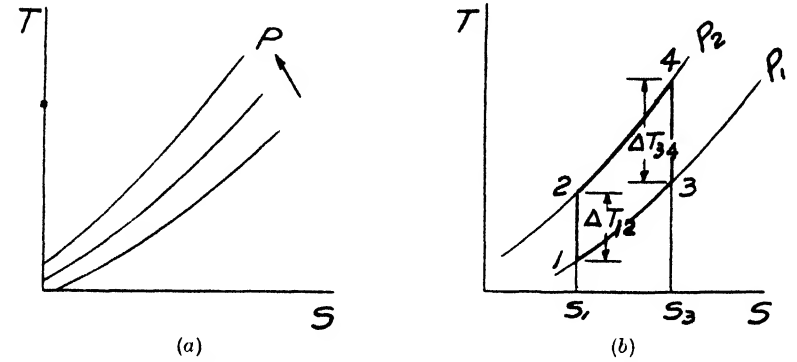

FIG. 3.1. Lines of constant pressure on a temperature-entropy diagram.

as the entropy increases, i.e. for an isentropic process the temperature interval between a pair of constant pressure lines increases as the entropy level increases, as shown in Fig. 3.1 (b).

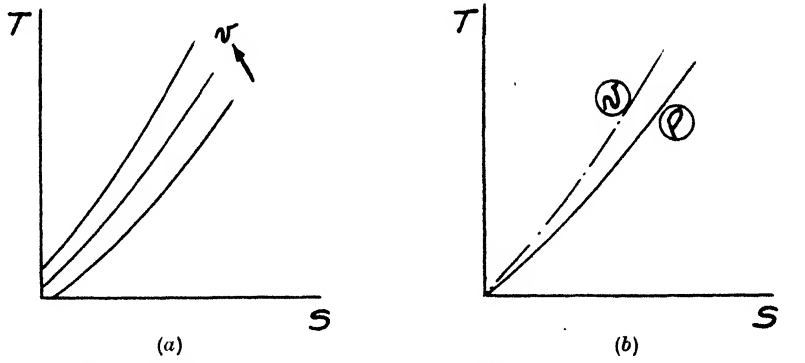

FIG. 3.2. (*a*) Lines of constant volume on a T-s diagram.
(*b*) Comparison of lines of constant pressure and constant volume on a T-s diagram.

For lines of constant volume, it can be shown in an analogous manner that

$$\frac{dT}{ds} = \frac{T}{c_v} \tag{3.6}$$

and

$$s - s_0 = \bar{c}_v \ln \frac{T}{T_0} + R \ln \frac{v}{v_0} \tag{3.7}$$

Constant volume lines are thus logarithmic, concave upward, and, for corresponding values of s and T, of greater slope than those of constant pressure, because $c_v < c_p$. Fig. 3.2 (a) shows a T-s diagram with lines of constant volume and Fig. 3.2 (b) shows a comparison with those of constant pressure.

3.2 *Differences between Actual Plant and Ideal Heat Engine*

The major differences in performance of the actual plant from those of the ideal heat engine as analysed in the previous chapter are due to:

(1) Internal irreversibility of the processes due to friction, turbulence, etc., and impossibility of obtaining 100% regeneration.

(2) Variation of specific heat with temperature and fluid composition.

(3) Variation of amount of the working fluid through the cycle.

(4) Loss due to incomplete combustion of fuel.

(5) Losses due to bearings, auxiliaries, etc., classed as mechanical losses.

(6) Loss of heat to surroundings, resulting in non-adiabatic compression and expansion and direct loss in the combustion chambers.

Of these, the first is the most important, and from it result the largest deviations from the ideal performance. The second has a definite, but secondary, effect, and depends on the choice of working medium, which, of course, is air for the " open cycle " plant. Since the variation of specific heat would affect an ideal heat engine working on the Joule cycle, it is possible to recalculate performance of an " air standard cycle " as is done for the spark-ignition engine, but here it will be considered as an attribute of the actual gas turbine plant. The third effect is small, although it is necessary to take it into account for precise results. Combustion loss is usually small under normal conditions, as are the mechanical losses, although the latter may vary considerably with application, size and operation of a given plant. The last deviation is usually quite small and can be obviated almost completely by insulation and hence is seldom taken into account, except for very precise evaluations of compressor and turbine efficiency. Before discussing these various effects in detail, some important generalizations can be made by considering only the effect of irreversibility of the compression and expansion processes. These have the major effect on performance and the other effects may be grouped as part of them if desired.

3.3 *Compression and Expansion Efficiency*

Irreversibility in compression and expansion causes an increase of entropy, as shown in Fig. 3.3. For a fixed pressure ratio, this results in a compressor delivery temperature $T_{2'}$ greater than T_2

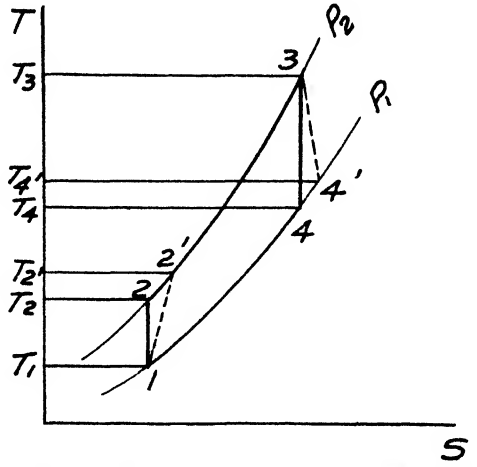

FIG. 3.3. Irreversible compression and expansion.

and a turbine exhaust temperature $T_{4'}$ higher than T_4. The degree of irreversibility can be taken as the ratio of ideal to actual work for compression and vice versa for expansion, rather than comparison of pressure ratios for fixed amounts of work, reversible or irreversible. In an adiabatic compression or expansion, the net work of the process, that is, including the flow work, is equal to the change of enthalpy Δh, or $c_p \Delta T$ for a perfect gas. Thus for compression, the efficiency η_c may be expressed as

$$\eta_c = \frac{W_{\text{ideal}}}{W_{\text{actual}}} = \frac{\Delta h_{\text{ideal}}}{\Delta h_{\text{actual}}} = \frac{\bar{c}_p \Delta T_{\text{ideal}}}{\bar{c}_p \Delta T_{\text{actual}}}$$

Now because the difference of specific heats for the ideal and actual processes is very small, the specific heat is usually taken as constant and the efficiency expressed as the ratio of temperature changes. η_c then becomes the *isentropic temperature efficiency*. Component efficiency can be expressed in many other ways, some of which will be discussed later, but when referred to without any other qualification, it may be taken as defined by the above. Note that this efficiency has meaning only for adiabatic processes, and that it is necessary to devise another standard, the isothermal process, if any cooling is attempted.

From Fig. 3.3, the compression efficiency then becomes

$$\eta_c = \frac{T_2 - T_1}{T_{2'} - T_1} \tag{3.8}$$

The values usually specified for a compression process are the required pressure ratio and the inlet temperature T_1, so that, using the isentropic relationships between pressure and temperature, the ideal temperature rise can be put into more convenient form. Thus

$$\eta_c = \frac{T_1(P_r^{\epsilon} - 1)}{T_{2'} - T_1} \tag{3.9}$$

and the actual work of compression is given by

$$W_{\text{actual}} = \Delta h_{\text{actual}} = \frac{c_p T_1}{\eta_c}(P_r^{\epsilon} - 1) \tag{3.10}$$

In a similar manner, the expansion or turbine efficiency, η_t, is given by

$$\eta_t = \frac{W_{\text{actual}}}{W_{\text{ideal}}} = \frac{\Delta h_{\text{actual}}}{\Delta h_{\text{ideal}}} = \frac{c_p(T_3 - T_{4'})}{c_p(T_3 - T_4)} = \frac{T_3 - T_{4'}}{T_3 - T_4} \tag{3.11}$$

For a turbine, the pressure ratio and initial temperature are usually known, so

$$T_3 - T_4 = T_3\left(1 - \frac{T_4}{T_3}\right) = T_3\left(1 - \frac{1}{T_3/T_4}\right)$$

$$= T_3\left(1 - \frac{1}{P_r^{\epsilon}}\right) = T_3\frac{(P_r^{\epsilon} - 1)}{P_r^{\epsilon}}$$

Hence

$$\eta_t = \frac{T_3 - T_{4'}}{T_3\left(\dfrac{P_r^{\epsilon} - 1}{P_r^{\epsilon}}\right)} \tag{3.12}$$

and the actual work of expansion is given by

$$W_{\text{actual}} = \eta_t c_p T_3 \frac{(P_r^{\epsilon} - 1)}{P_r^{\epsilon}} \tag{3.13}$$

3.4 *Effect of η_c and η_t on Cycle Performance*

The expressions for the work output and efficiency of the basic Joule cycle are now modified from the ideal case discussed in the

previous chapter. The net work is given by

$$W_n = W_t - W_c = \eta_t c_p T_3 \frac{(P_r^{\epsilon} - 1)}{P_r^{\epsilon}} - \frac{c_p T_1}{\eta_c}(P_r^{\epsilon} - 1) \quad (3.14)$$

If the works of compression and expansion are equated, the minimum temperature ratio $T_3/T_1 = T_r$ can be found for which net work is possible. Thus

$$\eta_t c_p T_3 \frac{(P_r^{\epsilon} - 1)}{P_r^{\epsilon}} = \frac{c_p T_1}{\eta_c}(P_r^{\epsilon} - 1)$$

and

$$\frac{T_3}{T_1} = T_r = \frac{P_r^{\epsilon}}{\eta_c \eta_t} \quad (3.15)$$

For $P_r = 5$ and taking reasonable average values of η_c and η_t as 0·85 with $k = 1{\cdot}4$, then the minimum temperature ratio for any net work is about 2·19. Thus with $T_1 = 59°$ F (15° C), T_3 must be 680° F (360° C). Eq. (3.15) furnishes the major reason why the gas turbine has been developed into a satisfactory prime mover only many years after it had been first demonstrated. Neither materials suitable for high temperature nor compressors of high efficiency were available until about the middle 1930's. Thus for $\eta_t = 0{\cdot}75$ and $\eta_c = 0{\cdot}7$, T_3 must be 1110° F (600° C) before the unit is self-driving and must be considerably higher than this before the efficiency becomes acceptable.

The difference between the efficiencies of steam turbine plants and gas turbine plants operating at the same temperature can be comprehended by consideration of the net work expression. For the former, the compression work is very small, because the working fluid is in the liquid state, and thus the degree of compression efficiency is a negligible factor. For the gas turbine, the " negative " work of compression is a considerable fraction of the total turbine work, the net work output being the difference of two large quantities and so the compressor efficiency is very significant. For example, taking $P_r = 5$, $T_3 = 1360°$ F (738° C), $\eta_c = \eta_t = 0{\cdot}85$ and $c_p = 0{\cdot}24$ Btu/lb F (Chu/lb C) for both processes, the ideal turbine work is 137 Btu/lb (76·1 Chu/lb) and the ideal compressor work is 85·5 Btu/lb (47·5 Chu/lb), giving a net work of 51·5 Btu/lb (28·6 Chu/lb). Small variations in compressor and turbine efficiency can thus have a considerable effect on the overall performance. The magnitude of the effect can be assessed by a parameter known as the *work ratio*, defined as the ratio of net work to total turbine work. The higher the value of work ratio, the less is the performance affected by variation of component efficiency. For the example given, the value of work ratio is 51·5/137 = 0·376.

$$\text{Work ratio} = \frac{W_{net}}{W_{tur}} = \frac{c_p\eta_t T_3 \dfrac{P_r^{\epsilon}-1}{P_r^{\epsilon}} - c_p \dfrac{T_1}{\eta_c}(P_r^{\epsilon}-1)}{c_p\eta_t T_3 \dfrac{P_r^{\epsilon}-1}{P_r^{\epsilon}}}$$

$$= 1 - \frac{P_r^{\epsilon}}{\eta_c\eta_t}\frac{T_1}{T_3} \qquad (3.16)$$

From this expression, it will be seen that the work ratio is increased by a high temperature ratio T_3/T_1 and by a low pressure ratio P_r. In general, the value of work ratio is not used as a major criterion, but it may be useful as a deciding factor or when there is some doubt about the compressor or turbine fulfilling expectations.

For the same point change of efficiency of turbine or compressor, the former usually exerts a greater effect on the work output, because it modifies a larger quantity, although this is not always the case. Taking the expression for net work, Eq. 3.14, and differentiating with respect to η_t, keeping all other terms constant, then

$$\left(\frac{\partial W_n}{\partial \eta_t}\right) = a = c_p T_3 \frac{P_r^{\epsilon}-1}{P_r^{\epsilon}}$$

Similarly, differentiating with respect to η_c, other terms constant,

$$\left(\frac{\partial W_n}{\partial \eta_c}\right) = \beta = \frac{c_p T_1}{\eta_c^2}(P_r^{\epsilon}-1)$$

Thus

$$\frac{a}{\beta} = \frac{T_3\left(\dfrac{P_r^{\epsilon}-1}{P_r^{\epsilon}}\right)}{T_1(P_r^{\epsilon}-1)/\eta_c^2} = \frac{T_3\eta_c^2}{T_1 P_r^{\epsilon}}$$

and

$$\frac{a}{\beta} > 1 \text{ when } \eta_c^2 > \frac{T_1 P_r^{\epsilon}}{T_3}$$

Substituting $T_1 = 59°\text{F}$, $T_3 = 1360°\text{F}$ and $P_r = 5$, then the turbine efficiency exerts a greater effect if $\eta_c > 0{\cdot}67$. However, for a pressure ratio of 16 and $T_3 = 1200°\text{F}$, then η_c must be greater than about 0·83 for the turbine to be the more important.

The pressure ratio for maximum work output can be obtained as for the ideal cycle, differentiating Eq. 3.14 and setting the result equal to zero, yielding

$$P_r = (\eta_c\eta_t T_r)^{\frac{k}{2(k-1)}} \qquad (3.17)$$

It is seen that the ideal cycle value is modified by the product $\eta_c\eta_t$ inside the brackets, thus lowering the pressure ratio at which the maximum work is obtained. For work output then, the effect

of component efficiencies is to qualify but not to change the conclusion for the ideal cycle that for a given temperature T_r, there is a pressure ratio for maximum work output.

Considering efficiency, this is expressed as the net work divided by the heat added, so referring back to Fig. 3.3,

$$\eta = \frac{(T_3 - T_{4'}) - (T_{2'} - T_1)}{(T_3 - T_{2'})}$$

$$= \frac{\eta_t(T_3 - T_4) - \dfrac{1}{\eta_c}(T_2 - T_1)}{T_3 - \left[T_1 + \dfrac{1}{\eta_c}(T_2 - T_1)\right]}$$

Substituting $T_2/T_1 = T_3/T_4 = P_r^{\epsilon}$ and $T_3/T_1 = T_r$, then

$$\eta = \frac{\eta_t T_r\,(1 - P_r^{-\epsilon}) - \dfrac{1}{\eta_c}(P_r^{\epsilon} - 1)}{T_r - \dfrac{1}{\eta_c}(P_r^{\epsilon} - 1) - 1} \tag{3.18}$$

Differentiation with respect to pressure ratio for finding a maximum value yields a relationship which may most conveniently be put into the form

$$P_r^{2\epsilon}\left(\frac{T_r - 1}{\eta_t T_r} - 1\right) + 2P_r^{\epsilon} = 1 + \eta_c(T_r - 1) \tag{3.19}$$

Although this may be solved as a quadratic in P_r^{ϵ} for given values of temperature ratio and component efficiencies, by itself it does not yield any useful simple results. Leaving further use of it for the moment, a very important result can be demonstrated in a graphical manner (Ref. 1).

Recalling the presentation in sec. 2.14 of dimensionless quantities W/c_pT_1 and Q/c_pT_1 for the ideal cycle, the same can be done for the cycle with component efficiencies. Thus

$$\frac{W_c}{c_pT_1} = \frac{P_r^{\epsilon} - 1}{\eta_c} \tag{3.20}$$

$$\frac{W_t}{c_pT_1} = \eta_t T_1 \frac{P_r^{\epsilon} - 1}{P_r^{\epsilon}} \tag{3.21}$$

$$\frac{W_n}{c_pT_1} = (P_r^{\epsilon} - 1)\left(\eta_t \frac{T_r}{P_r^{\epsilon}} - \frac{1}{\eta_c}\right) \tag{3.22}$$

and

$$\frac{Q_{in}}{c_pT_1} = \frac{T_3 - T_{2'}}{T_1} = T_r - \frac{1}{\eta_c}\frac{T_2}{T_1} - \left(1 - \frac{1}{\eta_c}\right)$$

$$= T_r - \frac{P_r^{\epsilon}}{\eta_c} - \left(1 - \frac{1}{\eta_c}\right) \tag{3.23}$$

The compressor work W_c/c_pT_1 is thus still linear with P_r^{ϵ} but has greater slope than the ideal and the turbine work W_t/c_pT_1 is modified directly by η_t. The heat added, Q_{in}/c_pT_1 is linear with P_r^{ϵ} again, but is less than the ideal because $T_{2'} > T_2$. Fig. 3.4 shows the ideal values in solid line and the values modified by component efficiencies of 0·85 in broken line. With $T_r = 1820/519$, then the maximum value of P_r^{ϵ} (zero net work) is reduced from 3·5 ($= T_r$) to 2·53 ($= \eta_c\eta_t T_r$) and the amount and position of maximum net work are both lower.

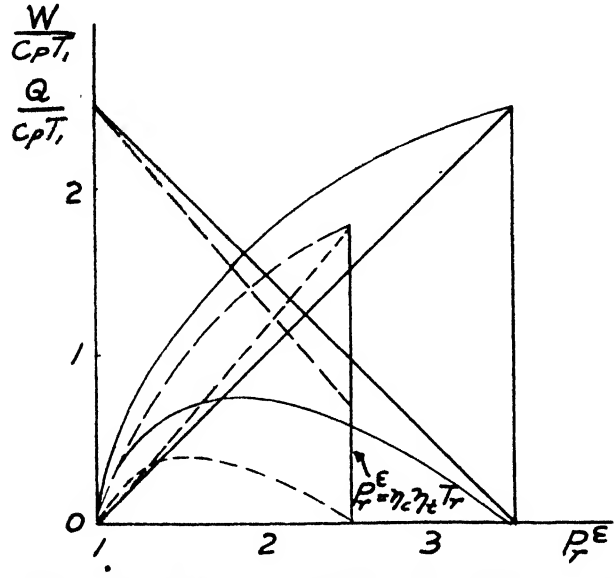

FIG. 3.4. Graphical representation of heat and work quantities—ideal and actual cycle.

Now the efficiency of the cycle is W_n/Q_{in} and the variation of this with P_r^{ϵ} may be demonstrated graphically. Fig. 3·5 shows the work and heat values of the cycle with real component efficiencies replotted in solid line. Another straight line BC is drawn to cut the net work line at E and F. Thus the ratios EG/HG and FJ/KJ represent the efficiencies at values of P_r^{ϵ} at G and J respectively and from simple geometry, they must be equal. The efficiency at both O and L must be zero, because W_n is zero and Q is positive and finite. Thus it is concluded that for a cycle with component efficiencies less than unity, the efficiency increases with P_r up to a point and then decreases, there being always two values of pressure ratio for any value of the efficiency. The point of maximum efficiency may be found graphically by drawing a straight line from B tangent to the net work

curve, line BD in the diagram. Thus for a real cycle there is a pressure ratio at which the *efficiency is a maximum*, as distinct from the ideal cycle in which the efficiency continuously increases with pressure ratio up to the limit where $T_2/T_1 = T_r$. It is also seen from Fig. 3.5 that the pressure ratio for maximum efficiency is higher than that for maximum work and so a compromise is necessary for the optimum pressure ratio for a particular application. This is a very important difference between the real and ideal cycles, and it remains true when the other effects of the actual plant are considered (i.e. specific heat, effect of fuel, etc.), as these only modify the result in a secondary quantitative aspect.

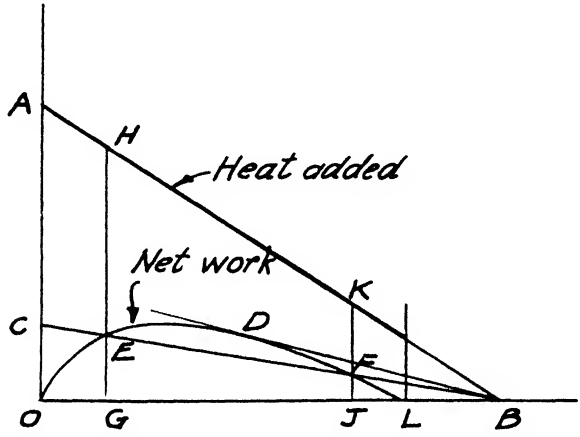

FIG. 3.5. Graphical representation of efficiency of actual cycle.

Returning now to the analytical statement, although the result of differentiating to find the pressure ratio for maximum efficiency was found to be unrewarding in itself, the substitution of the result into the relationship (3.18) above for efficiency yields the simple expression,

$$\eta_m = 1 - \frac{\eta_c \eta_t T_r}{P_{r_m}^{2\epsilon}} \tag{3.24}$$

where subscript m indicates the maximum efficiency value. Eq. (3.24) is seen to be similar in form to that for the ideal cycle, but modified by the product of efficiencies $\eta_c \eta_t$ and the fact that P_{r_m} is not the maximum pressure ratio.

Thus although no simple expression is available for the optimum pressure ratio for maximum efficiency, once P_{r_m} is known, the maximum efficiency is easily obtained from (3.24). A value of P_{r_m} for maximum efficiency can be obtained in conjunction with

the pressure ratio for maximum work and thus the two most important values for given component efficiencies and temperature ratio can be readily evaluated. Also as the work and efficiency are zero at $P_r = 1$ and (from the numerator of Eq. 3.18) at $P_r = (\eta_c \eta_t T_r)^{1/\epsilon}$, the general form of the curves can be sketched in. The work of calculation is relatively simple and much information can be obtained for a wide range of parameter values, from which a restricted range can be selected for detailed computation.

It should be noticed that the net work of the cycle (Eq. 3.14 for example) is increased by increase of T_3, the turbine inlet temperature, and by decrease of T_1, the compressor inlet temperature, a given percentage change of either having about equal effect. Thus for a given gas turbine operated at a fixed turbine temperature, the ambient air temperature has a considerable effect on the performance. If the design ambient temperature is 60° F, then more power will be obtained on a cold day and less power on a hot day. The gas turbine is singular in this respect of a widely varying power output with air temperature and it is an important aspect in application.

3.5 *Effect of Amount of Regeneration*

For the ideal cycle, the regeneration was taken as 100%, that is, the fluid from the compressor was considered to be heated up to the turbine discharge temperature. Thus in Fig. 2.13 (a), $T_{2_r} = T_4$ and, as the fluid has a constant specific heat and the mass rate of flow is everywhere the same, i.e. $T_4 - T_{4_r} = T_{2_r} - T_2$, then $T_{4_r} = T_2$. Heat transfer requires a temperature difference and, when this difference is infinitesimal, as it is in the ideal regenerator, then infinite area is required. For the actual regenerator, the required surface area increases very rapidly as the temperature difference available decreases and thus for economic reasons the amount of regeneration is limited. T_{2_r} is thus less than T_4 and correspondingly, $T_{4_r} > T_2$. For the actual gas turbine, the mass flow of expanded gas m_g is not quite the same as the mass flow of compressed air m_a, usually being slightly greater by the amount of fuel injected in the combustion chamber. The specific heat of the hot gases, c_{p_g}, is greater than that of the cooler air, c_{p_a}, by virtue of their higher average temperature and the presence of products of combustion (CO_2 and H_2O). Thus for a heat balance

$$m_a c_{p_a}(T_{2'_r} - T_{2'}) = m_g c_{p_g}(T_{4'} - T_{4'_r})$$

and

$$T_{2'_r} - T_{2'} = \frac{m_g}{m_a}\frac{c_{p_g}}{c_{p_a}}(T_{4'} - T_{4'_r}) > (T_{4'} - T_{4'_r})$$

The degree of regeneration or heat recovery is defined as the ratio of the temperature rise of the air ($T_{2'_r} - T_{2'}$) to the maximum temperature difference available, $T_{4'} - T_{2'}$, the latter being the temperature rise for the 100% regenerator. This ratio, expressed either as a fraction or a percentage, is called the *effectiveness* or *thermal ratio* and is given the symbol η_r. Thus

$$\eta_r = \frac{T_{2'_r} - T_{2'}}{T_{4'} - T_{2'}} \tag{3.25}$$

Although it has the symbol of efficiency and is sometimes called thus, it is not a true efficiency. Values of effectiveness in common use vary from 0·6 to 0·75, with 0·70 to 0·75 occurring most frequently as being an upper limit of the ordinary *recuperative* type based on size and cost. Recuperative is used with the meaning that the hot and cold fluids are at all times separated by a stationary metal wall, heat transfer taking place across this wall by conduction. A *regenerative* type is one in which the hot and cold fluids are cyclically in contact with a third medium which moves between the two, heat transfer taking place by convection. This latter type is not yet fully developed for the gas turbine, but it appears to have a possible potential to allow values of effectiveness up to 90%, or even greater, for a reasonable size and cost.

The use of Eq. 3.25 defining effectiveness then allows cycle calculations with regeneration to be readily made. Given the pressure ratio P_r, the inlet temperature T_1, the maximum temperature T_3 and the component efficiencies η_c and η_t, the compressor work is calculated by means of Eq. 3.10 and the turbine work by means of Eq. 3.13, the difference being the net work. To determine the heat input $c_p(T_3 - T_{2'_r})$, Eq. 3.25 is used to obtain $T_{2'_r}$, η_r being stated and T_4 calculated from Eq. 3.12.

For the ideal cycle with 100% regeneration, the cycle efficiency increased with decrease of pressure ratio and this holds true for the actual cycle with $\eta_r < 1{\cdot}0$, but modified by the effect of component efficiency to produce an optimum pressure ratio for given values of η_r, η_c and η_t.

3.6 *Flow Losses*

Although the irreversibility occurring in the compressor and turbine has the major effect on reducing the cycle performance from the ideal values, loss due to friction and turbulence occurs throughout the whole plant, since no fluid flow process can be wholly

reversible. This overall loss may be conveniently broken down into several distinct losses thus:

(a) Combustion chamber loss
(b) Heat exchanger loss, air side
(c) Heat exchanger loss, gas side
(d) Intercooler loss, air side
(e) Duct losses occurring between components and at intake and exhaust.

These losses are manifested as differences of pressure from the ideal values; all losses up to the turbine inlet may be considered as being equivalent to a reduction of compression ratio and all those following the turbine being equivalent to a reduction of expansion ratio. The various losses are shown graphically in Fig. 3.6, for a complex cycle. One immediate conclusion is that the pressure ratios for compression and expansion are not equal, as has been assumed heretofore and the "pressure ratio" of an actual cycle usually implies that between the compressor inlet and compressor discharge.

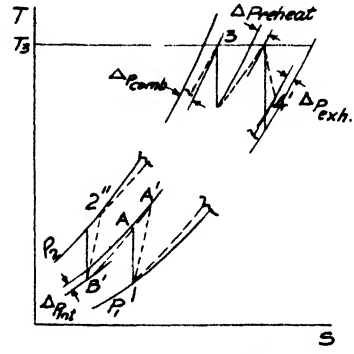

FIG. 3.6. Flow losses.

These fluid flow losses, sometimes called "parasitic" losses, are usually each small individually, compared with those of the compressor and turbine, but this is because they are controllable to a large extent by the cross-sectional area of the components and ducts. For flow considered to be incompressible, the loss of pressure due to friction and turbulence is usually expressed as a function of the dynamic pressure of the fluid at some arbitrarily chosen section of the component, thus

$$\Delta p = k \frac{\rho V^2}{2g_0}$$

For pure skin friction in a duct, k represents the product of a friction factor f and the length-diameter ratio of the duct, with ρ and V evaluated as mean values. For abrupt entrances and exits, as in the tubes of heat exchangers, k is a function of the area ratio. For diffusion, that is, the regain of static pressure by reducing velocity as in a duct following the compressor, k is a function of the diffuser efficiency, which in turn depends on the rate of diffusion and the area ratio. For the combustion chamber, k is a coefficient too complex to evaluate by analysis and is usually arrived at by empirical

means. These forms of loss will be studied in detail for the various components in subsequent chapters, and for the moment it is necessary to recognize only that for any given design, the loss is proportional to ρV^2. From the continuity equation $m = A\rho V$, $\rho V^2 \propto m/A^2\rho$ and hence $\Delta_p \propto m/A^2\rho$. Thus for a given mass flow rate m and density ρ, the pressure loss is inversely proportional to the square of the flow area or, assuming circular ducts of diameter d, $\Delta p \propto 1/d^4$. Losses can thus be minimized by increasing cross-sectional flow area, but the problem is not simple, because for certain components, diffusers and heat exchangers for example, the length must be increased if low velocities are required and thus overall bulk may be increased. The greatest difficulty is often on the exhaust side, that is, following the turbine, because the gases have a very low density due to their low pressure and high temperature. Hence the hot gas side of a heat exchanger and the final exhaust duct or stack may be critical design features.

Although it was stated above that individual flow losses were small compared with those due to irreversibility in compressor and turbine, nevertheless they are extremely important because of their cumulative effect and because there is little point in expending effort in obtaining the best component efficiencies if their effect is nullified by parasitic losses. Because flow losses are so dependent on size and shape, the actual layout of a gas turbine plant has a great influence on its overall performance. Furthermore, it makes it difficult to give standard performance figures for given pressure ratios and temperatures, as the application influences the degree to which flow losses can be minimized. To take extreme examples, an aircraft gas turbine sets a premium on size and weight, so that rather high pressure losses are tolerated, whereas for a stationary power plant, where normally space is a minor consideration, pressure losses are held to very small values in order to obtain the maximum output and efficiency.

The effect of varying flow losses on cycle performance can be generalized in a manner convenient for calculation. The analysis consists of finding the difference in output between the cycle without losses and the cycle with losses. In order to keep the algebra as simple as possible, the method will be demonstrated only for a loss of pressure Δp_c between compressor delivery, state 2, and turbine inlet, state 3, and a loss of pressure Δp_t between turbine discharge, state 4, and the atmosphere, state a.

For no pressure losses, $P_3 = P_2$ and $P_4 = P_a$, hence the turbine work is

$$W_t = \eta_t c_p T_3 \left[\frac{(P_2/P_a)^\epsilon - 1}{(P_2/P_a)^\epsilon} \right]$$

With pressure losses, $P_3 = P_2 - \Delta p_c$ and $P_4 = P_a + \Delta p_t$, hence

$$W_t' = \eta_t c_p T_3 \left[\frac{\left(\frac{P_2 - \Delta p_c}{P_a + \Delta p_t}\right)^\epsilon - 1}{\left(\frac{P_2 - \Delta p_c}{P_a + \Delta p_t}\right)^\epsilon} \right]$$

$$= \eta_t c_p T_3 \left[\frac{\frac{P_2^\epsilon \left(1 - \frac{\Delta p_c}{P_2}\right)^\epsilon}{P_a^\epsilon \left(1 + \frac{\Delta p_t}{P_a}\right)^\epsilon} - 1}{\frac{P_2^\epsilon \left(1 - \frac{\Delta p_c}{P_2}\right)^\epsilon}{P_a^\epsilon \left(1 + \frac{\Delta p_t}{P_a}\right)^\epsilon}} \right]$$

The terms $\left(1 \pm \frac{\Delta p}{P}\right)^\epsilon$ may be expanded to the series

$$1 \pm \epsilon \frac{\Delta p}{P} \pm - - - -$$

with higher terms omitted, because $\Delta p/P$ is small. Thus the turbine work with losses becomes

$$W_t' = \eta_t c_p T_3 \left[\frac{\frac{P_2^\epsilon \left(1 - \epsilon \frac{\Delta p_c}{P_2}\right)}{P_a^\epsilon \left(1 + \epsilon \frac{\Delta p_t}{P_a}\right)} - 1}{\frac{P_2^\epsilon \left(1 - \epsilon \frac{\Delta p_c}{P_2}\right)}{P_a^\epsilon \left(1 + \epsilon \frac{\Delta p_t}{P_a}\right)}} \right]$$

which reduces to

$$W_t' = \eta_t c_p T_3 \left[\frac{(P_2/P_a)^\epsilon \left(1 - \epsilon \frac{\Delta p_c}{P_2}\right) - \left(1 + \epsilon \frac{\Delta p_t}{P_a}\right)}{\left(\frac{P_2}{P_a}\right)^\epsilon \left(1 - \epsilon \frac{\Delta p_t}{P_a}\right)} \right]$$

Subtracting W_t' from W_t to obtain the loss,

$$W_{\text{loss}} = \eta_t c_p T_3 \left[\frac{\epsilon \frac{\Delta p_t}{P_a} + \epsilon \frac{\Delta p_c}{P_2}}{(P_2/P_a)^\epsilon \left(1 - \epsilon \frac{\Delta p_c}{P_2}\right)} \right]$$

The term $(1 - \epsilon \Delta p_c/P_2)$ can be taken as unity, because

$$\epsilon = (k - 1)/k \approx 0{\cdot}25$$

for exhaust gases and $\Delta p_c/P_2$ should not exceed 0·10. Thus the loss of output can be simplified (with $c_p\epsilon = R/J$) to

$$W_{\text{loss}} = \frac{\eta_t R T_3}{J(P_2/P_a)^\epsilon}\left[\frac{\Delta p_t}{P_a} + \frac{\Delta p_c}{P_2}\right] \text{(Btu) (Chu)/lb}$$

$$= \frac{\eta_t R T_3}{550\ (P_2/P_a)^\epsilon}\left[\frac{\Delta p_t}{P_a} + \frac{\Delta p_c}{P_2}\right] \text{hp/lb/sec} \qquad (3.26)$$

From this expression, it is apparent that the effect of a certain absolute pressure loss is dependent on the *pressure level* at which it occurs. A given loss on the high-pressure side is less important than a loss on the low-pressure side. Thus for a cycle with a pressure ratio of 5, for example, a combustion chamber loss of 2·5 psi has exactly the same effect as a loss of 0·5 psi at compressor inlet or at turbine exhaust. In the demonstration above, only two pressure losses were used, but the analysis can be generalized on the basis of effect of a loss being inversely proportional to the pressure level at which it occurs, so that

$$\sum \frac{\Delta p}{P} = \left[\frac{\Delta p_A}{P_A} + \frac{\Delta p_B}{P_B} + \frac{\Delta p_C}{P_C} + \ldots\right] \qquad (3.27)$$

Eq. (3.26) is not exact, but is sufficiently precise for initial calculations and particularly for estimating the effect of varying amounts of loss throughout the cycle.

One example will show the effect of pressure losses. For a cycle with $P_r = 5$, $T_{\max} = 1360°$ F (738° C) and $\eta_t = 0{\cdot}87$, having a loss of 1·25 psi through the air side of the heat exchanger, 1·5 psi through the combustor and 0·25 psi through the gas side of the heat exchanger, using $c_p = 0{\cdot}265$, then

$$\sum \frac{\Delta p}{P} = \frac{1{\cdot}25}{5(14{\cdot}7)} + \frac{1{\cdot}5}{5(14{\cdot}7)} + \frac{0{\cdot}25}{14{\cdot}7} = \frac{0{\cdot}80}{14{\cdot}7} (\equiv 5{\cdot}45\%)$$

and the loss of output is 5·5 hp/lb/sec. This represents about 7½% reduction of output from the cycle with no pressure losses.

3.7 *Effect of Variable Specific Heat*

The specific heat of air is independent of pressure within the limits of gas turbine operation, but varies considerably with temperature. Thus at 59° F (15° C), the constant pressure specific heat of air is 0·24 Btu/(lb) (F) or Chu/(lb) (C) but at 1360° F (738° C) it is 0·273 Btu/(lb) (F). Furthermore, the internal combustion of fuel

causes the expansion gas to contain products of combustion, principally CO_2 and H_2O vapour, both having higher values of specific heat than that of pure air. At 1360° F (738° C), a typical value of c_p for the gases after combustion is 0·281. Previously, the specific heat has been taken to be constant throughout the cycle, with a value of 0·24 where required. This assumption would seem to introduce a considerable error, because the difference between the cold air and hot gas values given above is nearly 17%. However, although there is an error, it is much less than this value, because of the compensating effect of a varying k. As the specific heat increases with temperature, the isentropic index k decreases, because $c_p - c_v = R$ remains constant and $k = c_p/c_v = [(R/c_v) + 1]$. As k decreases, the exponent $(k - 1)/k$ decreases and thus the change of temperature ΔT for a given pressure ratio and initial temperature likewise decreases. Because the change of enthalpy is $c_p \Delta T$, then the effect of increased c_p is somewhat neutralized. Actually the specific heat of air and of combustion gases changes continually during compression and expansion and for a precise calculation, an integration process is required. Keenan and Kaye (Ref. 2) have provided tables of air and gas properties in their " Gas Tables " and a brief explanation of the basis of these is now given.

As in Sec. 3.1, an expression for the change of entropy is

$$ds = c_p \frac{dT}{T} - R \frac{dP}{P} \tag{3.2}$$

and for an isentropic process, $ds = 0$, and hence

$$\frac{dP}{P} = \frac{c_p}{R} \frac{dT}{T}$$

Integrating between a datum state P_0, T_0, and any other state P, T, then

$$\ln \frac{P}{P_0} = \frac{1}{R} \int_{T_0}^{T} c_p \frac{dT}{T}$$

since c_p is a function only of temperature for a perfect gas, which we may consider air and combustion gases to be in normal gas turbine operation. Similarly one may obtain

$$\ln \frac{v}{v_0} = \frac{1}{R} \int_{T_0}^{T} \frac{c_v \, dT}{T}$$

Knowing c_p and c_v as functions of temperature, these expressions can be integrated and for any given temperature above T_0, there is a corresponding *relative* pressure ratio P_r and *relative* volume ratio v_r.

Thus for an initial P_1 and T_1 and given P_2/P_1, temperature T_2 can be found from the tabular value at P_{r_2} given by

$$P_{r_2} = \frac{P_2}{P_1} P_{r_1}$$

and, by using the values of v_{r_1} and v_{r_2} at temperatures T_1 and T_2,

$$v_2 = \frac{v_{r_2}}{v_{r_1}} v_1$$

The enthalpy at any state is given by

$$h = h_0 + \int_{T_0}^{T} c_p \, dT$$

and the internal energy by

$$u = h - RT$$

The entropy is given by integration of Eq. 3.2,

$$s = s_0 + \int_{T_0}^{T} c_p \frac{dT}{T} + R \ln \frac{P}{P_0}$$

The "Gas Tables" give the datum state as $T_0 = 0°$ R, where $h_0 = 0$ and $s_0 = 0$, with P_0 as unit pressure. Thus a change of entropy is given by

$$s_2 - s_1 = \int_{T_0}^{T_1} c_p \frac{dT}{T} - \int_{T_0}^{T_1} c_p \frac{dT}{T} + R \ln \frac{P_2}{P_1}$$

Because entropy is a function of both temperature and pressure, it cannot be given in tabular form directly, but must be calculated from the above relation. The gas tables give the temperature function as ϕ and, separately, tabular values of $R \ln N$, where $\phi = \int_{T_0}^{T} \frac{dT}{T}$ and $N = P_2/P_1$, so that

$$s_2 - s_1 = \phi_2 - \phi_1 + R \ln N$$

Tables for pure air are given in one degree intervals from 100° R to 3000° R and thence in ten degree intervals to 6500° R. Although the tables are based on isentropic values, they may be used for calculating actual adiabatic values in conjunction with the efficiency, defined either as a ratio of enthalpies or temperatures (Sec. 3.3). Thus the isentropic ΔT is first found and divided by η_c (for compression) or multiplied by η_t (for expansion), giving the actual $T_{2'}$. Entering the tables at this value of temperature, $h_{2'}$ can be found and $h_{2'} - h_1$ gives the work. Alternatively the isentropic Δh is modified by the efficiency and $T_{2'}$ found from the corresponding $h_{2'}$.

To show the use of the tables, a skeleton extract is given below, together with a simple example which also illustrates differences in methods and definitions.

T	t	h	P_r	u	v_r	ϕ
—	—	—	—	—	—	—
—	—	—	—	—	—	—
520	60·3	124·27	1·2147	88·62	158·58	0·59173
—	—	—	—	—	—	—
—	—	—	—	—	—	—
—	—	—	—	—	—	—
821	361·3	196·93	6·059	140·65	50·19	0·70189
822	362·3	197·18	6·085	140·82	50·04	0·70219
—	—	—	—	—	—	—
878	418·3	210·86	7·698	150·67	42·25	0·71830
879	419·3	211·11	7·729	150·85	42·13	0·71858
—	—	—	—	—	—	—

Table 3.1

(from Keenan and Kaye, Ref. 2)

Example. With an initial temperature of 520° R and for a pressure ratio of 5, find the final temperature if the compressor efficiency is 84% using (a) temperature basis and (b) enthalpy basis.

From the tables at 520° R,

$$h_1 = 124{\cdot}27 \text{ Btu/lb}$$

$$P_{r_1} = 1{\cdot}2147$$

Then $$P_{r_2} = 5 \times 1{\cdot}2147 = 6{\cdot}0735$$

Entering the tables at this value of P_{r_2} (interpolation required), then

$$T_2 = 821{\cdot}56° \text{ R}$$

$$h_2 = 197{\cdot}07 \text{ Btu/lb}$$

(a) $$T_2 - T_1 = 821{\cdot}56 - 520 = 301{\cdot}56° \text{ F}$$

$$\therefore T_{2'} - T_1 = \frac{T_2 - T_1}{\eta_c} = \frac{301{\cdot}56}{0{\cdot}84} = 359° \text{ F}$$

and $$T_{2'} = 520 + 359 = 879° \text{ R}$$

Entering the tables at this value of temperature,

$$h_{2'} = 211{\cdot}11 \text{ Btu/lb}$$

$\therefore$ Work of compression

$$= h_{2'} - h_1 = 211{\cdot}11 - 124{\cdot}27 = 86{\cdot}84 \text{ Btu/lb}$$

(b) $$h_2 - h_1 = 197{\cdot}07 - 124{\cdot}27 = 72{\cdot}8 \text{ Btu/lb}$$

$$h_{2'} - h_1 = \frac{h_2 - h_1}{\eta_c} = \frac{72{\cdot}8}{0{\cdot}84} = 86{\cdot}67 \text{ Btu/lb}$$

$$\therefore h_{2'} = 124{\cdot}27 + 86{\cdot}67 = 210{\cdot}94 \text{ Btu/lb}$$

At this value of enthalpy,

$$T_{2'} = 878{\cdot}3^\circ \text{ R}$$

and $$T_{2'} - T_1 = 878{\cdot}3 - 520 = 358{\cdot}3^\circ \text{ F}$$

Thus by using the efficiency based on the enthalpy values, the work of compression is about 0·2% less than if based on the temperature values, as is the temperature rise $\Delta T'$. The difference is small but significant, increasing at higher pressures.

Now, the temperature rise and work of compression will be calculated using a constant value of $c_p = 0{\cdot}24$ Btu/(lb) (R), with a corresponding value of $k = 1{\cdot}4$ and hence $k/(k-1) = 3{\cdot}5$. Thus

$$\Delta T' = T_{2'} - T_1 = \frac{T_1}{\eta_c}(P_r^{\epsilon} - 1) = \frac{520}{0{\cdot}84}\left(5^{\frac{1}{3{\cdot}5}} - 1\right) = 361{\cdot}3^\circ \text{ F}$$

$$\therefore \Delta h' = c_p \Delta T' = 0{\cdot}24(361{\cdot}3) = 86{\cdot}71 \text{ Btu/lb}$$

The change of temperature is 2·3° F or 0·64% greater than that found by using the gas tables, while the change of enthalpy is negligibly small. In this case the error is almost within normal slide rule limitations and although it may be a little greater over a larger pressure ratio, the results are sufficiently accurate for many calculations. This is not to deny the convenience of the tables for repeated calculations and the use of such accurate values is not only desirable but necessary for specifications and for published data. The purpose is rather to emphasize that many of the quick calculations so often required of the engineer may be handled with sufficient accuracy without recourse to tables. The author feels that too often the principles of analysis and calculation are obscured by too great dependence on tables and charts, whose significance is sometimes not completely understood.

Turning to the case of expansion of the combustion gases, tables are given for the gases resulting from the complete combustion of a hydrocarbon fuel of composition $(CH_2)_n$ with 400% of theoretical air (about 60/1 air-fuel ratio) and with 200% of theoretical air (about 30/1 air-fuel ratio). It can be shown that the use of the single composition can be used with negligible error for the products

of combustion of a wide range of hydrocarbon composition. Other air-fuel ratios may be obtained by interpolation. The gas tables are based on one pound-mole of products and it is necessary to calculate the molecular weight of the products for the actual fuel used in order to obtain the value per pound. As an example, suppose it is required to find the expansion work per pound of products through a pressure ratio of 5 with an isentropic temperature efficiency of 87% for the products of combustion of methane (CH_4) with 400% of theoretical air from an initial temperature of 1360° F. Using the tables at $T_1 = 1820°$ R, $h_1 = 13434{\cdot}3$ Btu/lb-mole and $P_{r_1} = 130{\cdot}21$. Then $P_{r_2} = 130{\cdot}21/5 = 26{\cdot}042$ and the tables give $T_2 = 1210{\cdot}8°$ R. The actual temperature drop is $0{\cdot}87\ (1820 - 1210{\cdot}8) \approx 530°$ R and thus $T_{2'} = 1290°$ R. At this value of temperature, the tables give $h_{2'} = 9247{\cdot}6$ Btu/lb-mole. Thus $\Delta h' = 13434{\cdot}3 - 9247{\cdot}6 = 4186{\cdot}7$ Btu/lb-mole. The molecular weight of the products of combustion of CH_4 with 400% of theoretical air is 28·63, so $\Delta h' = 146{\cdot}2$ Btu/lb.

As a comparison, using $c_p = 0{\cdot}24$ and $k = 1{\cdot}4$, then $T_{2'} = 1337°$ R and $\Delta h' = 140$ Btu/lb. A mean value of c_p for combustion gases through the expansion is 0·272, with $k = 1{\cdot}337$, giving $T_{2'} = 1293°$ R and $\Delta h' = 143{\cdot}5$ Btu/lb. Using the *air* tables (i.e. not taking into account the change of gas composition due to combustion) yields $T_{2'} = 1278{\cdot}5°$ R and $\Delta h' = 143{\cdot}8$ Btu/lb. The values of $T_{2'}$ and $\Delta h'$ by these different methods are compared in Table 3.2, giving the percentage differences from the most precise values represented by the " Gas Table " values.

Table 3.2

	Gas table values	*Per cent error*	*Using* $c_p = 0{\cdot}24$ *and* $k = 1{\cdot}4$	*Per cent error*	*Using* $c_p = 0{\cdot}272$ *and* $k = 1{\cdot}337$	*Per cent error*	*Using Gas Tables for air*	*Per cent error*
$T_{2'}$, R	1290	0	1337	+ 3·65	1293	+ 0·23	1278·5	− 0·89
$\Delta h'$, Btu/lb	146·2	0	140	− 4·23	143·5	− 1·85	143·8	− 1·64

The conclusion is that the use of c_p at a constant value of 0·24 Btu/lbF leads to the largest error, but not as great as might be expected at first sight. Using an average value of c_p consistent with the estimated range of temperature for the expansion can give a very close answer. The use of the air tables, that is, ignoring the effect of change of gas composition, likewise gives reasonably accurate

results. Thus one may conclude that for lean mixtures, say 90/1 and greater, the air tables may be used for calculations.

It is reiterated that the purpose of this discussion is to demonstrate that, although standard gas tables are necessary for precise work, very reasonable values may be obtained on the slide rule by using the basic relationships and fair estimates of the value of specific heat. To this end, values of the specific heat of air at different temperatures are shown in Fig. 3.7. Because the value of $R = c_p - c_v$ does not change with temperature and varies only very slightly from the value for pure air over the range of composition of combustion products, then the exponent $(k-1)/k$ may be obtained as follows:

$$\frac{k-1}{k} = \frac{c_p/c_v - 1}{c_p/c_v} = \frac{c_p - c_v}{c_p} = \frac{R}{c_p} = \frac{53{\cdot}34/778{\cdot}16}{c_p} = \frac{0{\cdot}06855}{c_p}$$

3.8 *Effect of Varying Mass Flow*

The first effect is that of the augmentation of the air flow by the amount of fuel added, so that the turbine gas flow, m_g, is greater than the compressor air flow, m_a, by the ratio $(1+f)$, where f is the fuel-air ratio by weight, m_f/m_a, i.e.

$$m_g = m_a + m_f$$

and

$$\frac{m_g}{m_a} = 1 + \frac{m_f}{m_a} = 1 + f$$

Although the fuel-air ratio, f, is convenient to work with in calculations, it is usually more meaningful to think in terms of its reciprocal, the air-fuel ratio, F. For hydrocarbon fuels, the theoretical or stoichiometric air-fuel ratio is about 15/1 in whole numbers, so that the 200% and 400% of theoretical air of the "Gas Tables" represent air-fuel ratios of about 30/1 and 60/1 respectively. A value of F of about 60/1 would correspond with the temperature rise required for a turbine temperature of 1350° F with an initial temperature of 59° F and a pressure ratio of 5/1. With $F = 60$, then $f = 0{\cdot}01667$ and the turbine flow is greater than the compressor flow by 1·67%.

However, there is nearly always a compensating effect due to the bleeding of air from the compressor, either at discharge or intermediately, for a variety of auxiliary purposes, such as cooling air for the bearings, turbine wheel, cabin cooling and so forth. It is seldom that the quantity of bled air is known exactly when design cycle calculations are being made and, as it is normally of the order of 1% or 2% of the total air, it is reasonable to assume that air and gas mass flows are equal. This assumption will be made in future

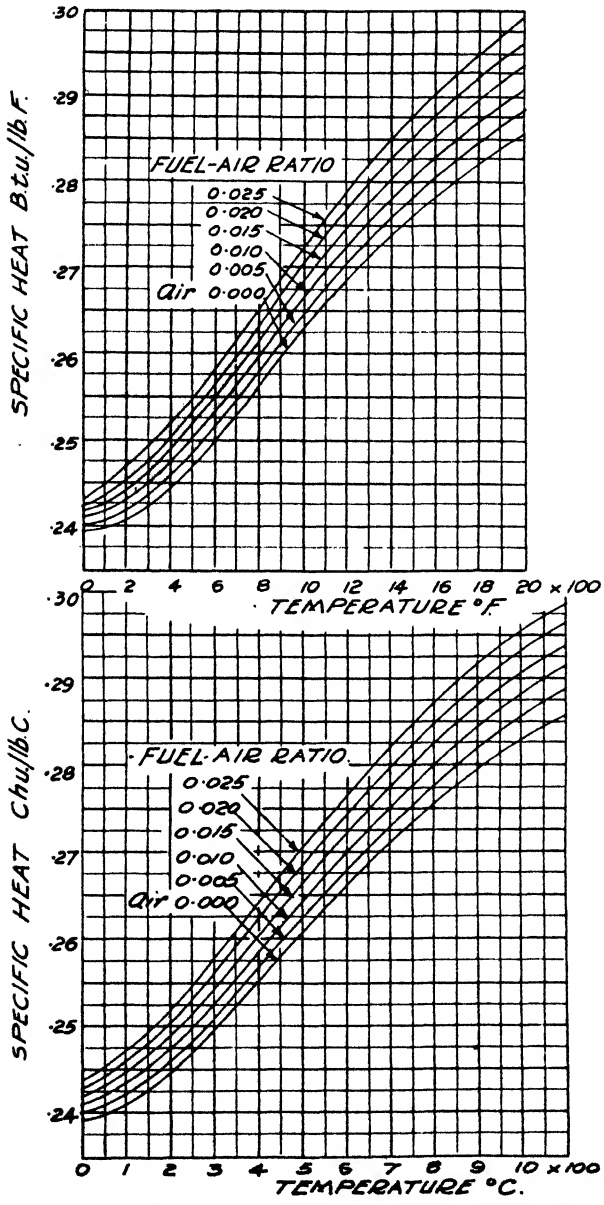

FIG. 3.7. Specific heat of air and combustion products.

throughout this text, so that $m_a = m_g = m$. For final calculations, it is necessary to know, or to estimate as exactly as possible, the amount of bled air, because it can be of such proportions as to reduce the nominal performance significantly. Because of the high speeds

of military aircraft and the use of higher combustion temperatures, with a correspondingly greater demand for cooling air, the demand for compressor bleed air is increasing.

3.9 *Loss Due to Incomplete Combustion*

At the design operating condition, combustion efficiency is usually very high, close to 100%, in the sense of the ratio of enthalpy released to the available enthalpy of the fuel. Combustion efficiency is extremely difficult to measure accurately to within 1% and it is conservative practice to assume it is 98% for purposes of cycle calculations. It is taken into account by dividing the theoretical amount of fuel required by 0·98 and it affects only the cycle efficiency and not the work output.

It is difficult to maintain combustion efficiency at this value at very lean mixtures, at low loads for example, or at very high altitude in turbo-jet engines, and it may be necessary to use lower values if operational requirements dictate considerable periods at these conditions. However, since both part-load and high-altitude conditions imply that the total fuel consumption is relatively small, a lower value of combustion efficiency may not be of very great importance.

3.10 *Loss Due to Mechanical Effects*

These losses may be divided into necessary losses, such as those due to bearing friction and the power required for the fuel pump and oil pump, and auxiliary power requirements which should not debit the inherent performance of the gas turbine, such as a reduction gear or electric generator. The friction loss of ball and roller bearings is extremely small, while that of plain bearings is somewhat higher. The pumping power for fuel and oil is a small fraction of the total power and a value of mechanical efficiency of 98% is a reasonable value in the absence of special auxiliary power requirements. This value is used to modify the net work value and thus also affects the efficiency.

3.11 *Effect of Heat Losses*

There is a loss of heat by radiation and convection from the combustion chambers and turbine casing, and these are usually insulated in industrial plants but not in aircraft engines. The fractional heat loss is very small and the insulation is more for the purpose of comfort in vicinity of the plant than for reasons of conserving efficiency. No allowance is usually made in calculations for this loss.

3.12 *Calculation of Fuel Consumption and Cycle Efficiency*

For the ideal cycle, the heat added, Q_{in}, was taken as $c_p \Delta T$ and c_p was taken as constant throughout the cycle. For the actual cycle, fuel is burnt internally and the equivalent of Q_{in} is the amount of a given fuel necessary to raise the air temperature at combustion chamber inlet to the gas temperature at turbine inlet. The delivered gases or *products* vary in composition from the entry fuel and air or *reactants*, and the specific heats will vary with composition and temperature. An actual gas turbine plant is then quoted as having a certain *specific fuel consumption*, *SFC*, lb fuel/hp hr, it being necessary to know the particular fuel used. As will be seen later, it is possible to change this to an efficiency, but the latter will not be absolute as for the ideal cycle, as again it is an efficiency for the particular fuel used.

A given fuel has a certain heating value, HV (or calorific value or heat of combustion), Btu/lb or Chu/lb, which is defined and measured in a certain way. As combustion in the gas turbine is at essentially constant pressure, the heating value is defined as the quantity of heat removed in returning the temperature of the products of complete combustion of unit quantity of fuel to the initial temperature of the reactants, the process occurring at constant pressure. The HV is quoted for a certain temperature, usually 25° C (77° F). In the gas turbine the reactants are at a temperature different from 77° F and probably with fuel and air temperature different from each other, while the products are certainly not cooled to the original temperature, as the object is to raise the air temperature to a given value. Hence, although the standard heating value is used in the calculation, care is needed in its application for accurate results to be obtained. Thus it is not sufficient to equate the sum of the enthalpy of the reactants and the heating value to the enthalpy of the products, and a more detailed heat balance is required. This can be visualized with the aid of Fig. 3.8 which represents an enthalpy-temperature diagram for reactants, fuel and air, with enthalpy H_2, including the chemical energy as well as the sensible enthalpy, at temperature T_2. An adiabatic combustion process then results in the reactant state 3, with

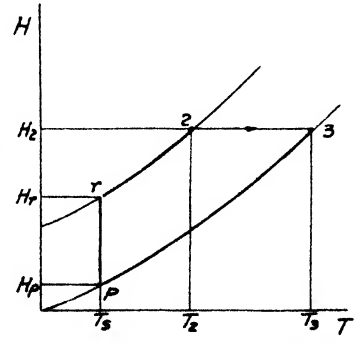

FIG. 3.8. Enthalpy-temperature diagram for combustion process.

$H_2 = H_3$. The problem is to determine the temperature of state 3 for a given mixture of air and fuel or, more usually, knowing T_3, which is given as the T_{max} of the cycle, to determine how much fuel is required to reach state 3 from state 2.

The information available is the heating value of the fuel at the standard temperature, T_s, and this is shown as the line rp on the diagram. Now because states 2 and 3 are thermodynamic states and endpoints of a process 2–3, then the path 2–3 may be replaced by the path 2–r–p–3. Thus

$$H_2 - H_3 = 0 = (H_2 - H_r) + (H_r - H_p) + (H_p - H_3) \quad (3.28)$$

where H is the enthalpy in Btu or Chu. For convenience in the diagram, state 2 represented both the reactants, fuel and air, but actually the fuel and air temperatures are different, so that $H_2 = H_a + H_f$. Using one pound of air as base, with a fuel-air ratio f, and taking the air at state 2 and the fuel at a state 2′, then Eq. (3.28) may be written as

$$0 = (h_2 - h_r)_{air} + f(h_{2'} - h_r)_{fuel} + f(HV)_s + (1 + f)(h_p - h_3)_{gas} \quad (3.29)$$

where $(HV)_s = h_r - h_p$ is the constant pressure, lower heating value of the fuel. It will be recalled that a fuel containing hydrogen has a lower heating value (LHV) if the water vapour resulting from combustion is not condensed and a higher heating value (HHV) if it is condensed. In all gas turbine combustion processes, the final temperature is far above the dew point, so that for the calculation of final temperature for fuel consumption, it is the LHV which is relevant. From Eq. (3.29), then

$$1 + f\left[\frac{(h_2 - h_r)_{air}}{f} + (h_{2'} - h_r)_{fuel} + (LHV)_s\right] + h_{p\,gas} \quad (3.30)$$

It will be observed from Fig. (3.8) that a simplified expression is obtained if the heating value at zero degrees absolute is used, when Eq. (3.28) becomes

$$H_2 - H_3 = 0 = H_2 + (H_{r_0} - H_{p_0}) - H_3$$

and, in terms of one pound of air,

$$h_3 = \frac{1}{1 + f}\left[h_2 + fh_{2'} + f(LHV)_0\right] \quad (3.31)$$

This may be convenient for repeated calculation, as, in the "Gas Tables" for example, the datum point for enthalpy values is zero absolute and thus values of h_2 and h_3 may be used directly. It must be noted that the term $(h_{2'} - h_r)$ relates only to the enthalpy without change of phase and that $(LHV)_s$ is assumed to be that from the

liquid phase. If the LHV is used from the gas phase and the fuel is actually injected as a liquid, then the enthalpy of vaporization at the standard temperature must be subtracted from the LHV. The specific heat of liquid hydrocarbon fuels is about 0·5 Btu/lb F (Chu/lb C) and as the enthalpy represented by $(h_{2'} - h_r)$ is very small in comparison with other terms, a precise value is unnecessary. In many practical applications, the fuel is injected at about ambient temperature and as this is very little different from that of the standard HV temperature (77° F), the fuel enthalpy term is often omitted. There are occasions, however, as with the use of a heated process-gas fuel, in which this enthalpy is not negligible and therefore the term is retained here.

The lower heating value of the fuel must be known and various sources are available. For pure hydrocarbons, the " Gas Tables " give both specific values for several fuels and a general formula for those of high molecular weight. For a mixed hydrocarbon, the heating value can be estimated quite accurately from its specific gravity (see Ref. 3).

To solve Eq. (3.29) for a particular unknown may be a tedious process. If the fuel-air ratio is known, then the solution is fairly straightforward. The " Gas Tables " may be used, the air table sections for $(h_2 - h_r)$ and the products tables for h_3 and $h_{p_{gas}}$. As mentioned previously, the latter are calculated for a fixed hydrocarbon composition $(CH_2)_n$, but are valid with considerable accuracy for most other hydrocarbons. Again, although tables are given only for 200% and 400% theoretical air, linear interpolation or extrapolation may be used with negligible error. However, the air tables are given with one pound of air as a basis and the products tables are for one pound mole of products as a basis, so that care must be taken in evaluating the various quantities.

The more usual problem in gas turbine work is to know the initial and final temperature, T_2 and T_3, and be required to find the fuel-air ratio f. As the enthalpy of the products depends on their composition and this in turn depends on f, then the solution may be a very tedious trial-and-error process. To obviate this, it is customary to prepare charts giving the combustion temperature rise $(T_3 - T_2)$ for a range of fuel-air ratios, with the entering air temperature as a parameter. Such charts will then be valid for a particular heating value only, and the sensible enthalpy of the fuel has to be taken at an arbitrary value. As the heating value and composition of most hydrocarbons do not vary too greatly, the charts may be used for other such fuels by adjusting the fuel-air ratio read from the charts in direct proportion to the ratio between the LHV used in the charts

to the *LHV* of the actual fuel used. Such a chart is shown in Fig. 3.9, which is based on an *LHV* at 77° F of 18,500 Btu/lb (10,278 Chu/lb), with the fuel in the liquid state. It represents a reasonable average value for hydrocarbon fuels, being typical for a kerosene, gasolines being slightly higher and fuel oils slightly lower. More complete charts covering a greater range and of extended scale for higher accuracy are given in Hodge (Ref. 4).

Returning to the question of obtaining fuel consumption of an actual gas turbine, the fuel-air ratio f required for a given turbine inlet temperature can be obtained from Fig. 3.9, or its equivalent. The fuel consumption in lb/hr then equals the product of f and the total air rate in lb/hr. The specific fuel consumption is the total fuel rate divided by the total output, i.e.

$$SFC = \frac{\text{lb fuel/hr}}{\text{hp output}} = \frac{\text{lb fuel/lb air/hr}}{\text{hp/lb air}} \times 3600 = 3600 \frac{f}{W_{h_p}} \quad (3.32)$$

where f is the fuel-air ratio and W_{h_p} is the specific power output.

The overall thermal efficiency is an inverse form of *SFC*, defined as the thermal equivalent of the rate of work output divided by the rate of heat input, or

$$\eta = \frac{550\ W_{h_p}}{Jf(HV)} \quad (3.33)$$

There is no complete agreement on which heating value to use. For obtaining a given temperature rise, only the *LHV* is effective, and the latent heat of vaporization of water is still contained in the gases when they are finally discharged following expansion in the turbine, as the discharge temperature is above the dew-point. One school of thought holds the view that this wasted thermal energy should be charged to the gas turbine plant, i.e. that the *HHV* should be used for Eq. (3.33). Others hold that the plant is not designed to utilize this latent heat so that the use of the *HHV* penalizes the plant unfairly if the fuel used has a high hydrogen content (meaning a high water vapour content of exhaust gases). Thus they advocate the use of the *LHV*. Others take the view that the correct value is neither of these, but a value based on the temperature at which the combustion occurs. There appears to be no one value which is at the same time precise thermodynamically, related practically to working conditions, and enabling direct comparisons to be made. An extensive and useful discussion is given in a " Symposium on Heating Values of Fuels " (Ref. 5). In practice, two distinct usages are made. In the U.S.A., the *HHV* at the standard temperature is almost universally used, while European practice tends to use the *LHV* at the standard temperature. As the

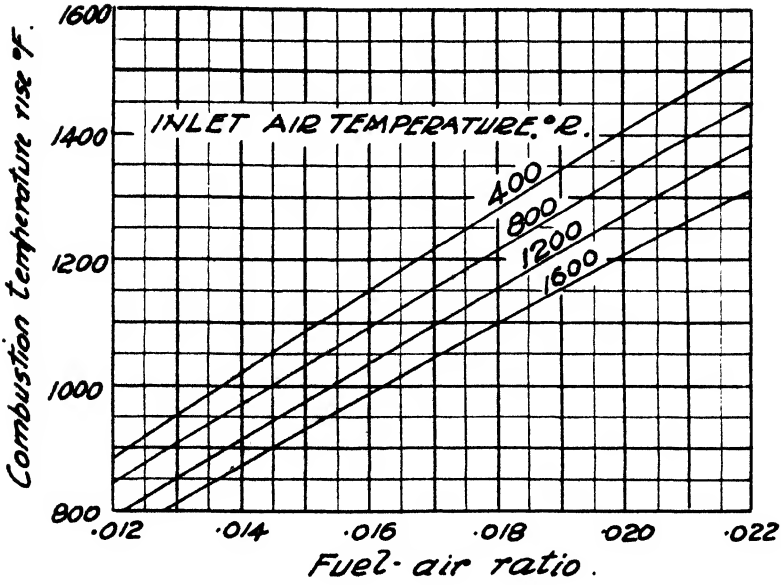

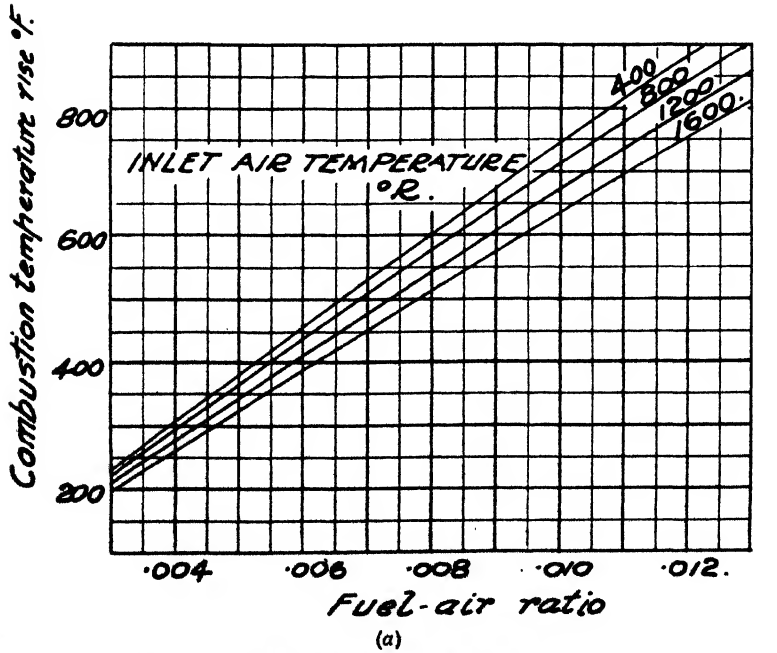

(*a*)

FIG. 3.9. Combustion temperature rise *versus* fuel-air ratio.

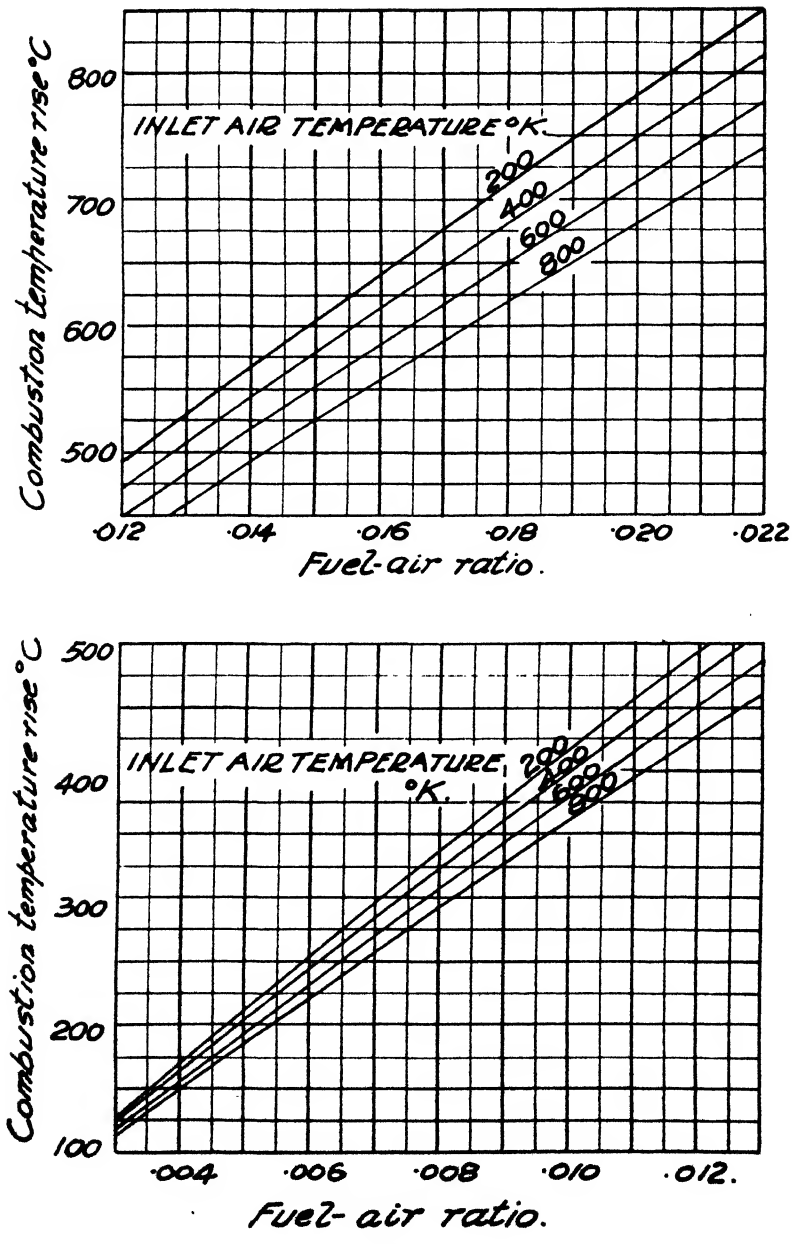

(*b*)

FIG. 3.9. Combustion temperature rise *versus* fuel-air ratio.

difference in LHV and HHV is of the order of 7% of the former, it is very necessary to know what value has been used when a value of efficiency is quoted.

Combining Eqs. (3.32) and (3.33), there results

$$\eta = \frac{2544{\cdot}5}{SFC \times HV} \tag{3.34}$$

For the LHV of 18,500 Btu/lb used previously, then

$$\eta = \frac{13{\cdot}75}{SFC} \text{ per cent} \tag{3.35}$$

and for the corresponding HHV of the typical hydrocarbon, (19,764 Btu/lb; 10,980 Chu/lb)

$$\eta = \frac{12{\cdot}87}{SFC} \tag{3.36}$$

Eqs. (3.35) and (3.36) are not absolute, but are useful for quick conversions between η and SFC, as both are in current use.

It is also necessary to distinguish exactly what the work output implies. From the point of view of the gas turbine itself, the work output is that obtained at the shaft, if all the essential auxiliaries such as fuel and oil pumps, etc., are driven by the plant itself. If any measurable amount of external power is necessary, then this should be subtracted from the shaft power. If a gearbox is used, then it must be decided if this is a necessary feature of the gas turbine plant, i.e. the actual shaft speed of the turbine may be too high for any practical application, in which case the loss due to the gearing should be debited to the plant. If, however, the gearing is necessary only for a particular application, then the loss is more reasonably debited to the system rather than to the prime mover.

3.13 *Representation of Gas Turbine Cycles*

Cycles may be shown pictorially in schematic form by using certain symbols for the components, with lines connecting the components showing the flow path. The conventional symbols are shown in Fig. 3.10. These diagrams may also show more than the necessary information for thermodynamic analysis, by indicating the relative positions of the compressors and turbines, if there are more than one of each, together with the relative position of the load. For example, it is often necessary to divide the compression among two or more separate rotors, which may each be driven by a separate turbine or all from one turbine. With separate turbines, the load may be taken from the high-pressure turbine or the low-pressure turbine or may be taken from a separate *power* turbine. From the

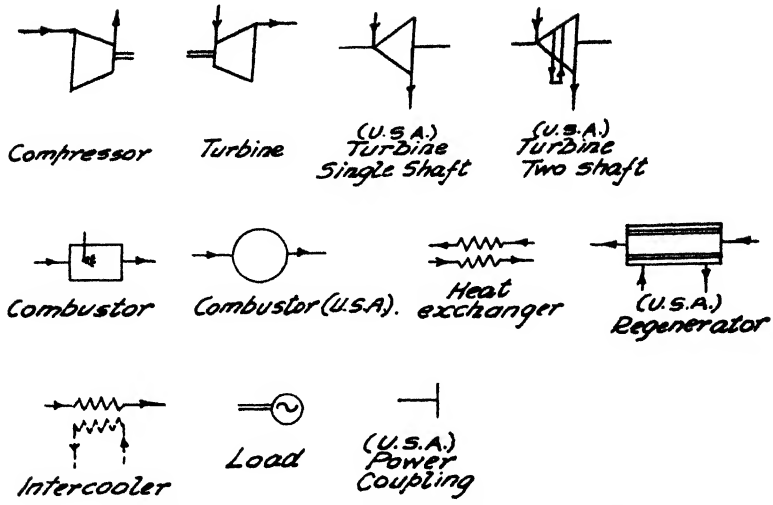

FIG. 3.10. Conventional symbols for cycle components.

point of view of thermodynamic analysis at the design point, the particular arrangement is immaterial, provided that any changes of component efficiency and extra flow losses in connecting ducts are taken into account. The importance of the arrangement of components lies in the design of the individual components and in the performance at off-design (part-load) points.

Starting with a simple Joule cycle with a single compressor and turbine, then the conventional schematic arrangement is shown in Fig. 3.11 (a). However, if a separate power turbine is used, then

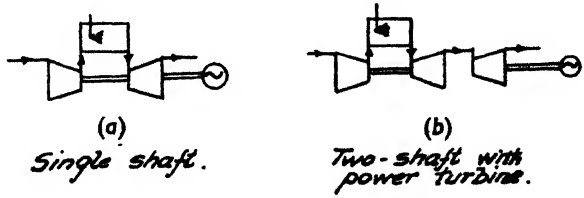

FIG. 3.11. Representation of simple cycle.

the cycle diagram appears as in part (b) of the figure. A cycle with two compression stages with intercooling, with each turbine driving a compressor, is shown in Fig. 3.12. Part (a), with high-pressure (HP) compressor and turbine on the same shaft and low pressure (LP) compressor and turbine on the same shaft, is known as a *straight compound* arrangement. Part (b), with HP compressor and LP turbine on one shaft and LP compressor and HP turbine on

another shaft, is known as a *cross compound* arrangement. There are many variants in layout of a given cycle, as the load may be taken from either turbine, the flow may be split and taken in parallel by two turbines, there may be a separate combustor for each turbine

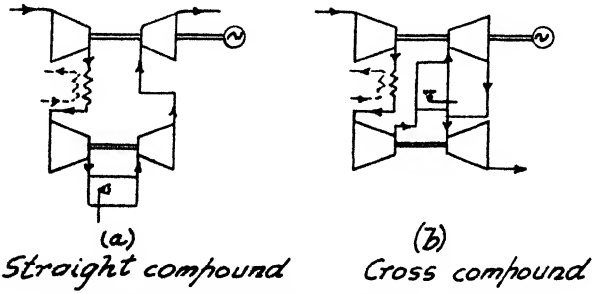

FIG. 3.12. Cycle with intercooling—compound.

and so forth, but the thermodynamic performance at the design point is independent of the physical arrangement. In the subsequent discussion of cycle performance, a conventional cycle diagram is given for each case in the simplest possible form, but the results are valid for more elaborate arrangements with separate power turbine, compounding, etc.

3.14 *Calculation of Cycle Performance*

Calculation of power output and efficiency of fuel consumption for a gas turbine cycle is carried out in a straightforward, step-by-step manner, starting at the air intake and ending at the point of discharge of combustion products. The negative work of compression is calculated from the known pressure ratio and estimated compressor efficiency by means of Eq. (3.10), using either a mean estimated specific heat or exact values from the " Gas Tables ". If the cycle has intercooling, then the calculation must be done in steps, allowing for pressure loss in the intercooler, and finding the air temperature after cooling by means of the equivalent of Eq. 3.25 for an assumed value of intercooler effectiveness.

The turbine inlet temperature, T_{max}, is known, and also the pressure, which is that of compressor delivery less estimated flow losses in the combustor and heat exchanger, if any. The turbine work is then calculated by means of Eq. 3.13, again allowing for flow losses in the heat exchanger and exhaust duct in obtaining the available turbine pressure ratio. The difference of turbine and compressor work is then the net rate of work output per lb per sec of air. The thermal units may then be converted to hp by multi-

plying by 778 ft lb/Btu or 1400 ft lb/Chu and dividing by 550 ft lb/(hp) (sec).

For obtaining efficiency or fuel consumption, it is necessary to find the fuel-air ratio f. For a cycle without regeneration, this can be found directly with the aid of a diagram similar to Fig. 3.9, as the combustion temperature rise is given by the difference of T_{max} and the final compressor delivery temperature, $T_{2'}$. Knowing f, the specific fuel consumption and efficiency can then be obtained from Eqs. (3.32) and (3.33). It should be noted that for cycles with reheat, there are two turbine work quantities and two additions of fuel. For cycles with a heat exchanger, the combustion temperature rise is the difference between T_{max} and the temperature of the air leaving the heat exchanger, $T_{2'_r}$. Recalling the definition of effectiveness (Sec. 3.5), then

$$T_{2'_r} = T_{2'} + \eta_r(T_{4'} - T_{2'})$$

where $T_{4'}$, the turbine discharge temperature, has been found from the turbine work calculation. An example of cycle calculation using mean specific heats is given as an appendix to this chapter.

3.15 *Performance of Actual Gas Turbine Cycles*

Work output and efficiency of all actual cycles are considerably less than those of the corresponding ideal cycles, due chiefly to the effect of compressor and turbine efficiencies and secondarily to the flow pressure losses incurred in other components. For cycles with a heat exchanger, the value of effectiveness possible will reduce the efficiency below the corresponding ideal regenerative cycle. With the many possible values of efficiencies, effectivenesses and losses, it is neither possible nor desirable here to give many charts of overall performance, but a few typical cycles are quoted so that a general idea may be obtained. The following " Standard " values are taken and may be regarded as typical of actual performance:

Inlet pressure	14·7 psia
Inlet temperature	59° F (15° C)
Compressor isentropic (temperature) efficiency	0·85
Turbine isentropic (temperature) efficiency	0·85
Turbine inlet temperature	1350° F (732·5° C)
Combustor pressure loss	0·02 P_{max}
Combustion efficiency	0·98
Exhaust pressure loss	0·2 psi
Fuel HHV	19,764 Btu/lb (10,980 Chu/lb)
Fuel LHV	18,500 Btu/lb (10,278 Chu/lb)
Mechanical efficiency	0·98

The compressor and turbine efficiencies should vary with pressure ratio and it will be shown later that the "polytropic" or "infinitesimal stage" efficiency is more realistic when comparing cycles with different pressure ratios. This analysis will be deferred, however, as it requires detailed discussion, and the use of a single isentropic efficiency allows comparison to be made more directly and obviously. The combustor pressure loss is an average value capable of attainment in plants of reasonable size, although in practice values may range from 1% to 4% of P_{max}. The combustion efficiency as used here represents the ratio of the actual rise of sensible enthalpy consequent on combustion to the ideal enthalpy rise. The exhaust pressure loss is negligible for many installations, but a finite value has been included here for the sake of conservatism. As no intake loss has been included, the exhaust loss may be thought of as allowing for the possibility of either.

The following variations of this basic simple cycle are shown in the next figures:

(1) Effect of varying T_{max}—values of 1200° F (649° C) and 1500° F (816° C).

(2) Effect of varying η_c and η_t—values of 0·8 and 0·9.

(3) T_{max} of 1200° F and 1500° F with $\eta_c = \eta_t = 0{\cdot}90$.

(4) Effect of regeneration—values of η_r of 0·60, 0·75 and 0·90, together with additional pressure losses of 0·02, 0·03 and 0·04 of P_{max} respectively.

(5) Effect of intercooling—value of $\eta_i = 0{\cdot}95$. Intercooling occurs at a pressure corresponding to the square root of overall pressure ratio, i.e. $P_{r_i} = \sqrt{P_r}$. Additional pressure loss due to intercooling—0·25 P_{r_i} psi.

(6) Effect of intercooling with regeneration for $\eta_r = 0{\cdot}75$.

(7) Effect of reheat and regeneration—$T_{reheat} = T_{max} = 1350°$ F (732·5° C), $\eta_r = 0{\cdot}75$. Reheating occurs at a pressure corresponding to the square root of available expansion ratio, i.e. $P_{r_r} = \sqrt{P_{r_{exp}}}$. Additional pressure loss due to reheating—0·5 P_{r_r} psi.

(8) Performance of complex cycle, with intercooling, reheat and regeneration.

(9) Effect of inlet temperature—T_1 from − 60° F to 120° F.

The various additional pressure losses are arbitrarily formulated, but are intended to yield reasonable values which increase with pressure ratio (increase of density). The calculations are based on average values of the specific heat of air, and of the combustion products. The performance is given in terms of specific output in hp/(lb) (sec) of air and efficiency as a function of pressure ratio.

The compressor temperature rise ΔT_{12} is sometimes used instead of pressure ratio as a base for comparison (Ref. 4, for example) as ΔT_{12} represents the work of compression for a given fixed rpm regardless of inlet temperature, whereas pressure ratio is dependent on the latter. Pressure ratio, however, is more readily visualized as a design parameter and is more suitable here in the presentation of typical performance possibilities as opposed to design formulation data. The figures should be used only as giving typical performance values and are useful chiefly in showing the effect of variation of the various parameters on a relative basis, rather than as giving absolute values.

Fig. 3.13 shows the variation of output and efficiency with pressure ratio, for three values of T_{max}. Both W and η have maximum values at a certain value of P_r, this value being lower for the former than for the latter at a given temperature, as was demonstrated earlier. The effect of increasing T_{max} is to increase both W and η for a given pressure ratio and to increase the pressure ratio at which the maxima occur. Increase of turbine inlet temperature T_{max} has a greater effect on work output than on efficiency and the importance of a high value in order to obtain reasonable performance is shown clearly in this figure. Taking a pressure ratio of 5 similar to that used for demonstration purposes in earlier discussion, then using the " standard " values yields an efficiency of about 19% and a work output of about 70 hp/(lb) (sec) of air. The efficiency is low compared to that of reciprocating combustion engines, but the power output is high, factors which sum up typical gas turbine performance, that is, relatively poor fuel consumption but relatively high size-to-power ratio. Thus the simple cycle gas turbine must use cheap fuels and have a high working temperature in order to compete in fuel cost with spark ignition and diesel engines, but may offer considerable advantages in size and weight.

Fig. 3.14 shows the effect of varying compressor and turbine efficiencies from 0·85 down to 0·80 and up to 0·90. Increased component efficiency increases markedly both W and η, and moves the maximum values to a higher pressure ratio similarly to increased T_{max}. It is worth noting that if low component efficiencies are expected, then it is not worthwhile to use high pressure ratios, as the maxima of both W and η occur at relatively low values of P_r.

In Fig. 3.15 the curves for $\eta_c = \eta_t = 0{\cdot}90$ and $T_{max} = 1200°$ F (649° C) show that a low turbine temperature may be used in conjunction with high component efficiencies in order to achieve a useful performance. This has been the approach to date of the Swiss gas turbine manufacturers; the use of low temperatures allows less

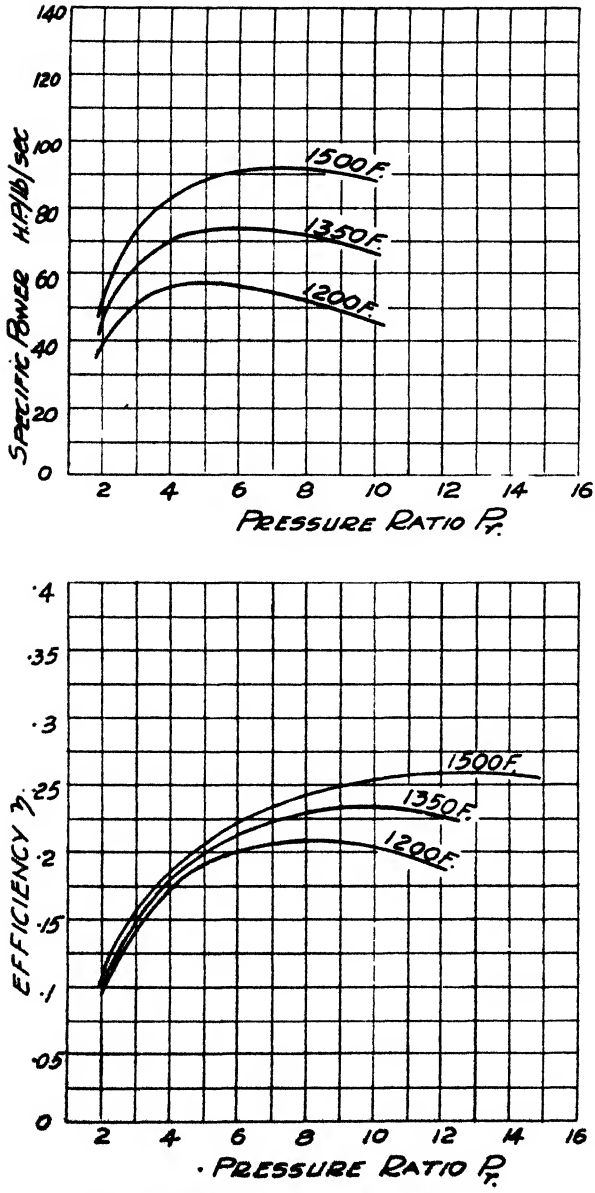

FIG. 3.13. Simple cycle—effect of T_{max}.

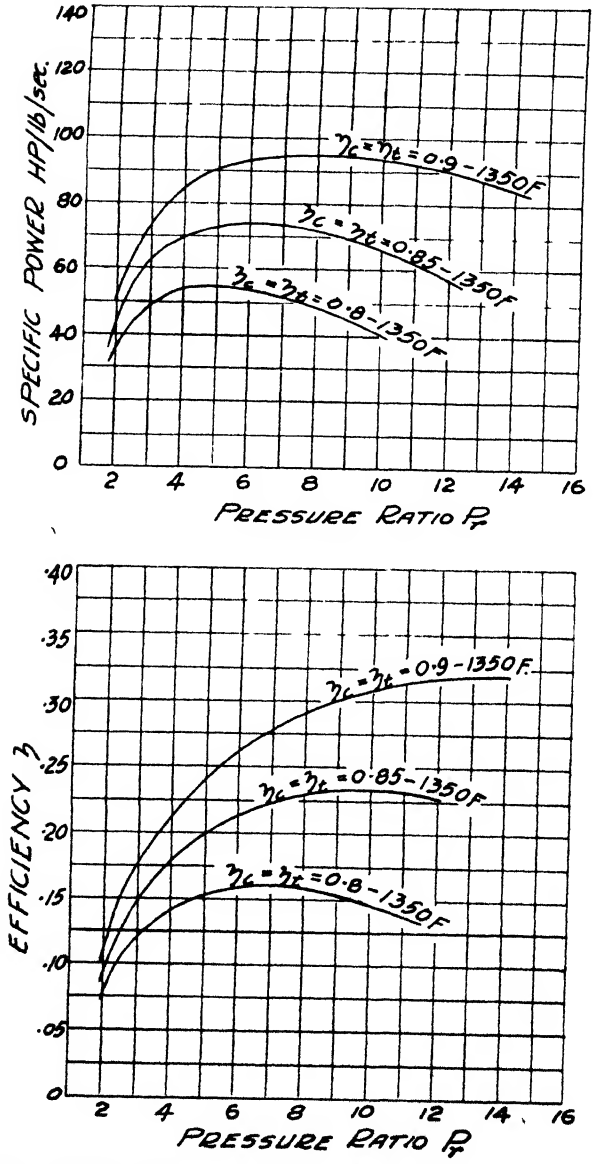

FIG. 3.14. Simple cycle—effect of compressor and turbine efficiency.

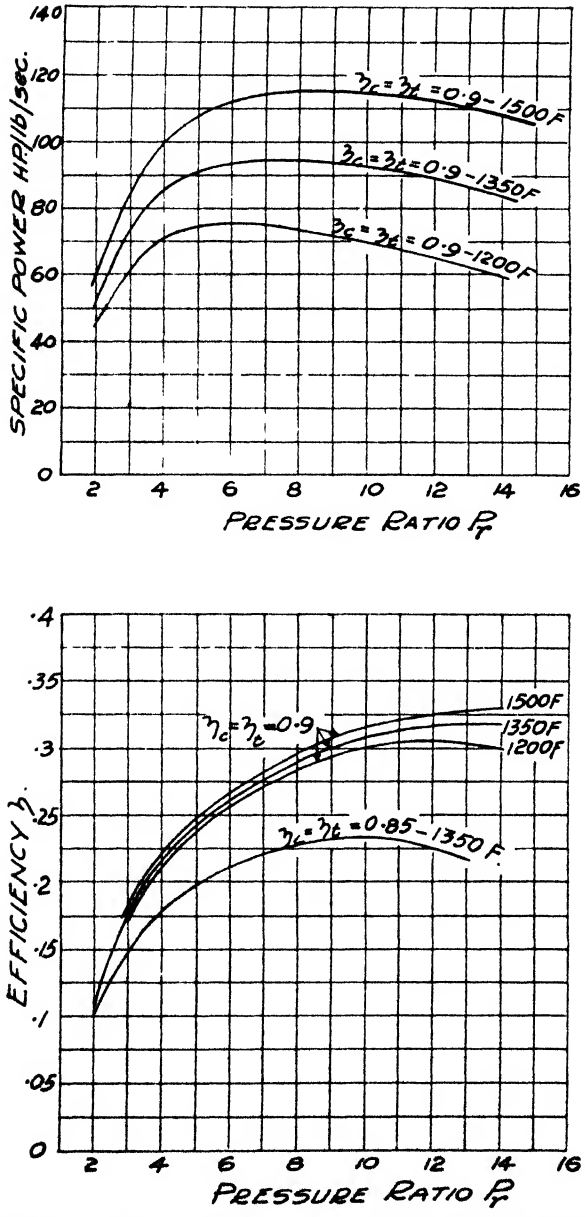

FIG. 3.15. Simple cycle—effect of T_{max}—high component efficiency.

expensive materials to be used and avoids possible fouling difficulties which are liable to occur with heavy fuels at higher temperature (see chapter on combustion). The curves for $\eta_c = \eta_t = 0{\cdot}90$ and $T_{max} = 1500°\,F$ (816° C) show what may be expected as a limit for the simple cycle for the near future. The turbine inlet temperature of 1500° F (816° C) is in use, but about 87–88% component efficiencies are the best yet achieved for industrial turbines. With these values, an efficiency approaching 30% is reached at a reasonable pressure ratio, still somewhat less than that of a good reciprocating combustion engine. For better fuel consumption then, it is necessary to elaborate on the Joule cycle by adding a heat exchanger in order to approach the regenerative cycle.

Fig. 3.16 shows the effect on performance of adding heat exchangers of 0·60, 0·75, and 0·90 effectivenesses to the simple cycle. The effect on work output is small, the reduction being due only to the increased pressure losses. The increase of efficiency is notable however, with a heat exchanger of 0·75 effectiveness giving a peak efficiency of about 29%. An almost equally important effect is that mentioned earlier, namely that regeneration lowers the pressure ratio at which the peak efficiency occurs. Thus with 0·90 effectiveness, the optimum pressure ratio is as low as 3, which holds the possibility of a simpler and cheaper compressor of high efficiency. With regeneration, the optimum pressure ratio for efficiency is lower than that for work output, but for the usual values there is less compromise than for the simple cycle. An effectiveness of 0·75 represents about the maximum value of the *recuperative* heat exchanger (Sec. 3.5), owing to limitations of size (hence cost), and a value of 0·90 can be achieved practically only by the *regenerative* type. The latter, however, represents a more difficult problem of design and construction and its possibilities are discussed in a later chapter. It should, however, be noted that an efficiency of over 30% is possible with the other standard values for the cycle, which makes the gas turbine directly competitive in fuel consumption with other combustion engines.

The next variation to the simple cycle is that of intercooling shown in Fig. 3.17. For the ideal cycle, it was shown that intercooling improved the work output but *decreased* the efficiency. The diagram for an actual cycle shows that the work output increases considerably and peaks at a much higher pressure ratio. The efficiency, however, is but little changed at low-pressure ratios and increases as the pressure ratio increases. This is because with irreversible compression the saving in negative work with intercooling outweighs the additional fuel necessary for the lower air

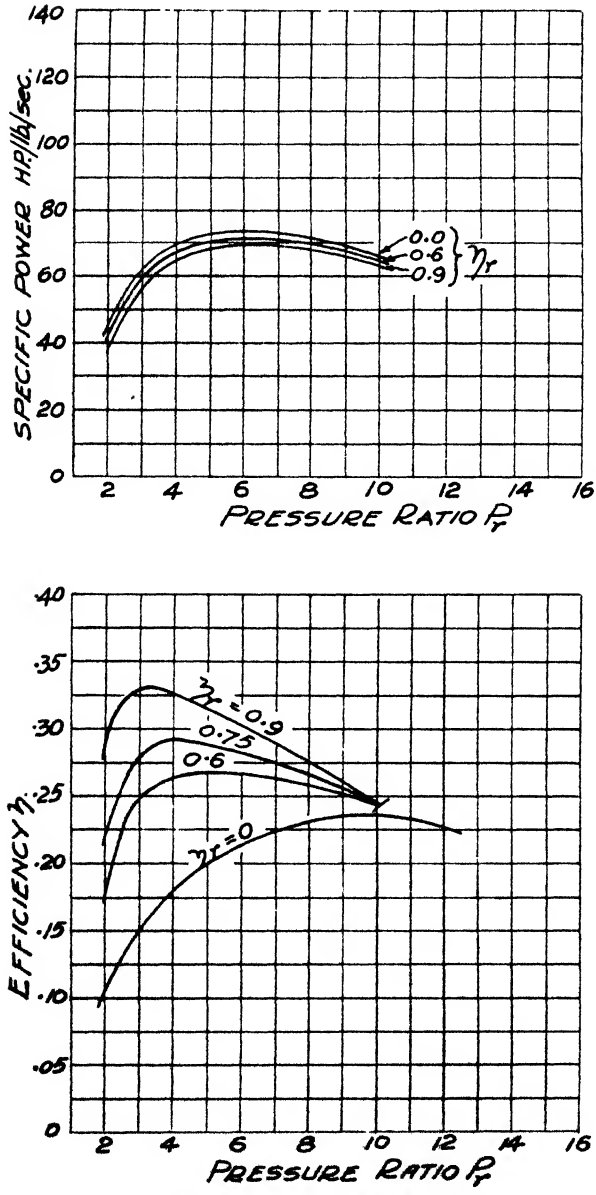

FIG. 3.16. Cycle with regeneration.

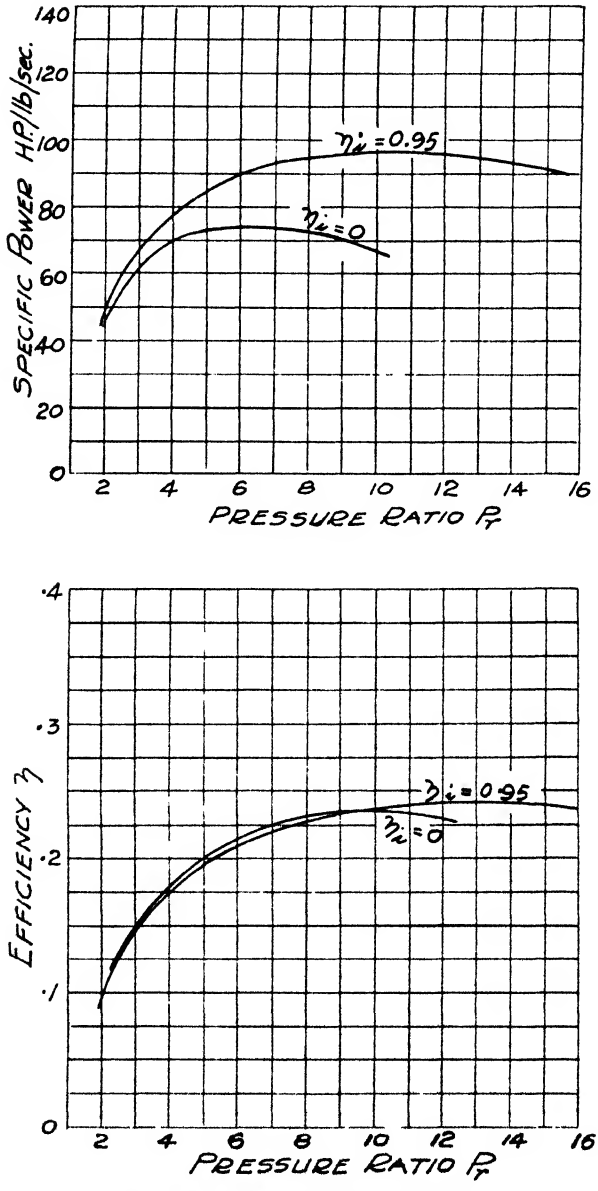

FIG. 3.17. Effect of intercooling.

delivery temperature. The increase in efficiency is not large and the main use of intercooling is to achieve a greater work output per lb of air, thus making a more compact unit. For high-pressure ratios, intercooling is almost a necessity, because as air temperature increases, the increment of pressure for a given amount of work decreases. As the limit of pressure ratio on a single shaft (i.e. blading running at a given speed) is of the order of 5, then with two rotors it is relatively simple to introduce cooling between the discharge duct of one rotor and the inlet duct of the next. Intercooling is usually restricted to a single unit, i.e. two stages of compression, but two stages of cooling improve performance still further and have been used in some plants. It should be remembered, however, that desirable as intercooling may be, it does detract from one of the principal merits of the gas turbine for many applications, namely that it is the only combustion engine which can be independent of water in all sizes.

Fig. 3.18 shows intercooling combined with heat exchange and this provides one of the most effective gas turbine cycles. Intercooling provides increased specific power, while both the intercooling and heat exchange improve the efficiency. The heat exchange modifies the effect of intercooling in moving up the pressure ratio for peak efficiency, with the result that for the standard figures used here, a peak efficiency of over 30% is obtained at a pressure ratio around 5.

Fig. 3.19 shows the results of reheat and heat exchange, somewhat similar to these for intercooling and reheat in increasing power and efficiency. Reheat by itself is not shown, as it is somewhat less effective than intercooling. Reheat has been used in practice only on experimental units, as the introduction of a second combustor leads to more complex installations and control difficulties.

Fig. 3.20 shows the *complex* cycle, that is, the cycle with intercooling, reheat and heat exchange, representing the closest practical approach to the ideal Ericsson cycle. It results in high efficiencies over a wide range of pressure ratio and very high power outputs. It has been used only in experimental plants, because in spite of its good performance, it requires an elaborate plant which, except for its more moderate use of cooling water, offers little advantage over a conventional steam plant.

Finally, Fig. 3.21 shows the effect of varying inlet air temperature T_1. In the discussion of ideal cycles, the parameter $T_r = T_3/T_1$ was used frequently, giving the idea that it was this ratio rather than the individual values which controlled the cycle performance. Usually it is not possible to control T_1, but its normal atmospheric

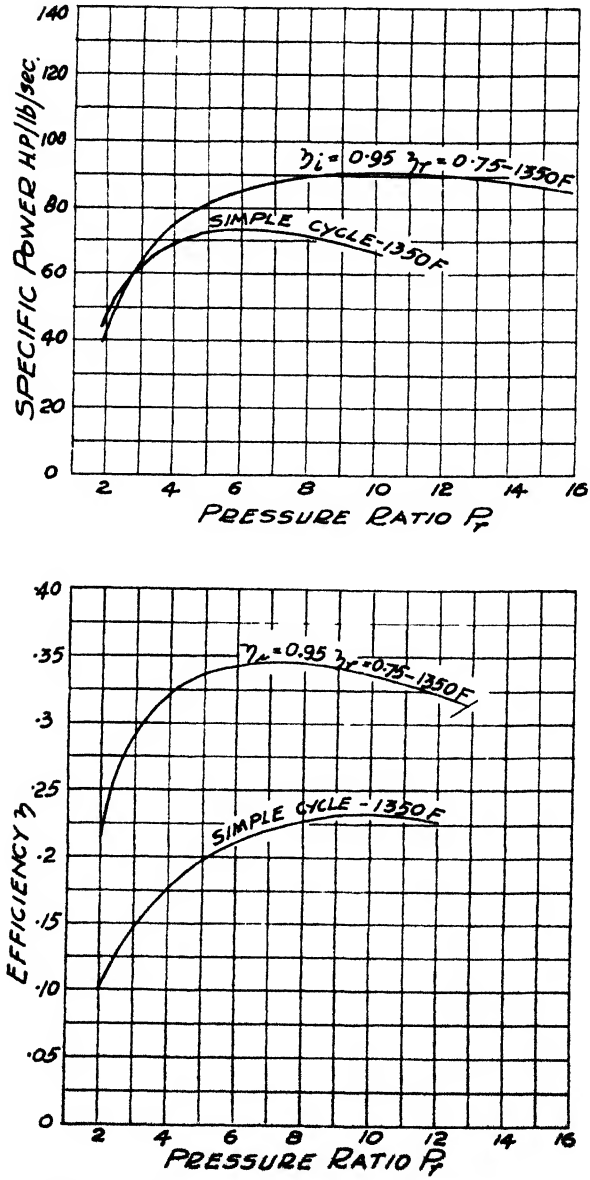

FIG. 3.18. Effect of intercooling and regeneration.

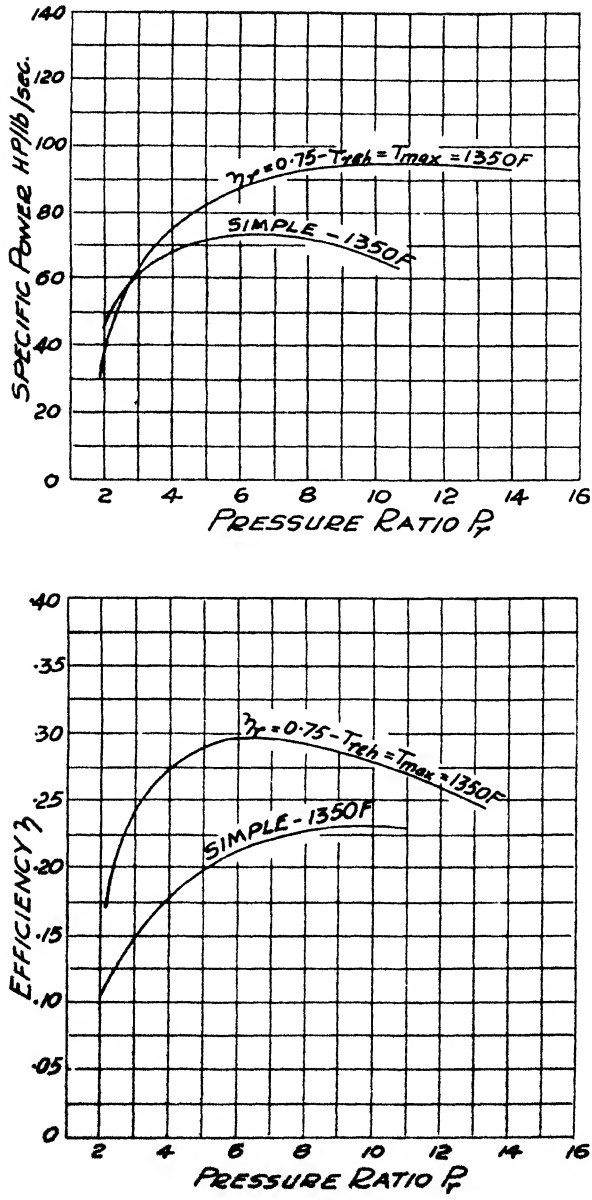

FIG. 3.19. Effect of reheat and regeneration.

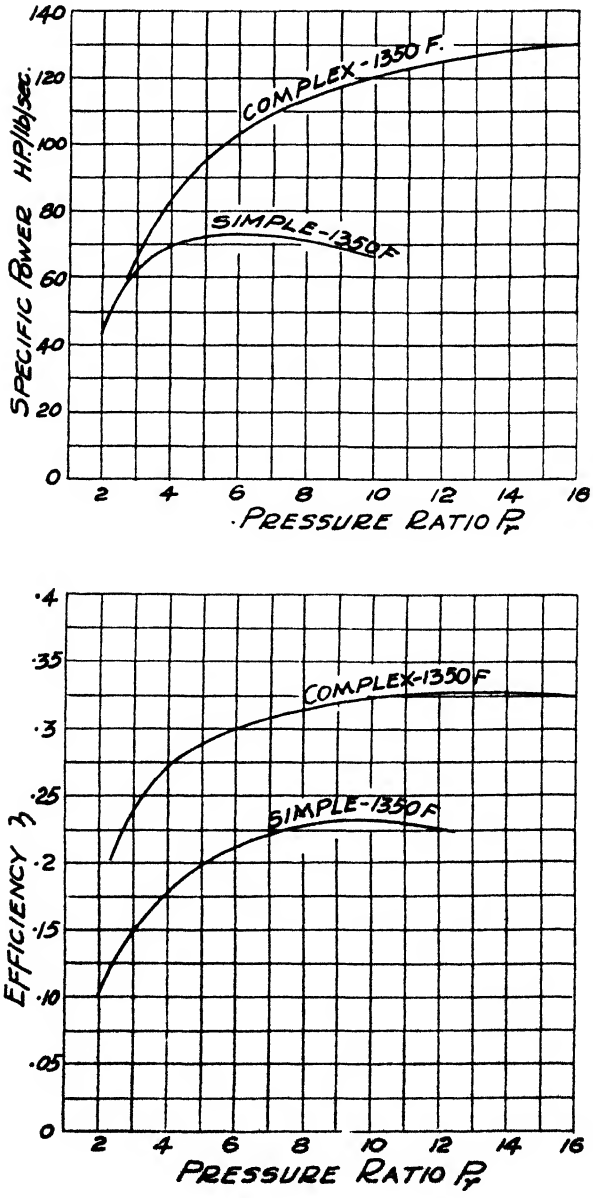

FIG. 3.20. Complex cycle.

variation has a considerable effect, as shown in the figure. The performance given here is based on a pressure ratio of 5, at an inlet temperature T_1 of 59° F as the design condition and then calculating the results at other values of inlet temperature using the same compressor work, which is equivalent to a constant speed, and the same T_{max}. At lower temperatures, therefore, the pressure ratio is increased, as $T_2/T_1 = (T_1 + \Delta T)/T_1$ increases. The opposite effect occurs at higher air temperature. The variation of efficiency and power output, particularly the latter, can be critical in some

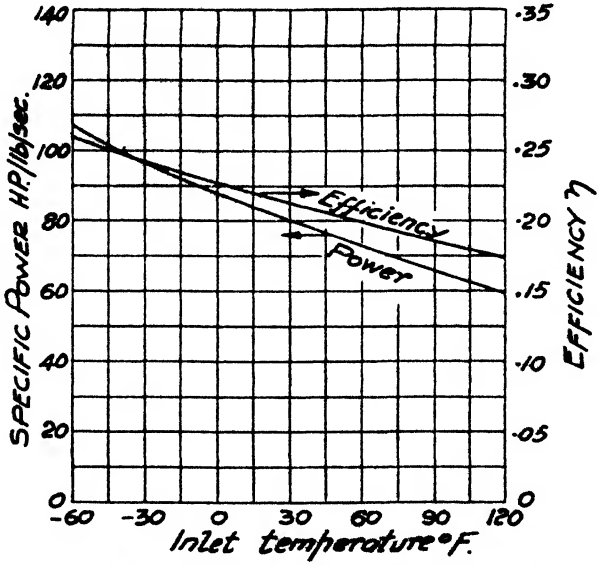

FIG. 3.21. Variation of performance with inlet temperature.

applications. For example, if the air temperature varies from — 20° F to 100° F, a not too extreme case, the power output varies from 125% of design to 87% of design. Thus if rated power must be maintained at high inlet temperatures, then the plant must be designed for the highest possible air temperatures. At low inlet temperatures, the plant may be run under reduced power conditions to produce only the rated output for the standard temperature or use may be made of the excess power. In the latter case, the unit must be designed mechanically to take the increased loading. The effect of an inlet pressure different from the standard sea-level figure is direct on power output and nil on efficiency. Varying ambient conditions affect the gas turbine more strongly than other combustion engines and the combination of pressure and temperature may exert a powerful influence on aircraft gas turbines, which more

than any other application have to meet a wide variety of such conditions. The effect of altitude on aircraft gas turbines is, of course, a study in itself and is part of the initial design procedure, but the variation of pressure and temperature can affect take-off performance considerably under so-called " normal " conditions. Fig. 3.21 should be interpreted qualitatively only, as it represents only the calculated performance under the assumed arbitrary conditions, and many other factors enter in practice which modify the actual figures, although the general result holds true.

It is important to remember, however, that the ambient pressure and temperature are important conditions to be stated in conjunction with a nominal rated output. Standard atmospheric values vary in different countries. In Europe, 15° C or 60° F are common values for intake temperature, but in the U.S.A., 80° F is a more usual value. In the latter country, standard conditions appear to be settling on 1000 ft altitude, corresponding to a pressure of 14·17 psia, and a temperature of 80° F.

3.16 *The Closed Cycle*

At the beginning of the chapter, it was pointed out that the usual form of the gas turbine plant did not operate on a true heat engine cycle, but that the term was commonly used thus. A true cycle is called a " closed cycle " and this introduces some additional elements. In the first place, the working fluid must be cooled down by an outside cooling medium between leaving the final turbine or heat exchanger and re-entering the first compressor. Secondly, the temperature rise of the air to turbine inlet temperature is carried out indirectly by heat transfer from an externally fired " air heater ", thus allowing any kind of fuel to be used with no risk of deposits on the turbine or heat exchanger. In the third place, control of output is not made by variation of the speed of the compressor and hence pressure ratio, or by turbine temperature, as in open-cycle turbines, but by means of the pressure level of the whole plant, this level being controlled by having a reservoir in the system. This last factor provides the great advantage of the closed cycle, as all pressure ratios and temperatures remain constant and only the mass flow rate of working fluid varies. Thus the cycle always operates at the design conditions of maximum efficiency, providing a flat part-load curve. Additionally, the system can be charged initially up to any practical datum pressure level, say 5 atmospheres, and with this high density, turbines of large output can be of relatively small size. Although a closed cycle can be composed of any of the elements, previously discussed for open cycles, it is most

effective in high-efficiency units, having two or more compressors with intercooling and heat exchange. Thus a typical closed cycle appears schematically as in Fig. 3.22. The cycle performance is calculated in similar manner to that of the open cycle, with the exceptions that the heat added is calculated from a combination of air heater effectiveness and actual combustion efficiency and that there may be additional flow loss through the *precooler*. The disadvantage of the closed cycle plant is that the air heater is in effect a heat exchanger operating with high fluid temperatures on both sides, thus giving a high metal temperature, and in addition requires a separate fan or compressor to supply the air for combustion. The size of the heat exchanger is mitigated by the fact that the air inside the plant is of a high density, which is conducive to high rates of heat transfer. These characteristics of the closed cycle plant will be more apparent after component performance has been analysed, and it will suffice now to note that, with the exceptions cited, the cycle performance of the design point is similar to that of the open cycle for similar values of component efficiencies, pressure ratios and temperatures.

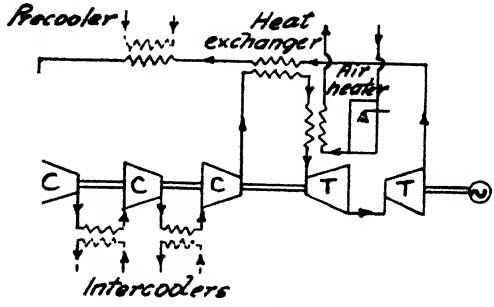

FIG. 3.22. Closed cycle.

The fact that the gas in the " closed cycle " plant suffers no change of composition implies that any suitable gas may be used, even a relatively expensive one, as the leakage is very small. Thus although only air is possible for the open cycle, gases offering more desirable properties may be used in the closed cycle. The major intrinsic properties of a gas which can affect the cycle performance are its molecular weight M_w, the value of its gas constant R and its specific heat c_p.

The density of a gas at a given pressure and temperature is directly proportional to its molecular weight, and thus from this standpoint, M_w should be large. The gas constant R affects the velocity of sound, a, in the gas, as $a = \sqrt{gkRT}$. For most common gases, $R = R_m/M_w$, where R_m is the *universal* gas constant, 1545·3 ft lb/lb mole F or 858·5 ft lb/lb mole C, so that a is also dependent on the molecular weight. The gas constant also enters into the value of $k = c_p/c_v$, the ratio of specific heats, since $R/J = c_p - c_v$ and $k(k-1) = Jc_p/R$. The index $k/(k-1)$ has

been seen to be a most important parameter, as it is the exponent of the pressure ratio-temperature ratio relationship in a isentropic process. The specific heat also enters in through the temperature rise for a given amount of heat transfer, as $Q = c_v \Delta T$.

Gases of high molecular weight (polyatomic gases) have a low value of R and a low value of k, yielding high values of the index $k/(k-1)$. Thus a small temperature ratio is associated with a large pressure ratio. The converse is true for the " light " gases of low molecular weight (hydrogen, helium). Thus different gases will require a varying number of compressor and turbine stages to achieve a certain pressure ratio for a given amount of work. The significance of the acoustic velocity is that the ratio of the fluid velocity to the acoustic velocity or *Mach* number has a profound effect on compressor performance (and to a lesser extent on turbine performance) when it reaches a certain critical value. A low value of a may then limit the performance of a machine before any of the other more usual limiting criteria are reached. The gas properties affect heat exchanger performance, which is critical in the closed cycle, because heat transfer depends on density, specific heat, viscosity and thermal conductivity.

It is almost impossible to generalize conditions in order to choose the optimum working fluid. It is necessary to know in detail the behaviour of compressor and turbine blading in relation to limiting values of Reynolds number, Mach number, stress and so forth. The desirable criterion for optimum performance may vary with application, for example, it may be size and weight of the rotating parts, cost of manufacture, design of heat exchanger, etc. Such analyses as have been made show that no outstanding overall gain is available over the use of air. An exception to this statement is made for the use of the closed-cycle gas turbine in connection with nuclear power plants. Here, it is desired to use the same fluid for the coolant of the reactor and for the power plant. Thus the working fluid must be chosen primarily for its nuclear properties and two attractive possibilities at the present time appear to be helium (very low M_w) and carbon dioxide (higher M_w).

3.17 *The Exhaust-Heated Cycle*

Yet another variant of the basic open cycle is that in which the air is heated indirectly through a heat exchanger between compressor and turbine, the fuel being burnt at low pressure immediately *following* the turbine. After this combustor, the gases pass through the hot side of the heat exchanger and thence to atmosphere. The cycle diagram then appears as in Fig. 3.23. The advantage of this

cycle is that a solid fuel may be used, as no ash or unburnt fuel passes through the turbine. The output is similar to that of the ordinary simple cycle with similar T_{max} and component efficiencies, but the efficiency with anything less than 100% regeneration is lower because the exhaust temperature is higher. Fig. 3.24 shows the cycle on a T-S diagram. 1–2 is compression, 2–3 is heating via

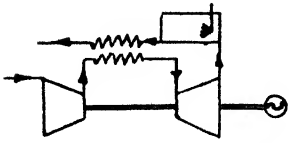

FIG. 3.23. Exhaust-heated cycle.

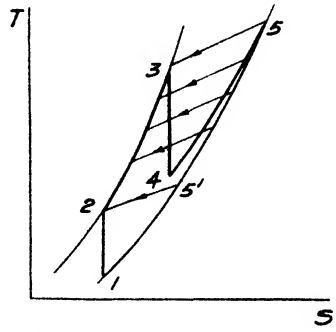

FIG. 3.24. Cycle diagram. Exhaust-heated cycle.

regeneration from 5–5′, 3–4 is expansion, 4–5 is the combustion process, 5–5′ is the heat transfer process to effect process 2–3, and 5′–1 is the rejection of heat to atmosphere. $T_{5'}$ is higher than the corresponding temperature for a heat exchanger of the same effectiveness in the normal position.

In Ref. 6, Mordell, the chief proponent of this cycle, shows that with 1400° F (760° C) inlet temperature and pressure ratio of 5, then a simple cycle has an efficiency of 19·35%, an ordinary heat exchange cycle an efficiency of 28·5% and the exhaust-heated cycle an efficiency of 22%, the latter two both for a heat exchanger of 75% effectiveness.

3.18 *Other Cycles*

There are many other possible variants of gas turbine cycles, showing one of the attractive features of the gas turbine plant—its versatility. Thus there is the semi-closed cycle, operating partly closed and partly open; the sub-atmospheric cycle, which utilizes air or very dilute gases at about atmospheric pressure from a previous process, the sequence being combustion, turbine, expansion, cooling and compression to atmospheric pressure for discharge; and combined cycles with steam. Some of these are described by Hodge (Ref. 4), while others are given in Refs. 7 and 8. Although some of these cycles have been put into practice, they are too numerous to

analyse here. The principles and methods described previously can be used in individual cases.

3.19 *The Gas Turbine Cycle for Jet Propulsion*

All the cycles discussed up to this point have had their useful output as shaft power. However, one of the major uses of the gas turbine is as an aircraft power plant in which the useful output is a stream of gas moving rearward at a high velocity. Such a use is a form of *jet propulsion* and the gas turbine used in this manner is usually called a *turbo-jet*. A gas turbine can be used in aircraft to drive a conventional propeller, when it is called a *turbo-prop*. Used in this manner, the useful output of the turbine is shaft power and so the previous analysis is valid. For use with a turbo-jet however, the cycle requires re-examination as the desired effect is different.

The turbo-jet cycle uses the basic Joule cycle, but the expansion is carried out in two stages, the first through a turbine to provide only just sufficient power to drive the compressor and the second through a simple nozzle to provide the highest possible velocity. The useful effect is the force or *thrust* produced by the net rate of change of momentum of the working fluid. The fluid has to be air taken from the atmosphere at inlet, which is changed to combustion products at outlet, since fuel is burnt internally. Disregarding the change of mass flow rate due to fuel addition (which again is usually negligible due to bleeding off the compressor for cooling purposes), then the *net thrust* F is

$$F = \frac{\mathrm{m}}{g_0}(V_j - V_i) \tag{3.36}$$

where V_j is the *jet velocity* at discharge and V_i is the inlet velocity. The product $\mathrm{m}V_j/g_0$ is called the *gross* thrust and $\mathrm{m}V_i/g_0$ is called the *intake drag* or *intake momentum*. For discussion of the cycle at this point, the turbo-jet will be considered as stationary, thus $V_i = 0$ and the *specific thrust* or thrust per lb per sec of air is simply V_j/g_0.

Fig. 3.25 shows the ideal Joule cycle for a turbo-jet with state points 1 to 5. Process 1–2 is compression and 2–3 is combustion, the usual processes as before; 3–4 is turbine expansion, with the work output $c_p(T_3 - T_4)$ just equal to the necessary compression work $c_p(T_2 - T_1)$. The remaining expansion from P_4 to P_1 is carried out in a simple propelling nozzle. Diagrammatically a turbo-jet may be sketched as in Fig. 3.26, which also shows the states corresponding to the cycle diagram. The useful output, the discharge velocity V_j, is produced by the expansion from 4 to 5.

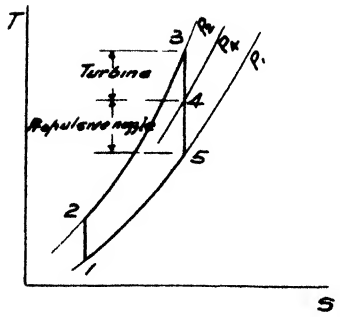

FIG. 3.25. Ideal Joule cycle for a turbojet engine.

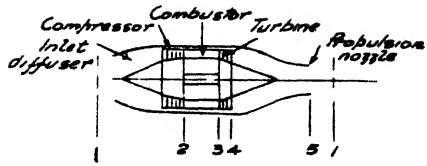

FIG. 3.26. Schematic representation of a turbojet.

The process 4–5 is one of constant stagnation enthalpy, as it is adiabatic and there is no shaft work. As any initial kinetic energy is here useful energy, then taking c_p as constant,

$$c_p T_4 + \frac{V_4^2}{2g_0 J} = c_p T_5 + \frac{V_5^2}{2g_0 J}$$

and
$$V_5 = [V_4^2 + 2g_0\, c_p J\, (T_4 - T_5)\,]^{\frac{1}{2}} \tag{3.37}$$

As before, the temperature drop can be put in terms of the ideal drop and an expansion efficiency, η_e, with

$$\eta_e = \frac{(T_4 - T_5)_{\text{act}}}{(T_4 - T_5)_{\text{isen}}} = \frac{(T_4 - T_5)_{\text{act}}}{T_4\left[\dfrac{(P_4/P_5)^\epsilon - 1}{(P_4/P_5)^\epsilon}\right]} \tag{3.38}$$

so that

$$V_5 = \left\{V_4^2 + 2g_0\, c_p J \eta_e\, T_4 \left[\frac{(P_4/P_5)^\epsilon - 1}{(P_4/P_5)^\epsilon}\right]\right\}^{\frac{1}{2}} \tag{3.39}$$

Normally, P_5 is the atmospheric pressure P_a. Utilizing the concept of stagnation or total temperature T_0 as the sum of static temperature T and dynamic temperature $V^2/2g_0c_pJ$, then Eq. (3.39) may be expressed as

$$V_5 = [2g_0\, c_p J\, (T_{0_4} - T_5)\,]^{\frac{1}{2}} \tag{3.40}$$

$(T_{0_4} - T_5)$ is the temperature drop from the stagnation pressure P_{0_4} at turbine discharge to the static pressure P_5 at nozzle discharge. With an expansion efficiency η_{es} defined in terms of the initial stagnation values of pressure and temperature, and final static pressure, i.e.

$$\eta_{es} = \frac{(T_{0_4} - T_5)_{\text{act}}}{(T_{0_4} - T_5)_{\text{isen}}} = \frac{(T_{0_4} - T_5)_{\text{act}}}{T_{0_4}\left[\dfrac{(P_{0_4}/P_5)^\epsilon - 1}{(P_{0_4}/P_5)^\epsilon}\right]} \tag{3.41}$$

then
$$V_5 = \left\{ 2g_0 c_p J \eta_{os} T_{0_4} \left[\frac{(P_{0_4}/P_5)^{\epsilon} - 1}{(P_{0_4}/P_5)^{\epsilon}} \right] \right\}^{\frac{1}{2}} \tag{3.42}$$

The calculation of actual performance with component efficiencies and flow losses then proceeds as follows. For a given pressure ratio, the work of compression is found, assuming a compressor efficiency η_c. Subtracting the combustion pressure loss from the compressor delivery pressure then gives the turbine inlet pressure. For a given T_{max}, the turbine work and compressor work are then equated to find the turbine outlet state 4, i.e.

$$c_p(T_{2'} - T_1) = c_p(T_3 - T_{4'})$$

$$c_p \frac{T_1}{\eta_c}(P_r^{\epsilon} - 1) = c_p T_3 \eta_t \left[\frac{(P_3/P_4)^{\epsilon} - 1}{(P_3/P_4)^{\epsilon}} \right]$$

Thus pressure P_4 and actual temperature $T_{4'}$ are known. To proceed with the calculation of V_5 requires a value of V_4 or the stagnation values T_{0_4}, and P_{0_4}. V_4 is generally high, possibly of the order of 1000 fps, and V_4^2 is an appreciable part of the expansion energy, but discussion of appropriate values is left for the future, after turbine performance has been analysed.

It is possible to circumvent this for the time being by using an overall expansion efficiency η_{0_e}, from turbine inlet tc propulsion nozzle discharge. This is adequate for cycle analysis, but it is necessary to use separate turbine and exhaust nozzle efficiencies in actual design. Using this method, the total expansion work is

$$c_p(T_3 - T_{5'}) = \eta_{0_e} c_p T_3 \left[\frac{(P_3/P_5)^{\epsilon} - 1}{(P_3/P_5)^{\epsilon}} \right]$$

Of this total, the turbine work is equal to the compressor work, so subtracting the latter yields the enthalpy available for useful work (gross thrust), i.e.,

$$\frac{V_5^2}{2g_0 J} = \eta_{0_e} c_p T_3 \left[\frac{(P_3/P_5)^{\epsilon} - 1}{(P_3/P_5)^{\epsilon}} \right] - c_p(T_{2'} - T_1) \tag{3.43}$$

from which the jet velocity V_5 can be calculated. For precise calculations, the variation of specific heat must be taken into account as for the shaft power cycle. This variation is greater for the turbo-jet cycle, because a higher turbine-inlet temperature is usually used to obtain high specific output, albeit at the expense of engine life.

The performance figures for turbo-jets are based on the useful output, the thrust, in terms of specific thrust, lb thrust/lb/sec of air and specific fuel consumption, lb fuel/hr/lb thrust. It is possible

to quote on a horse-power basis if the aircraft forward speed, U, is known, since $hp \propto FU$, but the value is correct only for that speed. It is sometimes useful to remember that a thrust of 1 lb when U is 375 mph is equivalent to one horse-power, since

$$hp = FU = \frac{1}{550}\left(375 \times \frac{5280}{3600}\right) = 1 \tag{3.44}$$

3.20 *Efficiency of a Jet Engine*

So far the term " efficiency " of a jet engine has not been used. For the preceding analysis, the unit was taken as stationary, thus producing a *static thrust* for a given amount of *energy* supplied (as fuel). When in forward motion, the gross specific thrust, V_j/g_0, is reduced by the inlet drag, V_i/g_0, to give the net thrust and thus the useful effect is dependent not only on the power plant itself but also on how the plant is being used, i.e. the aircraft speed, since $V_i = U$. The utilization of the gross thrust may be considered in terms of the *propulsion* (or Froude) efficiency. This is defined as the ratio of the useful propulsive energy to the available propulsive energy. The latter is equal to the sum of the former and the wasted propulsive energy, which is the residual kinetic energy of the gas discharged from the nozzle. Fig. 3.27 shows the velocity vectors, V_j the jet velocity, U the forward speed of the aircraft (equal to the inlet velocity) and V_e the residual or absolute exhaust velocity. The useful propulsive energy is $U(V_j - U)/g_0$ and the wasted energy is the kinetic energy of the exhaust gases, $V_e^2/2g_0$. Thus the propulsive efficiency, η_p, is

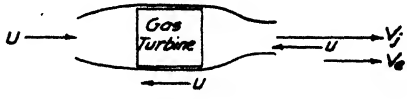

FIG. 3.27. Velocity diagram for turbojet.

$$\eta_p = \frac{\text{Useful energy}}{\text{Total energy}} = \frac{\text{Useful energy}}{\text{Useful energy + lost energy}}$$

$$= \frac{U(V_j - U)}{U(V_j - U) + V_e^2/2}$$

Substituting $V_e = V_j - U$, then

$$\eta_p = \frac{U(V_j - U)}{U(V_j - U) + (V_j - U)^2/2} = \frac{2U}{2U + (V_j - U)} = \frac{2U}{U + V_j} \tag{3.45}$$

From these relationships it is readily deduced that for a given jet velocity:

(1) The maximum thrust is produced when $U = 0$, i.e. the static condition, but the propulsive efficiency is zero.
(2) The maximum propulsive effort is produced when $U/V_j = \frac{1}{2}$, when the propulsive efficiency is 2/3.
(3) The maximum propulsive efficiency is produced when $U/V_j = 1$, but the thrust is zero.
(4) U/V_j cannot exceed unity or a negative thrust is produced.

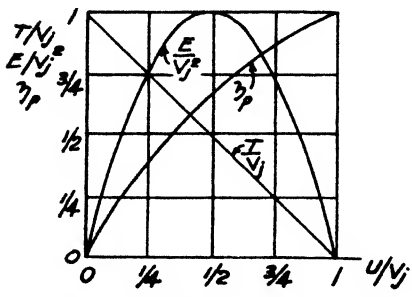

FIG. 3.28. Variation of thrust, propulsive energy and efficiency with U/V_j.

Fig. 3.28 shows the thrust, propulsive energy and efficiency in non-dimensional form as F/V_j, E/V_j^2 and η respectively plotted against U/V_j. This shows why the turbo-jet can be used satisfactorily only for the higher aircraft speeds, as V_j must be high in order to produce a reasonable thrust, and the propulsive efficiency is low unless U is high.

The propulsive efficiency is analogous to the transmission efficiency of a shaft-power unit, but its value changes considerably with the use of the vehicle. Thus it is not by itself an indication of the behaviour of the power plant, whose efficiency is expressed by the ratio of its useful effect to energy supplied. The useful effect of the power plant alone, that is not related to the vehicle, is simply the increase of kinetic energy of the air passing through it, i.e. $(V_j^2 - U^2)/2g_0$. The energy supplied is that of the fuel, h_f. Thus the intrinsic or internal power plant efficiency η_i is

$$\eta_i = \frac{V_j^2 - U^2}{2g_0 h_f} \tag{3.46}$$

The useful effect of the power plant and vehicle together is the resulting propulsive energy, $U(V_j - U)/g_0$, and the overall efficiency η_0 is

$$\eta_0 = \frac{U(V_j - U)}{g_0 h_f} \tag{3.47}$$

The propulsive efficiency expresses the efficiency of conversion of power plant energy to useful propulsive effort, i.e.

$$\eta_p = \frac{U(V_j - U)/g_0}{(V_j^2 - U^2)/2g_0} = \frac{2U(V_j - U)}{(V_j^2 - U^2)} = \frac{2U}{U + V_j} \tag{3.45}$$

which is, of course, the same result originally obtained by considering

the propulsion elements alone, without reference to the power plant. As a final result, then,

$$\eta_0 = \eta_p \eta_i$$

The efficiency of a turbo-jet is then always related to the aircraft speed and thus has meaning only for a specific condition. To assess performance thus requires considerable knowledge of the range of operating conditions and it is customary to use only the static condition for a single figure value to express the " quality " of performance. It is given as the specific fuel consumption, SFC, lb fuel/hr/lb thrust and not as an efficiency. The output likewise is quoted as the sea-level static condition in lb thrust/lb/sec of air. There is, however, some elaboration of these figures to the extent that an aircraft engine has more than one " rated output ". The maximum propulsive effort is needed at *take-off* (or for combat, in military aircraft), requiring the maximum turbine temperature and engine rpm. This is essentially an overload which the engine as a whole can sustain only for a very limited period. The normal engine operation is at the *cruising* condition, which power the engine can sustain indefinitely (subject to overhaul). The cruise conditions may not be very much lower in numerical values of temperature, rpm and output, but in terms of engine life there is a very great difference. A turbo-jet performance may then be given in terms of take-off and cruise, with maximum thrust for the former and minimum fuel consumption for the latter.

3.21 *Turbo-jet Performance*

As for a shaft-power engine, it is possible to deduce some qualitative answers to the effect on performance of variation of pressure ratio, maximum temperature and component efficiency. Initially, the ground-level static condition will be discussed.

It is useful in this analysis to consider the available energy Δh_{av} as equivalent to an amount of kinetic energy $V_{av}^2/2g_0$. This energy, for all gas turbine cycles, is the difference between the enthalpy drop in expansion and the enthalpy rise in compression, i.e. the net work. For the shaft-power cycle, this kinetic energy is used in the power turbine and the work of the turbine is directly proportional to it, i.e. $W_s \propto \Delta h_{av} \propto V_{av}^2$. For the turbo-jet cycle, the useful output is thrust, which is proportional to the velocity, so $F \propto V \propto \sqrt{\Delta h_{av}}$.

Considering first the specific thrust at a given pressure ratio, both increase of maximum temperature (or rather, the temperature ratio, T_m/T_1) and increase of component efficiency raise the thrust, because Δh_{av} is increased. The increase of thrust for a given per-

centage increment of either, however, is less than the corresponding gain for the shaft-power cycle, because it is proportional only to $\sqrt{\Delta h_{av}}$. For a given T_{max} and component efficiencies, the thrust at first increases with pressure ratio, passes through a maximum, and decreases, similarly to the power output for the shaft cycle and for the same reasons. The curve is not so peaked, however, again because the thrust is proportional to $\sqrt{\Delta h_{av}}$ and changes at a less rapid rate than W_s, which is proportional to Δh_{av}.

The specific fuel consumption improves with increase of component efficiency, other conditions fixed, but the effect of increased T_{max} is just the opposite to that of the power cycle, i.e. the SFC *decreases* with increase of T_{max}. It is difficult to prove this without an unwieldy analytical expression or using numerical examples. It can perhaps be appreciated by noting once again that the thrust is proportional only to $\sqrt{\Delta h_{av}}$ and although Δh_{av} increases with increase of T_{max}, it is insufficient to compensate for the increase of fuel required to obtain the higher T_{max}. This is true of the ideal cycle as well as the actual cycle with losses.

For other conditions fixed, increase of pressure ratio decreases the fuel consumption and this effect continues until a pressure ratio is reached which is considerably higher than that for maximum thrust, generally higher than the pressure ratios at present possible. This is due to the relatively flat thrust-pressure ratio relationship noted above. Initially, thrust increases with pressure ratio and the necessary fuel input decreases, because less temperature rise is required for a given T_{max}. After the maximum point is reached the thrust decreases, but less slowly than the decrease of fuel input, and so the SFC continues to decrease, albeit at a slower rate. Finally, a value of pressure ratio is reached at which the thrust falls off at a rate rapid enough to cause the SFC to increase.

Figs. 3.29 and 3.30 show thrust and SFC plotted against pressure ratio for the ground level stationary condition. The assumptions are as before, with the exception that all the losses with the exception of those in the compressor and turbine are grouped as $\Sigma\Delta p/p = 0{\cdot}12$. This may appear a high value, but a turbo-jet installation may entail a rather high intake loss and exhaust loss, together with a large combustor loss due to the necessity for the smallest possible size and weight. These figures, again to be taken as illustrative only, show the features of turbo-jet performance discussed above.

While the ground level stationary condition is often used as a basis for assessing turbo-jets, comparing one with another, their application as aircraft power plants introduces two very important

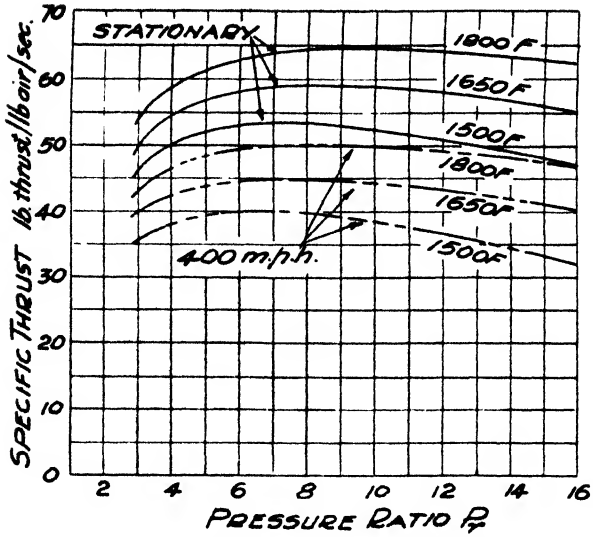

FIG. 3.29. Turbojet thrust—sea level, stationary and 400 m.p.h.

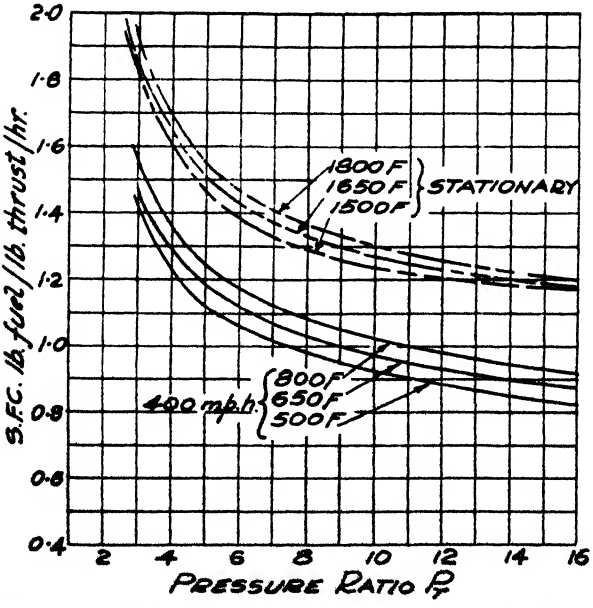

FIG. 3.30. Turbojet specific fuel consumption—sea level, stationary and 400 m.p.h.

variables. These are the effect of the aircraft speed (forward speed) and the effect of altitude. The latter, as variation of intake pressure and temperature, has been discussed for shaft-power plants, but the variation of pressure is much greater than for a land plant, while the temperature variation is inevitable and part of the design ambient conditions.

3.22 *Effect of Forward Speed*

Taking first the forward speed, this affects the compressor inlet pressure and temperature. The intake duct to the compressor acts as a diffuser, slowing down the air, which has a velocity relative to the compressor equal to the aircraft speed, and raising its pressure and temperature. Assuming the process is adiabatic, then the compressor inlet experiences the stagnation or total temperature T_{0_1} equal to the static (ambient) temperature T_a plus the dynamic temperature. Thus

$$T_1 = T_a + \frac{U^2}{2g_0 c_p J}$$

where U is the aircraft speed in fps (mph $\times$ 88/60). For $c_p = 0{\cdot}24$, the dynamic temperature reduces to $(U/110)^2$ for degrees F and $(U/147)^2$ for degrees C, which are useful expressions to remember for ready conversion. The centigrade expression is $(U/100)^2$ for U in mph.

If the intake diffusion effect is without loss, then the inlet pressure to the compressor would be the stagnation or total pressure, P_{0_1}, with

$$P_{0_1} = P_a + P_{\text{dyn}}$$

and from the isentropic relationship,

$$P_{0_1} = P_a \left(\frac{T_1}{T_a}\right)^{k/k-1}$$

This increase of temperature and pressure due to aircraft speed is called the *ram effect*, or simply *ram*. It becomes more and more important as the speed increases because of the U^2 term. Thus at 600 mph ground level, the increase of temperature due to ram is 64° F (36° C) and the stagnation pressure becomes 22·1 psia, an increase of 7·4 psi or about 50%.

In practice, although the ram effect is adiabatic within negligible limits, it is not reversible, i.e. there is a loss of pressure due to friction and separation so that the ideal stagnation pressure is not achieved. This may be expressed as a *ram efficiency* or intake efficiency. There are several different ways of defining this ram efficiency, η_r, some

based on pressures and some on temperature. One of the simplest, which will be used here for demonstration purposes, is to define it similarly to that for compressor efficiency, i.e.

$$\eta_v = \frac{\Delta T_{\text{isen}}}{\Delta T_{\text{act}}}$$

where ΔT_{act} is the dynamic temperature corresponding to the aircraft speed and ΔT_{isen} is the change of temperature corresponding to isentropic compression to the pressure actually achieved. This is demonstrated in Fig. 3.31, in which state (a) is that of the air at ambient conditions. If the air is stagnated relative to the compressor at aircraft speed U, then its temperature would be the stagnation value T_{0_1}. If the process were reversible it would have a pressure P_{0_1}, but it is actually irreversible. Being adiabatic, it still goes to temperature T_{0_1}, but suffers an increase of entropy so that it acquires only pressure P_1. The temperature corresponding to isentropic compression is $T_{1_{\text{isen}}}$. The ram efficiency is then defined as

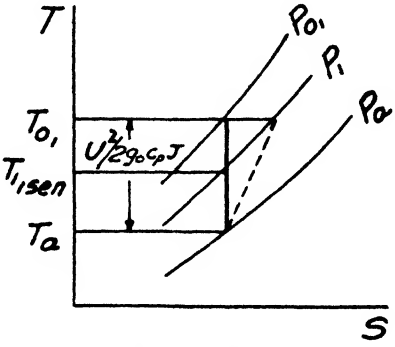

FIG. 3.31. Ram efficiency.

$$\eta_v = \frac{T_{1\,\text{isen}} - T_a}{T_{0_1} - T_a} = \frac{\Delta T_{\text{isen}}}{U^2/2g_0c_pJ} \tag{3.48}$$

Thus $\Delta T_{\text{isen}} = \eta_v U^2/2g_0c_pJ$, which is then used to calculate the inlet pressure P_1, with

$$P_1 = P_a\left(\frac{T_{1\,\text{isen}}}{T_a}\right)^{k/k-1} = P_a\left(\frac{T_a + \Delta T_{\text{isen}}}{T_a}\right)^{k/k-1}$$

$$= P_a\left[1 + \frac{\eta_v U^2}{2g_0c_pJT_a}\right]^{k/k-1} \tag{3.49}$$

Values of ram efficiency may vary widely according to the particular installation, but a value of 0·90 is reasonable and will be used here as typical. The ram pressure ratio is considerable at high forward speeds and both the efficiency and ambient temperature are important factors. For a given aircraft speed and ram efficiency, the ram pressure ratio increases as the ambient temperature decreases, i.e. at altitude.

The second effect of aircraft forward speed is in relation to the propulsion efficiency. As U increases, so does the inlet drag. If there were no ram effect, the net specific thrust would decrease, as the jet velocity would remain the same. With ram, the increase of inlet temperature reduces the gross thrust somewhat, but the increase of inlet pressure more than compensates for this, as the cycle pressure ratio is increased without shaft work being necessary. The overall effect of forward speed on inlet drag and ram is to reduce somewhat the net *specific* thrust, using normal values of cycle variables. Note that this discussion applies to *specific* thrust, thr/lb/sec of air. The *total* thrust will decrease at a lower rate or, at some conditions, may even increase, because the mass flow rate is higher. The specific fuel consumption increases with forward speed, because the reduction of temperature rise necessary between the increased compressor delivery temperature and a fixed turbine inlet temperature is not sufficient to outweigh the reduction in specific thrust.

3.23 *Effect of Altitude*

The effect of increased altitude on a turbo-jet is by virtue of the reduction of pressure and temperature. The temperature of the atmosphere varies considerably and continuously with location and time, so that a "standard" atmosphere is used for computing performance at various altitudes. There is more than one "standard" atmosphere according to season and latitude, "standard" in this case having the meaning of conventional rather than a true fixed value. The most general data used are those of the International Standard Atmosphere or ICAN atmosphere (International Commission on Navigation). It corresponds approximately to average values found in the middle latitudes and is formalized by using a linear decrease of temperature (or *lapse rate*) of 1·98° C (3·564° F) per 1000 ft of altitude, starting with a ground-level temperature of 15° C (59° F). With the temperature fixed, the pressure can be calculated according to the principles of hydrostatics, using 14·70 psia as the ground-level pressure. The standard lapse rate is taken only to the point where the temperature is reduced to — 56·5° C (— 69·7° F), corresponding to an altitude of about 36,000 ft, above which the atmosphere is considered to be isothermal, again in approximate conformity with the actual state of affairs. Above the "isothermal altitude", the pressure continues to decrease but according to an isothermal relationship. Some values of the International Standard Atmosphere are given in Table 3.3.

Table 3.3

Altitude (*ft*)	*Temperature*		*Pressure* (*psia*)
	(*F*)	(*C*)	
0	59	15·0	14·70
1000	55·4	13·0	14·17
5000	41·2	5·1	12·23
10,000	23·3	— 4·8	10·11
15,000	5·5	— 14·7	8·29
20,000	— 12·3	— 24·6	6·75
25,000	— 30·2	— 34·5	5·45
30,000	— 48·0	— 44·4	4·365
35,000	— 65·8	— 54·3	3·46
40,000	— 69·7	— 56·5	2·72
50,000	— 69·7	— 56·5	1·68
60,000	— 69·7	— 56·5	1·04
70,000	— 69·7	— 56·5	0·65

3.24 *Performance with Altitude and Speed*

The effect of the varying pressure with altitude on specific thrust and SFC is nil, because it is equivalent to altering the datum pressure only and the pressure ratios remain constant. It does, of course, alter the total thrust, which is directly proportional to mass flow and hence pressure, and thus has a profound effect on aircraft performance as a whole. It may affect the component performance indirectly by reducing the Reynolds number for the flow over the blading of compressors and turbines and this may be of great consequence, but the present discussion is limited to fixed values of component efficiencies.

The effect of a lowering of ambient temperature on cycle performance is (1) to increase the ram pressure for a given forward speed (Eq. 3.49), (2) to increase the compressor pressure ratio at a given engine rpm, since for a fixed ΔT of the compressor, $T_2/T_1 = (T_1 + \Delta T/T_1) = 1 + \Delta T/T_1$ increases as T_1 is reduced, and (3) to increase the necessary temperature rise $T_2 - T_1$. Effects (1) and (2) increase the thrust, as a greater expansion ratio is available, this increase being sufficient to counteract the additional fuel required by effect (3), so that the SFC is reduced. An important effect on component performance, as opposed to cycle performance, is to increase the Mach number at compressor inlet, as the acoustic velocity is proportional to $\sqrt{T}$. This can lead to a considerable reduction of compressor efficiency.

The effects of forward speed and altitude are shown in Figs. 3.29, 3.30, 3.32 and 3.33. Figs. 3.29 and 3.30 show a ground level

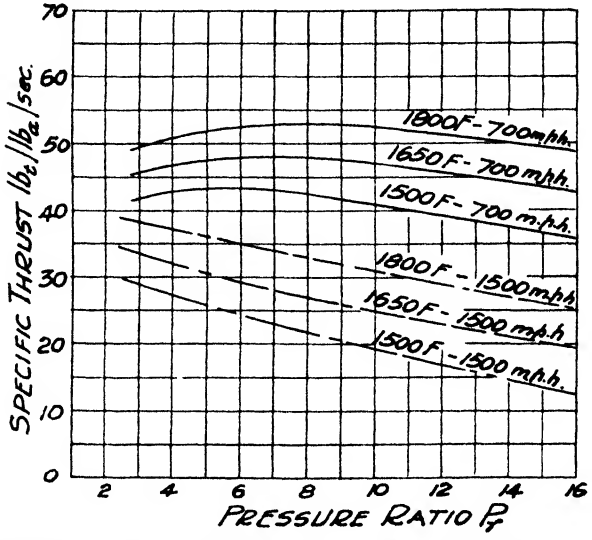

FIG. 3.32. Turbojet thrust—36,000 ft, 700 mph and 1500 mph.

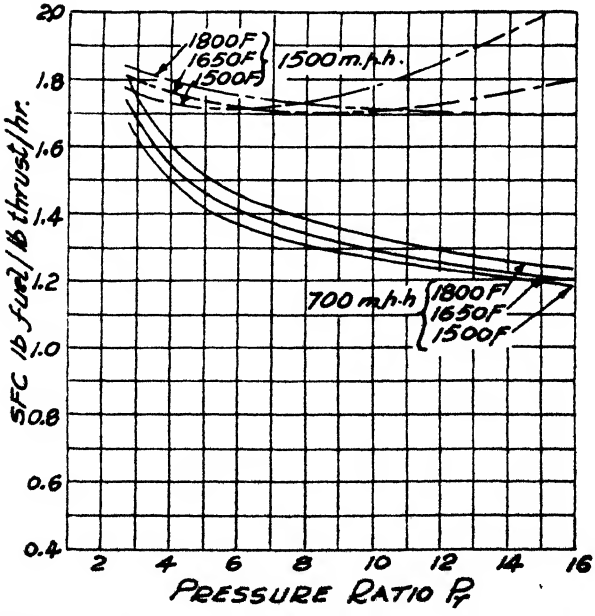

FIG. 3.33. Turbojet specific fuel consumption—36,000 ft, 700 mph—and 1500 mph.

condition at 400 mph, hence the effect only of aircraft speed. Figs. 3.32 and 3.33 show the performance at the isothermal altitude, 36,000 ft, for two speeds 700 mph and 1500 mph, corresponding to Mach numbers of 1·06 and 2·27 respectively.

3.25 *Modified Turbo-jet Cycles*

Additions to the basic cycle for shaft-power plants were those of intercooling, heat exchange and reheat, all of which were beneficial in various ways. Intercooling would improve turbo-jet thrust as it would reduce the compressor work, but a sufficient water supply is next to impossible for an aircraft. A short-term cooling effect is possible by injecting finely divided water (or water-alcohol mixtures to avoid freezing) into the compressor inlet, the evaporation of which tends to make the compression approach the isothermal process. Additionally it increases the mass flow rate. This procedure is sometimes adopted for take-off purposes, when maximum thrust is required for a matter of minutes. Heat exchange would improve the fuel consumption, but not to the same extent as for the shaft-power engine, because in the latter the heat is recovered after all the available work has been extracted. In the turbo-jet, on the other hand, the heat must be extracted intermediately in the expansion, between turbine and propelling nozzle. Thus some thrust is lost, because the final velocity is reduced. This loss of thrust is crucial, because one of the main advantages of the turbo-jet is its ability to produce a much greater propulsive effort for a given size of engine than the reciprocating engine or the propeller gas turbine. Thus, heat exchangers are not used in turbo-jets and do not appear likely to be used in the immediate future.

The third effect, reheat or afterburning, is adopted widely for military aircraft in the form of additional fuel added in the exhaust duct between turbine and nozzle. Because there are no moving parts, a much higher temperature is possible and a thrust increase of 30–40% is achieved. The efficiency is very poor, however, because the heating takes place at a very low pressure ratio, when even the ideal cycle has a low efficiency. A further disadvantage is that, in order to take full advantage of the reheat, a much larger exhaust pipe and propelling nozzle are needed, so that the latter has to be of varying area, thus necessitating increased weight for its own construction and that of its operating mechanism. In addition, the apparatus necessary for the combustion of the fuel causes a restriction, hence loss of pressure in the exhaust duct and more excess weight, which are present even when the reheat is not in operation. In spite of these drawbacks, most military turbo-jets are equipped

with reheat, because the additional thrust possible is invaluable at take-off, for interception, and for combat. No figures with reheat performance are given here, because the actual performance is extremely susceptible to the combustion efficiency achieved, the additional exhaust pressure loss and the degree of nozzle control, for which working data are extremely meagre because the application is purely military.

3.26 *Conclusions from Cycle Analysis*

The main conclusion from the preceding cycle analysis is the tremendous range and versatility of the gas turbine. In saying this, one has to remember that the gas turbine may have the highest power-weight ratio of any prime mover, because the efficiencies quoted are only moderate and in many instances very much lower than those of the steam turbine or reciprocating combustion engine. It is only in the more complex cycles, with at least intercooling and heat exchange, that the gas turbine can rival the fuel consumption of other types, when its power-weight ratio may be little different from its competitors. In its simple form, however, or even with a moderate heat exchanger, it is so much more compact than other types of similar output, that, in conjunction with its freedom from a water supply, it is very attractive for many applications. The extreme case of this is its use as a turbo-jet, where it has revolutionized the aircraft field.

The cycle analysis shows that performance is very sensitive to relatively small changes of the operating variables, and this is at the same time, a warning that disappointment is possible, if design skill is lacking or some condition impossible to fulfil, and a cause for believing that the gas turbine has by no means reached the limit of its performance.

APPENDIX

Cycle Calculation

The cycle is one having a pressure ratio of 5 and a maximum combustion temperature of 1500° F (815·5° C). The initial conditions (ambient air) are 14·17 psia and 80° F. The calculations have been carried out with a 10-in. slide rule and the results rounded off to a reasonable significant figure. Assumed component performance:

Compressor efficiency	$\eta_c = 0{\cdot}84$
Turbine efficiency	$\eta_t = 0{\cdot}87$
Combustion efficiency	$\eta_{cc} = 0{\cdot}98$
Mechanical efficiency	$\eta_m = 0{\cdot}98$
Regenerator effectiveness . . .	$\eta_r = 0{\cdot}75$

Pressure losses:

Combustor.	$\Delta p_c = 1{\cdot}5$ psi
H/E, air side	$\Delta p_a = 1{\cdot}0$ psi
H/E, gas side	$\Delta p_g = 0{\cdot}25$ psi
Stack exhaust	$\Delta p_e = 0{\cdot}10$ psi

Thermodynamic data:

Average specific heat, compression, $c_{p_a} = 0{\cdot}242$ Btu/lb F

Average specific heat, expansion, $c_{p_g} = 0{\cdot}275$ Btu/lb F

Average index, $(k-1)/k$, compression, $\epsilon_c = 0{\cdot}283$

Average index, $(k-1)/k$, expansion, $\epsilon_t = 0{\cdot}25$

The values of specific heat and ϵ are obtained by a trial-and-error process, making an initial guess and correcting for a second calculation. The values above are sufficiently correct for most purposes.

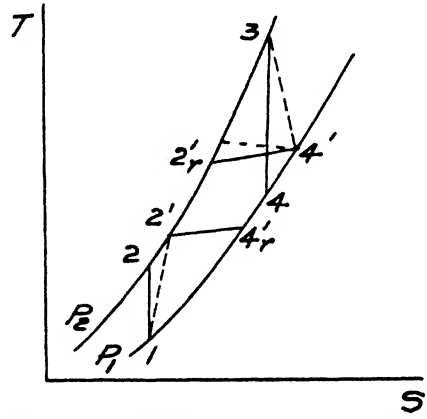

FIG. 3.34. Cycle diagram for illustrative calculation.

The state points are shown in Fig. 3.34

1. Compressor temperature rise.

From Eq. (3.9),

$$T_{2'} - T_1 = \frac{T_2 - T_1}{\eta_c} = \frac{T_1}{\eta_c}(P_r^{\epsilon_c} - 1)$$

$$= \frac{540}{0{\cdot}84}(5^{0{\cdot}283} - 1) = 371^\circ \text{F}$$

$\therefore$ Compressor delivery temperature,

$$T_{2'} = 371 + 80 = 451^\circ \text{F} = 911^\circ \text{R}$$

2. Compressor work.

From Eq. (3.10),

$$W_c = c_{p_a}(T_{2'} - T_1) = 0{\cdot}242\ (371) = 89{\cdot}8 \text{ Btu/lb}$$

3. Turbine temperature drop.

Turbine inlet pressure $= P_2 - \Delta p_a - \Delta p_{cc}$

$= 5\ (14{\cdot}17) - 1{\cdot}0 - 1{\cdot}5 = 68{\cdot}35$ psia

Turbine discharge pressure $= P_1 + \Delta_{p_e} + \Delta_{p_g}$

$= 14{\cdot}17 + 0{\cdot}1 + 0{\cdot}25 = 14{\cdot}52$ psia

$\therefore$ Turbine pressure ratio $= \dfrac{68{\cdot}35}{14{\cdot}52} = 4{\cdot}71$

From Eq. (3.11),

$$T_3 - T_{4'} = \eta_t(T_3 - T_4) = \eta_t T_3 \left(\frac{P_r^{e_t} - 1}{P_r^{e_t}}\right)$$

$$= 0{\cdot}87\ (1960)\left(\frac{4{\cdot}71^{0{\cdot}25} - 1}{4{\cdot}71^{0{\cdot}25}}\right) = 548^\circ \text{ F}$$

$\therefore$ Turbine discharge temperature,

$$T_{4'} = 1500 - 548 = 952^\circ \text{ F} = 1412^\circ \text{ R}$$

4. Turbine work.

From Eq. (3.13),

$$W_t = c_{p_g}(T_3 - T_{4'}) = 0{\cdot}275\ (548) = 150{\cdot}7 \text{ Btu/lb}$$

5. Net work.

$$W_n = \eta_m(W_t - W_c) = 0{\cdot}98\ (150{\cdot}7 - 89{\cdot}8) = 59{\cdot}68 \text{ Btu/lb}$$

$$= \frac{59{\cdot}68 \times 778}{550} = 84{\cdot}4 \text{ HP/lb/sec}$$

6. Combustion temperature rise.

With complete combustion,

$$\Delta t_{cc} = T_3 - T_{2'_r}$$

From Eq. (3.25),

$$T_{2'_r} = \eta_r(T_{4'} - T_{2'}) + T_{2'}$$

$$= 0{\cdot}75\ (1412 - 911) + 911 = 1286{\cdot}8^\circ \text{ R} = 826{\cdot}2^\circ \text{ F}$$

$\therefore \Delta_{t_{cc}} = 1960 - 1286{\cdot}8 = 673{\cdot}2^\circ$ F

For a combustion efficiency of 0·98, then $\Delta t_{cc} = 687^\circ$ F

From Fig. 3.9, the fuel-air ratio required for a combustion temperature rise of 687° F from an initial temperature of 1286·8° R is 0·0104 (air-fuel ratio = 96/1).

7. Specific fuel consumption.

From Eq. (3.32),

$$\text{SFC} = \frac{3600 \times 0{\cdot}0104}{84{\cdot}4} = 0{\cdot}443 \text{ lb/hp hr}$$

8. Efficiency.

From Eq. (3.33),

$$\eta = \frac{550 \times 84{\cdot}4}{778 \times 0{\cdot}0104 \times 18{,}500} = 0{\cdot}309$$

REFERENCES

1. Hawthorne, W. R., and Davis, G. de V. Calculating Gas-Turbine Performance. *Engineering*, **181**, No. 4706, 1956.
2. Keenan, J. H., and Kaye, J. *Gas Tables*. John Wiley and Sons, Inc., N.Y., 1948.
3. Craigoe, J. Miscellaneous Publication No. 97, *U.S. Bureau of Standards*, 1929.
4. Hodge, J. *Cycle and Performance Estimation*. Butterworths Scientific Publications, London, 1955.
5. Symposium on Heating Values of Fuels. *Trans. A.S.M.E.*, **70**, 1948, pp. 811, 819, 821, 823.
6. Mordell, D. L. The Exhaust-Heated Gas-Turbine Cycle. *Trans. A.S.M.E.*, **72**, 1950, p. 323.
7. Chambadal, P. The Possibilities of Combined Gas and Steam Turbine Installations. *Eng. Dig.*, **11**, 1950, p. 395.
8. Stys, Z. S. Gas Turbines for the Chemical Industry. *A.S.M.E.* Paper No. 57-GTP-9, 1957.

For a detailed analysis of gas turbine cycles, see Reference 4.

CHAPTER 4

COMPRESSORS AND TURBINES—ENERGY TRANSFER AND FLUID FLOW CHARACTERISTICS

THE rotating components, compressor and turbine, have many features in common and it is instructive as well as economical to consider their basic performance together. They are both concerned with *energy transfer*, from the rotor to the fluid for the compressor, to the rotor from the fluid for the turbine. The effectiveness of this transfer of energy is governed by the *fluid dynamics* of the system.

4.1 *Energy Transfer in Compressors and Turbines*

Consider the passage of a fluid through a rotor of any shape, as shown in Fig. 4.1. The rotor has an axis A-A and is turning at a

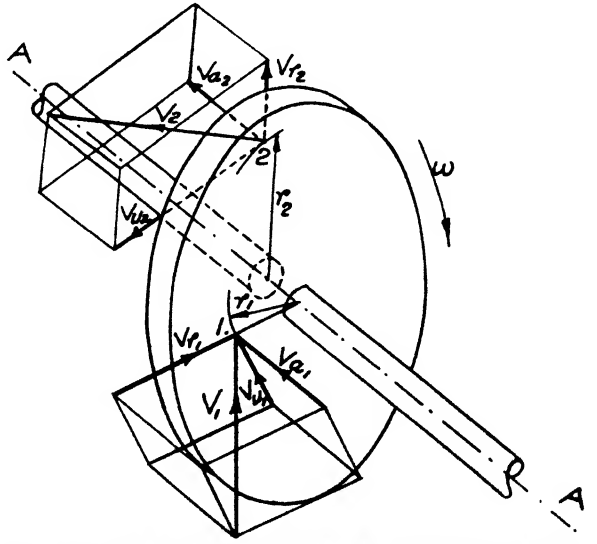

FIG. 4.1. Flow through a generalized turbomachine rotor.

steady rate of ω radians per second. At the entry station 1, the fluid has a velocity V_1 and is considered to enter at radius r_1. The velocity vector may be oriented quite generally with respect to the rotor, but it may be resolved into three mutually perpendicular components. It is convenient to make these three components (1)

axial, that is, in a direction parallel to the axis A-A, (2) *radial*, that is, in a direction normal to A-A and passing through it, and (3) *tangential*, that is, in a plane normal to A-A and in a direction normal to a radius. These components are labelled V_{a_1}, V_{m_1} and V_{u_1} in the diagram. Similarly at exit from the rotor, the velocity V_2 has axial, radial and tangential components V_{a_2}, V_{m_2} and V_{u_2}. Considering the interaction of fluid and rotor, reflection will show that the axial and radial components contribute nothing to the rotation, only thrust and radial forces, and that the tangential components V_u are wholly responsible for any rotational effect. Taking unit mass of fluid entering and leaving in unit time, the rate of change of *angular momentum* of the fluid is $(V_{u_1}r_1 - V_{u_2}r_2)$ and by Newton's Law, this is equal to the *torque* of the rotor. Thus

$$\tau = \frac{V_{u_1}r_1 - V_{u_2}r_2}{g_0} \tag{4.1}$$

where g_0 is the dimensional constant relating pounds force to pounds mass, 32·174 $(\text{lb}_m/\text{lb}_f)/(\text{ft}/\text{sec}^2)$.*

The product of torque, lb_f ft, by the rate of rotation, rads/sec, gives the *rate of energy transfer*, E, ft lb_f/sec, for unit mass flow rate, thus

$$E = \omega\tau = \frac{\omega}{g_0}(V_{u_1}r_1 - V_{u_2}r_2)$$

The product ωr is the linear rotor speed u, so that

$$E = \frac{1}{g_0}(U_1V_{u_1} - U_2V_{u_2}) \tag{4.2}$$

Eq. 4.2 is called the *Euler "turbine" equation* and is the basic relationship for both compressors and turbines. If the first term in brackets is larger than the second, then the energy transfer is positive from fluid to rotor, and the rotor is called a turbine. If $U_2V_{u_2} > U_1V_{u_1}$, then E is negative and the rotor is called a compressor. Recognizing that $U_2V_{u_2} > U_1V_{u_1}$ for a compressor, the relationship is usually inverted so that it is not necessary to work with a negative quantity all the time.

The simple turbine equation is subject to some restrictions. The flow must be steady, i.e. angular velocity, flow rate, fluid properties and heat transfer rate, if any, must be constant with time. The

* g_0 as a dimensional constant is the method preferred by the author to handle the vexed question of units brought about by the use of the pound for both force and mass in the basic relationship $f \propto ma$. Some may prefer to dispense with any distinction between pounds force and pounds mass by the use of g as an acceleration, ft/sec², while others may prefer to eliminate completely a numerical factor by using the slug for mass and pound for force, or pound for mass and poundal for force.

relationship applies strictly to every infinitesimal streamline, i.e. if the velocity is not uniform over the inlet and exit areas, then an integration over each area is required. There must be no discontinuity of pressure, giving a force component in the tangential direction, as there might be, for example, with a choked nozzle at the rotor discharge.

These conditions are readily met in the great majority of applications and Eq. (4.2) has great utility. If the inlet and outlet fluid velocities in the vector sense (both magnitude and direction) are known, together with the linear rotor speed at inlet and outlet, then it is immaterial what happens *inside* the rotor and the energy transfer may take place in any physical fashion whatsoever. Note that the tangential velocities V_u are the fluid velocities, not necessarily the same as the nominal physical rotor or blade angles.

Although the Euler equation in the form of Eq. (4.2) is basic, it is useful to transform it into a relationship which throws more light on the physical way the fluid energy is changed. Fig. 4.2 shows a velocity diagram at exit from a rotor, in a plane containing both V_2 and U_2. By vector principles, the combination of V_2 and U_2 gives the relative velocity V_{r_2}, that is, the fluid velocity relative to the rotor. The absolute velocity V_2 may be resolved into two components, V_{u_2}, the tangential component and V_{m_2}, the meridional component. V_{m_2} is perpendicular to the tangential direction and, for the time being, may be considered to be a constructional component, not necessarily having any particular significance.

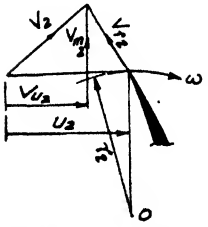

FIG. 4.2. Exit velocity diagram for generalized rotor.

From the geometry,

$$V_{m_2}^2 = V_2^2 - V_{u_2}^2$$

and also,

$$V_{m_2}^2 = V_{r_2}^2 - (U_2 - V_{u_2})^2$$

Equating these values of $V_{m_2}^2$ and expanding,

$$V_2^2 - V_{u_2}^2 = V_{1_2}^2 - U_2^2 + 2U_2V_{u_2} - V_{u_2}^2$$

Hence

$$U_2V_{u_2} = \tfrac{1}{2}(V_2^2 + U_2^2 - V_{r_2}^2)$$

A similar generalized expression may be obtained for the inlet, thus

$$U_1V_{u_1} = \tfrac{1}{2}(V_1^2 + U_1^2 - V_{r_1}^2)$$

Now the energy transfer relationship is

$$E = \frac{1}{g_0}(U_1V_{u_1} - U_2V_{u_2})$$

hence, also

$$E = \frac{1}{2g_0}\left[(V_1^2 - V_2^2) + (U_1^2 - U_2^2) + (V_{r2}^2 - V_{r1}^2) \right] \qquad (4.3)$$

Thus the energy transfer may be given by the sum of the differences of the squares of *absolute* fluid velocities V, *rotor* velocities U, and *relative* fluid velocities V_r at inlet and outlet of the rotor. (Note the inversion of the subscripts 1 and 2 in the V_r^2 term, in order to give the relationship as the sum of three quantities.) Squares of velocities represent energies and an analysis of the three terms shows the physical nature of the energy transfer.

The first term, $(V_1^2 - V_2^2)/2g_0$, is the energy transfer due to change of absolute kinetic energy of the fluid, a familiar concept. The second term, $(U_1^2 - U_2^2)/2g_0$, represents the change of energy due to the centrifugal effect. It will be recalled from fluid mechanics that a rotating fluid in equilibrium has a pressure gradient to balance the centrifugal force, with a pressure at any radius proportional to the product of the square of the radius and the angular velocity, $\omega^2 r^2$, i.e. U^2. The second term then represents the energy transfer due to transferring the fluid across this pressure gradient due to centrifugal effect. The third term, $(V_{r_2}^2 - V_{r_1}^2)/2g_0$, is the energy transfer due to change of the relative kinetic energy of the fluid. Relative to the rotor, i.e. to an observer having the same velocity as the rotor, the fluid changes its velocity from inlet to outlet. By the simple Bernoulli equation without any terms for change of potential energy due to position (which is negligible for a gas), then this change of velocity gives rise to a change of static pressure. The third term then expresses the energy transfer due to a change of pressure consequent on change of relative velocity in the rotor.

The first term represents energy transfer due to change of *kinetic* energy and the last two terms represent energy change involving change of *static* pressure, thus demonstrating that such energy transfer is dependent on a change of *stagnation* or *total* pressure, of which the dynamic component may be important. It is possible that only one of the three individual types of energy transfer is present and, in particular, the second form of the Euler equation shows that a *radial* path for the fluid can be effective, that is, that a substantial effect may be produced by allowing the fluid to enter and leave the rotor at different radii. It is also possible for one of the three components to be acting in the opposite direction to the other two, providing that the net effect is in the required direction. The result of all this is to show that a turbomachine may give a

desired effect in many different ways, so that design is not circumscribed only to attainment of a given fluid or mechanical power output, but because of this flexibility of method, may be directed to an optimum goal, such as simple construction, lowest size or weight, convenient arrangement with respect to other components of the system and so forth.

Apart from the obvious classification into compressors and turbines, dependent on the direction of energy transfer, the different methods of affecting this transfer give rise to two other broad fields of classification. The first is into *axial-flow* and *radial-flow* types. A large number of turbomachines have no significant change of radius between fluid entry and outlet, that is $U_1 \approx U_2$, and thus are called *axial-flow* machines. On the other hand, the *radial-flow* type is dependent to a substantial extent on energy transfer due to change of radius. These are often called *centrifugal* machines for compressors and *centripetal* machines for turbines. This is because if energy transfer due to a difference of U_1 and U_2 is used, then for a compressor, U_2 should logically be greater than U_1, that is the fluid should flow radially *outward*. The reverse holds true for a turbine. Outward-flow compressors and inward-flow turbines are the common forms of radial machines, but the requirement is not absolute, as it is the sum of the energy components as given in Eq. (4.3) which determines the overall effect. Although the majority of compressors and turbines in present use may be classified as axial- or radial-flow, it is possible to have *mixed-flow* types in which neither effect clearly preponderates. Here, following the general custom, the term radial-flow will include all machines which have any significant radial velocity component, leaving the term axial flow to those types in which any difference of U_1 and U_2 is negligible.

The second major classification is based on the relative proportions of the energy transfer consequent on change of kinetic energy and on change of static pressure. It is called *degree of reaction* or simply, *reaction*, and is defined as the ratio of energy transfer by virtue of change of static pressure to the total energy transfer. Denoting reaction by R, then for a turbine

$$R = \frac{\frac{1}{2g_0}\left[(U_1^2 - U_2^2) + (V_{r_2}^2 - V_{r_1}^2) \right]}{E} \tag{4.4}$$

where E may be expressed by either form of the Euler equation. The degree of reaction is usually between 0 and 1 but may be negative or greater than unity.

A zero value of reaction has special significance and a machine

with $R = 0$ is called an *impulse* machine. Impulse implies no change of static pressure in the rotor, so that in a turbine, for example, the energy transfer is wholly effected by a jet of fluid striking the blade. A simple example of pure impulse action is of a paddle-wheel, Fig. 4.3.(a). A reaction of unity implies that all energy transfer occurs by virtue of change of static pressure in the rotor. A simple example is that of Hero's steam turbine or, in a more familiar form, the ordinary lawn sprinkler, Fig. 4.3 (b). These examples are both

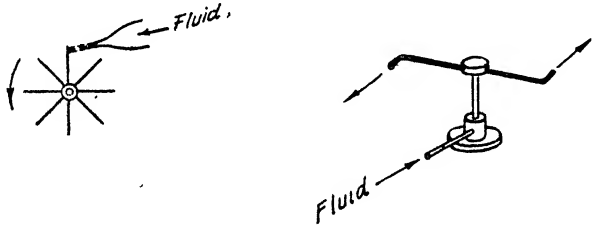

(*a*) (*b*)

FIG. 4.3. Impulse and reaction.
(*a*) Impulse principle—paddle wheel.
(*b*) Reaction principle—lawn sprinkler.

for turbines, because the processes are readily envisaged, but the principle applies for compressors. Here, impulse would mean that the energy transferred from the rotor to the fluid occasions no rise of static pressure in the rotor and that it is all given to an increase of absolute velocity of the fluid. A reaction of unity for a compressor means that the fluid enters and leaves with the same absolute velocity. It should be noted that for a radial-flow machine, the change of static pressure in the rotor is caused by two effects, the centrifugal action and the change of relative velocity. These may act in opposite directions to give a net value in either direction. To know the degree of reaction of a machine is then to have a considerable insight into its design and thus reaction is a useful major classification.

4.2 *Thermodynamics of Fluid Flow*

For cycle analysis, the work output or energy transfer was determined by purely thermodynamic considerations, using change of enthalpy in terms of pressure and temperature. The Euler turbine equation determines the energy transfer by the application of the principles of mechanics, in terms of rotor and fluid velocities. For a given rate of energy transfer, there must be an equivalence between the two sets of parameters and, taking into account the fact that the fluid is in motion, the exact quantitative link is provided by the steady flow energy equation.

Considering the generalized rotor used to obtain the Euler equation, an energy balance between the inlet and outlet stations for the steady flow of fluid is obtained by considering the energy quantities associated with the fluid flowing in and out, together with the quantities of heat and work crossing the boundaries of the system. Considering the steady flow of unit mass of fluid, its energy may be expressed by the internal energy u, the flow work Pv, the kinetic energy $V^2/2g_0$ and the potential energy due to position gz/g_0. Change of this total energy is associated with mechanical or shaft work, W_s, and heat, Q, being transferred in or out of the rotor. Using the usual convention that work is positive if being transferred from the rotor (as for the Euler equation) and that heat is positive if being transferred into the rotor, then the energy balance gives

$$u_1 + P_1v_1 + \frac{V_1^2}{2g_0} + \frac{g}{g_0}z_1 + Q = u_2 + P_2v_2 + \frac{V_2^2}{2g_0} + \frac{g}{g_0}z_2 + W_s \tag{4.5}$$

with u in ft lb_f/lb_m, P in lb_f/ft^2, v in ft^3/lb_m, V in ft/sec, z in ft and Q and W_s in ft lb_f/lb_m. The relationship between mechanical and thermal units, J, ft lb_f/Btu, will be introduced only when an exact numerical relationship is required. This relationship, Eq. (4.5), is valid for any fluid and, for a perfect gas, it may be considerably simplified.

In the first place, any change of potential energy gz/g_0 is usually negligible for a gas and the term can be omitted. In the second place, the sum of u and Pv is the enthalpy h, which for a perfect gas may be expressed by c_pT. Hence eq. (4.5) reduces to

$$c_{p_1}T_1 + \frac{V_1^2}{2g_0} + Q = c_{p_2}T_2 + \frac{V_2^2}{2g_0} + W_s \tag{4.6}$$

or

$$W_s = \left(c_{p_1}T_1 + \frac{V_1^2}{2g_0}\right) - \left(c_{p_2}T_2 + \frac{V_2^2}{2g_0}\right) + Q \tag{4.7}$$

For an adiabatic compression or expansion, Q is zero and will be taken as such from here on, as, in the cycle analysis, it was shown that cooling or heating during these processes was impractical and rarely attempted. Thus

$$W_s = (c_{p_1}T_1 - c_{p_2}T_2) + \left(\frac{V_1^2}{2g_0} - \frac{V_2^2}{2g_0}\right) \tag{4.8}$$

For unit flow *rate*, one lb_m/sec, then W_s is the rate of energy transfer and is given by the sum of the change of enthalpy of the gas and the change of kinetic energy and this must be the same as the rate of transfer E, obtained by the dynamic analysis, i.e. $W_s = E$. This is

the basic relationship which equates the thermodynamic expression of the problem to that of the dynamics of the energy transfer by means of a turbomachine.

It may be noted that in the cycle analysis as a thermodynamic statement, work was given by change of enthalpy only, whereas kinetic energy terms appear in Eq. (4.8). For a process in the thermodynamic sense, the fluid is simply a " working substance " which undergoes a change of state at rest. A process involving change of enthalpy or work gives a quantity of energy which is absolute and may be expressed in terms of temperature. The steady flow analysis breaks down this quantity of energy into various forms, in particular isolating that which may be expressed as kinetic energy. Thus from the thermodynamic viewpoint, a certain quantity of mechanical work transferred in an adiabatic process involves a change of enthalpy, $c_p \Delta T$. From the steady flow energy point of view, this same amount of work involves a change of enthalpy $c_p \Delta T'$ and a change of kinetic energy $\Delta V^2/2g_0$, i.e. ΔT and $\Delta T'$ are different, although the total quantity of energy involved is the same. Thus the temperature of a gas may vary with the velocity of the gas and it is necessary to be precise in distinguishing under what conditions the temperature is given. This can be made clearer by considering simply the flow of a gas in an insulated duct of varying area with no mechanical work being transferred. The steady flow energy equation then reduces to

$$c_{p_1} T_1 + \frac{V_1^2}{2g_0} = c_{p_2} T_2 + \frac{V_2^2}{2g_0} \tag{4.9}$$

i.e. the sum of enthalpy and kinetic energy is constant under such conditions and is called the *stagnation* or *total* enthalpy, h_0. (The subscript $_0$ will be used henceforward to denote stagnation or total states.) Regarding the specific heat as constant, Eq. (4.9) may be written as

$$T_1 + \frac{V_1^2}{2g_0 c_p} = T_2 + \frac{V_2^2}{2g_0 c_p} = T_0 \tag{4.10}$$

i.e. in adiabatic flow without work, the *stagnation* or *total* temperature T_0 is constant. The term stagnation is used because it expresses the value of a property when the fluid is brought to rest. From Eq. (4.9) the stagnation temperature T_0 is the sum of the *static* temperature T and the *dynamic* temperature, so that, in consistent units,

$$T_0 = T + \frac{V^2}{2g_0 c_p J} \tag{4.11}$$

The use of the dynamic temperature is such a convenient way of expressing kinetic energy in gas turbine analysis that it is often given the special symbol θ_v, the "temperature equivalent of velocity", and will be so used here.

The thermodynamic analysis is then equivalent to using the temperature of the fluid at rest or stagnation temperature, which is also expressed by Eq. (4.8) so that

$$W_s = c_p(T_{0_1} - T_{0_2}) \tag{4.12}$$

For a value of c_p of 0·24 Btu/lb F or Chu/lb C, and with $J = 778$ ft lb/Btu or 1400 ft lb/Chu, then with V in fps,

$$\theta_v \approx \left(\frac{V}{110}\right)^2 \text{ in degrees F} \tag{4.13}$$

$$\approx \left(\frac{V}{147}\right)^2 \text{ in degrees C} \tag{4.14}$$

The dynamic temperature can then represent a very appreciable amount of energy, as velocities in compressors and turbines are of the order of several hundreds of feet per second. The value of θ_v for a given velocity varies with c_p and so the above expressions are valid only for air at about atmospheric temperature and θ_v for high temperatures and for combustion gases must be evaluated with the correct value of c_p. However, when dealing with a gas undergoing a compression or expansion process, it is often sufficiently accurate to take an average value for the corresponding temperature change, expressing the work as $\bar{c}_p \Delta T_0$, with $T_0 = T + \theta_v$ and $\theta_v = V^2/2gJc_p$.

It is important to recognize that in compression or expansion, the work is represented by the change of *stagnation* enthalpy, because it has been seen by means of the second form of the Euler equation that the energy transfer is composed of a change of kinetic and a change of static pressure and the former may be considerable. Thus in the rotor itself, the change of static pressure represents a change of static temperature and the change of kinetic energy represents a change of dynamic temperature, the sum representing a change of stagnation temperature.

As the velocity of a fluid changes, so does the pressure. If the fluid is brought to rest, its temperature (i.e. static temperature) becomes the stagnation temperature, the process having to be adiabatic but not necessarily reversible. This is because the relationship is derived from the energy equation with $Q = 0 = W_s$, so that any effects of friction, turbulence, etc., remain in the system and appear as temperature. The process of the increase in pressure with reduction of velocity is a different matter, however, because the

effect of any irreversibility will result in a smaller increase of pressure being attained than for the ideal process. Because the degree of irreversibility can be of any value, the *stagnation* or *total pressure* of a fluid is defined as the pressure attained when brought to rest adiabatically and *reversibly*. Thus stagnation pressure, P_0, is a concept, since normally a flow process involves some degree of irreversibility. P_0 can be calculated from the isentropic pressure-temperature relationship, i.e.

$$\frac{P_0}{P} = \left(\frac{T_0}{T}\right)^{k/k-1} \tag{4.15}$$

Stagnation temperature and pressure can be represented on a temperature-entropy diagram. Thus in Fig. 4.4 (a), the state of a gas having a velocity V, pressure P and temperature T is located

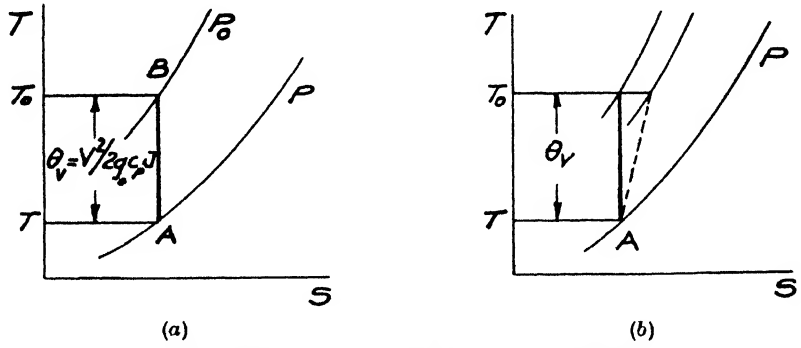

FIG. 4.4. Stagnation temperature and pressure.

at A. The state at rest, the stagnation state, is at B, with $\theta_v = V^2/2g_0c_pJ$, $T_0 = T + \theta_v$ and $P_0 = P(T_0/T)^{k/k-1}$. The process of stagnation AB is taken as isentropic, hence P_0 can be located. If it were adiabatic but not reversible, Fig. 4.4 (b), the stagnation temperature would remain the same, but with the increase of entropy due to irreversibility, the final pressure would be less than the ideal value P_0. Thus the stagnation pressure is a calculated value. It may also be seen from this analysis that, although the stagnation temperature will remain constant in adiabatic flow with no shaft work, the stagnation pressure will decrease, because of the irreversibility due to friction, which is ever-present, however small.

In some instances, particularly in the analysis of axial-flow compressors, the flow may be considered incompressible, i.e. constant density, and an alternative form for P_0 is found useful. Taking

Eq. (4.15), it may be written as

$$\frac{P_0}{P} = \left(\frac{T + \theta_v}{T}\right)^{k/k-1} = \left(1 + \frac{\theta_v}{T}\right)^{k/k-1}$$

For low values of V, i.e. θ_v small compared with T, this may be expanded by the series

$$(1 + x)^n = 1 + nx + \frac{n}{2}(n - 1)\, x^2 + \ldots .$$

Dropping terms of higher order than the first, then

$$\frac{P_0}{P} = 1 + \frac{k}{k-1}\frac{\theta_v}{T} = 1 + \frac{k}{k-1}\frac{V^2}{2g_0 c_p J T}$$

Now

$$\frac{k}{k-1} = \frac{c_p/c_v}{c_p/c_v - 1} = \frac{c_p}{c_p - c_v} = \frac{c_p}{R/J}$$

hence

$$\frac{P_0}{P} = 1 + \frac{V^2}{2g_0 RT} = 1 + \frac{\rho V^2}{2g_0 P}$$

and

$$P_0 = P + \frac{\rho V^2}{2g_0}$$

Thus stagnation pressure = static pressure + dynamic pressure, with dynamic pressure = $\rho V^2/2g_0$ for incompressible flow. This may be recognized as a form of the Bernoulli equation for incompressible flow of a gas ($\Delta z = 0$). $\rho V^2/2g_0$, often given the symbol q in aerodynamic work, is a very useful parameter. Often, loss in a particular process is given in terms of a multiple of " dynamic heads ", but it must be remembered that $\rho V^2/2g_0$ is the dynamic " head " or pressure only for *incompressible* flow. It is often used for gases where the change of density is inconsiderable for a given pressure change, and an average value of ρ is used for the process.

To sum up, we have three forms in which to express the energy transfer E, thus,

$$E = \frac{1}{g_0}(U_1 V_{u_1} - U_2 V_{u_2}) \qquad (4.2)$$

$$= \frac{1}{2g_0}\left[(V_1^2 - V_2^2) + (U_1^2 - U_2^2) + (V_{r_2}^2 - V_{r_1}^2)\right] \qquad (4.3)$$

$$= c_p(T_{0_1} - T_{0_2}) \qquad (4.12)$$

These provide the connecting link between the thermodynamic expression of the problem and the necessary turbomachine problem. The required pressure ratio in conjunction with the initial tempera-

ture gives the enthalpy change required, Eq. (4.12). This enthalpy change must then be effected by the rotor in accordance with Eq. (4.2) or (4.3).

4.3 *Compressor and Turbine Efficiencies*

In cycle analysis, turbomachine (compressor and turbine) efficiency was defined and used in terms of an isentropic efficiency based on enthalpy, or, as was pointed out, more usually on temperature. In view of the previous discussion on static and total values of pressure and temperature, it is necessary in dealing with the detailed design of components to specify exactly in what terms efficiencies are given. In what follows, it is still only the aerothermodynamic or internal efficiency, which is under discussion, that is, the machine efficiency including mechanical losses due to bearings, glands, etc., is not included. The latter are taken care of by applying a mechanical efficiency to a complete unit or component as required. Likewise, it is also assumed that only adiabatic processes are under consideration, as a different ideal standard is required in the normally rare cases of non-adiabatic turbomachine processes in gas turbine work. Compressor and turbine efficiencies are dealt with separately, as somewhat different methods can be used.

4.4 *Compressor Efficiency*

The isentropic temperature efficiency of compression, η_c, has been defined as

$$\eta_c = \frac{T_1(P_r^{\epsilon} - 1)}{T_{2'} - T_1} \tag{3.9}$$

with $T_{2'}$ the actual discharge temperature. Now T_1, $T_{2'}$ and the pressure ratio may all be based on either static or total values. The air at discharge from a compressor may have, for example, a static temperature of 370° F (187·7° C), a static pressure of 60 psia and a velocity of 440 fps. The corresponding stagnation values are 386° F (196·6° C) and 64·23 psia. Assuming for the present purpose that the inlet conditions are 60° F (15° C) and 14·7 psia, then the pressure ratios are 60/14·7 = 4·08 based on static discharge pressure and 64·23/14·7 = 4·37 based on stagnation discharge pressure. There is thus a 7% difference in pressure ratio. Using the same figures, the efficiency based on static values of pressure and temperature is 0·83. Based on stagnation pressure ratio and stagnation discharge temperature $T_{0_{2'}}$, then the efficiency is 0·837. Cycle analysis has shown the importance of small differences in component efficiency and therefore it is important to recognize clearly whether a given

efficiency value is based on static or total values. Either may be used, but generally the total pressure ratio and efficiency values are given, as they are higher numerically, and it is the change of stagnation enthalpy which represents the work of compression. If not stated, then the figures should be considered as total values, since this results in more conservative overall assessment.

For complete information, the velocity corresponding to the pressure and efficiency figures should be known. Diffusion of velocity into static pressure is difficult to accomplish without excessive space or high losses, and a compressor in which the air is delivered at a very high velocity, albeit with a high efficiency, may not be as effective as a component of the whole gas turbine plant as one with a lower efficiency and lower outlet velocity. The compressor, as a component, should include sufficient diffusion after the rotor so that the following component is not unduly penalized by having to accept the air at a high velocity.

In the preceding discussion, an inlet temperature and pressure were assumed and used for both static and total calculations. Total values are always used at entry, these normally being atmospheric values. This is because static values can be quite misleading, particularly for pressure ratio. For example, using the previous values for discharge with the compressor drawing from the atmosphere, the velocity right at compressor entry might be say, 550 fps. Assuming no losses between atmosphere and inlet, the inlet static temperature would be reduced by θ_{v_1}, $= (550/110)^2 = 25°$ F (13·9° C) and the pressure would be reduced to $14{\cdot}7/(520/495)^{k/k-1} = 12{\cdot}37$ psia. The static pressure ratio then becomes $60/12{\cdot}37 = 4{\cdot}85$. A different pressure ratio is obtained for each inlet velocity, which is a matter of individual design, not having any meaning as a cycle value. In the event that the intake ducting has a measurable loss, or if the compressor is receiving the air from a preceding component, then the actual stagnation pressure must be known or estimated.

4.5 *Turbine Efficiency*

Turbine efficiency is somewhat more complex than compressor efficiency owing to differences in evaluating both the useful output and the available energy. The actual shaft work produced has been seen to be $c_p(T_{0_3} - T_{0_{4'}})$, where state 3 is at turbine inlet and $_{4'}$ is the actual discharge state for a turbine with losses (see Fig. 4.5). Following steam turbine practice, the available energy is that for isentropic expansion from stagnation pressure at inlet to *static* pressure at discharge. For steam turbines, with their usually very

large pressure ratios, the kinetic energy at inlet is negligible compared with that available from expansion, hence a stagnation value at inlet is practically equivalent to the static value. Again, with steam

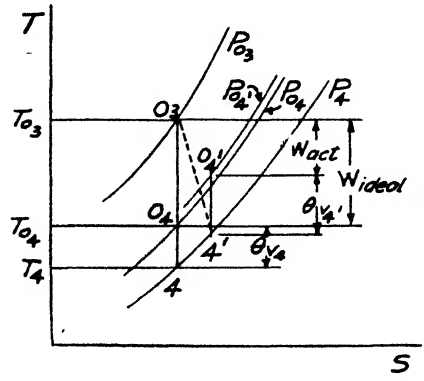

FIG. 4.5. Turbine process.

turbines, any discharge kinetic energy is unavailable, as it is dissipated in the condenser. On this basis then,

$$\eta_{t_s} = \frac{c_p(T_{0_3} - T_{0_{4'}})}{c_p(T_{0_3} - T_4)} = \frac{T_{0_3} - T_{0_{4'}}}{T_{0_3}\left[\dfrac{(P_{0_3}/P_4)^\epsilon - 1}{(P_{0_3}/P_4)^\epsilon}\right]} \tag{4.16}$$

where η_{t_s} is the "static" efficiency, essentially a "shaftwork" efficiency.

With the advent of the turbo-jet, however, only sufficient shaft work is required to drive the compressor, the remaining expansion energy being the useful output. Thus any kinetic energy at turbine discharge is useful and may represent a considerable proportion of the total energy. In this case, there is a choice of both numerator and denominator in defining an efficiency. One method is to use again only the actual shaft work as useful output but to evaluate the available energy from stagnation at inlet to stagnation at discharge, that is, not for complete expansion and thus not debiting the process with the residual kinetic energy. This "total" efficiency then becomes

$$\eta_{t_t} = \frac{c_p(T_{0_3} - T_{0_{4'}})}{c_p(T_{0_3} - T_{0_4})} \tag{4.17}$$

$$= \frac{T_{0_3} - T_{0_{4'}}}{T_{0_3}\left[\dfrac{(P_{0_3}/P_{0_4})^\epsilon - 1}{(P_{0_3}/P_{0_4})^\epsilon}\right]} \tag{4.18}$$

With the same idea of not debiting the turbine with the discharge kinetic energy, the useful output may be regarded as the sum of the shaft work and this kinetic energy. In this case, the available energy is that from stagnation pressure at inlet to static pressure at discharge, as for the first definition. Thus

$$\eta_{t_{t'}} = \frac{c_p(T_{0_3} - T_{0_{4'}}) + \dfrac{V_{4'}^2}{2g_0J}}{c_p(T_{0_3} - T_4)}$$

$$= \frac{T_{0_3} - T_{0_{4'}} + \theta_{v_{4'}}}{T_{0_3} - T_4} \tag{4.19}$$

$$= \frac{T_{0_3} - T_{4'}}{T_{0_3}\left[\dfrac{(P_{0_3}/P_4)^{\epsilon} - 1}{(P_{0_3}/P_4)^{\epsilon}}\right]} \tag{4.20}$$

Because the development of the gas turbine owes so much to the intensive work on the turbo-jet, Eq. (4.18), that based on shaft work and stagnation pressure ratio, is used most often. It does, however, give a somewhat higher value than Eq. (4.16).

4.6 *Polytropic or Infinitesimal Stage Efficiency*

The expressions for compressor and turbine efficiency are in terms of an overall performance. One question which arises is that of an overall efficiency if several similar stages of equal efficiency are used to obtain a given pressure ratio. In a compressor, for example, the temperature at entry to each succeeding stage is higher than that due to isentropic compression by virtue of the inefficiency of the preceding stage. Each successive stage is thus penalized, because for a given pressure ratio, more work is required if the initial temperature is increased, or alternatively, for a given amount of work, a lower pressure ratio is achieved. The effect is reversed for expansion.

The process can be demonstrated clearly on a temperature-entropy diagram, Fig. 4.6 (a) for compression and (b) for expansion. Using compression as example, A is the initial state and B' the final state for adiabatic compression from P_A to P_B. The overall isentropic efficiency η_c is equal to $\Delta T_{AB}/\Delta T_{AB'}$. If now the process of compression is accomplished by three stages, $P_A - P_1$, $P_1 - P_2$, $P_2 - P_B$, each of equal stage isentropic efficiency η_s, then the overall work is the same and represented by $\Delta T_{AB'}$. This amount

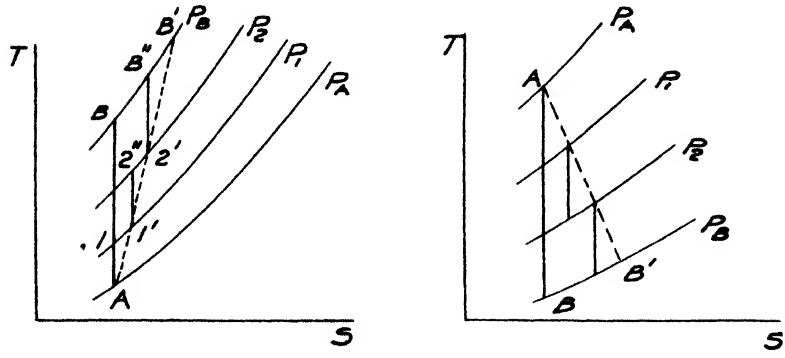

(*a*) Compression (*b*) Expansion

FIG. 4.6. Preheat and reheat effect.

of work can also be represented by the sum of $\Delta T_{A1'}$, $\Delta T_{1'2'}$ and $\Delta T_{2'B'}$, the actual stage temperature rise, thus

$$\Delta T_{AB'} = \Sigma \Delta T_s$$

where ΔT_s represents the work of a stage. Now from the diagram,

$$\Delta T_{A1'} = \frac{\Delta T_{A1}}{\eta_s}$$

$$\Delta T_{1'2'} = \frac{\Delta T_{1'2''}}{\eta_s}$$

$$\Delta T_{2'B'} = \frac{\Delta T_{2'B''}}{\eta_s}$$

and therefore

$$\Delta T_{AB'} = \frac{1}{\eta_s} (\Delta T_{A1} + \Delta T_{1'2''} + \Delta T_{2'B''}) \tag{4.21}$$

But, as was demonstrated in Sec. 3.1, lines of constant pressure diverge with increase of entropy, so that the *stage isentropic* temperature rise increases as the entropy increases (i.e. the inefficiency) of the previous stage increases, i.e.

$$\Delta T_{1'2''} > \Delta T_{12} \text{ and } \Delta T_{2'B''} > \Delta T_{2B}.$$

Thus

$$\Delta T_{A1} + \Delta T_{1'2''} + \Delta T_{2'B''} > \Delta T_{A1} + \Delta T_{12} + \Delta T_{2B} \text{ or } \Delta T_{AB}$$

From Eq. (4.21) then

$$\eta_s \Delta T_{AB'} > \Delta T_{AB}$$

and with $\Delta T_{AB} = \eta_c \Delta T_{AB'}$, then

$$\eta_s \Delta T_{AB'} > \eta_c \Delta T_{AB}$$

and

$$\eta_s > \eta_c$$

Thus the overall isentropic efficiency of compression is less than the stage isentropic efficiency of any of a number of stages of equal efficiency necessary to obtain a given pressure ratio. For a turbine a similar analysis yields the opposite effect, namely that $\eta_s < \eta_t$; for expansion, the reduced temperature drop with an inefficient stage means a slightly higher temperature at inlet to the next stage and thus an increase in work output for a given pressure ratio. The compressor effect is called *preheat* and the turbine effect is called *reheat*. The latter may be familiar from steam turbine practice, where the ratio $\Sigma \Delta W_s / W_s$ is called the reheat factor. The use of the term " reheat " is common to the process just described and to the process involving combustion, following a turbine expansion, that is, as an element of a cycle, and the distinction must be kept clear. The former is inherent in an expansion process and is a relatively small effect, while the latter is deliberate and usually means a considerable change of temperature.

The reheat or preheat effect was demonstrated qualitatively for three stages and raises two problems. The first one is that of a quantitative analysis to allow overall efficiency to be calculated from a knowledge of stage efficiencies. The second problem is raised by the thought that as the preceding analysis was quite general as to number of stages, the process must be proceeding continuously and infinitesimally, thus leading to the idea that there is an infinitesimal stage efficiency which is independent of pressure ratio or number of actual stages. From both viewpoints, it is desirable first to analyse the problem, using an infinitesimal stage pressure ratio and temperature rise.

For an increment of pressure, dP, from an initial pressure P, there is an isentropic efficiency η_p equal to dT/dT'. Thus, following the expression for a finite temperature change,

$$dT' = \frac{T}{\eta_p}\left[\left(\frac{P + dP}{P}\right)^{\epsilon} - 1\right]$$

and

$$\eta_p \frac{dT'}{T} = \left(1 + \frac{dP}{P}\right)^{\epsilon} - 1$$

Expanding the term in brackets and dropping second order terms,

$$\eta_p \frac{dT'}{T} = \left(1 + \epsilon \frac{dP}{P}\right) - 1 = \epsilon \frac{dP}{P}$$

and

$$\frac{dT'}{T} = \frac{\epsilon}{\eta_p} \frac{dP}{P}$$

Integrating over a finite pressure change P_1 to P_2 and temperature change T_1 to $T_{2'}$,

$$\ln \frac{T_{2'}}{T_1} = \frac{\epsilon}{\eta_p} \ln \frac{P_2}{P_1} \tag{4.22}$$

and

$$\eta_p = \frac{\frac{k-1}{k} \ln P_2/P_1}{\ln T_{2'}/T_1} \tag{4.23}$$

The last equation then gives an expression for η_p through a pressure ratio P_2/P_1 if the initial temperature T_1 and actual final temperature for an irreversible process, $T_{2'}$, are known. From Eq. (4.22), a relationship between the infinitesimal stage efficiency η_p and the overall efficiency, η_c or η_t, can be obtained. Using compression as example, Eq. (4.22) yields, after taking the anti-logarithm of both sides,

$$\frac{T_{2'}}{T_1} = \left(\frac{P_2}{P_1}\right)^{\epsilon/\eta_p}$$

from which

$$T_{2'} - T_1 = T_1 \left[\left(\frac{P_2}{P_1}\right)^{\epsilon/\eta_p} - 1 \right] \tag{4.24}$$

Now for the corresponding compression, the overall efficiency is η_c and

$$T_{2'} - T_1 = \frac{T_1}{\eta_c} \left[\left(\frac{P_2}{P_1}\right)^{\epsilon} - 1 \right] \tag{4.25}$$

Equating (4.24) and (4.25), then

$$\eta_c = \frac{(P_2/P_1)^{\epsilon} - 1}{(P_2/P_1)^{\epsilon/\eta_p} - 1} = \frac{P_r^{\epsilon} - 1}{P_r^{\epsilon/\eta_p} - 1} \tag{4.26}$$

Eq. (4.26) then allows η_c and η_p to be expressed in terms of pressure ratio. This is shown in Fig. 4.7 (a).

The corresponding expressions for expansion are:

$$\eta_p = \frac{\ln T_3/T_{4'}}{\frac{k-1}{k} \ln P_3/P_4} \tag{4.27}$$

and, using $P_3/P_4 = P_r$,

$$T_3 - T_{4'} = T_3 \left(\frac{P_r^{\eta_p \epsilon} - 1}{P_r^{\eta_p \epsilon}} \right) \tag{4.27a}$$

and

$$\eta_t = \frac{\frac{P_r^{\eta_p \epsilon} - 1}{P_r^{\eta_p \epsilon}}}{\frac{P_r^{\epsilon} - 1}{P_r^{\epsilon}}} \tag{4.28}$$

The relationship between η_i, η_p and pressure ratio is shown in Fig. 4.7 (b).

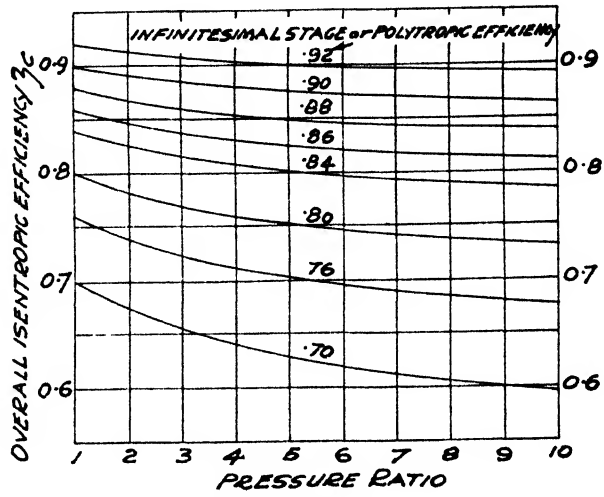

(*a*) Compression

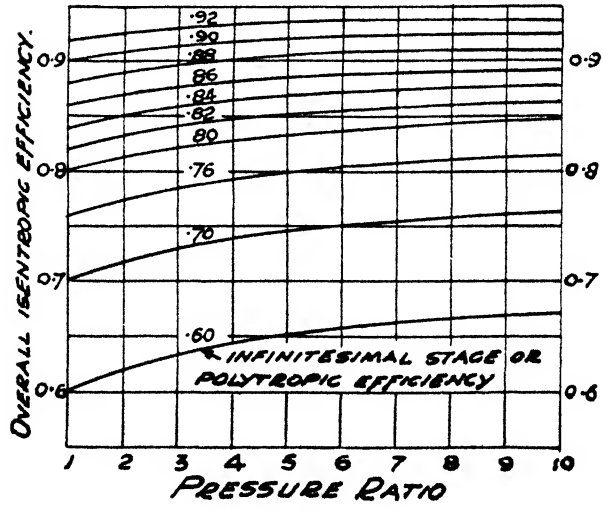

(*b*) Expansion

FIG. 4.7. Relationship of efficiencies and pressure ratio.

η_p, the infinitesimal stage efficiency, is more usually called the "polytropic" efficiency, but the former is more descriptive. Apart from its use in any other form, its importance lies in demonstrating the change in overall efficiency consequent on pressure ratio, an

inherent change due to the thermodynamics of the process which cannot be avoided. Thus, supposing a large number of stages of equal efficiency and each of small pressure ratio, approximating an infinitesimal pressure ratio, are used in series to produce a given pressure ratio P_r. The overall efficiency of compression, using Fig. 4.7 for example, is η_{c_1}. Adding more stages to obtain a higher overall pressure ratio yields a lower overall efficiency η_{c_2}, even though the additional stages are of equal efficiency. Thus, apart from any aerodynamic difficulties which may arise from attempting a high pressure ratio, the overall efficiency decreases with increase of pressure ratio. The reverse is true for expansion, larger pressure ratios yielding higher efficiencies. This is the underlying reason for the remark in Chapter 3, when typical cycle performances were given, that the compressor and turbine efficiencies should vary with pressure ratio. Eqs. (4.24) and (4.27a) show how a constant value of infinitesimal stage efficiency can be used for cycle calculations over a range of pressure ratio, as from them, compression and turbine work quantities can be obtained which automatically include the inevitable preheat and reheat effects. Alternatively, a plot such as is given in Fig. 4.7 can be used to obtain the overall efficiency at a given pressure ratio corresponding to a fixed value of infinitesimal stage efficiency. A value of the latter of 0·85 for both compression and expansion is typical of practice at the present time.

It remains to examine how a small, but finite, stage efficiency compares with the use of an infinitesimal stage efficiency. The derivation of the η_c and η_t in terms of such a finite stage efficiency will not be given here as it is rather long (see Ref. 1) and only the results will be given. For compression,

$$\eta_c = \frac{P_{r_s}^{m\epsilon} - 1}{\left[1 + \frac{1}{\eta_s}\left(P_{r_s}^{\epsilon} - 1\right)\right]^m - 1} \tag{4.29}$$

where P_{r_s} is the small or finite stage pressure ratio, m is the number of such stages and η_s is the efficiency of each stage. For expansion,

$$\eta_t = \frac{1 - \left[1 - \eta_s\left(\frac{P_{r_s}^{\epsilon} - 1}{P_{r_s}^{\epsilon}}\right)\right]^m}{\frac{P_{r_s}^{m\epsilon} - 1}{P_{r_s}^{m\epsilon}}} \tag{4.30}$$

with symbols as for compression.

These expressions, (4.29) and (4.30), are cumbersome to use and, with four variables, cannot be plotted conveniently. For a number

of stages greater than about six, the difference in overall efficiency in using the expressions for finite stage efficiency η_s, (4.29) and (4.30), and the expressions for infinitesimal stage efficiency, (4.26) and (4.28), are very small and consequently the latter are usually used, as they are very much more convenient.

4.7 *Efficiency-Summary*

It is obvious that there are many efficiencies of a compressor or turbine. In the first place, efficiency may be on the basis of total or static values. There is then the division into overall, finite stage and infinitesimal stage efficiency. The differences are small, but important, because in a gas turbine, 1% of efficiency in a component is magnified into 3% to 5% on net output and hence on fuel consumption. The overall isentropic efficiency is useful for cycle analysis, but in comparing values of efficiency at different ratios, the infinitesimal stage efficiency is the real criterion for evaluation, as it is independent of pressure ratio and thus measures the real design skill.

4.8 *Fluid Flow in Gas Turbines*

It has been seen that the energy transfer in compressors and turbines is effected by change of fluid velocities and that these changes are brought about by, or accompanied by, changes of pressure and temperature.

The overall performance of the gas turbine is analysed in thermodynamic terms, but the attainment of a certain efficiency is governed by the behaviour of the fluid as it flows through a passage or over an immersed surface. The following paragraphs will review some of the dynamics of fluids as they affect component performance, and discuss in some detail certain concepts and behaviour which are essential to understanding the performance and design of compressors, turbines and intermediate flow passages. As in the formal study of fluid dynamics, flow behaviour can be interpreted from the viewpoint of *duct* or pipe flow, with the performance expressed in terms of changes in the fluid itself, or from the viewpoint of flow over an *immersed body*, with the performance expressed in terms of forces on the body itself. For gas turbines, the most convenient or enlightening method is sometimes obvious, but in a number of cases, either type of analysis can be used. Some of the more important phenomena of duct flow will be reviewed first.

4.9 *Flow of Fluids in Ducts*

The important features of duct flow are the changes of pressure

and velocity which occur with area change and the type of flow pattern produced. Because energy transfer is dependent on velocity as a vector quantity, fluid direction as produced by duct direction is important. Only adiabatic flow will be considered, any specific problems associated with heat transfer or combustion of fuel being discussed later under those headings.

Duct flow in gas turbines is almost always turbulent, that is, the Reynolds number is above the critical value of about 2000 and is characterized (in a straight duct) by an almost uniform velocity profile across the duct except for the *boundary layer* near the walls, where the fluid has a much lower velocity, nominally zero at the surface. The effects of friction and turbulence are usually most conveniently given in terms of loss of dynamic pressure, $\rho V^2/2g_0$ for incompressible flow. Thus for skin friction loss in a straight duct, the loss of pressure Δp over a length of duct, L, having an equivalent diameter, d_e, is given by the Fanning equation,

$$\Delta p = f \frac{L}{d_e} \frac{\rho V^2}{2g_0} \tag{4.31}$$

where f is the friction factor, a function of Reynolds number. For ducts of any shape, the " equivalent diameter ", d_e, is defined as four times the hydraulic radius, the latter being the ratio of cross-sectional flow area and wetted perimeter. For a circular pipe, d_e reduces to the diameter d; for a rectangular duct of sides a and b, $d_e = 2ab/(a + b)$; and for an annulus of inner and diameter d_1 and d_2, $d_e = d_2 - d_1$. The friction factor f varies continuously with Reynolds number and pipe roughness (note that it is sometimes given as $4f$ in an alternative version of Eq. 4.31). Exact values can be obtained from plots in any fluid mechanics text, but for a first approximation, $f = 0{\cdot}3/R_e^{\frac{1}{4}}$ is valid for smooth pipes with Reynolds number between 5000 and 100,000. It is seldom possible to isolate pure friction values for flow in turbine and compressor rotors, but an estimate is often required for inlet and exhaust ducts of the complete plant and, most particularly, for the tubes of recuperative heat exchangers.

4.10 *Flow Around Corners*

Flow around corners leads to a different and larger type of loss than flow in straight pipes. Only bends of constant area are considered in this topic, i.e. bends in transfer ducts. Blade passages are duct bends, but they normally have area change and are considered in more detail under flow in blading. The centrifugal effect on the curved flow lines produces a pressure gradient which, acting

on the boundary layer, causes a spiral eddy motion and separation. The degree of separation and hence loss, is dependent on the degree of turning (the bend angle θ), the sharpness of the bend (radius ratio, mean radius of bend/width of duct in plane of bend), the cross-sectional flow shape (circular, rectangular, etc.) and, if not round or square cross-section, the aspect ratio (width/depth). Losses are expressed as $\Delta p = k\rho V_1^2/2g_0$ where V_1 is the inlet velocity and the coefficient k depends on the factors given above. Detailed data are not given here, as they cannot be succinctly expressed. Two references having such data are Wirt (Ref. 2) and Patterson (Ref. 3). 90° bends often have to be included to make a compact plant installation in and out of heat exchangers for example, and must be given careful consideration both from the point of loss and of introduction of an unbalanced flow distribution.

4.11 *Flow with Area Change*

Area change is, of course, an important part of compressors and turbine rotors, but for the time being, the problem will be considered from the point of view of large ducts, e.g. the intake duct to the compressor, the exhaust nozzle, etc.

Using incompressible flow to discuss the general problem of area change, it is seen from the continuity and Bernoulli equations that, as area decreases, velocity increases, and hence the pressure is reduced. Vice versa, as area increases, velocity decreases and the pressure rises. It is the direction of the pressure change and its effect on the boundary layer which is at the root of the flow behaviour in area change. Taking decrease of area with velocity increase, the pressure gradient is in the direction of flow, thus the slow-moving boundary layer is urged on, receiving energy from the main stream, and hence tends to become thinner. Thus in a *nozzle*, the flow is stable and the loss is very small. Expressing nozzle efficiency as the ratio of actual kinetic energy at outlet to ideal kinetic energy (that for isentropic flow), then its value for simple convergent nozzles is close to unity, from 0·95 to 0·98.

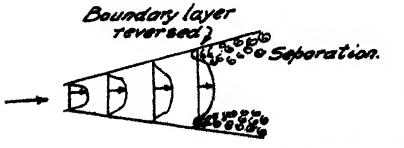

FIG. 4.8. Separation in a diffuser.

In the opposite case of a *diffuser*, increasing area with reduction of velocity, the pressure gradient is in the opposite direction to the flow. Thus the fluid in the boundary layer is further retarded, and, if the pressure gradient is too severe, the fluid near the walls reverses its direction and *separates* from the surface. This is shown in Fig. 4.8. The eddies and separation

cause considerable loss of useful energy and a flow pattern with a high-velocity core. A severe pressure gradient is caused by a rapid increase of area and thus diffusion must take place gradually, with small angles of divergence of the duct. Diffuser efficiency in incompressible flow may be expressed as the ratio of actual rise of static pressure to the ideal rise for the same initial and final flow areas. Thus

$$\eta_d = \frac{\Delta p'}{\Delta p}$$

and, from the Bernoulli relation,

$$\Delta p = \frac{\rho V_1^2}{2g_0} - \frac{\rho V_2^2}{2g_0}$$

and, from the continuity equation, $\rho A_1 V_1 = \rho A_2 V_2$,

$$V_2^2 = \left(\frac{A_1}{A_2}\right)^2 V_1^2$$

hence

$$\eta_d = \frac{\Delta p'}{\frac{\rho V_1^2}{2g_0}\left[1 - \left(\frac{A_1}{A_2}\right)^2\right]} \tag{4.32}$$

Diffuser efficiency is a function of the rate of area change, defined as the included angle 2θ, the overall area change, A_2/A_1, and the shape of cross-section. A summary of diffuser performance is given by Patterson (Ref. 4), some of whose results are adapted here in Fig. 4.9. The optimum angle 2θ is in the range 6°–10°, the efficiency

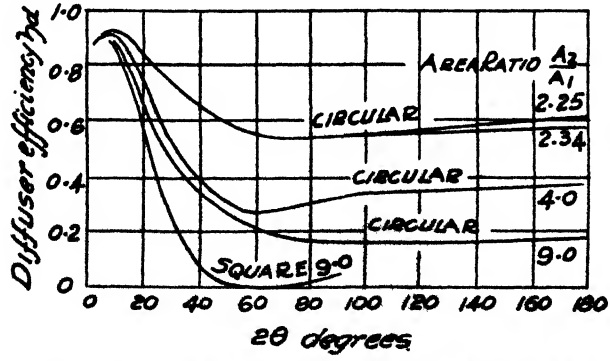

FIG. 4.9. Diffuser efficiency (after Patterson, Ref. 4).

decreasing rapidly for larger angles. The decrease at very small angles is due to the great length required for a given area ratio, skin friction then contributing the major effect. From Fig. 4.9, it is

seen that diffusion is a major problem in gas turbines, because even low rates of divergence yield an efficiency of little better than 90% and require a long length for any normal degree of diffusion. Very poor efficiency is obtained with large angles, so that a compromise between size and efficiency is always required.

For flow at sufficiently high velocities so that it can no longer be considered incompressible, diffuser efficiency can be expressed in similar fashion to that of ram efficiency, i.e.

$$\eta_d = \frac{\Delta T_{\text{isen}}}{\Delta T_{\text{act}}}$$

where ΔT_{isen} is the isentropic temperature change and ΔT_{act} the actual temperature change between the initial and final pressures. As the process is adiabatic, the stagnation temperature remains constant and therefore

$$\Delta T_{\text{act}} = T_{2'} - T_1 = \frac{V_1^2 - V_2^2}{2g_0 c_p J} = \theta_{v_1} - \theta_{v_2}$$

Thus

$$\eta_d = \frac{T_1 \left[(P_2/P_1)^{\epsilon} - 1 \right]}{\theta_{v_1} - \theta_{v_2}} \tag{4.33}$$

4.12 *Area Change in Compressible Flow*

Some very special effects occur in compressors and turbines when velocities are very high, reaching or exceeding the *acoustic* or *sound* velocity. The significance of the so-called " acoustic " velocity is that it is the velocity of propagation of pressure changes in the gas. A gas velocity greater than the acoustic velocity implies that no pressure change can be transmitted upstream and it is this fact that brings about the particular phenomena which are of special importance. The parameter expressing the ratio of velocities is known as the *Mach* number, M, defined as V/a, where a is the acoustic velocity. It can be shown that $a = \sqrt{g_0 kRT}$, with T the static temperature of the gas. For the standard ground level temperature of 59° F (15° C), $a = 1117$ fps, decreasing to 970 fps at the isothermal altitude. On the other hand, for gas at the turbine inlet temperature, say 1500° F (817° C), the acoustic velocity is about 2090 fps. With this considerable variation, then velocities themselves have no absolute significance and it is the Mach number which counts.

Some useful and important results can be obtained relating to subsonic ($M < 1$) and supersonic ($M > 1$) flow by considering isentropic compressible flow in a duct with area change. The basic

relationship is the momentum equation in the form of the one-dimensional, steady state form of the Euler flow equation,

$$\frac{dP}{\rho} + \frac{VdV}{g_0} = 0 \tag{4.34}$$

To bring in area change requires the continuity equation $m = A\rho V$, or, in differential form,

$$\frac{dA}{A} + \frac{d\rho}{\rho} + \frac{dV}{V} = 0 \tag{4.35}$$

The isentropic relation is used for connecting pressure and density, $P/P^k = \text{constant}$, in differential form,

$$\frac{d\rho}{\rho} = \frac{1}{k}\frac{dP}{P} \tag{4.36}$$

Finally, the Mach number, $M = V/a = V/\sqrt{g_0 kRT}$, is needed to eliminate velocity.

First, dividing (4.34) by V^2 and substituting $V^2 = M^2 g_0 kRT$ yields

$$\frac{dV}{V} = -\frac{1}{kM^2}\frac{dP}{P} \tag{4.37}$$

This shows that whatever the value of Mach number, an increase of pressure is accompanied by a decrease of velocity and vice versa.

Secondly, from (4.35) and (4.36),

$$\frac{dV}{V} = -\frac{dA}{A} - \frac{d\rho}{\rho} = -\frac{dA}{A} - \frac{1}{k}\frac{dP}{P} \tag{4.38}$$

Substitution for dV/V from (4.37) yields

$$\frac{dA}{A} = \frac{dP}{P}\left(\frac{1 - M^2}{kM^2}\right) \tag{4.39}$$

From (4.39) it is seen that with $M < 1$, i.e. $(1 - M^2)$ positive, then increase of area is accompanied by increase of pressure and from (4.37), decrease of velocity. This is the *subsonic diffuser* case. Similarly, decrease of area is accompanied by decrease of pressure and increase of velocity, the *subsonic* or *convergent nozzle* case.

If $M > 1$, i.e. $(1 - M^2)$ negative, then increase of area is accompanied by decrease of pressure and increase of velocity. Thus for supersonic flow, acceleration requires increase of area. Decrease of area is accompanied by increase of pressure and decrease of velocity, a *supersonic diffuser*.

Finally when $M = 1$, $dA/A = 0$, i.e. the sonic velocity is achieved only where there is no area change. Putting all these results together for flow from rest or from an initially very low velocity, it is

seen that a converging or decreasing area passage is required at first to accelerate the flow. If a Mach number of unity is reached, then the area change at that point is zero and to continue to accelerate the flow requires increasing area, or a divergent passage. A passage shape as in Fig. 4.10 is thus reached, with the minimum flow area where $dA = 0$ being known as the *throat*. While subsonic diffusion is important, supersonic diffusion does not occur in gas turbine components, except possibly in the case of supersonic axial-flow compressors, which as yet have not been used in other than experimental units. The convergent-divergent nozzle of Fig. 4.10, necessary for obtaining the highest possible discharge velocity, presupposes that the pressure ratio across the nozzle is sufficient to produce a Mach number of unity at the throat. With only a small pressure ratio, the gas accelerates to the throat, where it is still subsonic, and then slows down in the divergent part, which in this case acts as a subsonic diffuser, i.e. the duct acts as a simple Venturi tube. It is then necessary to examine the problem further in terms of pressure ratio.

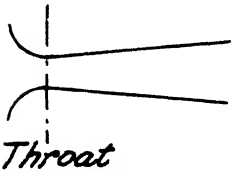

FIG. 4.10. Converging-diverging nozzle for $M > 1$.

In the first place, a simple but highly important relationship for the pressure at the throat can be obtained when the Mach number of unity occurs there. From the statement expressing stagnation temperature,

$$T_0 = T + \frac{V^2}{2g_0c_pJ}$$

and substituting $V^2 = M^2g_0kRT$,

$$T_0 = T + \frac{g_0kRTM^2}{2g_0c_pJ} = T + \left(\frac{k-1}{2}\right)M^2T$$

or

$$\frac{T_0}{T} = 1 + \frac{k-1}{2}M^2 \tag{4.40}$$

From the definition of stagnation pressure,

$$\frac{P_0}{P} = \left(\frac{T_0}{T}\right)^{k/k-1} = \left(1 + \frac{k-1}{2}M^2\right)^{k/k-1} \tag{4.41}$$

For the special condition at the throat when $M = 1$,

$$\frac{T_0}{T} = 1 + \frac{k-1}{2} = \frac{k+1}{2} \tag{4.42}$$

and

$$\frac{P_0}{P} = \left(\frac{k+1}{2}\right)^{k/k-1} \tag{4.43}$$

For flow under the conditions here (isentropic, no shaft work), both the stagnation temperature and pressure are constant. They thus represent the *reservoir* conditions. Eqs. (4.42) and (4.43) then show that there is a fixed temperature ratio and a fixed pressure ratio between the reservoir and the throat for a Mach number of unity at the throat, regardless of the down-stream pressure. These ratios are known as the *critical* temperature and pressure ratios respectively, T_{r_c} and P_{r_c}. For $k = 1{\cdot}4$ (atmospheric temperature), $T_{r_c} = 1{\cdot}2$ and $P_{r_c} = 1{\cdot}893$. For combustion cases ($k = 1{\cdot}3$), $T_{r_c} = 1{\cdot}15$ and $P_{r_c} = 1{\cdot}831$.

An important corollary of this state of affairs is that once $M = 1$ at the throat, reduction of the discharge pressure, even down to zero, will not change the mass flow rate which remains constant at its value for $M = 1$. From continuity

$$m = A\rho V = \frac{APV}{RT} = \frac{APM\sqrt{g_0kRT}}{RT} = \frac{APM}{\sqrt{T}}\sqrt{\frac{g_0k}{R}}$$

For $M = 1$,

$$m = \frac{AP}{\sqrt{T}}\sqrt{\frac{g_0k}{R}} \tag{4.44}$$

Thus for given reservoir conditions, P and T are fixed by the critical ratios and hence m is fixed. Making the substitutions,

$$m = \frac{AP_0}{\sqrt{T_0}}\sqrt{\frac{g_0k}{R}} \cdot \left(\frac{2}{k+1}\right)^{\frac{k+1}{2(k-1)}} \tag{4.45}$$

The condition of $M = 1$ at the throat, with the mass flow constant, is known as *choked* flow, or the nozzle is said to be *choked*. Choked flow occurs frequently in turbine nozzles and turbo-jet exhaust nozzles and has meaning for some conditions in compressors.

If the flow reaches a Mach number of one at the throat, then theoretically there is the possibility that with a diverging duct from the throat onwards, the flow may decelerate subsonically or accelerate supersonically. The former requires increasing pressure and the latter decreasing pressure, according to the qualitative relations given previously. This brings out the important point that the overall pressure ratio, P_{0_1}/P_2, from inlet to discharge of a convergent-divergent duct may be *less* than the critical ratio and yet allow $M = 1$ at the throat.

Consider a convergent-divergent duct of fixed dimensions supplied with air at stagnation or *reservoir* conditions P_{0_1}, T_{0_1}. The air discharges to a *receiver* in which the pressure is P_e. Note that the

discharge pressure in the nozzle, i.e. at the exit plane but with the fluid still ideally confined by the duct, may in certain circumstances be different from P_e and is denoted by P_2. The flow conditions will be now examined with P_e continuously varied from P_{0_1} down to zero, i.e. a vacuum.

As soon as P_e is slightly lowered below P_{0_1}, flow commences. The pressure along the nozzle decreases up to the throat but the Mach number there is still low, and the flow then continues to diffuse subsonically so that at discharge, $P_2 = P_e$. A plot of P_2/P_0, along

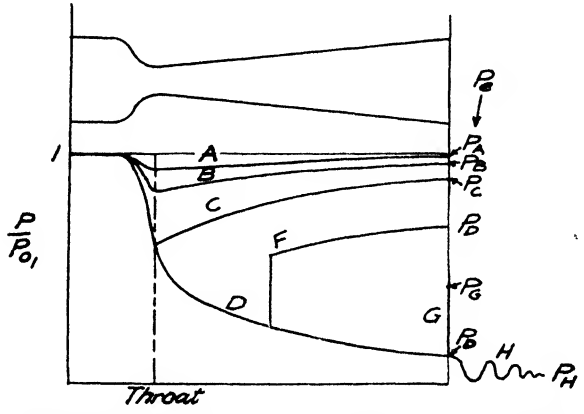

FIG. 4.11. Variation of pressure along a nozzle for various exhaust pressures.

the nozzle is shown in Fig. 4.11. The flow condition just described is represented by line A. The mass flow rate is wholly controlled by the initial temperature T_0, the overall pressure ratio P_0/P_2 and the area A_2. Thus

$$m = A_2\rho_2 V_2 = \frac{A_2 P_2 V_2}{RT_2}$$

T_2 is determined from the pressure ratio, since $T_0/T_2 = (P_0/P_2)^{\epsilon}$. V_2 is determined from the stagnation relationship, i.e.,

$$T_0 = T_2 + V_2^2/2g_0c_pJ$$

hence

$$V_2 = [2g_0c_pJ(T_0 - T_2)]^{\frac{1}{2}}$$

If P_e is lowered a further step, then the flow may be shown as following line B, determined as for A, but with a greater mass flow because P_0/P_2 is larger. The lowest pressure occurs at the throat and hence the highest velocity occurs there also. As the velocity is at a maximum, the temperature is at a minimum, i.e. the Mach number $M = V/\sqrt{g_0kRT}$ has its maximum value for the whole length of the nozzle at the throat.

As P_e is continually reduced, the mass flow increases, but eventually a Mach number of unity is reached at the throat. This condition is shown by line C in the diagram. If now P_e is further reduced, the mass flow remains constant, because the critical pressure ratio has been reached at the throat and it has been seen that downstream conditions do not then affect the throat state. With the mass flow and discharge area fixed, no random value of P_e will then allow the pressure P_2 to equal P_e for isentropic flow. The only other possibility for isentropic flow following the sonic state at the throat is for continuously increasing supersonic flow with continuously decreasing pressure, so that P_e has to be reduced to a much lower value to match the required P_2. This condition is shown by line D.

Now it is known that flow continues for receiver pressures P_e lying between P_C and P_D, but it cannot be isentropic and some other condition must be sought. The answer lies in a *shock wave*, a discontinuity of state which occurs in the divergent part of the duct. It is not necessary here to analyse the relations of a normal or plane shock and it will suffice to say that for a given Mach number before the shock, the ratio of state properties across the shock is fixed. In the first place, a shock wave can only occur from initially supersonic flow and the velocity after the shock is always subsonic. There is an increase of entropy, that is loss of available energy, represented by a decrease of *stagnation* pressure across the shock, although there is a rise of *static* pressure. There is an accompanying rise of static temperature, although as the process is not isentropic, it cannot be calculated from the pressure rise alone. The nozzle picture can now be completed for receiver pressure lower than P_c. After reaching the sonic state at the throat, the gas continues supersonically to some point when a plane shock occurs. The static pressure increases suddenly and the flow becomes subsonic from the downstream side of the shock to the nozzle discharge. For a given value of P_e, the shock occurs at a plane so that a combination of isentropic and supersonic flow up to the shock, a plane shock, followed by (for ideal flow) isentropic and subsonic flow to the discharge allows P_2 to equal P_e. Such a state of affairs is shown by line F in Fig. 4.11. The limit of a possibility of plane shock occurs when the pressure immediately following the shock is the receiver pressure P_e. This is shown by line G in Fig. 4.11. For pressures less than P_G but greater than P_D, a complex series of oblique shocks occur, but this will not be discussed in detail. For receiver pressures below P_D, the gas can expand in the nozzle itself down to P_D, the remaining expansion to P_H being a free expansion which occurs in oscillatory fashion (line H).

The loss of stagnation pressure across a plane shock itself is not

very large, at least for initial Mach numbers up to about 1·5, but the following subsonic diffusion does not occur isentropically as the ideal picture postulates. The sudden increase in pressure sets up a severe reverse pressure gradient, which causes the boundary layer to separate. Thus the actual loss due to *overexpansion* may be considerable. There is also, of course, a loss due to *underexpansion* (line H), as the kinetic energy is dissipated.

From the point of turbine performance, a convergent-divergent nozzle is then liable to lead to poor efficiency unless the design conditions are constant. Actually, the very high velocities are not necessary, as the blade speed for effective utilization of such gas velocities is not desirable for reasons of material stress. For the propelling or exhaust nozzle of turbo-jets, a supersonic nozzle is a possibility, although not widely used at the present. It is, however, necessary to appreciate the general features of normal shock, as shock phenomena occur in other manifestations, which will be discussed in particular instances for both compressors and turbines.

It is necessary to understand clearly the behaviour of a convergent nozzle when the pressure ratio P_0/P_e is greater than the critical value. The throat of a convergent nozzle is at the plane of minimum area, that is, at discharge. The gas attains some velocity at discharge when P_0/P_e is just the critical value. Subsequent lowering of P_e does not change the nozzle discharge pressure P_2 and the flow is *choked*. The expansion in the receiver from P_2 to P_e is a free expansion and the kinetic energy may be lost.

4.13 *Flow Through Blade Passages*

The parallel flow passages in axial-flow compressors and turbines formed by rows of blades are invariably curved, may increase or decrease in area and are likely to be affected by compressible flow effects. Thus the previous discussion may be used to form some qualitative conclusions with respect to compressor and turbine performance. Curvature, necessary to effect rate of change of angular momentum, must be limited and controlled in order to avoid large losses due to separation. If the flow is accelerating, as in a turbine, the efficiency is high and considerable change of direction is possible. If the flow is diffusing, as in a compressor, both the amount of diffusion and the amount of turning must be very limited to obtain reasonable efficiency. The phenomenon of choking is most obviously likely to arise in turbines where high velocities are utilized. It is also possible for shock to occur anywhere when a local velocity has reached a supersonic value, and this can occur both in compressors and turbines. To evaluate these problems in more detail,

it is necessary to discuss the phenomena of flow over immersed bodies.

4.14 *Flow Over Immersed Bodies*

An airfoil shape immersed in a flowing fluid is subject to a force which may be resolved into two components, the *lift* L and the *drag* D. This is shown in (a) of Fig. 4.12 for a compressor and in (b) for a turbine. The lift may be envisaged as due to an unbalanced

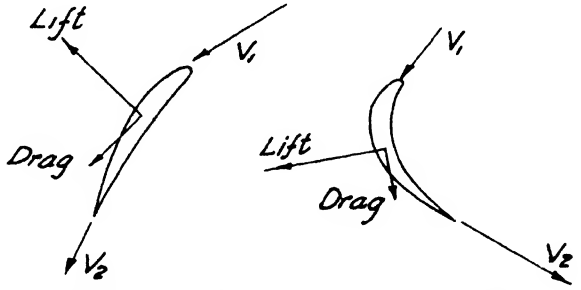

(*a*) Compressor blade (*b*) Turbine blade

FIG. 4.12. Lift and drag force on a blade.

pressure distribution, higher on the concave surface than on the convex surface, over which the pressure may be much below the free stream pressure due to the increase of local velocity. The drag is due to the shearing stress at the surface and the consequent boundary layer. The latter is usually *laminar* for a short distance downstream of the leading edge, changing then to *turbulent*. The drag due to a laminar boundary is less than that due to a turbulent one, and therefore one object in airfoil design is to prevent *transition* from the one to the other for as long as possible. Too great a rate of change of the airfoil profile or too great a curvature of the blade as a whole has an effect similar to decelerating flow in a duct or flow in an elbow, the consequent adverse pressure gradient causing separation of the boundary layer, with reduction of lift and increase of drag. Flow around blades in compressors or turbines is different from flow around isolated airfoils, because of the effect of adjacent blades. Two adjacent blades form a channel in which there is a pressure gradient, usually increasing pressure in the flow direction for a compressor and decreasing pressure for a turbine. Thus, the boundary layer in a compressor has very severe conditions under which to operate, and the rate of pressure change in the channel and the degree of curvature of the blade have to be very limited

in order to avoid separation. In a turbine, on the other hand, the pressure gradient is favourable and very large curvatures, 90° or more, can be used without severe losses.

The lift and drag performance of an airfoil section is measured in terms of lift and drag coefficients, C_L and C_D respectively, defined by the following expressions.

$$L = C_L \frac{\rho V^2}{2g_0} A \qquad (4.46)$$

$$D = C_D \frac{\rho V^2}{2g_0} A \qquad (4.47)$$

where V is a representative velocity and A is a representative surface area. The velocity may be either the inlet, outlet or mean velocity, and the area is usually the product of the length (height) of the blade and its chord length (line joining leading and trailing edges). C_L and C_D are, of course, dependent on the airfoil shape and degree of curvature and, for a given blade, dependent on Reynolds number, Mach number and the angle of attack, that is, the angle between the approach fluid and the blade.

This brief account of the behaviour of blades with respect to the lift and drag forces serves to show that the same considerations apply in these circumstances as when the flow is treated as channel flow. There must then be a quantitative relationship between energy transfer in terms of channel flow, i.e. rate of change of angular momentum and energy transfer in terms of actual forces on the blades.

Corresponding to the rate of change of angular momentum, it is the net *tangential* force on the blades which is effective in energy transfer. Fig. 4.13 shows the lift and drag forces resolved into

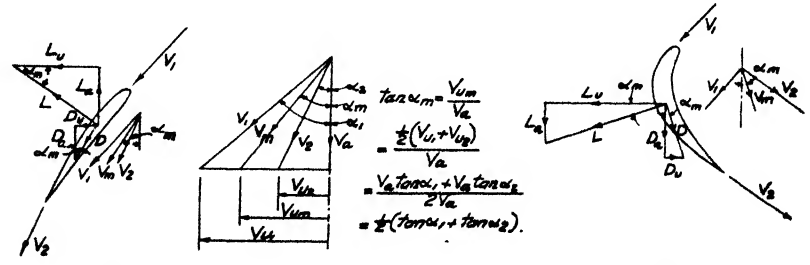

FIG. 4.13. Components of lift and drag forces.

tangential components L_u and D_u, and axial components, L_a and D_a. The resultant lift and drag forces L and D are normal and

parallel to the mean velocity V_m, which has an angle α_m with the axial direction. The mean angle α_m is defined so that

$$\tan \alpha_m = \tfrac{1}{2}(\tan \alpha_1 + \tan \alpha_2) \tag{4.48}$$

as shown in Fig. 4.13.

The net tangential force F_u is then

$$F_u = L_u \pm D_u = L \cos \alpha_m \pm D \sin \alpha_m$$

Substituting from Eqs. (4.46) and (4.47) then

$$F_u = \frac{\rho V_m^2}{2g_0} A(C_L \cos \alpha_m \pm C_D \sin \alpha_m)$$

For any satisfactory turbine or compressor blade, $C_L \gg C_D$, and the drag component may be dropped with negligible error. The area A is the product of chord length and the length of the blade, so the area per unit blade length is simply the chord length c. The mean velocity in terms of axial velocity is $V_m = V_a/\cos \alpha_m$, hence the tangential force per unit blade length is

$$F_u = \frac{\rho V_a^2}{2g_0} c \frac{C_L}{\cos \alpha_m} \tag{4.49}$$

The force due to rate of change of angular momentum, since the flow is axial, i.e. $r_1 = r_2$, is

$$F_u = \frac{m}{g_0}(V_{u_1} - V_{u_2})$$

For unit blade length, the rate of mass flow per blade is $m = \rho V_a s$, where s is the *pitch* of the blades or the tangential distance between corresponding points of adjacent blades. Thus the force per unit blade length due to rate of change of angular momentum is

$$F_u = \frac{\rho V_a s}{g_0}(V_{u_1} - V_{u_2}) \tag{4.50}$$

Equating the two expressions for F_u, Eqs. (4.49) and (4.50),

$$\frac{\rho V_a s}{g_0}(V_{u_1} - V_{u_2}) = \frac{\rho V_a^2}{2g_0} c \frac{C_L}{\cos \alpha_m}$$

Multiplying both sides by the blade speed u to obtain the work or rate of energy transfer, then

$$E = \frac{U}{g_0}(V_{u_1} - V_{u_2}) = \frac{UV_a}{2g_0} \frac{c}{s} \frac{C_L}{\cos \alpha_m}$$

A further reduction may be made by substituting $V_u = V_a \tan \alpha$ (see Fig. 4.13), when

$$C_L = 2 \frac{s}{c} \cos \alpha_m (\tan \alpha_1 - \tan \alpha_2) \tag{4.51}$$

In analogous fashion, the drag D must correspond to the loss of pressure, Δp, the difference of ideal and actual change of pressure. The drag per unit blade length in the direction of the mean velocity is

$$D = C_D \frac{V_m^2}{2g_0} c$$

The force due to Δp per unit blade length is Δp ($s \cos \alpha_m$), hence

$$C_D \frac{\rho V_m^2}{2g_0} c = \Delta p \, s \cos \alpha_m \tag{4.52}$$

or

$$C_D = \Delta p \frac{s}{c} \cos \alpha_m / (\rho V_m^2 / 2g_0) \tag{4.53a}$$

Substituting $V_a = V_m \cos \alpha_m$,

$$C_D = \frac{s}{c} \frac{\Delta p}{\rho V_a^2 / 2g_0} \cos^3 \alpha_m \tag{4.53b}$$

Eqs. (4.51) and (4.53) are then alternative methods of expressing energy transfer and blade performance. The use of the lift and drag coefficients reflects the use of aeronautical techniques in turbomachine design and sometimes provides a useful basis for analysis, although design data for compressor and turbine blades are more usually given in terms of fluid angles and pressure loss coefficients. Some of the properties of blades for axial-flow compressors and turbines will now be discussed from the viewpoint both of channel flow and of lift and drag coefficients.

4.15 *Blade Performance—General*

The most direct form in which blade performance can be given is in values of air deflection angle at some optimum condition of loss, for various blade settings, inlet fluid angles and blade spacings. The optimum condition of loss may have various interpretations, such as minimum pressure loss coefficient or minimum C_D, maximum C_L/C_D value, maximum deflection with specified maximum loss, Mach number limitation, etc. The correlation of results covering all the many variables is a difficult problem, but must always be attempted so that the possible design region can be delineated. Some of the very generalized results will be given here where possible, but they should be used only as indicating the range and order of performance. Unfortunately, British and American nomenclature and presentation of results differ somewhat, so that the data cannot be compared directly in simple fashion. The differences in definitions and symbols must be observed carefully, because in some cases the same terms and notations are used for different variables. Both

British and American basic usage will be described here, with the former being used when performance is being discussed generally, as it is in many ways easier to apply and more adaptable to the type of analysis used here.

4.16 *The British Method of Specifying Blade Performance*

A blade is specified by means of a *base profile* superimposed on a curved line, the *camber line*. A base profile is shown in Fig. 4.14, together with the nomenclature associated with it. The *maximum thickness t*, expressed as a fraction of the chord *c*, that is *t*/*c*, and the position of maximum thickness, are important characteristics of a profile. The base profile fitted to a camber line is shown in Fig. 4.15.

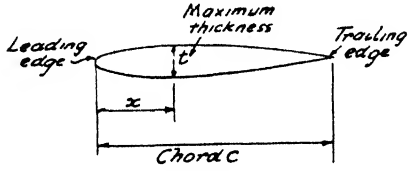

FIG. 4.14. Base profile.

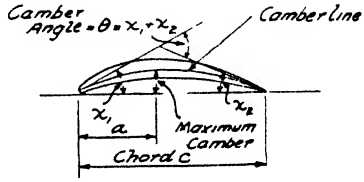

FIG. 4.15. Camber and camber angle.

The degree of camber can be expressed in several ways, but here will be given as *camber angle*, θ (called simply, the *camber*). θ is seen to be the sum of the angles χ_1 and χ_2 made by the chord and the tangents to the camber line at leading and trailing edge. θ represents the geometrical turning angle of the blade. The position of maximum camber as a/c, shown in Fig. 4.15, is an important parameter in blade performance. The camber line may be a simple geometrical shape, such as an arc of a circle or a parabola, such shapes controlling the position of maximum camber. In some cases, the camber line corresponds to no simple geometrical shape, but is constructed so that, in conjunction with the base profile itself, it gives a particular pressure distribution and hence lift coefficient.

A row of like blades gives rise to other geometrical characteristics, as shown in Fig. 4.16. The *blade* inlet and outlet angles β_1 and β_2 are given by the angles between the axial direction and the tangents to the camber line at inlet and outlet. The *axial* direction is always taken as the reference direction for axial-flow compressors, but only in some literature for turbines. For the latter, the long-established steam turbine nomenclature uses the tangential direction as datum and gas turbine data are given for both. The context should make clear which is being used in any given case in this text.

The distance apart of blades is given by the pitch, *s*, defined above,

but the spacing itself is not an absolute variable of performance. It is the relation of spacing to blade length, i.e. channel shape, which is the controlling parameter, expressed either as *pitch-chord*

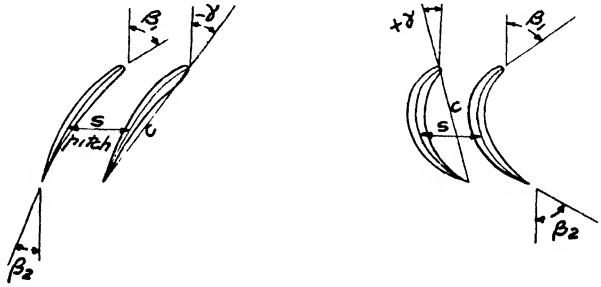

FIG. 4.16. Blade nomenclature.

ratio, s/c, or as the *solidity*, c/s. Both parameters are in use and as the usable range of either centres around a value of unity, care must be taken in application. Another parameter describing the setting of a row of blades of given form and spacing, is the *stagger* angle, γ, the angle made by the axial direction and the chord line, Fig. 4.16. Where necessary, angles are given positive or negative values, dependent on the quadrant in which they are located, as shown in Fig. 4.16.

Finally, the nomenclature with respect to the *fluid* angles must be defined, as these are seldom the same as the blade angles. The inlet and outlet angles are shown in Fig. 4.17 as α_1 and α_2. The difference

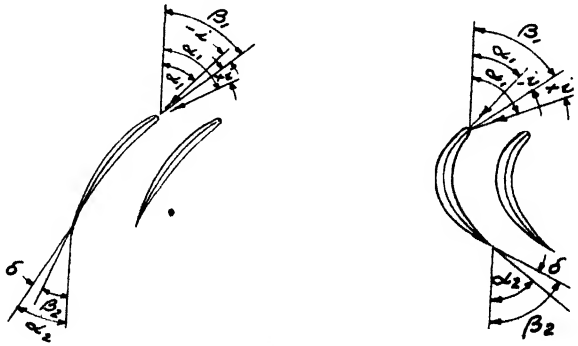

FIG. 4.17. Fluid angles, incidence and deviation.

between α_1 and β_1 is known as the angle of incidence or simply the *incidence*, i, positive or negative as shown. The difference between α_2 and β_2 is known as the *deviation*, δ, and is always positive described

in this manner as $\alpha_2 - \beta_2$. The total fluid turning angle is known as the *deflection*, $\epsilon = \alpha_1 - \alpha_2$.

4.17 *Cascades of Blades*

Because rotational tests of a full row of blades are costly and time-consuming, much useful information can be obtained from a linear row or *cascade* of blades in a wind-tunnel. Total pressures and fluid directions are measured before and after the blade row, thus giving directly the deflection $\epsilon = \alpha_1 - \alpha_2$, the deviation δ at a pre-set incidence i, and the loss of total pressure Δp_0. Lift and drag of airfoils in cascade are never measured directly, the coefficients being calculated from Eqs. (4.51) and (4.53). A total pressure survey across the inlet to a cascade should give a constant value, as shown in Fig. 4.18, because the inlet flow is made as uniform as possible to establish a fixed datum state for all similar tests. The total pressure across the outlet, however, reveals regions of low pressure, representing the losses due to the blade *wakes*, the regions of boundary layer shedding and separation. Integration across one blade pitch will then give the average loss of pressure Δp_0. Similarly, a survey of the fluid angles shows a uniform direction at inlet, since this is controlled, but at outlet the fluid angle varies across a blade pitch. On the concave face of the blade, the fluid may receive full guidance, but on the convex face there is a thicker boundary layer and possibly separation, while between blade surfaces, the fluid tends to receive less guidance. Thus, as with the discharge pressure, the outlet fluid angle is an average value. A short distance downstream from the trailing edge, mixing has taken place and hence a following blade row tends to receive the fluid in a state approximating the calculated average values.

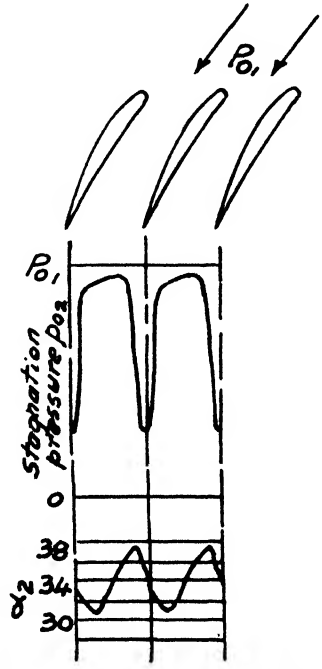

FIG. 4.18. Stagnation pressure distribution and fluid outlet angle across a cascade of blades.

A given set of blades, with certain values of pitch-chord ratio and stagger, are tested over a range of incidence, both positive and negative. The results may be plotted as deflection, ϵ, and pressure loss coefficient, $\Delta p_0/(\rho V_1^2/2g_0)$, or as C_L and C_D, against incidence,

i, as shown in Fig. 4.19. Over a considerable range of incidence, ϵ is almost linear with i, from which it may be inferred that the outlet angle a_2 is unaffected by inlet angle a_1. However, at some

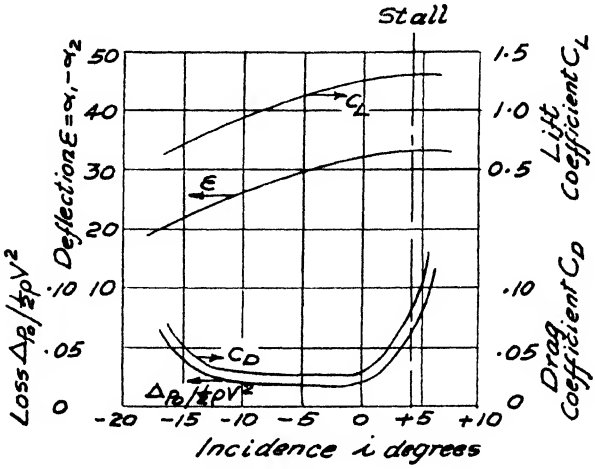

FIG. 4.19. Typical cascade result.

positive value of incidence, ϵ reaches a maximum value and then starts to decrease. Correspondingly, the pressure loss coefficient is fairly constant over the middle range of incidence, but at the positive value of i where the rate of increase of ϵ starts to decrease, the loss starts to increase rapidly. After the value of i, corresponding to maximum ϵ, the loss is large and increases rapidly. The fall in deflection and increase of loss occur due to *stalling* of the flow, that is, a large area of separation appears on the convex surface of the blade, Fig. 4.20. Thus the design conditions under which a blade is intended to operate must be a compromise between high deflection, for maximum energy transfer, and low loss, for maximum efficiency, and must never reach the stall point. The data plotted as C_L and C_D follow similar paths to ϵ and loss coefficient. Numerous cascade tests at other values of pitch-chord ratio and stagger allow complete information to be accumulated on a given set of blades.

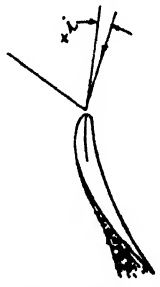

FIG. 4.20. Stalling due to separation at high positive incidence.

4.18 *American Method of Specifying Blade Performance*

Compressor blade data are based on the 65-series airfoil with basic mean line of varying camber, with camber expressed as the

design lift coefficient, C_{L0}, for the isolated airfoil. The blades have a 10% thickness occurring at about 40% chord. The maximum camber occurs at 50% chord. The camber expressed as a value of lift coefficient is not readily elucidated without reference to the original work and it will suffice to say that the range is from 0 to 2·7, with increasing values indicating increasing camber angle in the sense used previously. A blade is designated, for example, as a 65-series airfoil, with a twelve-tenths C_{L0} (i.e. 1·2) the thickness being 10%, the nomenclature then being given as 65-(12)010.

Turbine blade profiles are based on a specified *mean* (camber) line and a *thickness distribution* (profile shape). The curvature is given in terms of a camber angle, θ_c, similar to the British designation.

For both compressor and turbine blades the major line of designation is the chord, the line joining the leading and trailing edges. The angle between the chord and the direction of the entering fluid is the angle of attack, α. The angles made by the fluid with the axial direction at inlet and outlet are designated β_1 and β_2 respectively. The fluid deflection, $\beta_1 - \beta_2$, is denoted by θ. Incidence and deviation, as employed in the British notation, are not used. Fig. 4.21 shows a comparison of definitions and notation.

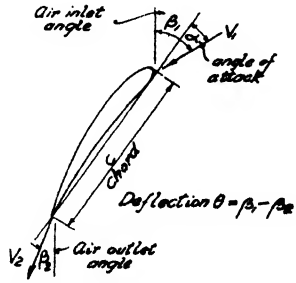

FIG. 4.21. American notation for cascades.

Performance of a cascade of blades is expressed in analogous terms to the British method, i.e., as a plot of θ or C_L, and C_D vs. angle of attack α. In addition, the pressure distribution is measured at each angle of attack and the blade design point is taken as that angle of attack for which no velocity peaks corresponding to pressure peaks occur. This criterion is based on the premise that the blade section will be required to operate at high Mach numbers.

4.19 *Arrangement of Blades*

There are many different ways of obtaining a given amount of energy transfer with one specified blade profile. A set of blades of given camber and fixed spacing will give variable energy transfer and variable change of velocity (amount of diffusion or acceleration) according to the setting angle or stagger. This can be visualized with the aid of Fig. 4.22, in which blades are represented by two straight lines of constant inclination one to another (same camber). At a given pitch, they are represented as hinged at the leading edge to give varying degrees of stagger, from negative values at the left to

positive values at the right. For negative stagger, it is seen that the flow is *diffused* and for positive stagger it is *accelerated*, passing through *impulse* for zero stagger. Thus negative stagger represents a typical compressor condition and positive stagger, a typical turbine condition.

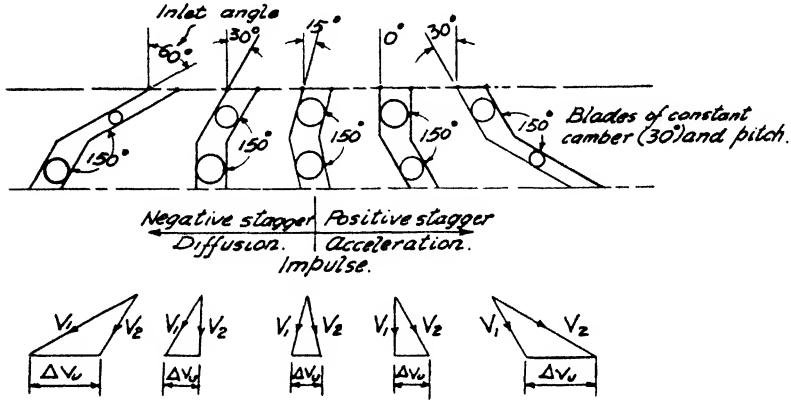

FIG. 4.22. Effect of blade arrangement.

The velocity diagrams below each blade setting show the relative changes of velocity and the relative changes of energy transfer represented by ΔV_u. Higher values of ΔV_u are obtained at high values of stagger (either positive or negative), with a corresponding greater change of total velocity. Now for negative stagger (compressor blades), the amount of diffusion must be limited to avoid high losses, while for positive stagger (turbine blades) a considerable amount of acceleration can take place at high efficiency. Thus a turbine blade section can be allowed to deflect the fluid considerably more than can a compressor blade section, that is, it can have a higher camber.

A given amount of energy transfer at a given level of efficiency is then a function of camber, stagger and blade speed. A given compressor condition, for example, may be achieved in many ways and the choice depends on many factors, such as the influence of Mach number, size and weight limitations, cost, range of stable operation required, and so forth.

4.20 *Stage Reaction*

Another variable which must be considered is that of the degree of reaction of the stage. Many factors may influence the choice of the optimum reaction, but one of the major ones is that of efficiency.

The following analysis has to make some simplifying assumptions but they are reasonable ones.

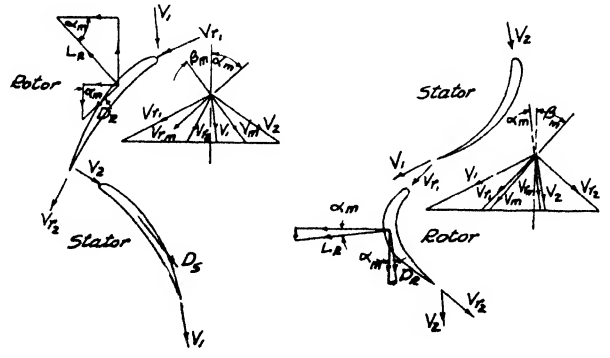

(*a*) Compressor (*b*) Turbine

FIG. 4.23. Diagrams of compressor and turbine stage for lift-and-drag analysis.

Fig. 4.23 shows the lift and drag forces on rotor and stator blades of a compressor stage and of a turbine stage, together with the corresponding velocity diagrams. The blade profile efficiency of the stage is

$$\eta_{ps} = \frac{E - \text{loss}}{E} = 1 - \frac{\text{loss}}{E}$$

In terms of lift and drag, using subscript R for the rotor and S for the stator,

$$E = U(L_R \cos \alpha_m \pm D_R \sin \alpha_m)/g_0$$
$$\approx UL_R \cos \alpha_m / g_0$$

omitting the drag component, as $D_R \ll L_R$

The loss in the rotor $E_R = D_R V_{r_m}$ and in the stator, $E_s = D_s V_m$. Thus

$$\eta_{ps} = 1 - (D_R V_{r_m} + D_s V_m)/UL_R \cos \alpha_m$$

Since $\Delta(UV_v) = \Delta(UV_{v_r})$, the tangential force on rotor and stator must be the same, i.e. $L_R \cos \alpha_m = L_s \cos \beta_m$, so

$$\eta_{ps} = 1 - \frac{1}{U}\left[\frac{D_R V_{r_m}}{L_R \cos \alpha_m} + \frac{D_s V_m}{L_s \cos \beta_m}\right]$$

Now the assumption is made that $D_R/L_R = D_s/L_s = D/L$, i.e. lift-drag ratio is the same in rotor and stator. Thus

$$\eta_{ps} = 1 - \frac{D}{L}\left[\frac{V_{r_m}}{U \cos \alpha_m} + \frac{V_m}{U \cos \beta_m}\right]$$

From the velocity diagrams, $\cos \alpha_m = V_a/V_{r_m}$ and $\cos \beta_m = V_a/V_m$, so

$$\eta_{ps} = 1 - \frac{D}{L}\left[\frac{V_{r_m}^2 + V_m^2}{UV_a}\right] \tag{4.54}$$

For a given stage, D, L, U and V_a are fixed, hence the stage profile efficiency depends on $V_{r_m}^2$ and V_m^2. By partial differentiation, it is readily found that η_{ps} is a maximum when $V_{r_m} = V_m$. The velocity diagram then shows that for this condition the diagram must be symmetrical about the axis. By substitution of $V_m = V_{r_m}$ in Eq. (4.54), and putting $V_{r_m}^2 = V_a^2 + (U/2)^2$, differentiating with respect to V_a/U and setting the result equal to zero, it follows that the maximum efficiency requires $V_a/U = \frac{1}{2}$, whence $\alpha_m = \beta_m = 45°$ and the reaction R is 0·5.

A reaction of 50% is very common for both compressors and turbines. Although the above analysis requires some rather broad assumptions, it is generally valid in that a middle value of reaction yields a better efficiency than do extreme values, either large or small. This may be seen qualitatively from a consideration of velocity triangles. With a symmetrical arrangement, no velocities, either relative or absolute, are extreme. On the other hand, a reaction near zero or unity results in a very asymmetrical diagram, with at least one velocity relatively high. Since losses are proportional to V^2, the stage efficiency suffers. Another advantage of 50% reaction blades is that, because of symmetry, rotor and stator are similar. This can have some possible advantage in manufacturing, although usually the differing requirements of root fixing militate against this.

4.21 *Three-dimensional Considerations*

All of the previous discussion of blade performance has been confined essentially to *two-dimensional* flow, that is, flow around a profile of infinite length and of the same shape throughout that length. A finite blade set in a rotor or stator row, introduces three-dimensional aspects, which may be considered under two heads: (1) variation of blade angles with radius due to varying rotor speed and other aspects of the effect of radius, and (2) losses additional to the profile or cascade loss, due to the presence of the bounding annuli walls and to the clearance between blade tip and wall.

Taking the former first, quite obviously varying blade speed from root to tip requires a varying velocity triangle in order to obtain optimum incidence at all radii. A more complex consideration is

that of radial variations of the fluid state which may occur due to the rotational component of velocity V_u. A rotational velocity introduces a centrifugal effect and radial motion may occur. Departure of a streamline from a given radius at the trailing edge of a blade row leads to uncertainty regarding the flow at the leading edge of the succeeding blade row and it is possible to minimize this by maintaining radial equilibrium.

Consider an infinitesimal segment of fluid at radius r, Fig. 4.24, subtending an angle $d\theta$ and bounded by radii $(r + dr)$ and r. The segment has an angular velocity ω and thus a tangential velocity $V_u = \omega r$. Equilibrium requires that the centrifugal force, F_c, acting radially outwards be balanced by a pressure force, F_p, due to pressure $p + dp$ at radius $r + dr$ and pressure p at radius r. The fluid is considered to be a gas, so that potential energy due to height above a datum is negligible, but also as incompressible to the extent that ρ is constant. The centrifugal force per unit depth perpendicular to the plane of rotation is F_c = mass $\times$ radial acceleration =

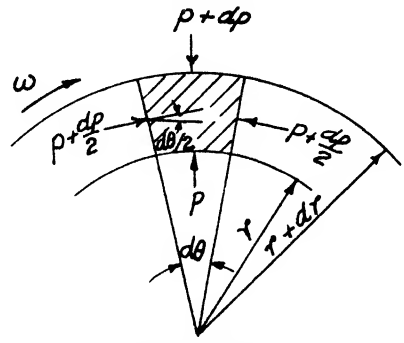

FIG. 4.24. Radial equilibrium diagram.

$$\frac{\rho}{g_0}\pi\,[\,(r + dr)^2 - r^2]\,\frac{d\theta}{2\pi}\,\frac{V_u^2}{r}$$

$$= \frac{\rho}{g_0}\,V_u^2\,dr\,d\theta, \text{ dropping second order differentials.}$$

The pressure force per unit length, taking into account the component on the radial surfaces, is

$$F_p = (p + dp)\,2\pi\,(r + dr)\,\frac{d\theta}{2\pi} - 2\left(p + \frac{dp}{2}\right)dr\,\sin\frac{d\theta}{2} - p2\pi r\,\frac{d\theta}{2\pi}$$

For infinitesimal angles, $\sin(d\theta/2) = d\theta/2$ and then, dropping terms of second order, $F_p = r\,dp\,d\theta$.
Equating F_p and F_c,

$$\frac{\rho V_u^2}{g_0}\,dr\,d\theta = r\,dp\,d\theta$$

and

$$\frac{dp}{dr} = \frac{\rho V_u^2}{g_0 r} \qquad (4.55)$$

Equation (4.55) gives the radial pressure gradient in terms of the tangential velocity and radius.

For flow in the absence of external torque and friction, the Euler flow equation applies along a streamline, that is

$$\frac{dp}{\rho} + \frac{VdV}{g_0} = 0 \tag{4.34}$$

For a fluid having a purely rotational motion, $V = V_u$, hence

$$\frac{dp}{\rho} + \frac{V_u dV_u}{g_0} = 0 \tag{4.56}$$

Combining Eqs. (4.55) and (4.56) gives

$$\frac{dp}{\rho} = \frac{V_u^2}{g_0 r} dr = -\frac{V_u dV_u}{g_0}$$

and hence $\dfrac{dV_u}{V_u} + \dfrac{dr}{r} = 0$

Integrating,

$$V_u r = \text{constant} \tag{4.57}$$

This relationship of tangential velocity and radius is known as a *free vortex* and occurs in nature in tornados and whirlpools. It can be deduced directly from Eq. (4.1), as with $\tau = 0$, then $V_{u_1} r_1 = V_{u_2} r_2 = \text{constant}$

Considering now the flow leaving the trailing edge of a blade in an annular row of blades in an axial-flow machine, the absolute velocity V has components V_u and V_a, thus the Euler flow equation becomes

$$\frac{dp}{\rho} + \frac{V_u dV_u}{g_0} + \frac{V_a dV_a}{g_0} = 0$$

Then for ideal flow with radial equilibrium, Eq. (4.55) must apply, giving

$$V_u^2 \frac{dr}{r} + V_u dV_u + V_a dV_a = 0 \tag{4.58}$$

A given relationship of V_u and r then requires a fixed relationship of V_a and r, determined from Eq. (4.58). For example, if a free vortex relationship is taken, i.e. the blade trailing edge angle is designed so that $V_u \propto 1/r$, then

$$V_u r = \text{constant}$$

and

$$\frac{dr}{r} = -\frac{dV_u}{V_u}$$

Substituting this into Eq. (4.58) yields

$$V_a dV_a = 0$$

which gives two possible solutions, the trivial one of $V_a = 0$ (no flow) or V_a = constant. Thus blading design for free vortex flow with radial equilibrium requires $V_u \propto 1/r$ and V_a constant with radius. This is a simple design condition and requires no special distribution of axial velocity initially, as without guide vanes, the flow of fluid into a row of axial-flow blades is uniform and axial. Furthermore, with free vortex flow into and out of a blade row, the energy transfer is constant with radius, since $E \propto \Delta(UV_u)$ and $U \propto r$ and $V_u \propto 1/r$.

However, although free vortex flow is a simple criterion and recommends itself as a naturally-occurring phenomenon, it has some drawbacks which will be discussed in the separate analyses of compressors and turbines. Other vortex flow patterns are possible and may be generalized into a vortex relationship $V_u r^n$ = constant. Thus free-vortex flow has $n = 1$. For any value of n except $n = 0$, which is a special case, combination of the radial equilibrium equation (4.55), the Euler equation (4.34) and the general vortex equation $V_u r^n$ = constant, yields after integration between stations 1 and 2,

$$V_{a_1}^2 - V_{a_2}^2 = V_{u_1}^2 \left(\frac{n-1}{n}\right)\left[\left(\frac{r_1}{r_2}\right)^{2n} - 1\right] \tag{4.59}$$

For free-vortex flow, with $n = 1$, this reduces to $V_{a_1}^2 = V_{a_2}^2$ = constant, as was shown previously. Another common pattern is that of *solid rotation*, i.e. as for a rigid body, which has constant angular velocity ω. Since $\omega = V_u/r$, then V_u/r = constant and n has a value of -1. Eq. (4.59) then reduces to

$$V_{a_1}^2 - V_{a_2}^2 = 2V_{u_1}^2 \left[\left(\frac{r_2}{r_1}\right)^2 - 1\right] \tag{4.60}$$

From this it is seen that as the radius increases, the axial velocity decreases. Thus for a given radius ratio or *hub ratio*, and a given tangential velocity at the root, there is a limiting value of root axial velocity which corresponds to a zero value of axial velocity at the tip. Alternatively, for fixed values of velocities, there is a limiting hub ratio.

A value of $n = 0$ corresponds to V_u = constant, i.e. it is indeterminate. Using the three relationships of radial equilibrium, Euler flow and V_u = constant and integrating gives

$$V_{a_2}^2 = V_{a_1}^2 - 2V_u^2 \ln (r_2/r_1) \tag{4.61}$$

Again this requires axial velocity decreasing from root to tip and a limiting value of hub ratio.

For an untwisted blade, i.e. constant outlet angle α referred to the *tangential* direction, then $V_a = V_u \tan \alpha$. Using this relationship, as before, then for radial equilibrium,

$$V_u r^{\cos^2 \alpha} = \text{constant} \tag{4.62}$$

i.e. $n = \cos^2 \alpha$. The corresponding axial velocity relationship is $V_a r^{\sin^2 \alpha} = \text{constant}$.

For small values of α, $\cos^2 \alpha$ is not far from unity and $\sin^2 \alpha$ is very small. Thus designing for free vortex flow with $V_{u_r} = \text{constant}$ and V_a constant, with a constant outlet angle, is not very far removed from a radial equilibrium condition. This is sometimes used in turbine nozzles, where α, the nozzle angle, is often small, and untwisted blades allow a simplification in manufacture.

An important consequence of designing for radial equilibrium with any kind of radial distribution of tangential and axial velocities, is that the *reaction* varies from root to tip. This generalization can be seen qualitatively by noting that through a stator row there is no change in total pressure (except for minor losses) but there is a change in velocity, varying from root to tip, and thus a radial variation of static pressure. At rotor discharge, there is again a uniform radial static pressure and the change of static pressure across the rotor will thus vary with radius. Only in special cases then will the reaction be constant with radius. Designation of a stage having vortex flow with radial equilibrium as having a certain degree of reaction can refer only to a particular radius, either the mean radius or a designated " design " radius.

4.22 *Three-dimensional Flow Losses*

The loss measured in a cascade is a pure *profile* loss, and the experimental conditions are rigorously controlled to this end, so that the length of the blade section and the wall conditions have no effect. For finite blades in an annular row, the bounding surfaces of the inner and outer annuli introduce a skin friction loss. A boundary layer develops from the leading edge of the bounding duct onwards, growing rapidly in the adverse pressure gradient of compressors and much less rapidly for turbines, in which acceleration occurs. The interaction of the tip and root of both rotor and stator blades with the boundary layers causes complex secondary flow effects. Such flow discontinuities appear as vortices, whose dissipation gives rise to areas of total pressure loss at root and tip. These three-dimensional losses may account for up to 50% of the total

loss in a well-designed compressor (i.e. one with low two-dimensional cascade loss) and thus are of considerable interest. Although much has been found out about the nature of the secondary flow, most of it is only qualitative and the quantitative aspects are still largely empirical.

The two-dimensional loss is accounted for by the drag coefficient, C_{D_p}, with the additional subscript p now indicating *profile* loss. Similarly, the wall friction or *annulus* loss is denoted by C_{D_a} and the *secondary flow* loss by C_{D_s}. Thus the total drag coefficient C_{D_0} is

$$C_{D_0} = C_{D_p} + C_{D_a} + C_{D_s} \tag{4.63}$$

The analysis of three-dimensional loss in terms of drag coefficient rather than pressure loss coefficient is useful because of the association with induced drag of the isolated airfoil. The coefficients C_{D_a} and C_{D_s} will be discussed in more detail separately for compressor and turbine.

REFERENCES

1. Shepherd, D. G. *Principles of Turbomachinery*. The Macmillan Co., N.Y., 1956.
2. Wirt, L. New Data for the Design of Elbows in Duct Systems. *General Electric Review*, **30**, 1927, p. 286.
3. Patterson, G. N. Note on the Design of Corners in Duct Systems. *Aeron. Res. Coun.* R. and M. No. 1773, H.M.S.O., London, 1936.
4. Patterson, G. N. Modern Diffuser Design. *Air. Eng.*, **9**, 1938, p. 267.

CHAPTER 5

THE CENTRIFUGAL COMPRESSOR

THE centrifugal compressor is best suited to small units of comparatively low pressure ratio where overall diameter is not a restricting criterion. Although the centrifugal unit led the way to the first British and American turbo-jets, following the pioneer work of Whittle (Ref. 1), it has been almost universally supplanted by the axial-flow compressor for jet aircraft, whose high speed necessitates the lowest possible frontal area. The centrifugal compressor is suitable for turbo-prop units, whose function is in medium-speed aircraft, but its chief use is in shaft-power units of small output, where simplicity, light weight and ruggedness are more important than maximum efficiency and low diameter.

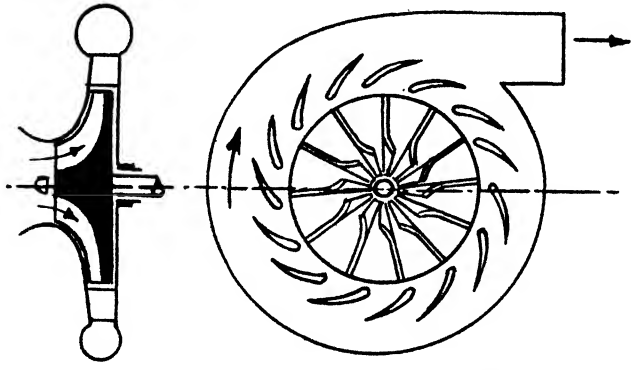

FIG. 5.1. Typical centrifugal compressor.

The centrifugal impeller has had a long history in pumps and fans, and as a medium pressure unit, as part of a multi-stage compressor. For the gas turbine, however, it has developed markedly in pressure ratio and efficiency at high speed, again largely due initially to the efforts of Whittle. A typical form is shown in Fig. 5.1, having three-dimensional vanes which extend into the inlet eye and having a radial discharge. The Euler equation, with signs reversed so that

E is positive (since it is recognized that the energy transfer is always from rotor to fluid), gives

$$E = \frac{1}{g_0}(U_2 V_{u_2} - U_1 V_{u_1})$$

$$= \frac{1}{2g_0}[(V_2^2 - V_1^2) + (U_2^2 - U_1^2) + (V_{r_1}^2 - V_{r_2}^2)]$$

From the viewpoint of energy transfer alone (i.e. pressure rise or pressure ratio), this shows that U_2 should be greater than U_1, V_{u_1} should be small, V_2 should be greater than V_1 and that the rotor should diffuse the flow ($V_{r_2} < V_{r_1}$). The simplest situation is with $V_{u_1} = 0$, that is purely axial flow into the eye. This is the most common practical case, because usually there is only a short fairing duct in front of the compressor and thus the air is induced straight in from atmosphere. The energy transfer E then becomes $U_2 V_{u_2}/g_0$ and is controlled entirely by the impeller discharge design. This will be analysed in the first place for ideal flow.

5.1 *The Ideal Impeller*

Fig. 5.2 shows a generalized velocity diagram for the impeller discharge. The air is considered to leave the impeller with relative velocity V_{r_2} at angle β_2, the discharge *vane angle*. Vector addition of the impeller linear velocity or *tip-speed* U_2 gives the *absolute discharge velocity* V_2. V_2 can be resolved into two components, the *tangential* velocity V_{u_2} and the *radial* velocity V_{m_2}. V_{u_2} is the component representing energy transfer and V_{m_2} is the component representing flow rate, as the product of V_{m_2} and the circumferential area $A_2 = \pi D b$ gives the volume flow rate. The Euler equation can be transformed into a more directly useful form as follows:

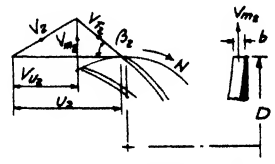

FIG. 5.2. Discharge velocity diagram for radial-flow impeller.

$$E = \frac{U_2 V_{u_2}}{g_0} = \frac{U_2}{g_0}(U_2 - V_{r_{u_2}}) = \frac{U_2}{g_0}(U_2 - V_{m_2} \cot \beta_2) \qquad (5.1)$$

For a given impeller running at a constant speed, i.e. fixed U_2 and β_2, E is then a linear function of V_{m_2}. Thus with $V_{m_2} \propto$ flow rate Q,

$$E = K_1 - K_2 Q$$

For $\beta_2 < 90°$, $\cot \beta_2$ is positive and the E-Q line has a negative slope as shown in Fig. 5.3. For $\beta_2 = 90°$, $\cot \beta_2 = 0$, and E does not

vary with Q. For $\beta_2 > 90°$, cot β_2 is negative and the E-Q line has a positive slope. At zero flow, E has the same value for any value of β_2. Vanes with $\beta_2 < 90°$ are called *backward-curved* vanes, with $\beta_2 = 90°$, *radial* vanes, and with $\beta_2 > 90°$, *forward-curved* vanes. Corresponding velocity diagrams for the same values of U_2 and V_{m_2} are shown in Fig. 5.3, thus the diagrams correspond to impellers of the same tip speed and flow rate. A plot of energy transfer E (as head or pressure) against flow rate (as Q or m) is known as a characteristic line or usually simply as a *characteristic*.

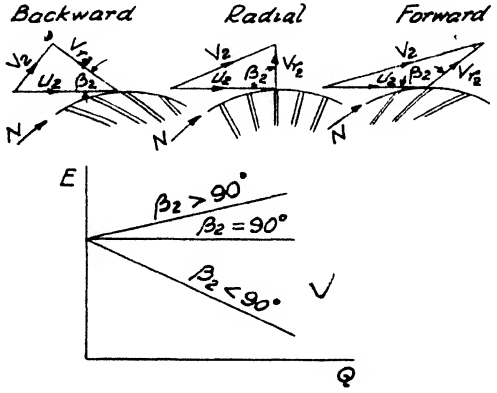

FIG. 5.3. Characteristics of backward-curved, radial, and forward-curved vanes.

5.2 *Analysis of the Ideal Diagrams*

Comparison of the three diagrams shows that the energy transfer, which is proportional to V_{u_2}, is least with backward-curved vanes, increasing with increase of β_2. Thus it would appear desirable for maximum pressure ratio with a given impeller always to use forward-curved vanes. However, it will be seen that nearly all the increase of E as β_2 increases is due to increase of discharge velocity V_2, that is to kinetic energy. This means that in order to obtain the equivalent high static pressure ratio, then a considerable amount of diffusion is necessary in the fixed casing following the impeller. This is difficult to do efficiently without an excessively large diffuser, with the result that the overall compressor efficiency is low. In terms of degree of reaction, a radial-vaned impeller ($\beta_2 = 90°$) has $R \approx 0{\cdot}5$, while for very large values of β_2, it can exceed unity. Evaluating the problem on an absolute basis, the impeller tip speed can have values up to about 1700 fps, from which it will be seen that V_2 can have high supersonic values for forward-curved vanes.

Diffusion of velocities of this value cannot be performed efficiently, as even with a low rate of diffusion to avoid separation, the friction loss would be high.

The result is that most centrifugal impellers for gas turbines have radial vanes, representing a compromise between maximum pressure ratio, maximum efficiency and size. An almost equally important reason, when high speeds are used, is that the radial-vaned impeller gives rise to the lowest disc stress due to the vane mass loading. With radial vanes, the vane loading imposes only a direct centrifugal stress, whereas any curvature of the vanes introduces bending stresses in addition. A third point is that purely radial vanes are much easier to manufacture than curved vanes, a criterion whose importance depends on the application.

The suitability of radial vanes is not absolute, however. Any reduction of the discharge velocity V_2 is beneficial for efficiency and a high value of energy transfer can still be obtained with backward-curved vanes if the radial velocity is made sufficiently small. Fig. 5.4 shows a comparison of radial vanes and backward-curved vanes, the latter with a much lower radial velocity and hence relative velocity. The difference in V_{u_2} is small, but the reduction in V_2^2 is considerable. However, another doubtful point arises in that V_{r_2} is now probably much smaller than V_{r_1}, so that considerable diffusion must take place in the impeller itself. This can lead to poor impeller efficiency, so that the gain in casing diffuser efficiency may be offset. There are insufficient data to be able to generalize on this feature, so that the best one can say is that no one particular feature should be made extreme. It is one of the unfortunate features of centrifugal compressors that little else but a rotating test of the complete compressor can give a reliable answer, as intake, impeller and casing are mutually dependent to a considerable extent. On the other hand, for both axial-flow compressors and turbines, a great deal of information can be obtained from static blade cascade tests. This is not to deny the importance of the proper analysis and testing of the component parts of a centrifugal compressor, that is the inducing section, the radial part of the impeller and the diffuser, but rather to emphasize the interdependence of these units.

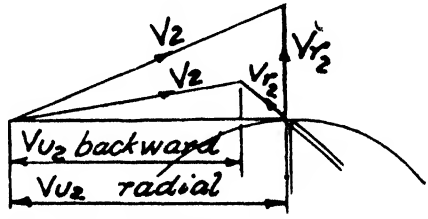

FIG. 5.4. Reduction of kinetic energy with backward-curved vanes.

5.3 *Modification of the Ideal Diagram—Slip*

For the ideal impeller, the fluid was assumed to follow the blade contour, so that at discharge the blade angle β_2 was used as the energy transfer criterion. In fact, the fluid always leaves the vane at an average angle which is *less* than the geometrical blade angle. Thus in Fig. 5.5 for an impeller with radial vanes ($\beta_2 = 90°$), the fluid leaves at an angle α_2 which is less than 90°, with the result that, for the same V_{m_2}, the tangential component V_{u_2} is reduced to $V_{u_{2'}}$. The difference between the tangential components of the relative velocities $\Delta V_{r_u} = V_{ru_2} - V_{ru_{2'}}$ is known as the *slip* of the impeller. For the radial-vaned impeller, the ratio of the tangential components of the absolute velocity with and without slip, $V_{u_{2'}}/V_{u_2}$, is known as the *slip factor*, denoted by μ. Slip may be explained, and quantitatively analysed, by means of the aerodynamic phenomenon of circulation or by other more sophisticated techniques, but here it will suffice to discuss it in terms of the original "relative eddy" method of Stodola. Qualitatively, a group of fluid particles having a particular orientation at entry to the impeller channel retains this orientation as the group moves radially outward along the channel. Thus in Fig. 5.6, at A the orientation is radial. At B, which represents the same channel at a small increment of time later, the group has moved outwards but has retained its orientation with respect to fixed axes by virtue of its inertia. A further stage is known at C, while D represents the group at the moment of discharge. The orientation, fixed with respect to the surroundings, has changed, in this particular representation, by 90° with respect to the channel, or has effectively rotated through 90° in the opposite direction to the impeller rotation. Thus the relative velocity of the fluid has received a tangential component, resulting in the slip shown in Fig. 5.5. This explanation is imprecise, but nevertheless the simple quantitative expression evolved by Stodola on this basis gives values surprisingly close to those given by much more complex analyses. The result may be expressed as

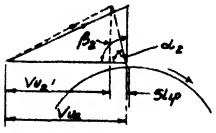

FIG. 5.5. Slip in an impeller.

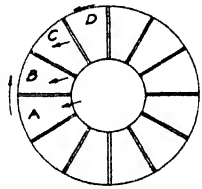

FIG. 5.6. Slip as represented by "relative eddy."

$$\Delta V_{r_{u_2}} = U_2 \frac{\pi \sin \beta_2}{n}$$

where n is the number of vanes or number of channels.

Thus

$$V_{r_{u_{2'}}} = V_{r_{u_2}} + \Delta V_{r_{u_2}}$$

and

$$V_{u_{2'}} = V_{u_2} - \Delta V_{r_{u_2}} = V_{u_2} - U_2 \frac{\pi \sin \beta_2}{n}$$

and

$$\mu = \frac{V_{u_{2'}}}{V_{u_2}} = 1 - \frac{U_2}{V_{u_2}} \frac{\pi \sin \beta_2}{n} \tag{5.2}$$

which for $\beta_2 = 90°$ reduces to

$$\mu = 1 - \frac{\pi}{n} \tag{5.3}$$

More exact analyses, corresponding well with test results, show that for $\beta_2 = 90°$,

$$\mu = 1 - \frac{0{\cdot}63\pi}{n} = 1 - 0{\cdot}315\,\theta \tag{5.4}$$

where $\theta = \dfrac{2\pi r}{nr} = \dfrac{2\pi}{n}$, the channel angle or angle subtended by adjacent vanes. This result, Eq. (5.4), is valid only for a fairly large number of vanes, about 8 or more, and may be further approximated by the simple expression $\mu = (n - 2)/n$.

For discharge vane angles less than 90°, the substantiation of theoretical analyses by test data is less satisfactory, but the Stodola expression may be used as giving a conservative estimate. Again, for $\beta_2 < 90°$, a complicating factor is introduced by virtue of non-uniform distribution of velocity in the axial direction and in the circumferential direction. This is not " slip ", although it gives rise to the same effect of reducing the possible amount of energy transfer. In the previous analyses, any velocity V has been taken as representing a uniform velocity over the cross-sectional area normal to it. However, a given flow rate Q may occur with any non-uniform distribution and it may be shown that the energy transfer for any given value of Q and fixed area A is less for any non-uniform velocity than for a uniform velocity. This effect may be represented by a velocity distribution coefficient C_v, with $C_v > 1$, applied to the radial velocity V_{m_2}. Hence, with no slip,

$$E = \frac{U_2}{g_0} (U_2 - C_v V_m \cot \beta_2)$$

For radial vanes, with $\cot \beta_2 = 0$, the distribution coefficient theoretically has no effect and this appears to be borne out by test

values of slip factor agreeing with theoretical values, with no further correction necessary for C_v. For $\beta_2 < 90°$ however, C_v does have an effect, but as the velocity distribution for a given impeller is not known exactly, it can only be included in empirically determined values of overall slip factor. Thus the Stodola expression for slip, which yields rather lower values than do more precise analyses, appears to be a reasonable working expression, as it compensates for lack of knowledge of velocity distribution.

To summarize the effect of slip and velocity distribution on energy transfer, we have first of all the " diagram " or *Euler* energy transfer, E_E, with fluid angles identical with blade angles, thus,

$$E_E = \frac{U_2 V_{u_2}}{g_0} = \frac{U_2}{g_0}(U_2 - V_{m_2} \cot \beta_2) \tag{5.1}$$

The actual energy transfer E is

$$E = \frac{U_2 V_{u_{2'}}}{g_0} = \frac{U_2}{g_0}(U_2 - C_v V_{r_{u_{2'}}})$$

For radial-vaned impellers,

$$\mu = \frac{V_{u_{2'}}}{V_{u_2}}$$

and

$$E = \frac{\mu U_2 V_{u_2}}{g_0} = \frac{\mu U_2^2}{g_0} \tag{5.5}$$

5.4 *Compressor Efficiency*

The expressions for energy transfer developed above give E, the rotor work input, all of which is transferred to the air, but not necessarily in useful form. For air, the useful form of energy is the pressure, mostly static pressure, but including some dynamic pressure if this can be utilized in the succeeding component. Recalling the discussion in the previous chapter, the overall stagnation isentropic efficiency is

$$\eta_c = \frac{\Delta h_0}{\Delta h_{0'}} = \frac{c_p \Delta T_0}{c_p \Delta T_{0'}} \approx \frac{T_{0_1}(P_{r_0}^{\epsilon} - 1)}{T_{0_{2'}} - T_{0_1}}$$

For a given pressure ratio, P_{r0}, the difference between the isentropic change of temperature, ΔT_0, and the actual change of temperature, $\Delta T_{0'}$, represents the energy which has been dissipated by fluid

friction, eddies and mixing, into internal energy. Thus for a radial-vaned impeller,

$$E = c_p J \Delta T_{0'} = \frac{\mu U_2^2}{g_0}$$

and hence

$$\Delta T_0 = \eta_c \Delta T_{0'} = \frac{\eta_c \mu U_2^2}{c_p J g_0} \tag{5.6}$$

or

$$U_2^2 = \frac{c_p J g_0 \Delta T_0}{\mu \eta_c} \tag{5.7}$$

where $\Delta T_0 = T_{0_1}(P_r{}'_0 - 1)$

Eq. (5.6) gives the isentropic work for a given blade speed and assumed slip factor and efficiency, from which the pressure ratio can then be calculated. Eq. (5.7) gives the blade speed required to produce a given pressure ratio for an assumed slip factor and efficiency.

It should be remembered that the efficiency η_c is usually the overall compressor efficiency from inlet to discharge and thus includes the diffuser. Energy can be transferred only in the rotor and only losses can occur in the diffuser. Thus the impeller efficiency must be higher than the compressor efficiency. The three main component elements of the compressor, the inducing section, the impeller and the diffuser, will be discussed from the viewpoint of their design and their effect on overall efficiency.

5.5 *Inducing Section*

The function of the inducer is to receive the air at the correct angle of incidence and to turn the air so that it is axial with respect to the impeller. For the usual case of the absolute inlet velocity being axial, the inlet vane angle α_1, Fig. 5.7 (a), may be small, thus requiring a large air deflection, $(90 - \alpha_1)$. The problem is really one of an axial-flow cascade and such data may be utilized wherever possible. Because the necessary fluid deflection is large, close vane spacing or low s/c is necessary. For low s/c, the vane chord should be large and the pitch small. The inducer should then be long in the axial direction with as many blades as possible. The latter requirement often conflicts with Mach number limitations at high flow rates and high rpm, as a serious blockage effect can

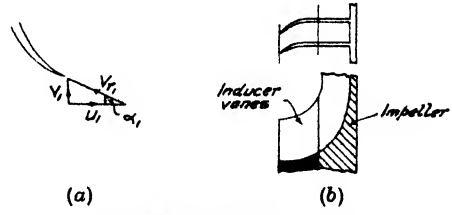

FIG. 5.7. Inducer section.

occur. Because it is difficult to obtain the optimum vane angles by bending a one-piece machined impeller, it is common practice to make a separate inducer which fits on to the impeller proper, Fig. 5.7 (b). The NACA have investigated the design of inducers, and Reference 2 may be consulted for detailed information. The vanes should operate with a few degrees of positive incidence (Sec. 4.16) as this minimizes choking effects.

For high flow rate and high rpm, the tip of the inducer vane is critical with respect to Mach number. For a given flow rate and eye root diameter, the annular intake area may be large, resulting in a low axial velocity and high eye tip speed, or it may be small, giving a higher axial velocity and lower eye tip speed. The critical velocity is that relative to the vane, V_{r_1}, and Fig. 5.8 (a) shows qualitatively

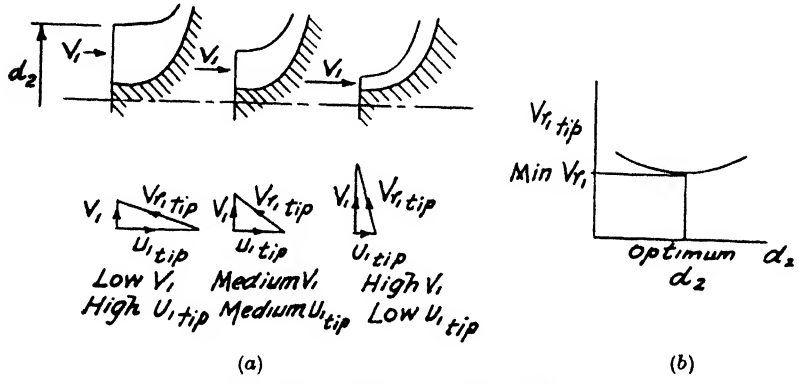

FIG. 5.8. Optimum inducer size.

how this varies between the two extremes. There is an intermediate value which gives the minimum value of V_{r_1}. By assuming a value of V_1, the annulus area, and hence the eye tip diameter d_2, is fixed from continuity. V_{r_1} can then be calculated from the velocity triangle and plotted against d_2. This results in a curve as in Fig. 5.8 (b), from which the minimum value of V_{r_1} can be selected. Since it is actually the Mach number $V_{r_1}/a_1 = V_{r_1}\sqrt{/gkRT_1}$ which is critical, it should be remembered that as V_1 increases, T_1 and P_1 decrease, since the stagnation values remain constant for reversible adiabatic flow. Thus the inlet density and the local acoustic velocity a_1 vary for each value of V_1 and d_2. Finally then M_{r_1} should be plotted to obtain the optimum solution.

While limiting values of Mach number are usually in the range 0·7–0·8 for flow over blades, the critical value for the inducer of radial-flow compressors is somewhat uncertain. The Mach number

decreases from the eye tip inwards and thus only a local effect occurs. It would seem possible that as the flow condition at the tip is usually poor because the air in that region almost immediately flows round the inside radius of a bend, then a high Mach number causes relatively little additional effect. Compressors have been used successfully with nominally high tip Mach numbers, but if possible it is best to design for low values.

If the eye tip Mach number is excessive, then it is possible to reduce it by means of *prewhirl*. Prewhirl is the name given to the deliberate introduction of a component of tangential velocity to the absolute velocity at intake, this component being in the direction of rotation. This is shown in Fig. 5.9. The prewhirl is given by a set of fixed intake guide vanes preceding the impeller. It is generally possible to obtain substantial reduction of V_{r_1} with a moderate amount of prewhirl, but it is accompanied by a reduction of energy transfer, as there is now a subtractive term $U_1 V_{u_1}/g_0$ in the Euler equation. However, as U_1 is usually considerably less than U_2, the reduction of energy transfer is not large. If a fixed pressure ratio must be maintained, then the impeller tip diameter must be increased over the nominal value without prewhirl. Note that prewhirl must be distinguished from *prerotation*, which is the name usually given to the departure from axial flow at entry which is caused, not deliberately, but by effects which occur due to the whole flow pattern. Thus it has been shown that sometimes there is a reverse flow at the eye tip due to separation in the impeller channel and this produces a rotational effect in the inlet duct. Prerotation is most likely to occur at off-design conditions, most commonly at flows less than design, and it may be caused by flow conditions right downstream in the diffuser casing. It is not subject to design, except in the sense that its occurrence may be minimized by endeavouring to avoid separation in the impeller channel and diffusion casing.

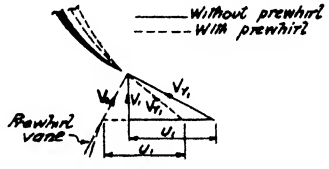

FIG. 5.9. Prewhirl.

5.6 *Impeller Channel*

As the radial-flow impellers for gas turbines usually have radial vanes or do not depart greatly from $\beta_2 = 90°$, the problem of channel shape is mostly in the design of the cross-section in the axial plane. Assuming that the eye dimensions have been calculated for the optimum intake condition and the discharge dimensions by the energy transfer requirement, then the problem is one of channel

flow round a 90° bend with certain dimensions fixed at inlet and outlet.

The impeller has been tacitly assumed up to this point to be open or *single-shrouded*, as at (a) of Fig. 5.10. This construction implies a radial clearance between the vane edges and the front casing, with the opportunity for leakage of air and with casing friction loss due to the absolute velocity. Alternatively, the impeller may be *closed* or *double-shrouded* as at (b). There is then no leakage around the vane edges and the friction loss in the channel is due to the relative velocity of the air. There is possible leakage between front shroud and casing, together with a disc friction loss. While the data are

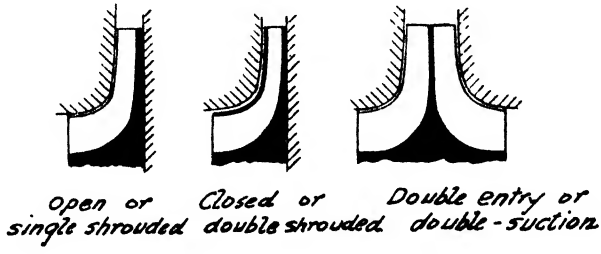

FIG. 5.10. Types of impeller construction.

not altogether conclusive, it appears that the efficiency of the open type is as good as or better than that of the equivalent closed type, if the clearance between vanes and casings can be made small, which is usually possible with precision construction. Furthermore, the closed type is difficult to manufacture except by casting and the stresses induced at the usual high speeds often preclude its use. Part (c) of the figure shows a double-entry type of impeller, which may be necessary if the mass flow requirement is high.

With respect to the cross-sectional shape of the channel, this is in general fixed by the number of vanes, dictated by considerations of slip and blockage, and the impeller tip width, which is largely governed by the desired discharge radial velocity. Within these limits, however, the area should preferably be square, as with friction loss proportional to the length-equivalent diameter ratio, L/d_e, then for a given flow area, d_e is a maximum when the quadrangular channel shape is square. While this requirement takes second place, it should be kept in mind so that the passage shape does not become excessively elongated in one direction. If possible, the number of vanes should be an odd number, as this minimizes harmonics of vibrations induced at the tip by downstream excitation.

The flow pattern in the channel can be calculated for ideal, com-

pressible flow, if only that part of the channel lying in a plane or conical sheet is considered. Several methods have been used (see Ref. 3 for a bibliographical survey) and the results are of considerable use in obtaining a picture of flow conditions. Thus the theoretical distributions of static pressure and relative velocity show where separation is mostly likely to occur due to the interaction of pressure gradient and viscous effects, while the changes in flow pattern as the major parameters of speed and flow rate are changed indicate the direction of performance variations. Valuable as such theoretical analyses are as qualitative indications, the effects of viscosity and departure from uniform inlet conditions limit their usefulness as complete design information. Furthermore, it is known that the diffuser system can exert a very powerful effect on the whole flow régime back to the inlet duct, and thus ideal channel design may produce disappointing practical results because it is not possible to ensure the corresponding ideal inlet and discharge conditions.

The torque is applied to the driving or leading face of the vanes and a higher static pressure results here than on the trailing face or, in other words, at a given radius across the channel, the pressure decreases from leading to trailing face. As the pressures must be equal at the vane tip at discharge, there is a large pressure gradient on the trailing face near discharge and this is usually severe enough to cause flow separation. The air then flows mostly on the leading face side of the channel. Such separation not only causes losses, but leads to an irregular velocity distribution from the impeller tip and hence affects the diffusion in the casing. A " half-vane " is sometimes advocated in the outer portion of the channel, located between the full vanes, in order to reduce slip and to produce a less irregular velocity distribution. This can be beneficial, but, if not placed in exactly the right position, it can intensify an already poor velocity distribution. Thus it is really necessary to know the flow pattern at the radius of the leading edge of the half-vane before it can be properly positioned.

The shape of the bend from the axial to the radial plane is governed by the consideration that, taking into account the variation of channel width with radius in the circumferential direction, the area should be such that the velocity as computed along the mean channel bend line should vary as uniformly as possible. A rather thick boundary layer is formed in the inducer section and some increase of area is needed to avoid possible choking. Furthermore, if the inducer area is not enlarged progressively, the rate of area change in the radial part of the passage may have to be high, thus promoting further the possibility of separation.

Disc stressing is complex, but can be handled by one of the conventional methods. Radial vanes introduce no bending stresses of themselves and are handled as an additional mass under centrifugal action. The vanes can be thin from the steady stress point of view, but it is advisable on a large, heavily loaded impeller to taper them into the disc, so that their cross-section is a blunt wedge shape. This is so that the transmission of vibrations, set up by the rotation of the vane tips past the varying pressure field at diffuser entry, is minimized down the vanes to the eye portion, where vibration fatigue is possible due to resonance with the longer cantilevered eye vanes. A separate inducer section lessens the vibration difficulty, as some additional damping is introduced. Neither stressing nor vibrations can be dealt with here in any detail, as each is a specialist topic and it is difficult to give any general design rules.

5.7 *The Diffuser System*

As previously mentioned, the diffusion casing following the impeller is at least as important as the impeller in its effect on efficiency because, with a radial-vaned impeller, about half the stagnation pressure is in the form of dynamic pressure and most of this must be transformed to static pressure for subsequent efficient use.

The section of the casing following the impeller must both collect the air from the several channels and diffuse it. The air leaving the tip has a high velocity, possibly supersonic, and has a direction making a small angle with the tangential direction, Fig. 5.11 (a).

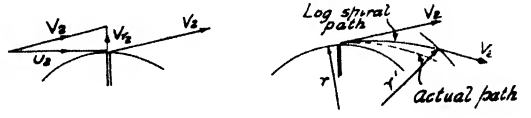

(a) (b)

FIG. 5.11. Flow leaving impeller.

As it travels radially outward, the flow area increases, even if the casing walls remain parallel, because of the greater radius, and thus the velocity is reduced. As there is no longer any torque, the angular momentum remains constant, assuming no frictional effect. Referring back to Eq. (4.1,) then with $\tau = 0$, $V_{u_r} =$ constant or the flow is a *free vortex* (see 4.21) with a superimposed radial flow. If the fluid were incompressible, then the radial velocity component would also vary inversely with radius, as with constant casing width, the area varies directly with radius, and from continuity, $m = A\rho V$, then $V_m r =$ constant. With both V_{u_2} and V_{m_2} varying inversely

with radius, then $V_2 \propto 1/r$ and the flow path may be shown to be a logarithmic spiral. Due, however, to the compressible nature of the flow, the density increases as V_2 is reduced and the path lies inside the log spiral, as shown in Fig. 5.11 (b). For ideal flow, it is possible to combine the free vortex flow relation, continuity and the compressible flow relations so that the velocity may be calculated at any radius. The resulting equation, although not complex, is of high order and requires trial-and-error solution. Likewise, although data are available for estimating friction factors for flow of this nature, the flow pattern is usually so far from uniform that only an approximate estimate can be made. A relatively simple procedure is to calculate for $V_u \propto 1/r$ and to assume a value for V_m at the required radius. This then gives a velocity V and, since the stagnation temperature is constant, a static temperature. Allowing for reasonable loss from entry to the required radius, say about half the total loss based on an assumed overall compressor efficiency, then the static pressure can be calculated. Then with the density known, continuity will give the necessary radial velocity. If this does not check with the assumed value, then a new estimate is made and the procedure repeated, until agreement is reached. This is a rather crude procedure, but owing to the uneven nature of the flow pattern, it is sufficiently exact until test data on the completed compressor allow a more exact calculation to be made and modifications instituted. To provide more diffusion than by simple free vortex with constant annular passage width, the latter may be made to diverge slightly, an included angle of about 6° being the best for maximum efficiency. It is also helpful according to NACA tests to form a throat between impeller discharge and beginning of this *vaneless diffuser*, with the object of smoothing out the flow. A contraction ratio of 0·72 was found to be satisfactory, but such a contraction is only possible for low initial Mach numbers, otherwise choking occurs.

Diffusion in this manner, that is basically by increase of radius with $V_u r$ constant, is reasonably efficient but the rate of diffusion decreases as radius increases and, if carried out to the required final velocity, would necessitate a very large diameter casing. For a more compact arrangement, free diffusion is taken only to a radius about 10–20% greater than the impeller tip radius and then the air is guided by vanes which form a number of separate channels, Fig. 5.12. The axis of the channels makes a greater angle with the tangential direction and the diffusion is governed by straightforward area change. The vanes are called *diffuser vanes* and their design follows those of blade cascades, or alternatively, channel theory may

be followed for the passages, leaving the vane profiles determined by channel boundaries. Adopting the latter viewpoint, then the angle of diffusion should be small, following the general pattern discussed in Sec. 4.10, although often the angle has to be somewhat greater than the optimum in the interests of overall dimensions. Best results are achieved with diffusion in one plane only, with passages as close to square as possible and with a linear axis. The optimum number of vanes is subject to conflicting considerations. From the point of view of rate of area change, the number should be large, as a given area divides into passages of decreasing included angle as the number of passages increases. However, the frictional loss increases (high L/d) and the necessary finite thickness of the vanes reduces the free flow area and increases the velocity. These considerations, however, are usually over-ridden by the fact that the flow from the impeller is not of uniform velocity, but of high velocity from the driving side of the vane and of low velocity from the separated region on the trailing face. If the diffuser channel opening receives air from several impeller channels, then an averaging effect occurs, although the flow pattern is far from ideal. If, however, the diffuser channel opening is smaller than the impeller channel, then it will at one moment receive far more flow than that for which it was designed and then, at the next moment, less flow. Thus the passage may be alternately choked and starved, leading most probably to *surging*, which is explained later. The number of diffuser vanes should then be a minimum consistent with a reasonable value of diffusion angle dictated by a compromise between efficiency and size.

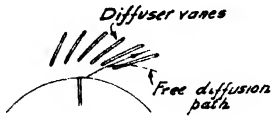

FIG. 5.12. Diffuser vanes.

Fig. 5.13 shows that the vane overlap forms a diffuser *throat* or minimum passage area bounded on both sides by a solid surface. The throat controls the flow rate unless choking occurs in the inducer section, and its area may be used to shift the operating point to some extent. The nominal throat area as computed from free vortex flow and continuity is usually increased some 15% due to the boundary layer and irregular velocity distribution.

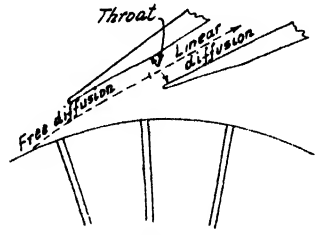

FIG. 5.13. Diffuser-vane overlap and throat.

Following either the vaneless or vaned diffuser, the air must either be collected into a single outlet or distributed into a given number of channels, for passage to the combustor or heat exchanger. If a

single outlet is required, then the diffuser is followed by a *scroll* or *volute* casing, Fig. 5.14 (a), consisting of a passage of increasing area from the tongue to the outlet flange. Although the volute may accomplish some diffusion, it is preferable to increase the cross-sectional area in direct proportion to the angle of advance from the tongue, that is, in proportion to increase of mass flow around the periphery. With no diffusion, then the velocity is nominally constant, and hence the pressure is also constant. If the passage mean-line has an increasing radius beyond that required for increase of mass flow, then some free vortex diffusion is possible, but under these circumstances, it is not an efficient process.

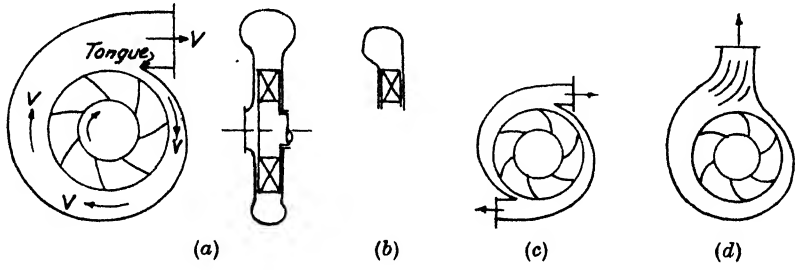

FIG. 5.14.

(*a*) Scroll or volute casing. (*b*) Offset casing. (*c*) Double outlet casing. (*d*) Radial outlet. Volute casings.

The cross-sectional shape of the scroll can be either approximately circular or rectangular. The former is stronger under the high pressures developed but is more difficult to manufacture unless cast. The exact shape does not appear to be important and often it is made asymmetrical in order to reduce the overall diameter, Fig. 5.14 (b). It is possible to have more than one outlet, as shown at (c), or the outlet may be made radial with the help of guide vanes (d).

A volute casing with a single tangential outlet is most often used for industrial gas turbines, in which a heat exchanger or single combustor is utilized. For aircraft engines, such an arrangement is not possible, because of space requirements, and following the diffuser vanes, the air must be turned at right angles into the axial direction. To do this requires guide vanes, as shown in Fig. 5.15. If separate combustors are used, the number of diffuser vane channels can be the same, each with its own set of turning vanes.

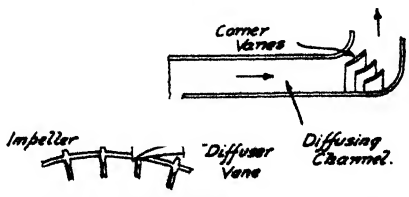

FIG. 5.15. Corner vanes for turning after diffusion.

A comparison of the performance of vaneless and vaned diffuser casings shows that the former is usually slightly less efficient at the design point flow, but has less decrease of efficiency at flows above and below design, that is, it has a wider operating range. The higher design point efficiency of the vaned type is, of course, dependent on a good design to avoid separation, but its narrow range is inevitable because with fixed vane inlet angles, off-design flows give rise to large angles of incidence (Sec. 4.15), with consequent high losses. On the other hand, the vaneless diffuser always has high friction loss due to the long flow path of the quasi-logarithmic spiral, but varying flow angles do not impose high incidence losses. Because the use of gas turbines with centrifugal compressors is tending towards small units where space and weight are important, diffuser vane casings are more generally used.

5.8 *Effect of Losses on the Compressor Characteristic*

The previous discussion of inducer, impeller channel and diffuser flow will show how the ideal characteristic (Sec. 5.1) is modified from a linear relationship. The losses may be divided into *friction* losses, which are proportional to V^2, and hence m^2, (the variation of friction factor with Reynolds number is a second-order effect) and into *incidence* losses, which, in terms of drag coefficient C_D, are proportional to $C_D V^2$. C_D is a minimum only at the design point, increasing more sharply at positive incidence due to stalling (Fig. 4.20). Flows less than design induce positive incidence, so that even the lower velocity does not compensate for increased C_D, with the result that the overall loss due to the wrong angle of attack has a minimum at or near the design point. Fig. 5.16 (a) shows qualitatively these losses plotted against flow rate. If these losses are subtracted from the ideal energy transfer for a radial-vaned impeller, then the linear characteristic becomes curved, with a maximum value of E at some particular value of flow, as shown at (b). For backward-curved vanes, with an ideal characteristic of negative slope, the actual characteristic is less peaked and, with very small values of β_2, may have no positive slope at all, i.e. the pressure always decreases with increase of flow. However, as gas turbine compressors usually

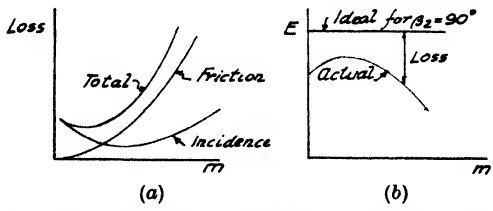

FIG. 5.16. Losses and actual characteristic for a compressor.

have radial vanes, or a limited amount of backward curvature, a typical pressure ratio-mass flow characteristic will have a point of maximum pressure ratio, with a positive slope for lower flow rate and a negative slope for higher flow rate. This fact has a very important bearing on the range of compressor operation, as it is the fundamental reason for surging.

5.9 *Surging*

Fig. 5.17 shows a typical characteristic resulting from the analysis of losses as described above. Suppose that the compressor is operating at point A, when a down-stream effect causes additional resistance to flow, or increases the "back-pressure". At constant speed, the compressor can operate only along its characteristic, so that the equilibrium point moves to B, having a lower flow rate at increased pressure. Further restriction causes the operating point to move successively to lower flow rates, eventually arriving at point C. From this point on, restriction of flow results in a *lower* compressor delivery pressure. Momentarily then, there is a higher pressure in the downstream system than at compressor delivery and the flow stops and even reverses its direction. A very short interval of time later, the duration being dependent on the capacity of the whole system, the compressor again starts to deliver fluid. The pressure starts to increase from a very low value and the operating point will move rapidly along the characteristic from right to left. If the down-stream conditions are unchanged however, then once again flow will break down after point C of maximum pressure, and the cycle will be repeated, usually with a high frequency. This phenomenon is known as *surging* or pumping. Its manifestation is dependent on the level of fluid and rotor velocities and the capacity of the discharge system. At low pressures with a relatively flat characteristic, there may be only a mild instability, denoted by a changed tone of compressor noise and fluctuating pressure, but at high pressures the effect may be almost explosive, with continued operation likely to lead to physical damage due to impact loads and high-frequency vibration. The onset and severity of surging are also controlled by the downstream system, as a small volume will clear rapidly and possibly allow operation on the part of the characteristic with positive slope. It is also possible that resonance occurs, and so changing the natural frequency of the fluid system

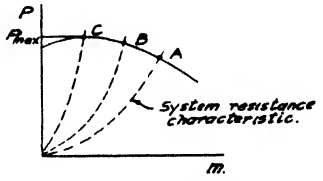

FIG. 5.17. Surging.

can change surge characteristics, although normally this is not possible.

As a result of surge, it is conservative to assume that the compressor cannot be operated at any point to the left of the maximum pressure point, that is, on the positive slope of the characteristic. In a gas turbine, surging may be instituted by a rapid increase in fuel flow, as this may cause the turbine nozzles to choke, or if they are already choking, may cause a sudden reduction of mass flow. A compressor by itself may surge at a sufficiently high speed. The air leaving the impeller tip is diffused rapidly in the vaneless space and more rapidly still when traversing the area between the diffuser tip and the diffuser throat. At high speed, the deceleration may be so rapid that the adverse pressure gradient causes separation, reducing the flow rate so that the compressor operates in the surge area.

At high tip speeds, with radial blades, the absolute velocity is of the order of 1500 fps or greater and, even at the increased temperature due to compression, this represents a Mach number greater than unity. This supersonic velocity is, however, singular in that diffusion in the vaneless space is accomplished without shock, as static pressure measurements at the casing walls give no indication of a discontinuity. A simple explanation may be given by considering the total velocity as resolved into two components, the tangential and the radial. The tangential component, which is supersonic, is governed only by the free vortex law and not by area. The radial component is governed by the area change, but is subsonic. Thus one may assume that the supersonic component passes smoothly to subsonic values without shock when governed only by the law of constant angular momentum.

5.10 *Choking*

At points on the characteristic to the right of the maximum pressure points, that is, at higher mass flow rates, a different situation occurs. As the rotor speed remains constant, the tangential velocity component at the impeller tip remains constant. As mass flow increases, however, the pressure decreases and hence the density is decreased. These effects result in a considerably increased radial velocity, which both increases the absolute velocity and the incidence angle at the diffuser vane tip. There is thus a rapid progression towards a choking state, so that the slope of the characteristic steepens and finally becomes vertical, i.e. the mass flow cannot be increased further.

5.11 *Actual Compressor Characteristic*

The result of losses, surging, and choking is to modify the ideal linear characteristics into the form shown in Fig. 5.18. A large part of the region to the left of the maximum pressure points is inoperable due to surge, this region being delineated by the *surge line*. At the higher rpm, there is only a limited range of possible operation between the surge point and the choking mass flow. The *range* of a compressor may be assessed as the percentage increase of mass flow which is obtainable between the surge point and the point where the efficiency has decreased from its maximum value an arbitrary amount due to the onset of choking. The range can obviously be a very important aspect, because the compressor cannot be operated arbitrarily when it is part of a gas turbine. Its operating line must match that of the turbine driving it and the combination is governed by the load characteristic and the fuel input as it regulates the combustion temperature. The figure shows that the peak efficiencies at each speed are rather close to the surge line, and that if the running line of the complete turbine is not accurately gauged then trouble will occur, due either to surging or to low efficiency. The peak efficiency of a compressor as determined on a separate test may not be realized when it is part of a complete plant, and thus the form of its characteristics may be at least as important as its peak performance.

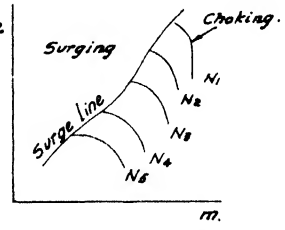

FIG. 5.18. Actual characteristic of a centrifugal compressor.

The centrifugal compressor is a long-established form, but for many years the stage pressure ratio was quite limited owing to a low limit of tip speed dictated by industrial standards. The development of the turbo-supercharger required pressure ratios of 2–2½/1, and the vision of Whittle for the turbo-jet raised it to 4–4½/1. Pressure ratios of 6/1 and even higher have been developed by the Boeing Company (Ref. 4). Pressure ratio is a function of tip speed, slip factor and efficiency; thus, from Sec. 5.4,

$$\Delta T_0 = \frac{\eta_d \mu U_2^2}{c_p J g_0}$$

and

$$\frac{P_{0_2}}{P_{0_1}} = P_{r_0} = \left[\frac{T_{0_1} + \Delta T_0}{T_{0_1}}\right]^{\frac{k}{k-1}}$$

$$= \left[1 + \frac{\eta_d \mu U_2^2}{c_p J g_0 T_{0_1}}\right]^{\frac{k}{k-1}}$$

With values of $\mu = 0{\cdot}9$, $c_p = 0{\cdot}24$ and $T_{0_1} = 519°$ R (288° K), the table below gives values of attainable pressure ratio for a range of tip speeds and efficiencies.

U_2	η_c	P_{r_0}
1500	0·75	4·07
	0·80	4·4
	0·85	4·72
1600	0·75	4·75
	0·80	5·17
	0·85	5·6
1700	0·75	5·57
	0·80	6·1
	0·85	6·65
1800	0·75	6·55
	0·80	7·2
	0·85	7·9

This table gives an idea of the possibilities if high tip speeds can be used. It also shows the great importance of efficiency, not only for its own sake, but in its effect on pressure ratio at a given tip speed.

Efficiency decreases with increase of pressure ratio, 80% being possible at about 2·5/1, about 78% at 4/1 and about 75% at 5/1. Painstaking work and detailed development can slowly raise efficiencies, although no very great improvement is very likely. However 78% efficiency at 1700 fps tip speed would give a pressure ratio of about 6/1, which would give a very reasonable cycle efficiency in conjunction with already achieved turbine efficiencies and combustion temperatures.

5.12 *Effect of Size and Speed*

For small-output gas turbines, where the air mass flow may be only of the order of one to two lb/sec, the impeller can be quite small. For a given tip speed, the rpm must then be high. For example for $U_2 = 1500$ fps, the impeller o.d. is 34·4 in. for 10,000 rpm, 17·2 in. for 20,000 rpm, 8·6 in. for 40,000 rpm and 5·73 in. for 60,000 rpm. The question then arises as to any effect of size and speed on efficiency.

Size effects are, of course, best correlated in terms of Reynolds number, with the characteristic dimension the impeller tip diameter,

the characteristic velocity the impeller tip speed and with the fluid properties evaluated at the inlet conditions. Balje (Ref. 5) presents a detailed analysis of the possible effect of Reynolds number, which shows a considerable reduction with decrease of R_e, a reduction of approximately 8 to 10 points for a tenfold change of Reynolds number for example. Detailed data on the effect of Reynolds number alone are difficult to come by, but the reduction does not appear to be nearly as large as indicated above.

With respect to the effect of speed of rotation alone, there may be a change in performance due to varying proportions of energy transfer from increase of angular velocity and from increase of radius of rotation. Data available on this effect are limited to one series of NACA tests, which indicates that for a given tip speed, better performance is given by increasing angular velocity than by tip diameter. Thus a small impeller running at high rpm appears to be better than a larger impeller at a lower rpm. This is in spite of a higher Mach inlet number in the former case and a lower nominal Reynolds number. One cannot, therefore, generalize with confidence on the effect of rotor size on efficiency.

REFERENCES

1. Whittle, F. Reference 1 of Chapter 1, and Cheshire, L. J. Centrifugal Compressors for Aircraft Gas Turbines. *Proc. I. Mech. E.*, **153**, 1945; reprinted by *A.S.M.E.* 1947, *Lectures on the Development of the British Gas-Turbine Jet Unit.*
2. Johnson, I. A., and Ginsburg, A. Some N.A.C.A. Research on Centrifugal Compressors. *Trans. A.S.M.E.*, **75**, 1953, p. 805.
3. Shepherd, D. G. *Principles of Turbomachinery.* The Macmillan Co., N.Y., 1956.
4. Hage, S. D. *et al.* Compressor Development for Small Gas Turbines. *A.S.M.E.* Paper No. 57-A-258, 1957.
5. Balje, O. E. A Contribution to the Problem of Designing Turbomachines. *Trans. A.S.M.E.*, **74**, 1952, p. 451.

CHAPTER 6

THE AXIAL-FLOW COMPRESSOR

For most aircraft and industrial gas turbines, the axial-flow compressor is used in preference to the radial-flow type, because it has a higher efficiency and is capable of a higher pressure ratio on a single shaft. The basic reasons for this are that the fluid flow is deflected in one plane only and that the average velocities are much lower. As a result, the energy transfer in a single *stage* is very limited, a stage pressure ratio of about 1·2 being a high value for conventional compressors. However, the ease of combining axial-flow stages, as compared with the difficulty of staging the radial-flow type, leads to overall pressure ratios of up to 6/1 or even higher in some instances. Thus the axial-flow compressor is normally considered as consisting of a number of stages, with a single stage being considered as a fan. The breakdown into stages has led to a very detailed knowledge of the axial-flow compressor, both with respect to design procedure and with respect to the flow pattern, so that considerable empirical data and theoretical analysis are available. Having said this, it must also be emphasized that axial-flow compressor design is extremely complex from the point of view of obtaining the optimum design for a given duty, because of the very large number of variables involved. This chapter can discuss certain principles only, with no attempt at indicating an optimum design procedure. Chapter 4 indicated not only that there was a difference between American and British blade terminology, but also that there can be a basic difference in outlook, as exemplified by the channel approach and the airfoil approach, that is, in the expression of performance in terms of either fluid deflection or of lift coefficient. Together with the possible variations in number of stages, diameter and speed, choice of which depends on the application of the gas turbine, then it is possible here only to indicate the effect of the major design variables. The British method of analysing design performance is used, because more generalized data are available for use and its application is relatively straightforward in principle.

6.1 *Energy Transfer*

For axial flow, with $U_1 = U_2 = U$, then the Euler equation

becomes

$$E = \frac{U}{g_0}(V_{u_2} - V_{u_1})$$

or

$$E = \frac{1}{2g_0}[(V_2^2 - V_1^2) + (V_{r_1}^2 - V_{r_2}^2)]$$

For a stage in general, there is a whirl component both at inlet and outlet, so that V_{u_1} cannot be omitted as was done for the radial-flow compressor. It will be seen from the second form of the equation that in general the absolute velocity is increased in the rotor and that the relative velocity is decreased. Regarding a stage, that is rotor and stator, as one of many, then the rotor increases the energy, both kinetic and static, and the function of the stator is twofold, first to transform the increased kinetic energy to pressure and secondly to discharge the fluid at the proper angle for the succeeding stator. In most compressors, the increase of static pressure in the rotor is about equal to that in the stator, i.e. the stage has a reaction of about 50%. Thus both sets of blades diffuse the flow, and both turning and diffusion are limited for good efficiency, so the stage energy transfer is also limited compared to what is possible in the radial-flow stage or in a turbine stage.

6.2 *Velocity Diagrams*

Fig. 6.1 shows a typical stage with associated velocity diagrams. Because the density change is usually small and the area change for constant throughflow velocity is small, the axial velocity is usually considered constant across a stage. This is important, because it leads to many simple relationships for axial-flow compressors. In practice, the axial velocity is usually kept constant by a progressive reduction of area from inlet to discharge of the whole rotor, so that the assumption is justified. Exceptions do occur, most frequently in the last stage or so, when it may be desirable to reduce the axial velocity in order to avoid too large a value of leaving velocity which might penalize the following component. As a consequence of constant axial velocity, the inlet and outlet velocity diagrams may be superimposed, as shown in the *combined* diagram of Fig. 6.2. Such a diagram gives a considerable amount of information, both qualitative from inspection and quantitative by further analysis.

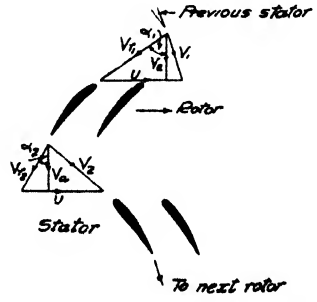

FIG. 6.1. Typical axial-flow stage.

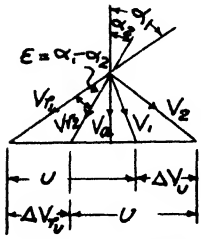

FIG. 6.2. Combined diagram.

The angle between V_{r_1} and V_{r_2}, $(\alpha_1 - \alpha_2)$, is the air *deflection*, ϵ. The difference of absolute tangential velocity, $\Delta V_u = V_{u_2} - V_{u_1}$, is a measure of the energy transfer. With constant V_a, then the change of absolute tangential velocity is equal to the change of relative tangential velocity, because from the diagram,

$$U = V_{r_{u_1}} + V_{u_1} = V_{ru_2} + V_{u2}$$

$$\therefore V_{u_2} - V_{u_1} = V_{r_{u_1}} - V_{r_{u_2}} \tag{6.1}$$

This relationship also gives a means of expressing the basic Euler equation in a more useful form in terms of flow rate (expressed as axial velocity V_a) and fluid angles at the rotor (α_1 and α_2), and hence rotor blade angles. From the Euler equation,

$$E = \frac{U}{g_0}(V_{u_2} - V_{u_1}) = \frac{U}{g_0}(V_{r_{u_1}} - V_{r_{u_2}})$$

and substituting $V_{r_u} = V_a \tan \alpha$, then

$$E = \frac{UV_a}{g_0}(\tan \alpha_1 - \tan \alpha_2) \tag{6.2}$$

The combined diagram also shows graphically the degree of reaction. The reaction R has been defined as, (Sec. 4.1),

$$R = \frac{\frac{1}{2g_0}[(U_1^2 - U_2^2) + (V_{r_2}^2 - V_{r_1}^2)]}{E}$$

For the axial-flow compressor, $U_1 = U_2$, and reversing the signs for compression, then

$$R = \frac{V_{r_1}^2 - V_{r_2}^2}{2U(V_{u_2} - V_{u_1})} \tag{6.3}$$

From the diagram it is seen that

$$V_{r_1}^2 = V_a^2 + V_{r_{u_1}}^2$$

and

$$V_{r_2}^2 = V_a^2 + V_{r_{u_2}}^2$$

hence

$$V_{r_1}^2 - V_{r_2}^2 = V_{r_{u_1}}^2 - V_{r_{u_2}}^2$$

Substituting in (6.3) and also using (6.1),

$$R = \frac{V_{r_{u1}}^2 - V_{r_{u2}}^2}{2U\,(V_{r_{u1}} - V_{r_{u2}})} = \frac{V_{r_{u1}} + V_{r_{u2}}}{2U} \qquad (6.4\text{ a})$$

Defining a mean tangential relative velocity, $V_{r_{u_m}}$,

$$V_{r_{u_m}} = \frac{V_{r_{u1}} + V_{r_{u2}}}{2}$$

then

$$R = \frac{V_{r_{u_m}}}{U} \qquad (6.4\text{ b})$$

This relationship is shown in Fig. 6.3 (a) for a general case, with $R \approx 0{\cdot}7$, (b) for 50% reaction, and (c) for a special case with rotor outlet velocity V_2 in the axial direction. For the last case, the

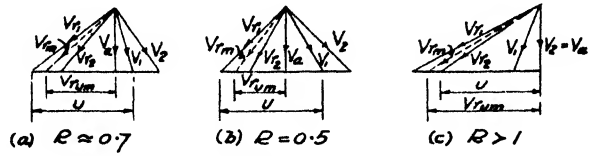

FIG. 6.3. Mean relative velocity.

reaction is *greater* than unity, with the absolute velocity being decreased in the rotor. A value of $R > 1$ implies that the energy transfer in the rotor by virtue of change of static pressure is greater than the total stage energy transfer, i.e. the air is *accelerated* in the stator, so that the static pressure at rotor inlet is below that at entry to the previous stator. This naturally places the burden of a large change of static pressure, i.e. ΔV_r^2, on the rotor, but the argument for it is that the stator acceleration gives the best possible velocity distribution to the rotor, which can then operate at peak efficiency.

It will be seen that the definition of $V_{r_{u_m}}$ also defines a mean relative velocity, V_{r_m}, shown in Fig. 6.4, not as the mean of V_{r_1} and V_{r_2}, but given by the tangential components. Eqs. (6.4) are very useful to keep in mind for obtaining a quick estimate of stage reaction from a velocity diagram. For quantitative use, knowing the fluid angles, it can be put into the following form.

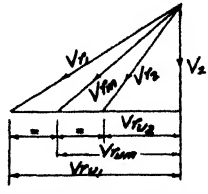

FIG. 6.4. Degrees of reaction.

$$R = \frac{V_{r_{u1}} + V_{r_{u2}}}{2U} = \frac{1}{2}\frac{V_a}{U}(\tan\alpha_1 + \tan\alpha_2) \qquad (6.5)$$

Eqs. (6.2) and (6.5) for energy transfer and reaction are basic forms for the axial-flow compressor stage, as they are in terms of blade speed U and flow rate V_a, both probably known from initial decisions, while values of α_1 and α_2 are determined from cascade data.

6.3 *Actual and Ideal Energy Transfer*

The energy transfer is given in terms of *fluid* angles, α_1 and α_2 and in terms of axial velocity V_a. It was noted in Sec. 4.16 that fluid angles are seldom the same as blade angles, because of incidence at inlet and deviation at outlet. Incidence is controllable and is a design parameter adjusted for a given performance from cascade data in relation to desired operating range, Mach number behaviour and so forth. The deviation, however, is a phenomenon akin to slip of the radial-flow compressor and due to the same basic aerodynamic reasons. The deviation occurs so that the energy transfer is always less than that calculated from blade angles, that is, less than the " Euler head ". Again, this does not affect efficiency, but modifies only the possible energy input. Exact knowledge of deviation is important, because the fluid deflection is limited in axial-flow blading and only a degree or so of deflection less than estimated can have a serious effect on energy transfer. It is reasonable to suppose that deviation is a function of blade spacing (as for slip), of degree of blade curvature, that is, of blade camber, and of blade profile. Test data show that these factors may be grouped into an expression

$$\delta = m\sqrt{\frac{s}{c}}\,\theta \tag{6.6}$$

where m is a factor dependent on blade profile and blade setting. A constant value of $m = 0{\cdot}26$ was used in early work and is still a fair value to use in the absence of precise blade data. However, Fig. 6.5 shows m plotted against stagger angle for two common blade forms, as given by Carter and Hughes (Ref. 1). Using Eq. (6.6) with $m = 0{\cdot}26$ shows that the deviation is considerable. Thus for $\theta = 30°$ and $s/c = 1$, then $\delta = 0{\cdot}26\ (30°) = 7{\cdot}8°$, over one-quarter of the geometrical change of direction of 30°.

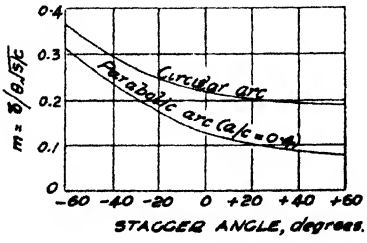

FIG. 6.5. Deviation factor as a function of blade stagger (adapted from Carter and Hughes, ref. 1).

For the annulus of an axial-flow compressor, the axial velocity distribution from inner to outer radius (root to tip) is designed to conform to a certain pattern. The form of distribution is connected

with the vortex pattern (Sec. 4.21) and will be considered in more detail shortly, but no matter what the ideal form, it is modified by the boundary layer at the inner and outer surfaces. Considering a constant axial velocity for simplicity, Fig. 6.6 (a) shows a typical modification of velocity profile through several stages. The effect

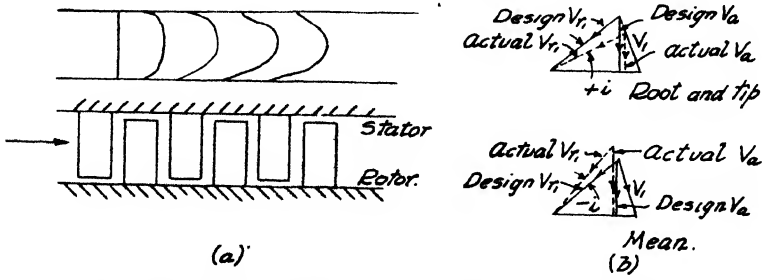

FIG. 6.6. Effect of peaked velocity distribution on air angle.

is more marked than in pipe flow because of the severe adverse pressure gradient. The growth of boundary layer causes a lower velocity near root and tip and a higher velocity in mid-span. The effect on the velocity diagram is shown in Fig. 6.6 (b), resulting in a higher positive incidence at root and tip, and a lower incidence, possibly negative, at mid-span. Ideally, the reduced energy transfer at mid-span due to reduced α_1 is compensated by higher energy transfer at root and tip. However, the blade is probably designed on the basis of a certain uniform axial velocity, so that the design point deflection is a little less than the stalling deflection (Fig. 4.19). Hence little, if any, increased deflection is obtained at root and tip, which may be in the stall region at the extreme. The overall result is a reduction of energy transfer E due to reduced change of whirl velocity. In this instance, there may be an accompanying effect on efficiency if the root and tip sections are stalled to any appreciable degree, but this is indirect, as again the main phenomenon is akin to a reduction of Euler energy transfer.

It is very difficult to predict the change of axial velocity distribution for any particular compressor, but Howell (Ref. 2) has given the generalized results of a considerable number of compressor tests in the form of a " work-done factor " Ω to be applied to the nominal energy transfer, plotted against number of stages, as shown in Fig. 6.7. Thus the actual energy transfer becomes

$$E = \Omega \frac{UV_a}{g_0} (\tan \alpha_1 - \tan \alpha_2) \qquad (6.7)$$

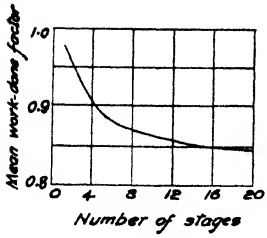

FIG. 6.7. Value of mean work-done factor (adapted from Howell and Bonham, ref. 2).

Fig. 6.7 shows that Ω decreases rapidly for the first few stages, levelling off to a value around 0·85 for a large number of stages. In this diagram, Ω is the coefficient to be applied to each stage of a compressor of a given number of stages, that is, it is a mean value, not an individual value, for each stage. It should be noted that not all compressors appear to exhibit this reduction of energy transfer, as the effect depends on the nominal design point with respect to the stall point and on the growth of boundary layer. Thus, although Fig. 6.7 does represent a considerable amount of experience, its application may be regarded as conservative practice.

6.4 *Coefficients of Performance and Efficiency*

Some dimensionless coefficients of performance have been found useful in various methods of analysis. A brief account of the method and use of dimensional analysis is given in Chapter 10 and this should throw some light on the meaning of dimensionless groups and their advantages. Here the parameters will be deduced directly from relationships already used.

The first such dimensionless parameter is the *flow* coefficient, ϕ, defined as

$$\phi = \frac{V_a}{U} \tag{6.8}$$

The second parameter is the *pressure coefficient*, ψ_p, defined as

$$\psi_p = \frac{\Delta P_0}{\rho U^2/2g_0} \tag{6.9}$$

The third parameter is the *temperature rise coefficient*, ψ_T, defined as

$$\psi_T = \frac{c_p \Delta T_0}{U^2/2g_0 J} \tag{6.10}$$

(6.9) and (6.10) can be transformed into terms of U, V_a, α_1 and α_2. The energy transfer in thermodynamic terms is equated to that in terms of the Euler equation (cf. Chapter 4), thus

$$E = c_p \Delta T_0 J = \frac{\Omega U V_a}{g_0} (\tan \alpha_1 - \tan \alpha_2)$$

Hence

$$\psi_T = \frac{c_p \Delta T_0 J}{U^2/2g_0} = 2\Omega \frac{V_a}{U} (\tan \alpha_1 - \tan \alpha_2) \tag{6.11}$$

Further, from Fig. 6.2, $U = V_a (\tan \alpha_1 + \tan \alpha_0)$

$$\therefore \psi_T = 2\Omega \frac{\tan \alpha_1 - \tan \alpha_2}{\tan \alpha_1 + \tan \alpha_0} \tag{6.12}$$

Introducing the stage stagnation isentropic efficiency, η_s, with

$$\eta_s = \frac{(\Delta T_{0_{12}})_{\text{isen}}}{(\Delta T_{0_{12}})_{\text{act}}} = \frac{T_{0_1} [P_{r_0}^{\epsilon} - 1]}{\Delta T_0}$$

and using the relationship for infinitesimal stage efficiency (4.24), with $P_{r_0} = P_{0_2}/P_{0_1} = (1 + \Delta P_0/P_{0_1})$, then

$$\Delta T_0 = T_{0_1} \left[\left(1 + \frac{\Delta P_0}{P_{0_1}} \right)^{\epsilon/\eta_s} - 1 \right] \tag{6.13}$$

With $\Delta P_0/P_{0_1} \ll 1$, then the first term in round brackets can be expanded to $\left(1 + \frac{\epsilon}{\eta_s} \frac{\Delta P_0}{P_{0_1}} \ldots\right)$, dropping terms of second order or higher as being negligible small. Thus there results

$$\Delta T_0 = T_{0_1} \frac{\epsilon}{\eta_s} \frac{\Delta P_0}{P_{0_1}}$$

or

$$\Delta P_0 = \frac{P_{0_1}}{T_{0_1}} \frac{\eta_s}{\epsilon} \Delta T_0$$

Substituting $P_{0_1}/T_{0_1} = \rho_0 R = \rho J(c_p - c_v) = \rho_0 J c_p (k - 1)/k$, then

$$\Delta P_0 = \eta_s \rho_0 c_p \Delta T_0 J$$

Hence

$$\psi_p = \frac{\Delta P_0}{\rho_0 U^2/2g_0} = \frac{\eta_s \rho_0 c_p \Delta T_0 J}{\rho_0 U^2/2g_0} = \eta_s \psi_T \tag{6.14}$$

The simple expression (6.14) depends on the assumption of a small pressure rise and nominally constant density. This is satisfactory for most axial-flow compressors.

Regarding a row of blades, either moving or stationary, as a means of increasing static pressure by virtue of decreasing the velocity, absolute in the stator and relative in the rotor, then the static isentropic efficiency may be regarded as the same as the incompressible flow diffuser efficiency. In Fig. 6.8, the flow through the blade passage is represented as shown by 1–2′. If the process were isentropic, then it would be as shown by 1–2, with the isentropic efficiency η_{s_s} given by $\Delta T_{\text{is}}/\Delta T_{\text{act}}$.

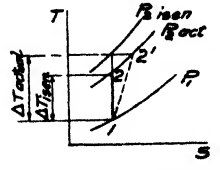

FIG. 6.8. Blade Efficiency.

Now

$$\Delta T_{is} = T_1 \left[\left(\frac{P_{2act}}{P_1} \right)^{\epsilon} - 1 \right] = T_1 \left[\left(\frac{P_1 + \Delta P_{act}}{P_1} \right)^{\epsilon} - 1 \right]$$

Expanding by the binomial theorem as previously demonstrated and dropping terms of the power of two and higher, as $\Delta P/P$ is very small, then

$$\Delta T_{is} \approx T_1 \cdot \frac{\epsilon \Delta P_{act}}{P_1}$$

Similarly

$$\Delta T_{act} = T_1 \left[\left(\frac{P_{2is}}{P_1} \right)^{\epsilon} - 1 \right] \approx T_1 \epsilon \frac{\Delta P_{is}}{P_1}$$

Hence

$$\eta_{s_s} = \frac{\Delta T_{is}}{\Delta T_{act}} \approx \frac{\Delta P_{act}}{\Delta P_{is}} \tag{6.15}$$

From the Bernoulli equation,

$$\Delta P_{is} = \frac{\rho}{2g_0} (V_1^2 - V_2^2) = \frac{\rho V_1^2}{2g_0} \left(1 - \frac{V_2^2}{V_1^2} \right)$$

Referring to Fig. 6.2,

$$V_1 = \frac{V_a}{\cos \alpha_1} \text{ and } V_2 = \frac{V_a}{\cos \alpha_2}$$

$$\therefore \Delta P_{is} = \frac{\rho V_1^2}{2g_0} \left(1 - \frac{\cos^2 \alpha_1}{\cos^2 \alpha_2} \right) \tag{6.16}$$

thus

$$\eta_{s_s} = \frac{\Delta P_{act}}{\frac{\rho V_1^2}{2g_0} \left(1 - \frac{\cos^2 \alpha_1}{\cos^2 \alpha_2} \right)} \tag{6.17}$$

The efficiency η_{s_s} may also be expressed as

$$\eta_{s_s} = \frac{\Delta P_{act}}{\Delta P_{is}} = \frac{\Delta P_{is} - \Delta P_{loss}}{\Delta P_{is}} \tag{6.18}$$

From Eq. (4.53), relating pressure loss and drag coefficient, replacing V_a by $V_1 \cos \alpha_1$,

$$\Delta P_1 = \frac{\rho V_1^2}{2g_0} \frac{C_D}{s/c} \frac{\cos^2 \alpha_1}{\cos^3 \alpha_m} \tag{6.19}$$

Using Eqs. (6.16), (6.18) and (6.19), then

$$\eta_{s_s} = 1 - \frac{\frac{C_D \cos^2 \alpha_1}{s/c \cos^3 \alpha_m}}{1 - \frac{\cos^2 \alpha_1}{\cos^2 \alpha_2}} \tag{6.20}$$

The above relationships are useful in plotting characteristics and in calculating stage performance. Thus plotting $\phi = V_a/U$ against $\psi_p = 2g_0\Delta P_0/\rho U^2$ gives the stage characteristic in dimensionless co-ordinates. The relationship $\psi_p = \eta_s\psi_T$ with $\psi_T = 2\Omega V_a$ $(\tan\alpha_1 - \tan\alpha_2)/U$ gives the pressure rise in terms of fluid angles. Eq. (6.20) expresses the blade row efficiency as a ratio of actual to ideal static pressure rise in terms of fluid angles, blade parameters and drag coefficient.

6.5 *Blade Cascade Data*

The previous section gave relations governing energy transfer and efficiency. For a given performance, it is then necessary to select fluid angles, stagger and blade spacing, from which blade angles can be determined for a chosen incidence and calculated deviation. Recollecting the discussion of Sec. 4.19 on the effect of stagger on amount of diffusion, together with the variables of blade profile and spacing, it will be appreciated that the problem of generalizing blade performance data is difficult. However, Howell

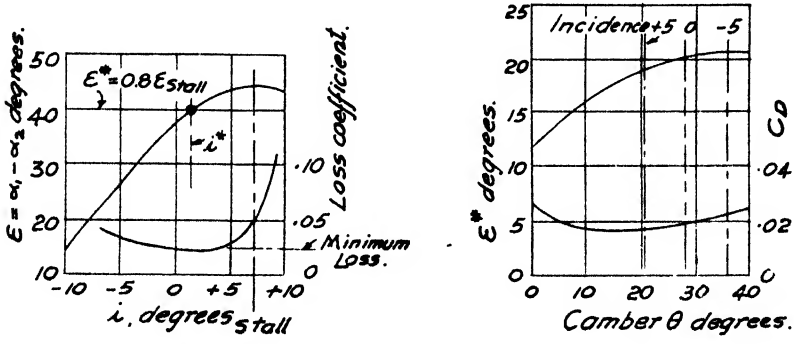

FIG. 6.9. Generalization of results using nominal values.
(*a*) Nominal values of ϵ and i. (*b*) ϵ^* and blade camber.

and his co-workers at the National Gas Turbine Establishment have presented results of a very large number of cascade tests covering a considerable range of variables. The method of generalizing the many performance plots such as Fig. 4.19 lies in selecting a *design point* for each plot. The design point is arbitrary, that used by Howell being defined as that where the fluid deflection ϵ is 0·8 of the stalling value of deflection, with the latter defined as that corresponding to a loss coefficient twice that of minimum loss. These individual design points, with corresponding incidences are denoted by "starred" values, i.e. ϵ^*, i^*, etc., and called *nominal* values.

Fig. 6.9 (a) shows a typical plot with the nominal values indicated. Nominal values for many arrangements can then be collected and generalized results presented.

Fig. 6.9 (b) shows nominal deflection ϵ^* as a function of blade camber θ for a fixed value of outlet angle α_2 and blade spacing. It is seen that at the higher values of ϵ^*, the amount of camber has little effect, i.e. for high camber, the associated nominal values of incidence and deviation result in an approximately constant deflection. Thus $\epsilon^* = 20°$ for a camber of 30° with zero incidence would be a suitable design condition for this particular blade arrangement. The loss associated with this is given by a drag coefficient (profile drag only) of about 0·018, another typical generalized design value.

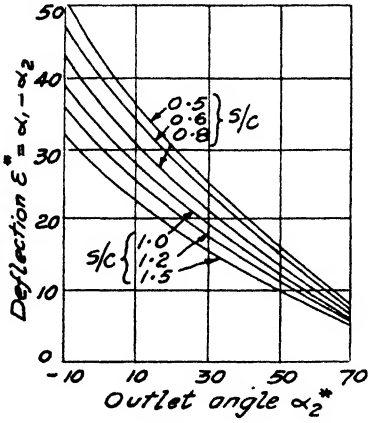

Fig. 6.10. Nominal deflection ϵ^* *vs* α_2^* (adapted from Howell, refs. 2 and 5).

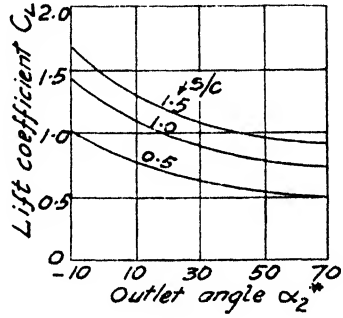

Fig. 6.11. Nominal lift coefficient C_L^* *vs* α_2^* (adapted from Howell, ref. 5).

With ϵ^* almost independent of θ, then blade data can be plotted as ϵ^* or C_L^* against stagger (i.e. blade setting) for the nominal loss condition, with blade spacing as a parameter. Howell gives his results in terms of nominal outlet fluid angle α_2^* rather than of stagger angle, as this is a more useful form for design. Figs. 6.10 and 6.11 show ϵ^* and C_L^* respectively, plotted against α_2^*, for a range of s/c. Permissible deflection or lift coefficient decreases with increased outlet angle (increased stagger, see Fig. 4.22) and increased pitch-chord ratio (or decreased solidity). Fig. 6.12 shows these results plotted as $(\tan \alpha_1 - \tan \alpha_2)$ against α_2, which gives the most direct form for energy transfer. From this, it is seen that over a considerable range of α_2, the effective energy transfer is almost independent of α_2. Between 0° and 40°, it is possible to approximate

the tangent difference by

$$\tan \alpha_1 - \tan \alpha_2 = \frac{1{\cdot}55}{1 + 1{\cdot}5\, s/c}$$

which represents a simple rule for a preliminary design calculation.

For conditions other than design, Fig. 6.13 shows actual/nominal values in non-dimensional form. These then can be used for estimating off-design points, that is, for calculating the characteristic of pressure rise or pressure ratio against mass flow for a given speed.

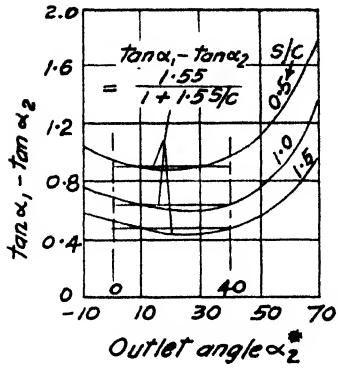

FIG. 6.12. Nominal values in terms of (tan α_1–tan α_2) (adapted from Howell, ref. 5).

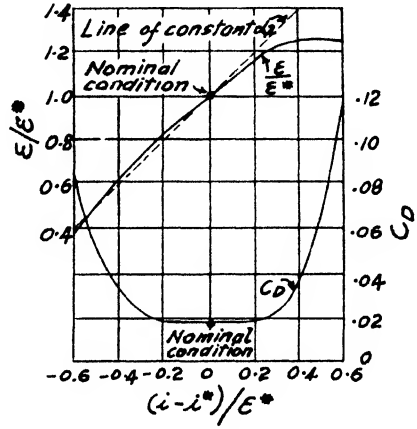

FIG. 6.13. Off-design data in terms of nominal values (adapted from Howell, ref. 5).

Figs. 6.10–6.13 represent the reduction of a considerable amount of data in very useful form, but it should be remembered that it is generalized information. It allows blades to be designed within the range of the charts with reasonable certitude of obtaining the desired performance. Such performance may not be the optimum possible, because of the necessary generalizations, but exact data can be obtained from individual cascade tests confined to the region indicated by the chart values. It should also be remembered that the nominal values are based on $\epsilon^* = 0{\cdot}8\epsilon$ at the stalling point, so that in some cases it may be possible to operate at higher values.

The NACA method of generalization is based on a design point angle of attack (see Fig. 4.21) for which the measured pressure distribution shows no velocity peaks on either surface. This criterion allows operation at high critical Mach numbers. In general, the design point indicated by this method is near the middle of the low-drag range, so that it allows efficient operation at off-design conditions on either side. The NACA data cover the 65-series blading

of varying camber as expressed by the design lift coefficient C_{L_0} of the isolated airfoil, and with nominal 10% thickness ratio. The blading nomenclature is given by the profile series identification 65 — followed by C_{L_0} in tenths and finally by the thickness number 10, i.e. 65– (12) 10 indicates a blade of the above type with a C_{L_0} of 1·2. The published results include cambers from C_{L_0} of 0 to 2·7, inlet angle β_1 of 30°, 45°, 60° and 70° and solidity c/s of 0·50, 0·75, 1·00, 1·25 and 1·50. (Very approximately, $C_{L_0} = \theta/24$, with θ the blade camber angle of British usage.) Three plots of results from Ref. 3 are reproduced here as Figs. 6.14, 6.15, and 6.16, for c/s of

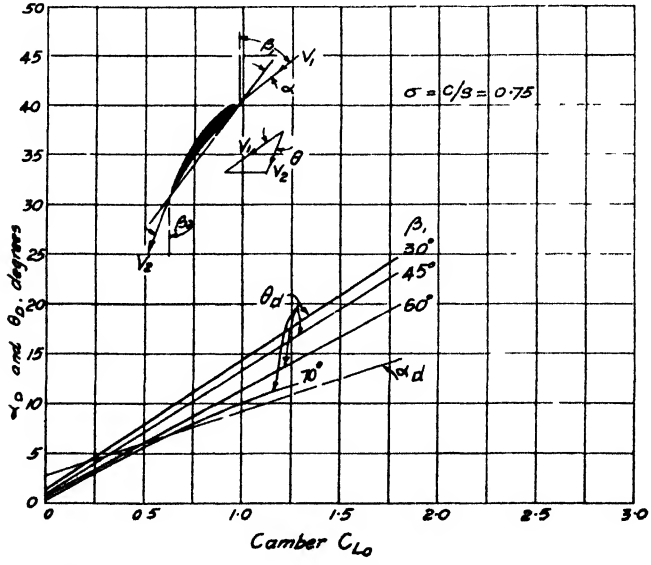

FIG. 6.14. Design deflection and angle of attack as a function of blade camber-solidity of 0·75.

0·75, 1·00 and 1·50 respectively, showing the design angle of attack a_d and design air deflection θ_d as ordinate against c/s as abscissa, with β_1 as parameter. These summary curves are only a small part of the data given in the quoted report, which gives full details of limits of useful operating range of each blade arrangement. In addition, the surface pressure distributions are given together with drag coefficient C_D, lift-drag ratio, L/D, and an additional loss coefficient C_{W_1}. The latter, called the *wake coefficient*, expresses the momentum difference between the wake flow and the downstream flow outside the wake, and is used in assessing the contribution of the wake in the summation of forces.

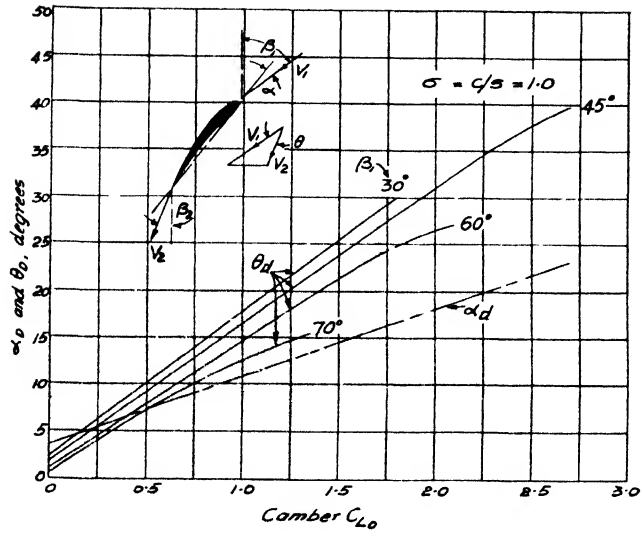

FIG. 6.15. Design deflection and angle of attack as a function of blade camber-solidity of 1·0.

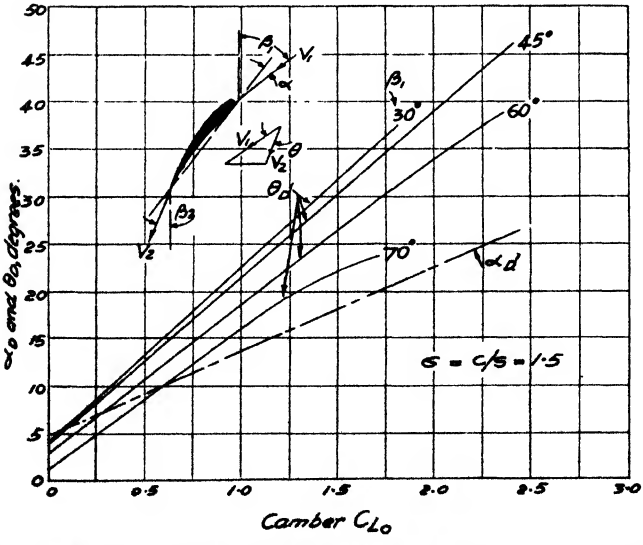

FIG. 6.16. Design deflection and angle of attack as a function of blade camber-solidity of 1·5.

Comparative tests of NGTE and NACA blading have shown close correspondence. It should be emphasized that cascade tests require extreme attention to detail, otherwise the data may be valid only for the conditions of the particular wind-tunnel used. The wall boundary layer exerts a powerful effect and great care is taken to remove the tunnel boundary layer immediately prior to the test section by means of suction, usually through porous walls. The level of turbulence is a controlling parameter as well. Incompatibility of data on the same blade sections is usually attributable to either or both of these reasons. Although it may be argued that blades in service will have to operate over a wide range of turbulence and boundary layer conditions, it is desirable for all cascade tests to be made under conditions which are standardized, so that valid comparisons can be made.

6.6 *Reynolds and Mach Number Effects*

The blade data given previously are valid for "low speed" cascades, where the velocity is low enough so that compressibility effects do not occur, i.e. there are no effects due to Mach number. On the other hand, the Reynolds number must be sufficiently high so that it is above a certain critical value. The Reynolds number $\rho Vc/\mu$, is based on the chord length c as characteristic dimension. Data on the effect of Reynolds number are not very precise, although a value of 2×10^5 is often given as a critical value below which the loss increases quite rapidly. The critical value is dependent on the level of turbulence (hydrodynamic turbulence), a high value allowing a lower Reynolds number. It seems certain that a value of Re of less than 1×10^5 results in considerably increased loss, while above 2×10^5 there is only a very gradual decrease in loss. For low-speed cascade tests, say a velocity of 200 fps, then at atmospheric pressure and temperature, the blade chord must be at least two inches in order for the Reynolds number to be above 2×10^5.

The Mach number affecting the blades is that of the absolute velocity for the stator and of the relative velocity for the rotor, with the temperature being the local static temperature. Thus the rotor Mach number is proportional to $V_{r1}/\sqrt{T_1}$ and the following stator Mach number is proportional to $V_2/\sqrt{T_2}$. The local velocity increases on the convex surface of the blade and it may become supersonic. Then toward the rear of the blade, the velocity is reduced as the pressure increases and the deceleration is accompanied by a shock wave, as depicted in simplified fashion in Fig. 6.17. There is a certain loss of total pressure across the shock, as discussed

in Sec. (4.12) for plane shock in a channel, and a sudden rise in static pressure. It is the latter which causes most of the loss, because the adverse pressure gradient causes separation in the boundary layer. If the velocity is further increased, then the loss increases very rapidly until the passage chokes. Three values of Mach number for blades are distinguished: (1) the *critical* Mach number M_c, at which the local velocity first equals the local acoustic velocity; (2) the *drag-critical* Mach number M_{dc}, at which the loss or drag coefficient has increased to 1·5 times its minimum value at the same incidence; and (3), the *maximum* Mach number M_m, at which choking occurs. M_c and M_{dc} are not the same for a blade in a cascade as for the isolated airfoil, because the adjacent blades form a channel which has a varying pressure gradient. M_m, of course, has no meaning except for a channel.

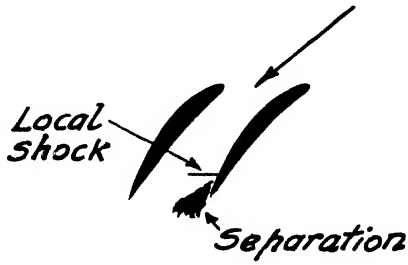

FIG. 6.17. Local shock and separation.

Critical values of Mach number depend largely on blade form, both for thickness, which should not exceed a t/c of 8–9% for high limiting values, and for profile shape. The latter affects not only M_c, but the relative values of M_{dc} and M_m. Carter (Refs. 1 and 4) gives information on the use of blades with circular-arc and parabolic-arc camber lines, with the former giving higher values of M_{dc} and lower values of M_m than the latter, that is Mach number effects are postponed for circular-arc blades, but the working range to the choking point is reduced. Because the critical values of Mach number are so dependent on blade form, it is again not possible to generalize, but for a thin profile, a value of M_{dc} of 0·75–0·80 should be possible. The angle of incidence affects M_{dc}, with zero incidence usually being best. Mach number is particularly a problem for aircraft gas turbines because the air temperature decreases with altitude and thus either the operating value at ground level must be conservative or deterioration of performance at altitude must be expected.

6.7 *Blade Loading and Diffusion Factor*

It has been emphasized that compressor cascade performance is governed by the degree of diffusion and turning possible with reasonable loss. Much attention has been given from time to time to correlation of blade performance in terms of diffusion parameters, such as pressure rise (Howell, Ref. 5), inlet and outlet velocity ratio (de Haller, Ref. 6), etc., with a varying degree of success. A satis-

factory criterion would seem to demand consideration of degree of deflection (turning), of degree of diffusion and of degree of fluid guidance (pitch-chord ratio). A new criterion embodying these factors has been developed at the NACA and recently made available. This blade-loading or *diffusion* factor D is developed from consideration of the local surface velocity and overall velocity characteristics and geometry of the blade. The end result is the diffusion factor D, which can be expressed as (Ref. 7).

$$D = 1 - \frac{V_{r_2}}{V_{r_1}} + \frac{V_{u_2} - V_{u_1}}{2V_{r_1}c/s}$$

$$= 1 - \frac{\cos a_1}{\cos a_2} + \frac{\cos a_1}{2c/s}(\tan a_1 - \tan a_2)$$

(For a cascade or stator row, the relative velocities V_r become the absolute velocities V.) For values of D up to about 0·3, the loss is a minimum and nearly constant, but increases more rapidly thereafter, with a doubling of loss for $D \approx 0{\cdot}4$ and tripling for $D \approx 0{\cdot}6$. Subsequent work (Ref. 8) suggests another value of equivalent diffusion factor for minimum loss, called D^*, with

$$D^* = \frac{\cos a_2}{\cos a_1}\left[1{\cdot}12 + 0{\cdot}61\frac{\cos^2 a_1}{c/s}(\tan a_1 - \tan a_2)\right]$$

A value of D^* of greater than 2 may result in blade stall.

Considerable success has been achieved with test compressors designed according to the diffusion factor criterion. In particular, it has allowed much higher Mach numbers to be used, because losses ascribed to Mach number have been found to be due not wholly to shock losses, but also to blade loading. Thus so called *transonic* blading has been developed, with relative Mach numbers of up to 1·2. This allows much higher pressure ratios per stage than the conventional compressor value of about 1·2 maximum, up to 1·5 having been achieved at high efficiency. High Mach number not only allows these higher stage-pressure ratios and thus fewer stages for a required delivery pressure, but also results in higher flows per unit frontal area, i.e. smaller compressors for a given output. It must be noted that the transonic design is based on blade loading at high Mach number and that loss due to Mach number effects will still occur for conventional compressors designed for subsonic flow as outlined in Sec. 6.6.

The logical development of the diffusion factor requires a detailed analysis and a good knowledge of fluid dynamics with respect to boundary layer and velocity distribution around a blade surface. It is not possible to summarize the analysis here, but the develop-

ment is discussed because it appears to be a significant step forward in blading design. The information has only recently become available, so that sufficient data from any number of applications are not available by which its general applicability can be judged.

6.8 *Supersonic Compressors*

In Chapter 4, the phenomena of shock waves were discussed briefly. Across a plane shock, there is an abrupt rise of static pressure when the supersonic velocity becomes subsonic. Although there is a loss of stagnation pressure, this is not large for Mach numbers between 1 and 1·5. The ratio of static pressures after and before shock is given by the expression

$$\frac{P_2}{P_1} = \frac{7M_1^2 - 1}{6} \text{ (for } k = 1{\cdot}4)$$

Thus for $M_1 \approx 1{\cdot}36$, $P_2/P_1 = 2$ and such values would suggest the use of supersonic velocities in compressors, as the pressure ratio per stage could theoretically be high, up to 5 or 6 for example. Single rotors using supersonic velocities have been made and tested, giving very good results, that is, high stagnation pressure ratio at high efficiency. The drawback is that the leaving velocity is high and has to be diffused in a stator to realize a high static pressure ratio. So far efforts at providing an efficient stator have failed, so that the overall stage efficiency is unacceptably low. Thus it would not seem that the supersonic compressor has an immediate future for the gas turbine.

6.9 *Effect of Stage Reaction*

The degree of reaction characterizes the proportion of static pressure change in rotor and stator. It is possible to have reaction greater than unity and less than unity and, of course, with any intermediate value. It was shown in Sec. 4.20 that 50% reaction gave maximum efficiency in an idealized case. This remains true for actual stages, although the variation in efficiency is not great around 50% as a median value of reaction. Another advantage of 50% reaction lies in the symmetrical diagram, so that $V_{r_1} = V_2$, which are the values significant for critical Mach number. Thus any particular value of limiting Mach number applies to both rotor and stator and one is not penalized in favour of the other. Also, for a given amount of energy transfer $E = U\Delta V_u$, the highest value of any of the velocities V_{r_1}, V_{r_2}, V_1 and V_2 is less for $R = 0{\cdot}5$ than the highest value for any other degree of reaction. Fig. 6.18 shows

these factors graphically. All three velocity diagrams are for the same U, V_a and ΔV_u, but (a) is for $R = 1$, (b) is for $R = 0{\cdot}5$ and (c) is for $R = 0$. Taking the symmetrical diagram (b), any degree of reaction greater than 0·5 causes V_{r_1} and V_{r_2} to move to the left and increase in magnitude. It will be observed that (a) is a mirror image of (c), that is a reaction of unity is aerodynamically equivalent to zero reaction (impulse), with rotor and stator blades interchanged.

Although a value of reaction of around 50% is very generally used, an unbalanced value can have a certain advantage for particular applications. Thus $R > 1$ implies that the pressure change in the stator is negative, i.e. the stator accelerates the air. Acceleration through a converging passage provides the most uniform velocity distribution, because the boundary layer is thin and there is no danger of separation. Hence the rotor receives the air in optimum fashion and can thus operate most efficiently. Such a stage is only possible when the velocities are generally low, as otherwise the critical Mach number is exceeded. A value of $R = 1$ or $R = 0$ implies no change of pressure across either the stator or the rotor respectively. Across that particular blade row, there is then minimum leakage past the tip and the clearance may be large without affecting the efficiency greatly. Such an arrangement may be advantageous if it benefits the mechanical construction, for reasons of economy for example.

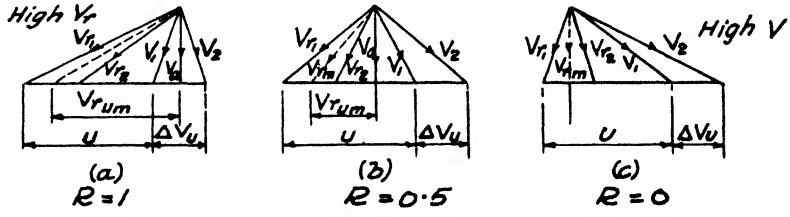

FIG. 6.18. Effect of stage reaction.

Fig. 6.12 showed that the energy transfer as given by ($\tan \alpha_1 - \tan \alpha_2$) increased for $\alpha_2 > 40°$, which implies, from consideration of Fig. 6.18, a high value of reaction. Thus a greater stage energy transfer is possible for a high reaction stage, but again this is true only if Mach number is not limiting.

6.10 *Effect of Blade Stagger*

For a given degree of reaction and a given flow rate (V_a), then there is a choice of blade stagger and blade speed. Using the NGTE method, stagger is expressed in terms of outlet angle α_2.

Some generalizations can be made using the expressions for energy transfer and reaction, that is

$$E = \frac{UV_a}{g_0}(\tan \alpha_1 - \tan \alpha_2)$$

$$R = \frac{V_a}{2U}(\tan \alpha_1 + \tan \alpha_2)$$

Now using the simplified expression obtained from Fig. 6.12, for a value of s/c of 0·8,

$$\tan \alpha_1 - \tan \alpha_2 = \frac{1{\cdot}55}{1 + 1{\cdot}5\, s/c}$$

$$= \frac{1{\cdot}55}{2{\cdot}2} = 0{\cdot}705$$

For a reaction of 0·5, then from

$$\frac{V_a}{U} = \frac{1}{\tan \alpha_1 + \tan \alpha_2}$$

by substitution from above,

$$\frac{V_a}{U} = \frac{1}{0{\cdot}705 + 2 \tan \alpha_2}$$

Thus increasing stagger (α_2) implies a decreasing value of V_a/U, and for a given flow rate, higher rotor speed. From the energy equation,

$$E = \frac{0{\cdot}705}{g_0} UV_a = \frac{0{\cdot}705}{g_0} V_a^2 (0{\cdot}705 + 2 \tan \alpha_2)$$

Thus the energy transfer increases with increasing stagger for a given flow rate. Again, as $(\alpha_1 - \alpha_2)$ decreases with increasing α_2, then the blade camber decreases with increasing stagger.

From the previous relationship,

$$\tan \alpha_1 = \frac{U}{V_a} - \tan \alpha_2,$$

substitution into the energy transfer equation gives,

$$E = \frac{UV_a}{g_0}\left(\frac{U}{V_a} - 2V_a \tan \alpha_2\right)$$

$$= \frac{U}{g_0}(U - 2V_a \tan \alpha_2)$$

whence

$$\left(\frac{\partial E}{\partial V_a}\right)_U \propto (-\tan \alpha_2)$$

Thus at a fixed speed, the energy transfer or pressure varies with air flow rate at a greater rate as α_2 increases, i.e. high stagger blading tends to have a steep characteristic. On the other hand, the point of maximum efficiency is usually further removed from the surge point, so that somewhat more flexibility is possible.

It is possible to pivot blades so that variable stagger is obtained. Although requiring a rather complex mechanical design, this is done on the stators of some aircraft gas turbines to alleviate starting difficulties and to provide more efficient operation over the whole working range.

6.11 *Three-dimensional Flow Patterns*

The general considerations of radial equilibrium and vortex flow were discussed in Chapter 4. As applied to axial-flow compressors, four types of blading flow have been used quite extensively and will be discussed here, although it must not be thought that these are exclusive.

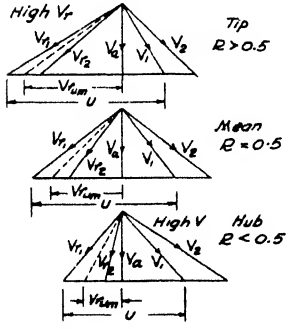

FIG. 6.19. Velocity diagrams at hub, mean and tip radii for free-vortex blading—50% reaction at mean radius.

The *free-vortex* type, with $V_u r = \text{constant}$ and V_a constant from root to tip, is a simple design criterion, but suffers from the disadvantage that the highest Mach number occurs at the rotor tip and at the stator hub (i.e. inside radius). This can be seen from Fig. 6.19, which shows the velocity diagrams for the hub, mean, and tip radii, with 50% reaction at the mean radius. It will be remembered from Chapter 4 that with radial equilibrium, the reaction varies with radius, so that a "design" reaction can be obtained only at one designated station. Thus a limiting Mach number applies only at the extremes of rotor and stator, implying that the remainder of the blade is not loaded to capacity with respect to Mach number.

The second type of blading is *constant reaction*, shown in Fig. 6.20 for 50% reaction. For true radial equilibrium, the axial velocity should vary with radius, but constant-reaction blading has been commonly used with constant V_a, as shown in the diagram. The inlet rotor Mach number, as represented by V_{r_1}, decreases only slightly from tip to root, as does V_2. Thus constant-reaction blading has an almost constant Mach number.

In both types of blading, the energy transfer is the same at all

radii. For the same mass flow rate (V_a), hub ratio, and limiting Mach number, constant reaction blading allows a higher blade speed than free vortex, and hence higher stage energy transfer. Thus for a required pressure ratio, fewer stages are necessary. However, there now enters one of the many complicating factors in making an optimum axial-flow compressor design, because, although fewer stages are required, the overall length and weight of compressors with free-vortex and constant-reaction blading may not be very different. This is because the lower root Mach number of the former allows a thicker root section than the latter and, together with the lower blade speed, allows a considerably smaller chord for a given limiting blade stress. Hence the design requires to be carried out in some detail before a decision can be made if a criterion for use is minimum weight. These remarks apply to any type of blading, that is, the overall application must be continually in mind before deciding on the apparent merits of a particular kind of blading.

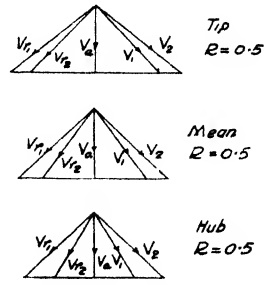

FIG. 6.20. Velocity diagrams at hub, mean and tip radii for 50% reaction blading of all radii—constant axial velocity.

A third type of blading used in many compressors, based on NGTE data, is the so-called "*half-vortex*" design, which is based on making the tangential components of velocity at exit equal to the arithmetic means of the corresponding components of the free-vortex and constant-reaction designs. This obviously has characteristics midway between the two extremes.

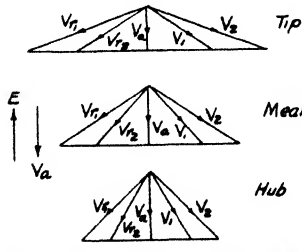

FIG. 6.21. Velocity diagrams at hub, mean and tip radii for solid rotation blading—varying axial velocity.

The fourth type of blading is that of *solid rotation*, with V_u/r = constant. This is shown in Fig. 6.21, with variable axial velocity, decreasing from root to tip as required for radial equilibrium (Eq. 4.60). This gives less variation of Mach number than does free vortex. For a given energy transfer and flow rate, the maximum Mach number is lower, or alternatively, the energy transfer or flow rate can be higher for a given Mach number. With $E = U\Delta V_u$ and $V_u \propto r$, the energy transfer increases from root to tip, in distinction to the previous three types of blading in which the energy transfer is the same at all radii. The restriction on hub ratio with solid rotation should be noted, that is, as V_a decreases towards the tip, there is a theoretical

limit when V_a is zero, and a practical limit of some minimum operating value.

Design for radial equilibrium seems to be a desirable condition, but the exact degree of benefit is not certain. The flow through a compressor eventually achieves equilibrium, as it must, leaving the question as to whether in doing so, losses occur due to mixing and incorrect incidences. Radial equilibrium design is predicated on a certain velocity distribution and the deformation due to wall boundary layer has already been discussed. Added to this are secondary flow effects, so that certainly the full effect of designed radial equilibrium is not realized. It would appear that at higher values of hub ratio, about 0·75 and over, then radial equilibrium has little effect. Hub ratios of aircraft gas turbine compressors, however, with the great emphasis on low frontal area, may be 0·50 and lower. At such values, the pressure gradient from root to tip is large and design for radial equilibrium would seem to be necessary. There is also evidence that although radial equilibrium may not raise efficiency in the normal operating range, it can be helpful at near-critical conditions with respect to stalling.

6.12 *Three-dimensional Blade Losses*

In addition to the profile loss as measured by cascade tests, there are the losses due to annulus friction and secondary flow (Sec. 4.22). Taking the former first, the loss due to wall friction may be expressed by the Fanning equation,

$$\Delta p = f \frac{L}{d_e} \frac{\rho V^2}{2g_0} \tag{4.31}$$

where in this case, L is taken as the blade chord c, V is the mean velocity V_m, and d_e is four times the hydraulic radius, equal to flow area hs (h = blade height) divided by *wetted* perimeter $2s$. Thus

$$\Delta p = f \frac{c}{4hs/2s} \cdot \frac{\rho V_m^2}{2g_0} = f \frac{c}{2h} \frac{\rho V^2}{2g_0}$$

The corresponding drag is equal to this pressure loss times the channel area, i.e. $D_a = \Delta p.\ hs$. From Eq. (4.47),

$$D_a = C_{D_a} \frac{\rho V_m^2}{2g_0} \cdot hc$$

Combining these equations, there results

$$C_{D_a} = \frac{f}{2} \frac{s}{h}$$

The friction factor f is higher than the usual pipe flow value because

of the adverse pressure gradient and $f = 0{\cdot}040$ is recommended. Thus the annulus drag coefficient for compressors becomes

$$C_{D_a} = 0{\cdot}02 \frac{s}{h}$$

Many effects combine to give the secondary flow and accompanying losses. In the first place, visualizing stationary cascade flow only, adjacent blades act as an elbow (Sec. 4.10), setting up a double eddy. In conjunction with the boundary layers from blade surfaces and bounding walls, vortices are shed at the trailing edge, resulting in a blade *wake*. The wake region represents loss of total pressure, showing peaks at the root and tip, Fig. 6.22.

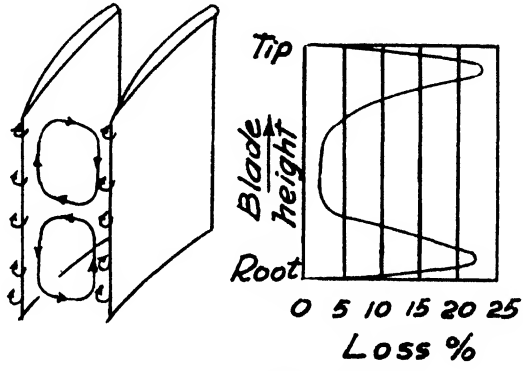

FIG. 6.22. Secondary flow losses.

Now taking into account the clearance space between the rotor blade tip and outer casing and between the inner end of the stator blade and rotor hub, then there is the additional element of leakage. The higher pressure on the convex surface has been mentioned (Sec. 4.14) and the consequent flow over the blade tip is augmented in the rotor by the relative motion between blade tip and casing. There is also a pressure gradient opposite to the flow direction all through the compressor (except for the infrequent cases of reaction of zero or less and reaction of unity or greater). Thus the secondary flow is a complex phenomenon and it is difficult to analyse quantitatively. Howell recommends a value of secondary flow drag coefficient,

$$C_{D_s} = 0{\cdot}18\, C_L^2$$

although it is recognized that this is an interim value pending more exact knowledge. Finally, then, the overall drag coefficient for estimating efficiency as in Sec. 6.4 becomes

$$C_{D_0} = C_{D_p} + C_{D_a} + C_{D_s}$$

with C_{D_p} the appropriate value from two-dimensional cascade data and with C_{D_a} and C_{D_s} as given above.

Sometimes the stator blades are shrouded at the tips, replacing radial clearance with axial clearance, which can be controlled more closely.

6.13 *Compressor Stall and Surge*

Blades are subject to stalling at excessive positive incidence, leading to complete flow breakdown in the extreme. Incidence becomes more positive as axial velocity is reduced, as shown in Fig. 6.23, and thus blade stall is most likely to be associated with reduced flow rate. Such conditions are encountered in axial-flow compressors during starting and low-speed operation, because at low rpm there is very little pressure rise, and the design point of the compressor is for high rpm and high pressure rise from the first to the last stage. Thus at low speed, the absence of pressure rise in the last stages leads to an axial velocity higher than design, leading to choking. Choking limits the flow rate, which then causes excessive positive incidence in the first stages and hence the possibility of stall. Stalling may be caused at any speed by choking effects downstream, by too great a rate of fuel injection for example, when the turbine cannot pass the necessary flow because the instantaneous temperature is high ($m\sqrt{T}/P$ = constant, Eq. 4.44).

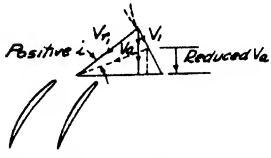

FIG. 6.23. Increase of positive incidence at reduced flow rate.

Low-speed stall occurs in the front stages. At high speeds, the last stages are more likely to stall, because their characteristic is steep and a small reduction in flow rate produces a considerable reduction of velocity and thus a large change of incidence. Quite frequently, stalling is accompanied by a hysteresis effect, that is, once stalled, the condition must be over-corrected in order for the blades to become unstalled. Low-speed and starting stall may be eliminated by *blow-off* or *variable stator* rows. Blow-off is accomplished by fitting valves at intermediate stations, or following the last stage, which remain open until the rotor reaches a predetermined speed or pressure, when they shut automatically. This permits a large flow at low speed and obviates positive incidence. Variable stators can obviously regulate incidence, and the initial stator row or *inlet guide vane* row, is particularly important and, at the same time, the easiest row to control. Stalling is seen to be a greater problem as the pressure ratio is increased, due to mis-

matching of stages at various conditions. This is what limits the pressure ratio on a single rotor, with fixed geometry blading, regardless of the number of stages. With the first few stator rows variable, pressure ratios of 8–9/1 are possible with conventional blades. Hence the use of the compound arrangement (Sec. 3.13), with separate compressor rotors driven at different speeds. Such an arrangement is used even on aircraft gas turbines, with one shaft inside another. This form of layout is sometimes called a " twin-spool " arrangement.

Investigation of blades in a stalled condition with instruments of high sensitivity and rapid response rate, such as the hot-wire anemometer, reveal that stall is a periodic phenomenon rather than a static condition. Such studies show that not all blades are stalled at the same time, but that a stall region, initiated locally at one region of a blade, is propagated from blade to blade in a direction opposite to the blade rotation, but at a lower speed. Thus the stall appears to be in the direction of rotation. If the stall condition is intensified, other stall regions are initiated and several such disturbances may be propagating at the same time.

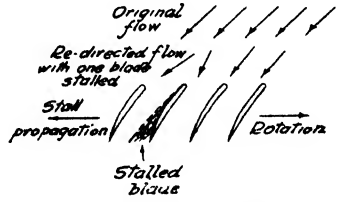

FIG. 6.24. Stall propagation.

A qualitative explanation of propagating stall has been given by Emmons *et al.* (Ref. 9). Referring to Fig. 6.24, in a set of blades operating close to stall, a transient condition or very small permanent change of conditions will cause one blade to stall, this blade having a slight difference in form or setting which predisposes it to react first. The passage containing the stalled surface of the blade is then restricted, so that the flow is directed locally to the adjacent passages. The neighbouring blade in the direction of rotation receives the flow at reduced incidence, with no ill-effects beyond a reduction of energy transfer. The neighbouring blade in the opposite direction of rotation, however, receives the redirected air at an increased incidence and will then itself stall. The stalling condition then corrects the flow over the adjacent blade in the direction of rotation, i.e. the originally-stalled blade, and thus in effect the stall condition has been propagated against the rotation. This condition continues from blade to blade and thus the rotating stall condition is set up. At the present time, the investigation of rotating stall is in its preliminary stages and although many independent studies have been made, and some quantitative analyses made (Ref. 10), it cannot be said that design data are available.

Stall has been distinguished from surging in this section, with the former being the cause of the latter. Thus, stalling does not necessarily cause a complete breakdown of flow, but possibly only a mild instability and reduction of efficiency. If the *stall* is sufficiently extensive to result in a sizeable reduction of the total flow, then the mechanism analysed in Sec. 5 may come into play and *surging* takes place.

Axial-flow compressors can be made highly efficient, up to 87–88%, if the pressure ratio is not too high (4–5/1) and if the stage blade loading is low. Their development is largely directed towards extending the range at high pressures, that is range of mass flow between stalling and choking. Prediction of the surge characteristics is important because the surge line often shows " kinks " which approach the operating line too closely for safe operation.

6.14 *Axial-flow Compressor Characteristics*

Fig. 6.25 shows a plot of typical axial-flow compressor characteristics, with pressure ratio plotted against mass flow for various speeds,

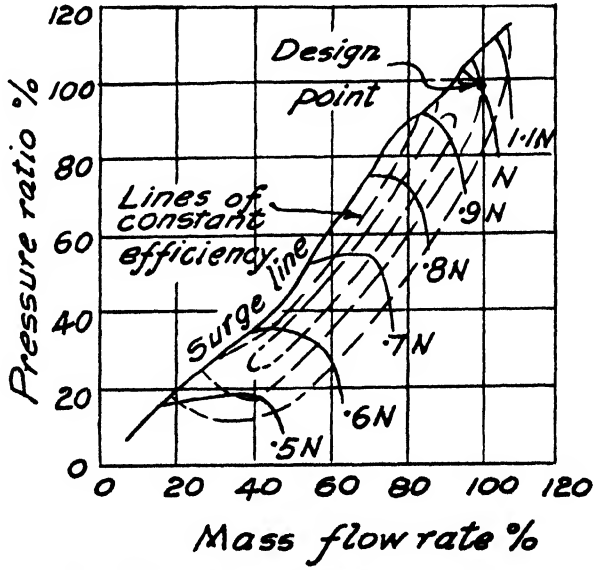

FIG. 6.25. Axial-flow compressor characteristics.

lines of constant efficiency being shown in broken line. The characteristics are usually somewhat steeper than those of a radial-flow compressor at the same pressure ratio, for the reasons discussed above, that is, mismatching of first and last stages at other than the design point. However, this is a matter of detailed design and

depends on the application, with development being directed towards increased range at high-pressure ratios.

Stage pressure ratios of about 1·2 are reasonable for industrial application, where weight and size are not over-riding conditions. For aircraft use, 1·3–1·35 is a possible figure, while 1·4 is a top limit for very advanced designs. Axial velocities of 400–500 fps represent industrial use, with 500–600 fps for aircraft use, the latter being used with small hub-tip ratios ($\gtrsim 0{\cdot}50$) in order to minimize the outside diameter. Higher axial velocities, up to 800 fps, have been used on experimental compressors, but require special blade design.

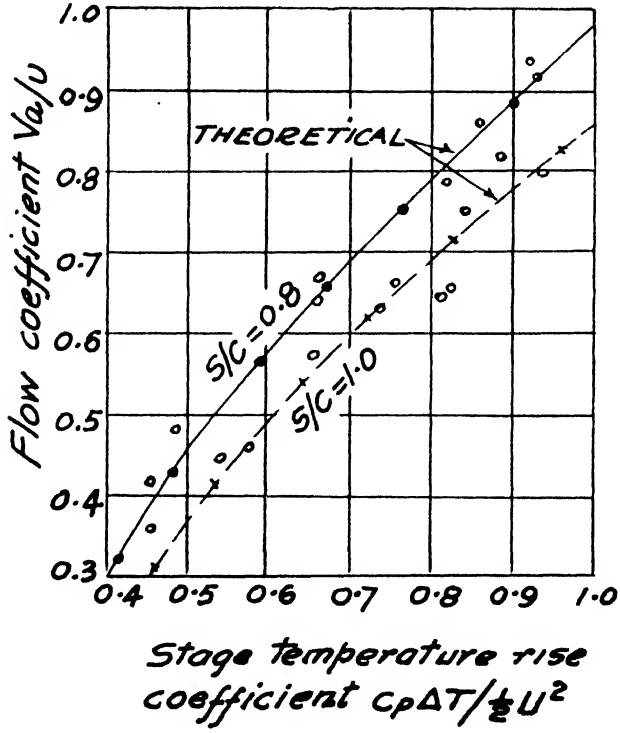

FIG. 6.26. Design-point flow and temperature-rise coefficients—actual and calculated (adapted from Howell and Bonham, ref. 2).

Fig. 6.26 from Howell shows theoretical characteristics of flow coefficient V_a/U against temperature rise coefficient, $c_p\Delta T/1/2U^2$, for two pitch-chord ratios, 0·8 and 1·0, using the generalized data from Sec. 6.5. The design is for 50% reaction and the numbers along the lines give the corresponding values of fluid outlet angle α_2, representing stagger. Superimposed on this plot are the test design point values of 19 different compressors. The figure shows that the

generalized cascade data correspond satisfactorily to actual compressor performance. It is useful as an initial guide to possible performance and for comparing a new design with established performance.

6.15 *Compressor Design*

The previous sections have discussed various aspects of axial-flow compressor performance, with a view to understanding the main characteristics. It will be realized that the design of a multi-stage compressor is a very complex matter, even in terms of the simplified viewpoints taken here. With so many variables, it is difficult to choose an optimum solution. Much depends on the application, whether military or industrial, whether efficiency or range of operation is the main target, if first cost, size or weight are prime considerations, and so forth. Some generalizations are given by Howell in Refs. 2, 5 and 11, which are useful guides in laying down a framework and in estimating performance. Reference to later work of the NGTE is desirable in detailed design.

The American viewpoint is contained in Ref. 12, representing in a single work a collation of the NACA work. This contains a great deal of detailed information on a correlated basis, using much of the NGTE and other studies for analysis and comparison. This report, released in 1958, shows a tendency to adopt some of the basic British parameters for design use, e.g. incidence and deviation, rather than those outlined earlier as representing American usage. However, the latter are used for much of the individual data on blade performance.

REFERENCES

1. Carter, A. D. S. and Hughes, H. P. A Theoretical Investigation into the Effect of Profile Shape on the Performance of Aerofoils in Cascade. *Aeron. Res. Coun.*, R. and M., No. 2384, 1950.
2. Howell, A. R. and Bonham, R. P. Overall and Stage Characteristics of Axial-Flow Compressors. *Proc. I. Mech. E.*, **163**, 1950, p. 235.
3. Herrig, L. J., Emery, J. C. and Erwin, J. R. Systematic Two-Dimensional Cascade Tests of N.A.C.A. 65-Series Compressor Blades at Low Speeds. *N.A.C.A.* TN 3916, 1957.
4. Carter, A. D. S. Some Tests on Compressor Cascades of Related Aerofoils Having Different Positions of Maximum Camber. *Aeron. Res. Coun.*, R. and M. 2694, 1953.
5. Howell, A. R. Fluid Dynamics of Axial Flow Compresors. *Proc. I. Mech. E.*, **153**, 1945, p. 441; reprinted by the *A.S.M.E.*, 1947, *Lectures on the Development of the British Gas-Turbine Jet Unit.*
6. De Haller, P. Das Verhalten von Tragflügelgittern in Axialverdichtern und um Windkanal. *Brennstoff-Wärme-Kraft*, **5**, 1953, p. 333.

7. LIEBLEIN, S., SCHWANK, F. C. and BRODERICK, R. L. Diffusion Factor for Estimating Losses and Limiting Blade Loadings in Axial-Flow-Compressor Blade Elements. *N.A.C.A.* R.M. E53D01, 1953.
8. LIEBLEIN, S. Loss and Stall Analysis of Compressor Cascades. *A.S.M.E.* Paper No. 58-A-91, 1958.
9. EMMONS, H. W., PEARSON, C. E. and GRANT, H. P. Compressor Stall and Surge Propagation. *Trans. A.S.M.E.*, **77**, 1955, p. 455.
10. EMMONS, H. W. A Survey of Stall Propagation—Experiment and Theory. *A.S.M.E.* Paper No. 58-A-150, 1958.
11. HOWELL, A. R. Design of Axial Compressors. *Proc. I. Mech. E.*, **153**, 1945, p. 452; reprinted by *A.S.M.E.*, 1947, *Lectures on the Development of the British Gas-Turbine Jet Unit.*
12. *Aerodynamic Design of Axial-Flow Compressors*, Vols. I–III *N.A.C.A.* R.M. E56B03, a, b, 1956.

For a concise analysis summarizing methods of axial-flow compressor design, see HORLOCK, J. H., *Axial Flow Compressors*, Butterworths Scientific Publications, London, 1958.

CHAPTER 7

THE TURBINE

THE turbine, like the compressor, may be of the radial-flow or the axial-flow type. However, as yet the former is used only in small sizes for particular applications, with by far the greatest number of gas turbines of all varieties having the axial-flow type. Owing to its limited usage and relatively new development, few design data are available for radial-flow turbines for compressible flow. Both types will be discussed in this chapter, with most emphasis on the axial-flow type, but first an analysis of energy transfer in general will be made.

7.1 *Energy Transfer*

The Euler energy transfer equations for the turbine are

$$E = \frac{1}{g_0}(U_1 V_{u_1} - U_2 V_{u_2}) \tag{4.2}$$

or

$$E = \frac{1}{2g_0}[(V_1^2 - V_2^2) + (U_1^2 - U_2^2) + (V_{r_2}^2 - V_{r_1}^2)] \tag{4.3}$$

It should be noted that for the development of Eq. (4.2), the change of angular momentum was taken as $(V_{u_1} r_1 - V_{u_2} r_2)$, with the implicit assumption that the tangential velocities V_u were both in the same direction as vector quantities, this direction being that of the rotor velocity U. If V_{u_2} is oppositely directed to U, then it is negative, i.e.

$$E = \frac{1}{g_0}[U_1 V_{u_1} - U_2(-V_{u_2})] = \frac{1}{g_0}(U_1 V_{u_1} + U_2 V_{u_2})$$

This is important because quite often V_{u_1} and V_{u_2} are oppositely directed in the turbine, that is, the fluid is given a very large change of whirl velocity, so that the energy transfer is high.

Recollecting the discussion of Sec. 4.4, in which the shaft work was seen to be equal to the change of *stagnation* enthalpy, $c_p \Delta T_0$, the available energy is that from stagnation conditions at inlet to static conditions at outlet, i.e. any discharge kinetic energy is wasted as far as shaft work is concerned. This kinetic energy is represented

by $V_2^2/2g_0$ and it is useful for analytical purposes to separate this term from losses due to irreversible flow, i.e. friction and turbulence losses. For any finite throughflow, V_2 must have a certain value and the corresponding energy loss is that due to blade arrangement or geometry, rather than to flow processes. Thus even for ideal flow, the overall efficiency cannot be unity, and this effect is conveniently taken into account by defining a turbine *utilization factor*, ϵ, as the ratio of actual energy transfer for ideal flow to available energy, i.e.

$$\epsilon = \frac{E_{\text{id}}}{E_{\text{av}}}$$

The difference between these two quantities is the discharge kinetic energy, $V_2^2/2g_0$, thus

$$\epsilon = \frac{E_{\text{id}}}{E_{\text{id}} + V_2^2/2g_0} \tag{7.1}$$

The aerodynamic blading efficiency, η_b, is the ratio of energy transfer for the actual flow to that for ideal flow, thus

$$\eta_b = \frac{E_{\text{act}}}{E_{\text{id}}}$$

Hence

$$\eta_t = \frac{E_{\text{act}}}{E_{\text{av}}} = \eta_b \epsilon$$

The turbine utilization is sometimes called the "diagram efficiency", because it is the same as the efficiency using an ideal velocity diagram. It has considerable use in turbine analysis, because it categorizes types of turbine with respect to potential energy transfer with ideal flow. It may be likened to the idea of the ideal cycle, provided that the analogy is not drawn too closely, with the inevitable loss of available energy due to discharge kinetic energy akin to the inherent irreversibility by operation of the second law of thermodynamics.

7.2 *The Radial-Flow Turbine*

The Euler equation shows that the logical form for the radial-flow turbine should be inward flow, with $U_1 > U_2$, in order to benefit from the centripetal energy transfer. Thus for gas turbines it becomes a reversed centrifugal compressor, which indeed it resembles closely, as shown in Fig. 7.1. This figure shows an impeller with radial vanes, which are desirable in order to minimize bending stresses at the high gas temperature. If the vanes are not radial, then they are backward curved, so that a higher nozzle

velocity can be used and a greater energy transfer obtained. The nozzles are fed from a volute with single inlet and there are considerable advantages to be gained from pivoting the nozzle vanes so that both discharge angle and area can be controlled. Although this has been done in a few cases, it has not been applied extensively.

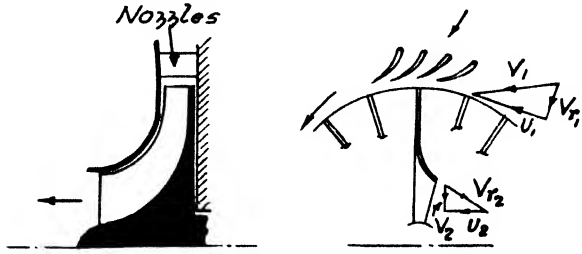

FIG. 7.1. Radial-flow turbine.

At discharge, the vanes are bent in similar fashion to the inducer of a compressor, in order that the absolute exit velocity should be axial or nearly so. It is obviously desirable that the gas should discharge axially from the point of view of disposal into an exhaust duct, but an even more important reason is concerned with the effectiveness. For a given flow rate, that is axial component of the absolute velocity, then V_2 is a minimum when it is wholly axial, hence $V_2^2/2g_0$ is a minimum and ϵ is a maximum, Eq. (7.1). Note that although the energy transfer is increased if V_2 is directed opposite to the direction of rotation as in Fig. 7.2, because then E is increased from (U_1V_{u2}/g_0) to $[U_1V_{u_1} - U_2(-V_{u_2})]/g_0 = (U_1V_{u_1} + U_2V_{u_2})/g_0$, the available energy must also have increased, because V_{r_2} is larger, requiring a higher pressure drop. Giving V_2 a tangential component V_{u_2} oppositely directed to rotation is a means of increasing energy transfer from a given size and speed of rotor, but more of the available energy is wasted as discharge kinetic energy. The discharge region may be a problem for optimum design, because the gases have a very low density (low pressure, high temperature), and a high outlet velocity may be necessary if the area is restricted.

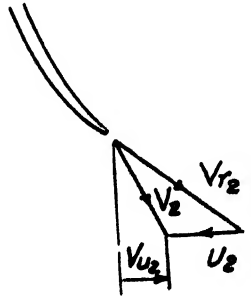

FIG. 7.2. Increase denergy transfer—reduced utilization.

Expansion through a large pressure ratio is possible in a single stage of a radial-flow turbine, values of 3–4/1 being achieved with good efficiency. Much higher pressure ratios are capable of being

used if high blade speeds are possible. The limiting factor is the allowable stress at the high temperatures of the combustion gases.

Very little proven design information is available with respect to the effect on efficiency of channel shape, number of vanes, etc. It would seem that the same general flow considerations apply as for radial-flow compressors, with the difference that the number of nozzle vanes may be considerably larger than the number of diffuser vanes, as the surging criterion does not apply. Balje (Ref. 1) has presented a theoretical analysis of the flow through each component part of a radial-flow turbine, which shows the relative importance of various elements. One result of this flow analysis is to show the effect of Reynolds and Mach number. Owing to the varying gas velocities and dimensions throughout the whole turbine, both parameters must be evaluated with arbitrarily chosen variables. The Reynolds number is calculated with density and viscosity at the inlet conditions, velocity that of the *impeller* tip and characteristic dimension the impeller diameter, thus

$$R_e = \frac{\rho_1 U_1 D}{\mu}$$

Likewise, the Mach number is evaluated as the ratio of the impeller tip speed and the acoustic velocity a^* at the critical temperature corresponding to the inlet stagnation temperature, thus

$$M = \frac{U_1}{a^*}, \text{ where } a^* = \sqrt{\frac{2k}{k+1} g_0 R T_0}$$

For the relatively small impellers of the radial type as at present in use, together with appropriate fluid properties, the Reynolds number is of the order of 10^6–10^7 and the Mach number is 0·7–0·8. With these values, the Balje analysis shows an efficiency variation of about 0·8 to 0·87, increasing with R_e and decreasing with M. The few reported test efficiencies available would indicate that such estimated values may be on the high side, but there is also some evidence that the estimated rate of decrease of efficiency with decrease of Reynolds number is pessimistic.

The typical radial-flow turbine has been shown in Fig. 7.1 with three-dimensional vanes extending from inlet to discharge. A simpler type of rotor is possible with cantilevered blades of small chord as shown in Fig. 7.3. With such blades, the rotor can be almost an impulse type, with very little contribution from the centripetal effect. As an addition to this type, more than one row of blades may be used with corresponding stator rows on the casing,

thus providing opportunity for a much greater expansion ratio with a single rotor.

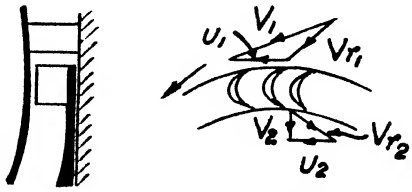

FIG. 7.3. Cantilever blades.

The radial-flow turbine is particularly favoured for very small units running at high rpm, for applications other than as simple gas turbines. Such applications are as air turbines in auxiliary power units in aircraft or as expanders in refrigerating units for airborne systems of many kinds. Their compactness, ruggedness and one-piece construction are their attractive features.

7.3 *The Axial-Flow Turbine*

The axial-flow turbine is used generally for nearly all medium and large sizes of plant and a wealth of design data is available. Design is rooted in that of the steam turbine, with extensions and modifications for the differing conditions and, often, for the different outlook engendered by the aerodynamic advances of recent years. In spite of the relatively long history of axial-flow turbine development, knowledge is still incomplete with respect to design for optimum performance for the many different conditions encountered. Because the plant performance is dependent on net work, the relatively small difference of two large quantities, turbine efficiency is critical and close attention to detail is necessary. The discussion here will deal first with general considerations of energy transfer and stage reaction, followed by more detailed consideration of blade behaviour and finally with overall turbine performance.

7.4 *Utilization and Reaction*

Fig. 7.4 shows a velocity diagram for an axial-flow turbine stage, with α the *nozzle* angle and β_1 and β_2 the *rotor* blade angles. In general, the absolute velocity is increased in the stator and the relative velocity is increased in the rotor, i.e. there is a pressure drop in both rotor and stator and the reaction has a value between zero and unity. For axial flow, $U_1 = U_2 = U$, hence

$$E = \frac{U}{g_0}[V_{w_1} - (-V_{w_2})] = \frac{U}{g_0}(V_{w_1} + V_{w_2}) \qquad (7.2)$$

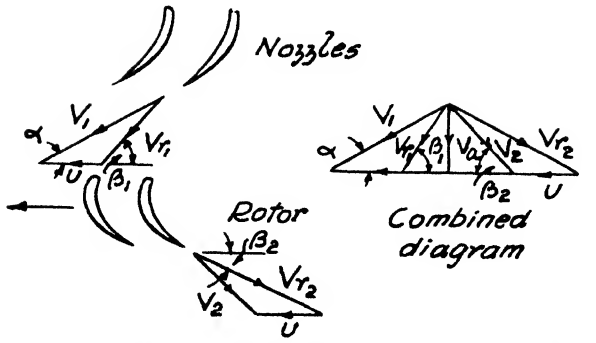

FIG. 7.4. Velocity diagram for an axial-flow turbine stage.

and

$$E = \frac{1}{2g_0}\left[(V_1^2 - V_2^2) + (V_{r_2}^2 - V_{r_1}^2)\right] \tag{7.3}$$

The reaction is

$$R = \frac{V_{r_2}^2 - V_{r_1}^2}{2g_0 E} \tag{7.4}$$

where E can be expressed as (7.2) or (7.3) as convenient.

The utilization factor is

$$\epsilon = \frac{E}{E + V^2/2g_0} \tag{7.5}$$

with E that for ideal (isentropic) flow. Now for a given mass flow rate, that is fixed V_a, then the blade geometry can be arranged so that V_2 can be either side of V_a, with varying E and varying R. For maximum utilization, however, V_2 must be a minimum and it is seen that then V_2 is coincident with V_a, i.e. V_2 is *axial*. Thus for maximum shaft work in a given stage, the absolute velocity at rotor discharge should be axial. The diagram then becomes as shown in Fig. 7.5.

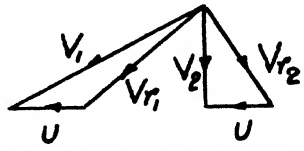

FIG. 7.5. Stage diagram for axial absolute outlet velocity.

It was noted in Chapter 4 that with blading designed for vortex flow, the degree of reaction varies with radius. Thus, unlike conventional steam turbine blading, a gas turbine stage has no fixed reaction, because it is usual to design for radial equilibrium, commonly with free vortex flow. However, it is usual to describe a blading design as having a particular amount of reaction at some specified radius and for this purpose, it is desirable to discuss the properties of zero reaction (impulse) and 50% reaction stages.

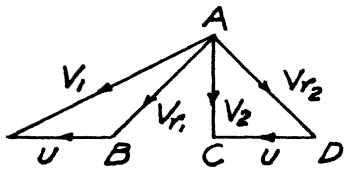

FIG. 7.6. Impulse stage operation at maximum utilization.

Fig. 7.6 shows an impulse stage operating at maximum utilization. For $R = 0$, $V_{r_1} = V_{r_2}$, hence triangles ABC and ADC are similar, with BC = CD, with CD representing the blade speed U. Thus $V_{u_1} = V_1 \cos \alpha = U + U = 2U$ and

$$\frac{U}{V_1} = \frac{\cos \alpha}{2} \tag{7.6}$$

For a given nozzle velocity V_1, V_{u_1} should be a maximum for the highest energy transfer, which means that the nozzle angle α should be small. It is limited by consideration of blade length, as $V_a = V_1 \sin \alpha$ and therefore a low value of α entails a longer blade. Values of nozzle angle of 15°–22° are general for impulse blading.

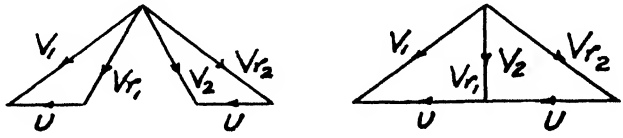

FIG. 7.7. 50% reaction stage.

Fig. 7.7 (a) shows a general case for a 50% reaction stage, operating at constant axial velocity. As discussed in Sec. 4.18, a 50% reaction stage is symmetrical and thus $V_1 = V_{r_2}$ and $V_{r_1} = V_2$. For maximum utilization, V_2 must again be axial, so that the diagram reduces to Fig. 7.7 (b), with V_{r_1}, V_2 and V_a co-incident. It is seen that for this case,

$$\frac{U}{V_1} = \cos \alpha \tag{7.7}$$

so that the optimum value of the *velocity ratio*, U/V_1, is twice that for the impulse case.

The relationship for velocity ratio can be generalized for any degree of reaction, with the result that

$$\frac{U}{V_1} = \frac{\cos \alpha}{2(1 - R)} \tag{7.8}$$

The maximum effectiveness, ϵ_{max}, becomes, from (7.5)

$$\epsilon_{max} = \frac{UV_1 \cos \alpha}{UV_1 \cos \alpha + (V_1^2 \sin^2 \alpha)/2}$$

Using the general relationship (7.8), then

$$\epsilon_{max} = \frac{\cos^2 \alpha}{1 - R \sin^2 \alpha} \tag{7.9}$$

For the impulse stage, $\epsilon_{max} = \cos^2 \alpha$, and for 50% reaction, $\epsilon_{max} = \cos^2 \alpha/(1 - 0{\cdot}5 \sin^2 \alpha)$.

For $\alpha = 20°$, then ϵ_{max} for impulse blading is 0·883 and for 50% reaction blading, 0·937. Eq. 7.9 differs from the conventional value of $\epsilon_{max} = \cos^2 \alpha$ for both impulse and reaction turbine stages. The difference lies in the definition of reaction, which here is given in a general form applicable to both compressors and turbines, but is given a special definition for steam turbines, for which the $\cos^2 \alpha$ value for ϵ_{max} is associated. For a discussion of this matter, Ref. 2 may be consulted, but here it will suffice to note that the maximum shaft energy transferable is less than unity even with ideal flow, as a certain amount of kinetic energy is always lost at discharge. This kinetic energy is a minimum when V_2 is axial. At other than the design condition, the value of U/V_1 is useful in order to assess the loss. Fig. 7.8 shows this for the impulse and 50% reaction cases. It should be noted that utilization factor is a criterion only when shaft work is the desired effect and, for the turbine of a turbo-jet, it may not be relevant.

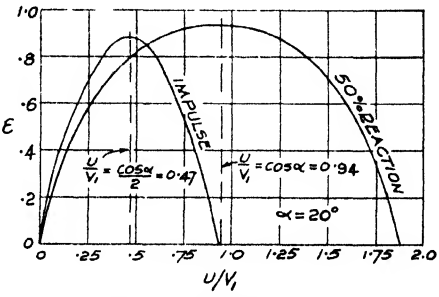

FIG. 7.8. Variation of utilization factor with U/V_1 for R 0 and R 0·5.

Comparing impulse and 50% reaction stages, it has already been seen that the latter gives the better actual efficiency with certain simplifying assumptions (Sec. 4.18), but the former can be shown to have a greater potential for energy transfer. Any turbine stage is likely to be operated at a blade speed corresponding to the highest blade and wheel stress consistent with the material and life considerations for the particular application. Thus, using subscripts i for impulse and r for 50% reaction, $U_i = U_r = U$. Now at maximum utilization, $E = UV_{u_1}/g_0 = UV_1 \cos \alpha/g_0$, hence using Eqs. (7.6) and (7.7),

$$E_i = 2U^2/g_0$$

and

$$E_r = U^2/g_0$$

The conclusion is that for a given limiting blade speed, the energy transfer in an impulse stage can be twice that for a 50% reaction stage, or, for a required total work output, an impulse rotor will have fewer stages. Where either low weight or initial cost is important, then impulse blading is used, as for example in aircraft gas turbines, where the former is a prime requisite. Industrial turbines for shaft-power output more commonly have reaction blading for maximum efficiency.

With the free-vortex design, the degree of reaction increases with radius, so that the impulse condition can only be realized at the root. Dependent on the hub ratio, the reaction may even be greater than 50% at the tip, but the blading may be called " impulse ", with the implication of this being at the root only. With " 50% reaction " blading, this can be realized only at one radius, often the mean radius, so that R is greater or less than 0·5 toward the tip and root respectively.

The degree of reaction also has an effect on the actual temperature experienced by the rotor blades. The blade is subject to the static temperature at nozzle exit plus some fraction of the dynamic temperature corresponding to the blade inlet relative velocity V_{r_1}. In an impulse stage, all the pressure drop and hence temperature drop, occurs in the nozzle, so that the static temperature is considerably lower than for the corresponding reaction stage. Although V_{r_1} may be somewhat higher for the impulse stage, the combined effect is such that for a given nozzle inlet temperature, the impulse blade experiences a lower temperature than one having any degree of reaction. Although this may occur only at the root of the blade, this is the critical region, because the blade stress is highest there. For the high gas temperatures usually used, a reduction of actual metal temperature of only 50° F may mean a proportionately much larger allowable stress or length of service for a given stress.

7.5 *Torque*

In addition to work output and efficiency, the torque of a turbine may be important in some applications, traction units for example, when acceleration under load is a prime consideration. In the first place, it must be realized that a separate power turbine is desirable for rapid acceleration, as then the compressor–compressor turbine combination can be kept idling as a gas producer, with the power turbine free to respond when required. The following analysis is for a turbine with separate gas supply, so that its speed is independent of the compressor. The torque relationship is developed for an

impulse stage, Fig. 7.9 (a), as the principle can be developed simply. The tangential force, and hence the torque τ on the blade is proportional to the change of tangential velocity, i.e.

$$\tau \propto (V_1 \cos \alpha + V_2 \cos \gamma)$$
$$\propto (V_{r_1} \cos \beta_1 + U) + (V_{r_2} \cos \beta_2 - U)$$

For the ideal turbine with $V_{r_1} = V_{r_2}$ and $\beta_1 = \beta_2$, hence

$$\tau \propto (2V_{r_1} \cos \beta_1) \propto 2(V_1 \cos \alpha - U)$$

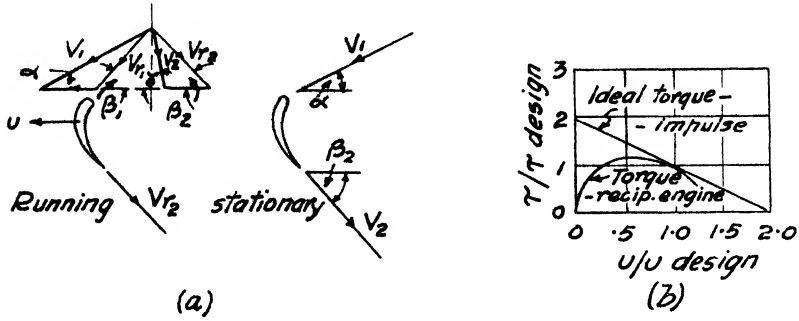

FIG. 7.9. Turbine torque relationships.

Thus for fixed inlet conditions, the torque is a linear function of blade speed. When $U = 0$, $\tau \propto 2V_1 \cos \alpha$ and when $U = (V_1 \cos \alpha)/2$, the design condition, $\tau \propto V_1 \cos \alpha$. Thus the zero speed or starting torque is twice the design torque. When $U = V_1 \cos \alpha$, then $\tau = 0$, which is the runaway speed, or maximum speed under no load. The ideal torque-speed relationship for an impulse turbine then appears as in Fig. 7.9 (b), with a typical reciprocating engine relationship shown as well. It is the high starting torque of a free turbine which is one of the attractive features of the gas turbine for traction applications, as it simplifies, if not eliminates, the gearbox. In effect, the turbine provides in itself the hydrodynamic transmission of automobiles.

The above analysis is idealized and is modified for real flow, but remains valid in principle. The ratio of starting torque to design torque varies with degree of reaction and may be increased by designing for U/V_1 greater than the optimum value for maximum utilization, thus sacrificing a little efficiency for torque ratio.

7.6 *Blade Performance*

Data on blade performance are required with respect to loss and actual fluid deflection as a function of blade shape, camber angle, stagger (degree of reaction), pitch-chord ratio, Reynolds and Mach

number. These are usually assessed for two-dimensional (cascade) flow, with three-dimensional effects superimposed in terms of blade aspect ratio. Because the function of the gas turbine blading is basically similar to that of steam turbine blading, much of the latter technology is applicable. Due, however, to the aerodynamic approach of late years, the performance of gas turbine blading is couched in different terms, usually those discussed generally in Chapter 5, rather than in terms of velocity coefficient.

7.7 *Blade Shape*

Blade profiles are not so critical as for compressors, although here perhaps the behaviour has not been studied so intensively, because the accelerating nature of the flow does not give rise to obviously limiting problems of separation and Mach number effects.

British work, mostly originating at the NGTE, has been based on both airfoil profiles with circular-arc and parabolic-arc camber lines, and on simplified or " conventional " profiles made up of circular arcs and straight lines for ease of manufacture. The latter developed from consideration of the flow passage shape rather than of flow around a blade and thus the consequent profile shape and camber line are arbitrary. Conventional blading is represented by a " T-6 " section (Ref. 3), consisting of circular arcs fitted to a parabolic camber line.

American data from the NACA are for blade shapes developed from loading considerations, that is, pressure and velocity distributions, so that the camber line and thickness distributions are a result of this, rather than vice versa. Details of such a related blade series are given in Ref. 4.

A most important factor in turbine blade performance is that of the degree of reaction, i.e. acceleration through the blades, and this is reflected in optimum blade shape. With high reaction, that is, in general for nozzle blades, there is little chance of separation due to local areas of retardation, as the passage formed by neighbouring blades has a large pressure gradient in the flow direction. However, with such blades, the entering Mach number is low, increasing continuously to outlet. Thus, it would seem that the highest loading (greatest turning) should take place in the forward section, leaving the rear section with a minimum of curvature. This is the basis of the NACA profile series, which have nearly straight upper-surface trailing edges. NGTE data tends to show that at low Mach numbers, trailing edge curvature is unimportant, but leads to higher losses at high values of Mach number. For impulse blading, the Mach number is relatively constant throughout the passage and the

loading should be more evenly distributed. British opinion, as represented by the NGTE (Ref. 5), regards optimum loading for low-reaction blading as an unsettled question requiring more study. The NACA work mentioned above discards the straight trailing edge requirement for the impulse blade section.

The degree of reaction affects the choice of blade thickness. For nozzle blading, the profile thickness as represented by t/c is relatively unimportant (up to t/c of 20%), but as reaction is decreased, increasing thickness causes higher loss. Trailing edge thickness appears to be very important and should be kept to the minimum consistent with strength requirements. This may be significant for internally cooled turbine blades, in which profile shape may have to be subordinated to flow and heat transfer requirements.

7.8 *Blade Profile Loss*

Loss may be expressed either from the channel flow viewpoint, as a pressure-loss coefficient λ, defined as

$$\lambda = \frac{\Delta P_0}{P_{0_2} - P_2}$$

or from the blade force viewpoint, as a drag coefficient C_D. The latter is most frequently based on the mean velocity V_m through the blade row Eq. (4.53 a), but sometimes either the inlet or the outlet velocity is used, so that care must be taken when using drag coefficient data. Referring to the analysis associated with Eq. (4.53 a) and taking $(P_{0_2} - P_2)$ as equal to $\rho V_2^2/2g_0$ (not exact for compressible flow, Sec. 4.2) then it can be shown that the relationship between λ and C_D based on mean velocity is given by

$$C_D = \lambda \frac{s}{c} \frac{\cos^3 \alpha_m}{\cos^2 \alpha_2} \tag{7.10}$$

British usage finds λ more convenient as a rule, although C_D is useful when considering secondary flow losses, while American practice is mostly given in terms of C_D.

Turbine blades usually have a relatively high tolerance of incidence, with this tolerance increasing with degree of reaction. Fig. 7.10 shows a typical variation of λ with i for impulse and nozzle blades. The impulse blade shows a higher loss everywhere, and greater sensitivity. The very low loss area within a narrow range of incidence is usually disregarded, as it is a typical cascade result signifying laminar flow over most of the blade, whereas in a turbine, the highly turbulent flow would not result in such laminar flow. In Ref. 5 a correlation of reasonable accuracy is given for the

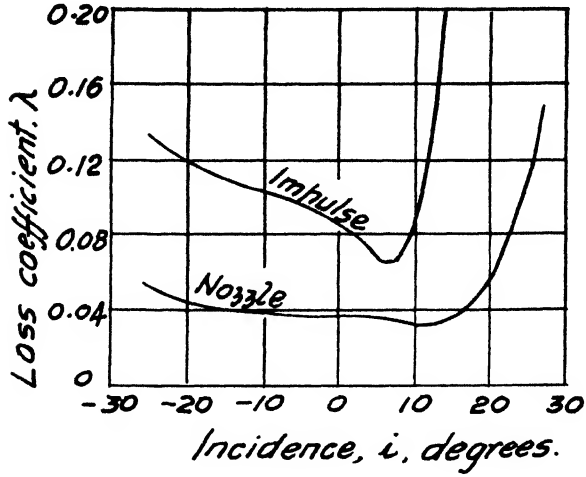

FIG. 7.10. Typical variation of turbine blade loss coefficient with incidence.

variation of λ with i for blades in general, showing the ratio of loss at any incidence to that at zero incidence, against the ratio of incidence to that at the stalling incidence (that incidence where $\lambda = 2\lambda_{min}$). This is given as Fig. 7.11.

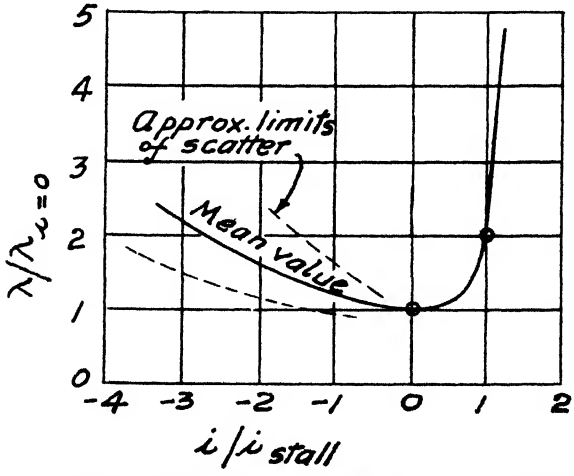

FIG. 7.11. Generalized variation of relative loss with incidence (adapted from Ainley and Mathieson, ref. 5).

The loss is usually a minimum at zero incidence and using this as a datum, Fig. 7.12 from Ref. 5 shows typical profile-loss coefficients for blades of conventional profile. These data are valid for $t/c = 20\%$,

$R_e = 2 \times 10^5$ and $M < 0{\cdot}6$. Fig. 7.12 shows that loss increases with deflection, as might be expected, and that for any required deflection, there is a certain value of blade spacing, s/c, for minimum

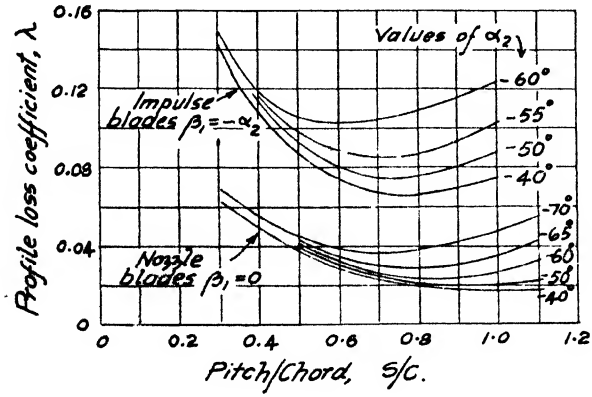

FIG. 7.12. Loss coefficient for convential section blades at zero incidence ($t/c = 20\%$, $R_e = 2 \times 10^5$, $M < 0{\cdot}6$) (adapted from Ainley and Mathieson, ref. 5).

loss. (Note that these data are given in terms of angles with respect to the axial direction, Sec. 4.16 and Fig. 4.17.) It should also be noted that the results are given in terms of *gas* angles, not *blade* angles, as for zero incidence, $\beta_1 = \alpha_1$ and the deflection parameter is α_2, not β_2.

For the design of blades for a required fluid deflection, it is necessary to estimate the deviation angle. For turbine blades, it has been found more convenient to represent deviation in terms of the gas efflux angle and the angle $\cos^{-1} o/s$, where o is the blade "opening" or throat, see Fig. 7.13. The procedure stems from the practice with steam turbine nozzles, which used to be of plate type with straight trailing edges forming passages having a definite linear axis. For such nozzles, it was found that the gas efflux angle could be represented by $\cos^{-1} o/s$ and this has been found useful for turbine blades, even with curved trailing edges for which no definite passage axis is apparent. For blades with straight trailing edges, the relationship can be expressed by

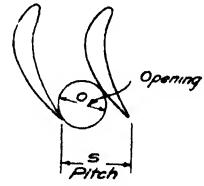

FIG. 7.13. Blade opening.

$$\alpha_2 = \frac{35}{30}(10 - \cos^{-1} o/s) \qquad (7.11)$$

This expression, deduced from results given in Ref. 5, gives α_2 as a negative angle in accordance with previous remarks and is valid for $M_2 < 0{\cdot}5$. For blades with curved trailing edges, α_2 is increased (numerically) by the order of 1°–2°, depending on the degree of curvature. For higher Mach numbers, the efflux angle approaches more closely to the value of $\cos^{-1} o/s$, reaching that value for a Mach number of unity. These rules are approximate and, for refinement, Ref. 5 should be consulted.

U.S. data on blade profile performance are expressed in somewhat different terms. Fig. 7.14, from NACA work (Ref. 4) shows the nomenclature used, with β_1 and β_2 the actual air inlet and outlet angles, with deflection or *air turning angle* $\theta = \beta_1 - \beta_2$, and θ_c the *blade* turning or camber angle; α_1 is the angle of attack, the angle between the chord and the entering streamline, and $\Delta\theta_d$ is the deviation at exit. At inlet, $\Delta\theta_i$ represents the " induced flow angle ", or change in direction of the stagnation streamline locally just ahead of the leading edge. This induced angle is caused by the effect of circulation round the blade and is measured by closely-spaced pressure taps on the blade surface itself.

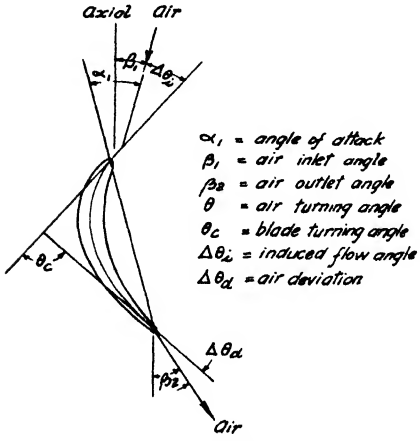

FIG. 7.14. N.A.C.A. turbine blade nomenclature (adapted from Dunavant and Erwin, ref. 4).

From the geometry of the figure, the blade camber angle is the sum of the deflection, induced angle and deviation, i.e.

$$\theta_c = \theta + \Delta\theta_i + \Delta\theta_d$$

Performance is given in terms of deflection θ against angle of attack α_1, together with two loss coefficients and the lift-drag ratio. The loss coefficients are C_{D_1}, coefficient of total force parallel to the mean velocity (C_D as previously defined) and C_{W_1}, a wake momentum difference coefficient, subscript 1 indicating that they are based on the *upstream* dynamic pressure, $\rho V_1^2/2g_0$.

Fig. 7.15 shows the type of performance data obtained. This particular result is for a cascade of blades having a blade turning (camber) angle θ_c of 95° and solidity c/s of 1·8, the inlet air angle β_1 being 45°. A design point condition is indicated by an arrow at an angle of attack of about 61°. This design α_1 is that angle of attack

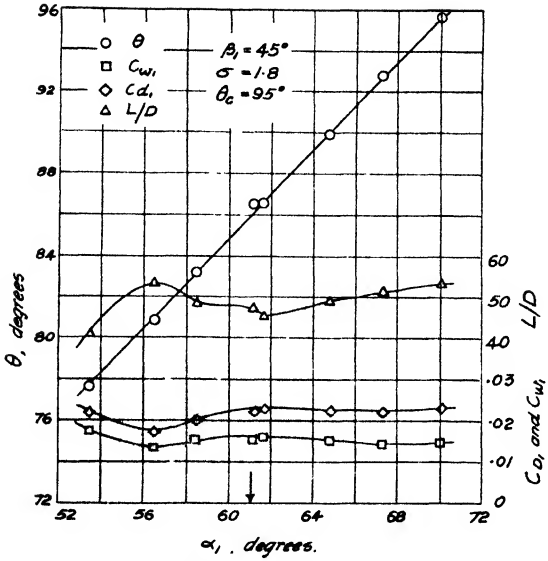

FIG. 7.15. Typical cascade data for turbine blades, N.A.C.A. (adapted from Dunavant and Erwin, ref. 4).

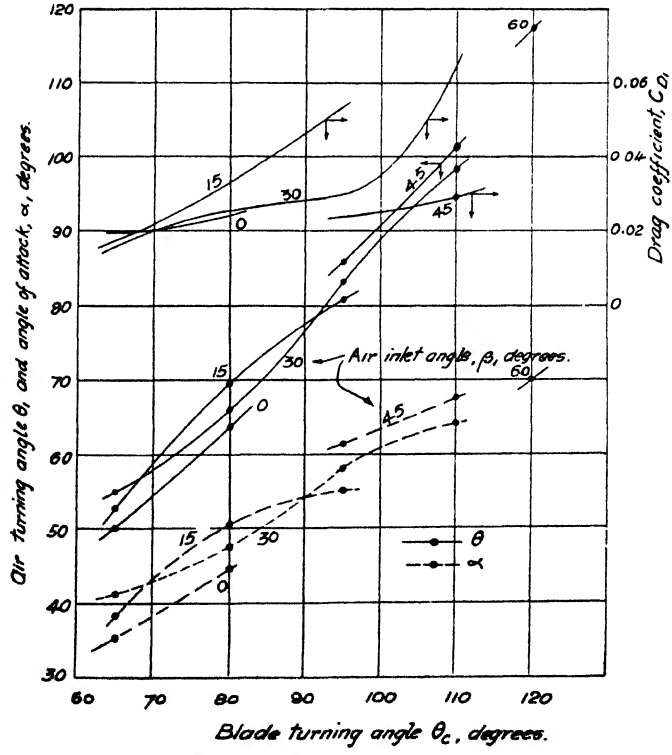

FIG. 7.16. Deflection, angle of attack and drag coefficient as a function of blade turning angle (adapted from Dunavant and Erwin, ref. 4).

at which stream stagnation pressure is obtained at an orifice located at the end of the mean line and for which orifices on either side indicate equal pressure drop.

Reference 4 gives data for a range of blade camber angle from 65° to 120°, air inlet angle from 0° to 60° and for two solidities, 1·5 and 1·8. The many results cannot be given here, as they are too numerous, but a replot of some of the data is given for illustration in Fig. 7.16, showing deflection θ, design angle of attack a_1 and the corresponding drag coefficient C_{D_1}, plotted against blade turning angle θ_c, for various values of air inlet angle β_1, all for one solidity σ of 1·8 ($s/c = 0{\cdot}55$).

The data shown by the figures for both NGTE and NACA cascades are intended only as a means of illustrating design methods and the type of results obtained. The data have been simplified and, for design work, the original or similar reports are necessary.

7.9 *Effect of Reynolds and Mach Numbers*

The Reynolds number for turbine blades is based on blade chord, but as there may be a considerable change in velocity and fluid properties through the blade passage, there is a choice of inlet, outlet, or mean conditions from which to choose. British practice, as exemplified by NGTE work, is based on outlet values, while U.S. practice, represented by NACA data, is based on a mean value, the average of upstream and downstream conditions.

For the former, Ref. 3 indicates a critical value of about 2×10^5 from cascade tests (low turbulence) and about 1×10^5 from turbine tests, losses increasing rapidly at lower values than these. A later report from the same source (Ref. 6) suggests that NGTE data for turbine blades corresponds to a mean value of Reynolds number of 2×10^5 and that for a turbine operating at values very different from this, the overall turbine efficiency obeys the law

$$(1 - \eta_t) \propto R_e^{-0{\cdot}2}$$

This is reasonably valid down to a Reynolds number of about $0{\cdot}5 \times 10^5$, below which the loss increases more rapidly.

The NACA data (Ref. 4) are based largely on mean Reynolds numbers from $3{\cdot}2 \times 10^5$ to 5×10^5, with high speed tests of a limited nature reaching values up to 15×10^5. In the quoted reference on turbine blade cascade results, no assessment is made of the effect of lower Reynolds numbers.

While for many designs, the value of Reynolds number is above any possible critical value, for very small turbines of low pressure ratio and possibly for those of turbo-jets at high altitude, some loss

may be anticipated. It is also possible that starting troubles may be accentuated by low values of Reynolds number.

The influence of Mach number on profile loss is really not clearly delineated. An effect is first felt when a local shock wave appears at the point of maximum suction pressure on the convex surface, the thickening of the boundary layer due to the adverse pressure gradient leading to an increase in loss coefficient. Increase of Mach number may then produce either a further increase of loss or, quite often, a decrease. The latter is quite contrary to the effect of Mach number on flow over blades generally, but may be explained by the movement of the shock wave downstream as the channel pressure gradient increases, with decreased loss due to a smaller area affected by the thickened boundary layer. However, for blades with considerable curvature in the trailing edge region, the loss may increase considerably. It would appear that in these circumstances, the laminar boundary layer separates rather than turning to a turbulent boundary layer (Sec. 4.14). Thus the effect of Mach number is associated with the degree of turbulence, as a high level of the latter would tend to induce early transition and minimize the possibility of separation.

7.10 *Three-dimensional Flow Losses*

In addition to the profile loss, there are the losses due to secondary flow and to tip clearance. Analytical study of these losses is immensely complex and visual methods of demonstrating three-dimensional effects confirm the expected complicated flow patterns, as well as showing unsuspected results in some instances. Analysis is very useful qualitatively, however, in elucidating the controlling parameters, leaving the numerical values to be determined empirically. For blading operating at the correct incidence (about minimum profile loss), the secondary flow loss may account for half or more of the total loss, with the clearance and profile losses each contributing about one quarter. At off-design conditions, the profile loss increases its relative proportion until at excessive positive incidence it is the main factor, resulting in blade stall. This shows two important points, firstly the necessity for cascade data to establish incidence limits, and secondly, the fact that at design conditions, much more knowledge of secondary flow effects is required in order to improve efficiencies. Studies of secondary flow have been made by both the NGTE and the NACA, for which Refs. 7 and 8 may be consulted.

The secondary flow loss is in many ways analogous to that of induced drag coefficient for isolated airfoils and therefore it is not

surprising that the loss depends very largely on the blade loading as given by lift coefficient. A parameter of secondary loss drag coefficient is given in Ref. 5 as

$$C_{D_s} = \lambda_s C_L^2/(s/c) \tag{7.12}$$

where λ_s is an empirical coefficient of the order of 0·006–0·025 depending on velocity variation and blade geometry.

Tip clearance loss has long been a subject for study, as it is a matter of considerable interest for steam turbines. A theoretical expression which seems to correlate reasonably well such measured values as are available is given in Ref. 5 as

$$C_{D_c} = \tfrac{1}{2} C_L^2 \frac{t_c}{s/c} \tag{7.13}$$

where t_c is the fractional tip clearance, gap over annulus height. This leads to reductions in turbine efficiency of 2–3 t_c. Clearance losses may be appreciable if radial tip clearance has to be large to allow for differential expansions, turbine growth and possible casing distortion. It is possible to replace radial tip clearance by axial clearance by means of tip shrouds, as shown in Fig. 7.17. The axial clearance can be adjusted by "end-tightening", with possible reduction of clearance loss by one half.

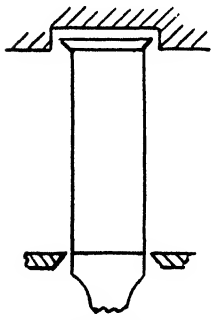

FIG. 7.17. Tip shrouds with axial clearance —diagrammatic.

Apart from loss of efficiency, there is a direct loss of output with tip clearance, as the fluid which passes through the gap does no work. This is equivalent to a lower value of outlet gas angle, so that the mean deflection must be increased to allow for this. Leakage depends on the degree of reaction, since obviously the pressure difference across the blade is an important factor. Although an analysis is possible in terms of blade parameters (Ref. 5), a very rough figure of 5% loss in work output may be used for reaction blading.

7.11 *Vortex-flow Design*

Because of the finite length of the blade, the design must allow for the variation of conditions from root to tip, not only for variation of blade speed, but for radial equilibrium as discussed in Chapter 4. For turbines, the free vortex flow condition has been most frequently applied, particularly as it is simple to use. This requires constant axial velocity from root to tip and inverse variation of whirl velocity with radius.

A free-vortex pattern requires more twist in the blade from root to tip than does a pattern ignoring radial equilibrium, but this is seldom a real complication in manufacture, because never are rotor blades made totally untwisted, as is possible in the first stages of steam turbines, in which the hub ratio (root diameter/tip diameter) is high. It is sometimes possible to make the nozzle vanes untwisted, because, with small outlet angles, the variation of angle may be only some 6°–7° from root to tip for free vortex flow. Thus a mean value will not cause a great departure from the nominal conditions and may affect efficiency to only a negligible extent. If machined from bar stock, an untwisted vane may represent quite a saving in manufacturing cost, but if, as is common, the vanes are precision-cast, then little is gained.

It has been previously pointed out that vortex flow involves varying degrees of reaction from root to tip. For free-vortex flow, the reaction increases with radius and thus a stage cannot be completely characterized as having a particular value. The designation impulse is sometimes given to blading having zero reaction at the root, with the reaction possibly increasing to a value of 0·6 or more at the tip, depending on the hub ratio. For stages of maximum work output for a limiting blade speed, it has been shown that impulse conditions are desirable. With free-vortex flow, this can obtain only at the root, so this becomes the design starting point. If any other radius is used as a design radius, the root conditions must be checked at an early stage, because negative reaction must be avoided. For a turbine, negative reaction implies a *rise* of static pressure across the rotor blade and although the required energy transfer may be obtained (i.e. $(U\Delta V_u)$ still positive), the diffusion or *recompression* is obviously detrimental to efficiency. This point is emphasized because it is often convenient to use the conditions at the mean radius for preliminary design calculations in order to establish the main design dimensions of a gas turbine for a given duty.

Turbines are not subject to a " work-done factor ", as discussed for compressors in Chapter 6, because, in the first place, the boundary layer is much thinner due to the high velocities and accelerating flow. In the second place, it is readily seen, by drawing a diagram in analogous fashion to that for an axial-flow compressor stage, that a peaked velocity profile leads to increased incidence at the centre section and reduced incidence at root and tip. For a turbine, however, the changed incidence is small for the reasons given above, and its greater tolerance does not lead to stall.

7.12 *Blade Stress and Blade Temperature*

This text does not seek to discuss stress considerations of gas turbines, but it is necessary to have sufficient knowledge to avoid inoperable designs. To this end, an elementary analysis of the main blade stress, that due to centrifugal effect, is given here.

A rotating blade is subject to (1) a direct centrifugal force, (2) a bending force consequent on (1) if the centroids of all blade sections are not radial and (3) a bending force due to fluid pressure and change of momentum. Stress due to the last-named is taken care of by blade chord and thickness, while that due to non-radial centroids may often be utilized to offset the direct bending stresses. It is the tensile stress due to direct centrifugal action which is the main limiting stress.

With R and r the blade tip and roof radii and A the blade profile area (constant), the mass of the blade is $\rho A(R - r)$, considered as concentrated at the centroid at the mean radius $r_m = (R + r)/2$. The stress S_c due to centrifugal force F_c on area A due to blade rotation is then

$$S_c = \frac{F_c}{A} = \frac{M\Omega^2 r_m}{g_0 A} = \left[\frac{\rho A(R - r)}{g_0 A}\right]\left[\frac{2\pi N}{60}\right]^2\left[\frac{R + r}{2}\right]$$

which may be reduced to

$$S_c = 0{\cdot}376\,\rho\left(\frac{N}{1000}\right)^2 A_a \tag{7.15}$$

where S_c is the stress in psi, ρ is the material density in lb/cu ft, N is the rotational speed in rpm and A_a is the annulus area in sq ft. Tapering the blade section from root to tip results in lower stress, the constant becoming about 0·25 for blade tip area/root area of 0·35. Eq. (7·15) (or modified for taper) then allows a rapid estimate to be made of allowable speed with a given throughflow (since $A_a \propto 1/V_a$) or vice versa.

Blade design may be used to minimize the actual metal temperature for a given maximum cycle temperature, as noted in Sec. 7.4. Thus lowered reaction gives lower metal temperature, a very important factor in blade life, due to the life-temperature-stress relationship of blade alloys. It may be noted that the effect of increasing reaction from root to tip in free-vortex blading is compatible with this effect, because the blade stress decreases with radius and a higher temperature towards the tip is not limiting.

7.13 *Turbine Overall Performance*

A turbine stage, or a group of stages, behaves in very similar fashion to a simple nozzle with respect to the pressure-flow relation-

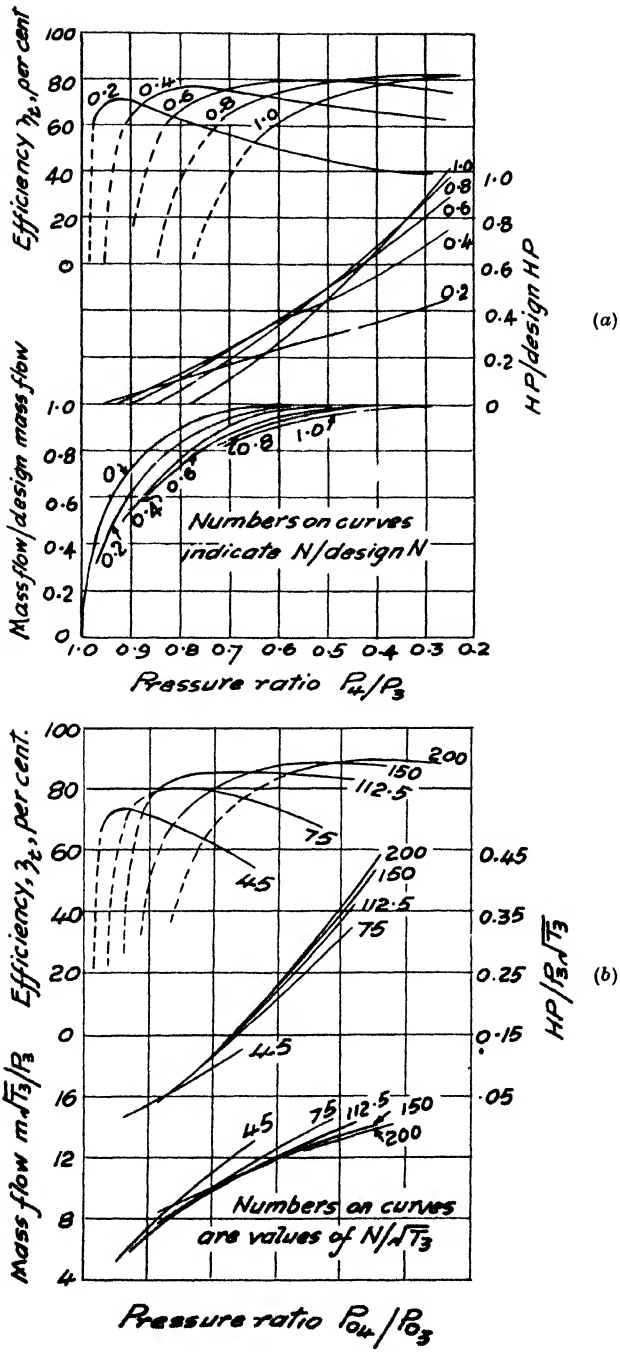

FIG. 7.18. (*a*) Two-stage impulse turbine (impulse at root); (*b*) Four-stage reaction turbine (50% at mean diameter). Performance characteristics of impulse and reaction turbines (adapted from Ainley, ref. 3).

ship. The independent parameter of speed has very little effect except at extreme conditions where incidence causes blade stalling. Two typical turbine characteristics are shown in Fig. 7.18 (following Ref. 3), (a) for a 2-stage impulse turbine of high pressure ratio and (b) for a 4-stage reaction turbine of low pressure ratio. The coordinates are dimensionless groups (these are discussed in Chapter 10), because in a gas turbine, it is seldom that only one performance variable (mass flow, pressure, temperature or speed) is altered at a time. The ordinate, pressure ratio P_3/P_4, is obvious and the abscissa, $m\sqrt{T_3}/P_3$, may be regarded simply as flow rate. Likewise the speed parameter is given as the ratio of speed to design speed.

The impulse turbine characteristic shows the phenomenon of choking, discussed in Chapter 4, that is, the limitation of mass flow at a certain pressure ratio. Gas turbine nozzles are always only convergent in physical shape because of the limitation of blade speed through the U/V_1 relationship and the poor performance of the convergent-divergent type at other than design conditions. However, an impulse stage is often run in the choked condition and due to the discharge expansion and shape of the nozzle blade row passages, a supersonic flow occurs. Fig. 7.19 shows a simplified view of the state of affairs. When the pressure ratio P_3/P_x exceeds the critical value, then choking occurs and the gas velocity is the acoustic velocity at the throat (Mach number of unity). The pressure P_x is less than the critical pressure at the throat and thus the gas expands. The convex trailing edge region of the adjacent blade forms in effect one side of the divergent part of a nozzle. The region downstream of the other blade is unbounded, however, and the fluid expands as if turning a corner (Prandtl-Meyer expansion). The net result is that the velocity is increased in magnitude and changed in direction, being deflected toward the axial direction. This velocity can most easily be determined on the basis of continuity of flow, with blade outlet conditions fixed and a known annulus area. This expansion to supersonic velocity without a physical divergent nozzle is accomplished with little loss at the moderate pressures in gas turbines.

FIG. 7.19. Gas expansion and deflection in choked flow.

The range of the constant-speed lines in Fig. 7.19 is greater than normally used, as usually pressure ratio and mass flow increase with speed. Thus for the purposes of estimating the turbine characteristic for part-load performance (see Chapter 10), it is common practice to reduce it to a single line, thus giving single values of pressure ratio

and flow rate at any speed. Admittedly, this is not completely accurate but is usually sufficiently so for the purposes for which it is used.

7.14 *Blade Cooling*

As far back as the days of World War II, when the gas turbine was in its initial development phase, the possibilities of cooling the turbine blade material, to permit the use of higher gas temperatures, was being actively considered. In Germany, hollow air-cooled nozzle blades were used, and hollow rotor blades, cooled by water under supercritical conditions, were in active preparation for experimental testing.

Increase of gas temperature would benefit the output and efficiency of nearly all shaft-power machines, but not necessarily of turbo-jet engines (see Chapter 3). The disadvantages are, in addition to complexity in manufacture and possibly in operation, the sacrifice of optimum blade design to make provision for circulation of cooling fluid and the loss of energy in the cooling process itself.

The cooling medium may be gaseous or liquid. The former appears advantageous because of the available supply of compressed air, thus requiring only a piping system from compressor discharge. However, gas offers a much lower heat transfer coefficient than does a liquid, and thus a relatively large quantity is required. A much lower flow rate of liquid is required, but unless a highly pressurized system is used, boiling occurs with wasteful and uncontrolled local cooling. There is also the possibility of deposits and gradually restriction of the cooling flow area.

Much work has been done on the thermodynamic effects, that is, improvement of performance due to higher T_{max}, balanced against losses due to poorer aerodynamic performance of blades and losses due to heat-rejection. A very careful balance is required, as it is easy to lose most of the ideal thermodynamic advantage. Likewise, much theoretical and experimental work has been done on the heat transfer problem itself. One of the major difficulties is to cool adequately the leading and trailing edges of the blades without sacrificing too much profile efficiency. Three major methods of cooling may be distinguished. The first is by convection in the ordinary sense, using small passages, high velocities and generous employment of finned surfaces inside the blade shell. The second method is by film cooling, that is, the injection of thin layers of coolant through slots into the boundary layer on the external blade surface. The third method is that of transpiration cooling, in which the fluid is forced through a porous wall so that the entire surface is

cooled, by effectively making an almost infinite number of very small flow passages. This last method is the most effective from the point of view of maximum coverage with a minimum of coolant flow. However, it requires special materials and methods of construction.

Up to the present time, although several experimental cooled turbines have been run, there does not appear to be an operational unit in regular use. A good summary of blade cooling, with an extensive bibliography, is given in Ref. 9.

REFERENCES

1. Balje, O. E. A Contribution to the Problem of Designing Radial Turbomachines. *Trans. A.S.M.E.*, **74,** 1952, p. 451.
2. Shepherd, D. G. *Principles of Turbomachinery.* The Macmillan Co., N.Y., 1956.
3. Ainley, D. G. Performance of Axial-Flow Turbines. *Proc. I. Mech. E.*, **159,** 1948; reprinted by *A.S.M.E.*, 1949, "Internal Combustion Turbines."
4. Dunavant, J. C. and Erwin, J. R. Investigation of a Related Series of Turbine-Blade Profiles in Cascade. *N.A.C.A.* TN 3802, 1956.
5. Ainley, D. G. and Mathieson, G. C. R. An Examination of the Flow and Pressure Losses in Blade Rows of Axial-Flow Turbines. *Aeron. Res. Coun.*, R. and M. No. 2891, 1955.
6. Ainley, D. G. and Mathieson, G. C. R. A Method of Performance Estimation for Axial-Flow Turbines. *Aeron. Res. Coun.*, R. and M. No. 2974, 1957.
7. Carter, A. D. S. Three-Dimensional Flow Theories for Axial Compressors and Turbines. *Proc. I. Mech. E.*, **159,** 1948.
8. Rohlik, *et al.* Secondary Flows and Boundary-Layer Accumulations in Turbine Nozzles. *N.A.C.A.* Report No. 1168.
9. Esgar, J. B. Turbine Cooling. Gas Turbine Progress Report, 1958, *A.S.M.E.* Paper No. 58-A-46C, 1958.

CHAPTER 8

COMBUSTION

THE function of the combustion chamber or *combustor* is to accept the air from the compressor and to deliver it to the turbine at the required temperature, ideally with no loss of pressure. For the common open-cycle gas turbine, this implies the internal combustion of fuel and thus a problem of fuel preparation, mixing and burning. The fuel is commonly gaseous or liquid, with solid fuel presenting a very difficult problem which has not yet advanced beyond the experimental stage. Gaseous or liquid fuels are almost invariably hydrocarbons, the former usually being natural gas, mostly methane, with some small proportion of heavier compounds such as propane and butane, while the latter may range from highly refined gasoline through kerosene and light diesel oil to a heavy residual oil (Bunker C or No. 6 fuel oil). It may be said that the combustion problem itself is seldom difficult, as all the fuels used for gas turbines are used in combustion apparatus of one sort or another and have been so used for many years. The difficulty arises in the combination of combustion with low pressure loss in a size of combustor compatible with the high power-weight or high specific output potentialities of the rotating elements. Almost any fuel can be burnt successfully if sufficient pressure drop is available to provide the necessary turbulence for mixing of air and fuel and if sufficient volume is available to give the necessary time for combustion to be completed.

8.1 *Criteria for Combustion Performance*

The desirable criteria for gas turbine combustion are listed below, with the order not necessarily indicating relative importance, because all must be satisfied for a successful design.

(1) Complete combustion of the fuel.

Any fuel unburnt, in the sense of the full heating value per pound not having been realized, is directly reflected in the fuel consumption or thermal efficiency.

(2) Minimum loss of total pressure.

Combustion pressure loss is one of the flow losses discussed in Chapter 3 and its effect may be judged from the loss expression (3.26).

(3) Absence of deposits.

As all normal fuels contain carbon, there is a tendency for free carbon to be deposited on the walls of the combustor or carried through to appear as smoke. Any accumulation of carbon will upset the designed flow pattern and increase pressure loss due to blockage, while eventually pieces may break off and damage the turbine blades. Smoke is always objectionable, sometimes to a limiting degree, although a light haze is usually allowable, if undesirable.

(4) Rapid and reliable ignition.

As the gas turbine is a steady-flow machine, ignition is required only at starting, the combustion being self-sustaining once the fuel is ignited by outside means. This allows a considerable simplification of the ignition system, as no distributor mechanism is needed as for the spark-ignition engine, nor again is the gas turbine dependent on a self-igniting fuel as for the diesel engine. Nevertheless, the certain ignition of a liquid fuel under all conditions is not always easy, taken in conjunction with the fact that the igniting means is likely to be permanently exposed to the combustion gases.

(5) Controlled temperature and velocity distribution at turbine inlet.

It is very important that the gas temperature at the turbine be either uniform or have a designed gradient, because at the high general level of temperature the strength of the blade material may be critical to within small limits. It is possible for the fuel-air mixture to have burnt to yield the required average temperature, but with the mixing to be poor so that there are hotter and less hot regions. The ideal turbine inlet temperature distribution might be that to give material properties to correspond to the stress levels in the blade, so that a uniform combustor outlet temperature is not necessarily the most desirable. Control of the temperature distribution is difficult to achieve to the desirable limits and sometimes the best that can be accomplished without compromising other qualities is to avoid excessive " hot spots ". Velocity distribution is not so important, but some attention to this may be necessary to avoid particularly bad conditions, for example where the turbine immediately follows a bend.

(6) Minimum volume and weight.

These criteria are always desirable, of course, but in some applications, the aircraft gas turbine being the prime example, they may be limiting. Even for a static industrial application,

the size and weight of the combustor must be suitable for the turbine as a whole and this imposes restrictions on design, as compared with other steady-flow combustion devices.

(7) Reliability and endurance.

These are again obviously desirable criteria, but the importance of the former is paramount in gas turbines, because a failure may wreck the turbine, as, owing to the high speed of the latter, only a small solid element, may cause considerable damage. Reliability and endurance are differentiated, because in an aircraft turbine, for example, a relatively short life may be acceptable, while reliability for that period is essential.

All these performance criteria must be satisfied to some degree, the importance of each depending on the application and the problem is to arrange a satisfactory compromise. It must be noted that in most cases it is not only the main operating or design point conditions that must be satisfied, but part-load and idling conditions as well, with the variables of altitude and forward speed affecting the aircraft plant. Thus both pressure level and mass flow rate may cover a wide range, with the inlet air temperature varying with pressure ratio (and with altitude for aircraft turbines). The variation of turbine inlet temperature over the usual operating range may be such as to require combustion to remain satisfactory over at least a 2/1 range of air-fuel ratio, with the additional requirement that the flame not be extinguished for occasional limited periods of operation with abnormally rich or lean mixtures. The design air-fuel ratio is proportional to the required combustion temperature rise, as was seen in the cycle analysis, and this depends on the pressure ratio, degree of regeneration and maximum temperature. The turbo-jet engine usually requires the richest overall mixture or lowest air-fuel ratio, which may be about 50/1. An industrial gas turbine of more conservative rating may be about 70/1, while with a heat exchanger, the mixture strength may be as lean as 100/1. Part-load conditions may require lowered temperatures, so that these air-fuel ratios are increased considerably, possibly to give the 2/1 range mentioned above. Note that for cycle calculations, fuel-air ratio was used, but for the combustion problem, its reciprocal, air-fuel ratio, is used as being capable of more ready apprehension as a numerical value.

Although both pressure and mass flow rate may vary considerably, they are to a large extent interdependent, and, together with the adiabatic relationship of compressor delivery pressure and temperature, the result is that the air velocity at entry to the combustor is

relatively constant. This is fortunate, because the velocity is a controlling parameter in combustion performance.

8.2 *The Nature of the Combustion Process*

Before attempting any analysis of the combustion process, it must be said that of all the component processes in the gas turbine, the least amount of firm design data is available for combustion. In contrast with compressor, turbine and heat exchanger design, for which data are available to ensure that adequate performance is reasonably assured for a conservative design, only certain guiding principles can be given for combustor design, with bench testing and modification being mandatory before full operational engine testing is possible. This is to a considerable degree inherent in the basic combustion problem itself, which is to obtain intimate mixing of fuel and air under conditions in which the resulting flame is self-sustaining and the chemical reaction is complete. Thus whereas compressor and turbine design is aimed at approaching ideal flow conditions and represents aerodynamic conditions only, combustion design involves the formation of turbulent zones, with the complication of both aerodynamic and thermochemical effects. The whole body of aerodynamic technology is available for the design of flow around streamlined bodies and through channels, whereas the production of exactly controlled turbulent mixing zones is so complex that the only resort is to empiricism. The problem in combustion is to produce only enough turbulence for mixing and burning, with any excess not only leading to additional pressure loss, but possibly being deleterious to the maximum reaction rate of fuel and air. Thus in spite of the tremendous research effort on combustion over the last twenty years, there is still no exact mechanism for flame stabilization in steady flow which would be generally agreed upon, and the formulation of rules for similarity in combustion, comparable to the use of Reynolds number and Mach number in purely aerodynamic problems, is still only in a tentative form. With this in mind, an attempt will be made here to summarize some of the general principles and broad correlations which have been established and which are useful in gas turbine combustion.

In a gas turbine combustor, the overall problem of obtaining complete reaction between fuel and air (actually fuel and oxygen) has a chemical aspect and a physical aspect. Although the physical aspect, considered as mixing, has been recognized all along, any attempt at exact understanding of the steady-flow combustion processes has been attempted mostly along chemical lines until recently. However, the approach through reaction kinetics, which

has been so valuable in explaining combustion in the reciprocating engine, does not seem likely to be very fruitful for gas turbine combustion. In the former case, a given quantity of combustible mixture is undergoing a change of state, occasioned by adiabatic compression and the local ignition of a small part of it, the flame spreading out into the mixture. Thus it is possible to fix attention on a certain part of the mixture and analyse the chemical process which is taking place. In the latter case, it is impossible to isolate any one quantity of material, because the process is one of mixing, with a burning zone fixed in space but with composition and temperature varying everywhere in the zone. While the chemical processes must occur and a knowledge of them is helpful for understanding in most, if not all, gas turbine combustor conditions, the physical processes are controlling and lead to such quantitative relationships as are available. Thus it has been shown by Longwell and Weiss (Ref. 1) that for adiabatic combustion of a homogeneous, stoichiometric mixture of a hydrocarbon fuel and air under conditions simulating as far as possible instantaneous and complete mixing with burning combustion gases, the maximum space heat release rate, or combustion intensity, is of the order of 3×10^8 Btu ($1{\cdot}7 \times 10^8$ Chu) per cu ft per hr per (atm) $^{1{\cdot}8}$. In this approach to a " perfectly stirred " reactor, the limiting condition is one of chemical reaction time. The value of overall maximum heat release rates at the design point in existing combustors is in the range $1\text{–}3 \times 10^5$ Btu/(ft^3) (hr) (atm$^{1{\cdot}8}$), so that, even allowing for the weaker mixture and the volume required for mixing with diluting air to obtain the limiting turbine inlet temperature, it is apparent that the chemical limit is not controlling.

The combustion reaction process requires the collision of molecules of fuel and oxygen, the collision having a sufficiently high energy level so that the molecules are broken down into simpler molecules, atoms and radicals, subsequent collisions of various combinations of the elementary particles leading to the final products of combustion. Although the overall reaction may be written as a simple chemical equation according to stoichiometrical relations, even the simplest reaction, hydrogen and oxygen for example, is known to involve a number of intermediate steps. In theory, a knowledge of all these steps, including the associated energy levels, called the *reaction kinetics* of the process, would allow the solution of the combustion problem. The knowledge of the problem for the combustion of a complex hydrocarbon under widely varying conditions is so scanty that no quantitative answer seems likely. The general nature of the chemical kinetic approach, however, is necessary and

useful in appreciating some overall features of the combustion process.

In a *bimolecular* gas reaction, that is, one involving the reaction of two molecules, it can be shown from the kinetic theory of gases that the rate of reaction expressed as the mass rate per unit volume of conversion of one component, the fuel for example, can be expressed as

$$r \propto m_0 \, m_f \rho^2 \sigma^2 \, T^{\frac{1}{2}} \, M^{-3/2} \, e^{-E/RT} \tag{8.1}$$

where
m_0 = fractional concentration of oxygen
m_f = fractional concentration of fuel
ρ = density
σ = measure of molecular diameter
T = absolute temperature
M = mean molecular weight
E = energy of activation
R = gas constant

The exact definitions and units need not concern us here, as only qualitative information is needed (or, for the practical case, is possible).

The first six terms on the right-hand side represent the number of collisions occurring and the last term, $\exp(-E/RT)$, represents the fraction of such collisions with an *activation* energy E sufficiently great to give rise to successful collisions, i.e. resulting in reaction. This exponential term is very important, as for fixed values of E and R, it is very sensitive to temperature. Thus it is this factor which accounts for the simple rule of elementary chemistry that a rise in temperature of 10° C at room temperature doubles the reaction rate. While this relation does not hold exactly, it is the key to understanding the non-reactance of a fuel mixture at atmospheric temperature and shows that a high mixture temperature is necessary for a fast reaction. The chemical kinetics of a reacting system here interpose a complicating factor, with the idea of *chain-branching* and *chain-breaking* mechanisms, each governed by a collision rate theory and occurring simultaneously, so that the overall reaction rate is not simply determined. However, from the measured rates of reaction of a fuel-air mixture, it is possible to deduce an *apparent* activation energy E, which appears to be of the order of 40,000 cals/gm mol for hydrocarbons.

The concentrations of oxygen and fuel, m_0 and m_f, are functions of temperature. This is apparent by considering that an increase of temperature is caused by reaction, that is a reduction of fuel and air concentrations, with an increase of products. Initially, before

reaction takes place, the concentrations are at a maximum and the temperature is a minimum. At the highest temperature, either m_0 or m_f or both are zero. The density of the mixture is a function of pressure and temperature and the molecular values σ and M are fixed for a given system. Thus Eq. 8.1 may be written

$$r = Ap^n f(T) \tag{8.2}$$

where A is a factor dependent on the initial mixture, p is the pressure and $f(T)$ is a complex function comprising all the temperature dependent factors discussed. The exponent n replaces the exponent two for the bimolecular reaction to generalize the expression for any order of reaction. The conclusions to be drawn from Eq. (8.2) are that the reaction rate is sensitive to pressure with the order of reaction n indicating the degree of sensitivity, and very dependent on temperature, with the exponential function in $f(T)$ having a controlling effect. The explicit nature of the pressure dependence is useful in forming combustion parameters. The evidence to date shows that a probable value of n for stoichiometric hydrocarbon mixtures is about 1·8, with a possibility of lower values for leaner mixtures. This accounts for the exponent of 1·8 in the combustion intensity expression quoted previously. It gives warning of the difficulties experienced with combustion in aircraft at high altitudes, where the pressure is much reduced. The temperature dependence shows that poor combustion is probable at mixture strengths not too far removed from the stoichiometric, as the adiabatic combustion or flame temperature is reduced, and also that some effect may be expected from the initial temperature of the reactants.

A property of a combustible mixture at a given initial state of pressure, temperature and air-fuel ratio is the *flame speed*, defined as the velocity of the flame front in a direction perpendicular to its surface (normal velocity) relative to the unburned mixture. It has a precise value only for propagation in a quiescent mixture or for laminar flow, as, in turbulent flow, the intensity and scale of turbulence introduce independent variables. Thus flame speed, usually denoted by S_u, is sometimes called the laminar flame speed, with laminar being implicit, if not otherwise denoted. While it seems that, under the extremely turbulent conditions of an unhomogeneous mixture of air and fuel in a gas turbine combustor, laminar flame propagation is remote, nevertheless S_u is a measure of the basic combustion process. Because the combustion process represented by a laminar flame is the simplest form which can be taken by a steady-flow combustion process and is susceptible to analysis, considerable attention has been given to experimental measure-

ments under varying conditions and their correlation with theoretical analyses. Values of S_u are very low in comparison with the bulk velocities necessary in combustors, being of the order of only a few fps for hydrocarbons. The dependence on mixture composition, pressure, and temperature, however, is useful in correlating with a reaction rate expression such as (8.2) and in predicting variations of performance in actual combustors, as ultimately the reaction takes place by laminar flame propagation locally, however small and disordered are these local zones. Thus it is possible to show (Ref. 2) that

$$S_u \propto B\,(p^{n-2})^{\frac{1}{2}} \tag{8.3}$$

The factor B covers the nature of the mixture, i.e. the type of fuel and the mixture strength. A flame is governed by heat and mass transfer and a balance between the reaction, which increases the temperature, and the heat conduction away from the reaction zone, is possible only within a narrow range of mixture strengths. Maximum flame speed occurs when the mixture strength is close to stoichiometric, which is the condition giving maximum temperature and hence reaction rate. Either side of stoichiometric, the flame speed decreases rapidly, until it is impossible to initiate any flame at all.

If $n = 2$, then flame speed is independent of pressure and as n appears to be about 1·8, the pressure dependence is not large and is inverse, i.e. S_u decreases as p increases. Alternatively, this expression may be used to estimate the order of reaction n by experimental values of S_u at various pressures.

Apparent flame speed is increased by turbulence and one theory of combustion postulates that turbulent combustion is similar to laminar combustion except that a flame front is wrinkled and distorted to a degree determined by the intensity and scale of turbulence. This has been developed quantitatively to some extent, with an expression for turbulent flame speed as a function of laminar flame speed and scale of turbulence, but the difficulties of application are considerable. It is apparent, however, that with laminar flame speeds of the order of a few fps, increased by turbulence as they may be, then a steady flame fixed in space cannot be expected for a gas turbine combustor by simple injection of fuel into the air stream of velocity one or two magnitudes greater than the laminar flame speed. Even if ignited initially, the flame would be immediately carried downstream, so that ignition would have to be continuous. It is obvious then that a means of flame *stabilization* must be found, that is, a system whereby part of the high-temperature products of combustion can be caused to recirculate in order

to ignite fresh reactants. Of course, flame stabilization in fact, if not by name, has been part of combustion practice since forced air circulation has been used, but, although successful systems are legion, for gas turbine combustion it is desirable to be able to analyse the basic controlling features of a stabilizing system in order that a good efficiency with respect to pressure loss may be established and so that the performance under varying conditions of flow rate, pressure, temperature, mixture strength, etc., may be estimated.

Many of the present-day stabilizing zones of gas turbine combustors which have been developed purely empirically are somewhat complex and cannot be well analysed on the basis of any singular dimension or air velocity. This is because one major requirement is vaporization of the liquid fuel and mixing with air before the combustion process can be initiated. Here again, however, the process of stabilization in a homogeneous mixture with a simple system is qualitatively effective in understanding the more complex combustor process.

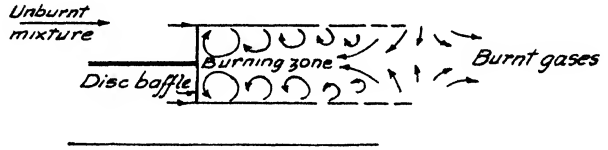

FIG. 8.1. Stabilizing zone—schematic.

Fig. 8.1 shows the basic elements of a stabilizing zone, with a disc *baffle* causing an eddy region in the flow of fuel-air mixture flowing steadily in a duct. Once reaction starts, mixing of burnt and unburnt gases occurs along the mixing region, with burning gases being drawn down into the eddy zone, completing the reaction, and being returned into the mixing zone to provide the steady circulation. At a fixed value of flow velocity, it is found that there is a limiting range of mixture strength for which the flame is stable, i.e. above and below which the flame is extinguished. This is called the *blow-out* velocity, V_{BO}. The range of mixture strength is reduced as the velocity is increased, a condition eventually being reached for which no stable flame is possible for any fuel-air mixture. This is called the maximum or peak blow-out velocity. A typical plot of mixture strength as fuel-air ratio on a mass basis against blow-out velocity is shown in Fig. 8.2. Different shapes of baffle (or " bluff body ") will show different curves of the same general nature, but with wider or narrower mixture limits for a given velocity and a differing peak velocity. Increase of size of baffle will increase the

blow-out limits and reduction of pressure will reduce the limits. The last two factors are important for design, because increase of baffle size will increase the pressure loss and the effect of pressure will throw light on altitude limits of stable burning.

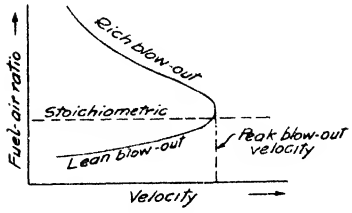

FIG. 8.2. Typical stability diagram.

At a given velocity the rich and lean limits of operation represent the limits of flame propagation under the conduction and transfer conditions in the recirculation zone, with the peak blow-out velocity usually occurring near the stoichiometric mixture strength. At this peak point, the rate of flow of the fuel-air mixture into the reaction zone just exceeds the reaction rate possible in the zone and flame extinction occurs. The mixture mass flow rate at this point is assumed to be proportional to the mixture velocity V_{BO}, the area of the reaction zone and the density of the mixture. The area of the zone is taken to be proportional to the stabilizer area or, in general, as d^2, where d is a characteristic dimension (e.g. disc diameter, plate width, etc.). For a given inlet temperature, the density is proportional to the pressure p. Hence mixture mass flow rate $\propto V_{BO}d^2p$. The reaction rate is the rate per unit volume, r, times the reaction zone volume, taken as proportional to d^3. Hence for the blow-out condition

$$V_{BO}d^2p \geq rd^3 \tag{8.4}$$

From Eq. (8.2), $r \propto p^n$ for a given mixture and temperature level. Thus, substituting in (8.4),

$$\frac{V_{BO}}{p^{n-1}d} \geq \text{constant} \tag{8.5}$$

This simple analysis resulting in Eq. (8.5) shows a dependence of blow-out velocity on pressure and baffle size. Experimental results with a variety of simple baffles and fuels shows that this expression is very reasonable, with the exponent of p being slightly less than unity, indicating an order of reaction slightly less than two (cf. $n = 1{\cdot}8$ discussed earlier) and with d having an exponent either close to unity as required by (8.5) or about half this value. The latter result has been postulated as due to a laminar flow wake, which would change the simple hypotheses above.

A similar result is possible by means of a considerably more complex analysis (Ref. 3) containing the collision rate parameters associated with r, that is, the effect of temperature, mixture strength, etc. The correlating expression is $m/vP^{1{\cdot}8}$ as a function of tem-

perature, fuel consumption, efficiency of oxygen consumption, activation energy, etc., where m is the mass rate of flow, v is the reaction volume and p is the pressure in atmosphere; $m/vp^{1\cdot8}$ is reducible to $V_{BO}/p^{n-1}\,d$ for a reaction order of 1·8. In the first form it suggests immediately a logical form of expressing combustion intensity for gas turbine combustors, even if the conditions therein are not similar to the homogeneous, controlled reactions for which it was developed.

8.3 *Form of Combustor*

The previous discussion, though barely scratching the surface of the subject, serves to indicate the necessary features of a practical combustor. First of all, it is necessary for the reaction zone to operate near the stoichiometric mixture strength in order to develop the highest possible temperature for a rapid reaction or rate of flame propagation. This mixture strength for most hydrocarbons is about 15/1, so for an overall air-fuel ratio of 60/1, only about one-quarter of the total air must be admitted to the reaction or *primary* zone, leaving the rest as *diluting* air to be admitted to reduce the gas temperature to the required turbine inlet temperature. It was stated earlier that the operating range of air-fuel ratio was usually at least 2/1, with combustion having to be sustained, if not necessarily efficiently, over a wider range. This immediately raises the question of designing for wide stability limits, that is, well below the peak blow-out velocity.

The primary zone must have a baffle to establish a recirculation zone, but, in addition to stabilization, a vigorous mixing action must be provided in order first to mix air and fuel and then to mix unburnt mixture with burnt gases. The stability parameter indicates that it is better to provide a small number of larger baffles than a greater number of smaller baffles. The pressure factor in this parameter shows that if the combustor is for an aircraft engine, then this must be taken into account at the start.

The necessity of high temperature for significant reaction rate shows that the diluting air must either be added only when it is certain that the reaction has gone to completion or that it must be added in slow degree so that the reaction is not immediately quenched. Because of the problem of mixing air and fuel, it is common to introduce some air as " secondary " air, that is, it has a function in the combustion process in promoting mixing and ensuring adequate oxygen for the fuel downstream of the nominal reaction zone.

The necessary outline structure of many combustors then appears

as in Fig. 8.3, yielding a typical annular form, with a central *liner* or *flame tube* containing the primary zone and baffle, surrounded by the *outer casing* or *air casing*. The annular space serves the purpose not only of separating the required primary air from the total air, but of providing a cooling air stream which limits the

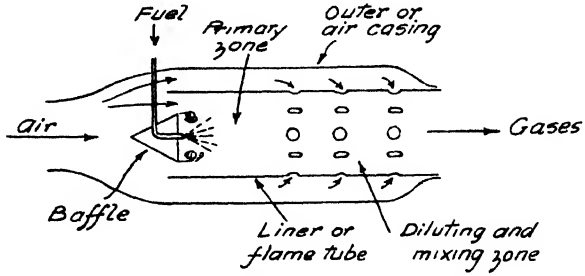

FIG. 8.3. Typical combustor—schematic.

temperature of the liner, which contains the reaction zone where the gas temperature may reach locally a value of the order of 3500 °F (2000° C) corresponding to the stoichiometric mixture temperature. In actuality, the stabilizing baffle is often considerably more complex than the simple bluff bodies hitherto mentioned.

8.4 *Stabilizing or Primary Zone*

Swirl vanes may be used, to give the primary air a considerable tangential component at entry, which mixes air and fuel over the cross-section and gives a recirculation pattern by means of vortex action. A free vortex (Sec. 4.21) has increasing tangential velocity with decreasing radius. By the Bernoulli principle, the higher velocity at the centre entails a lower static pressure and thus a radial pressure gradient. There is also an axial pressure gradient as velocities decrease due to dissipative effects and the vortex is strongest at entry. The resulting circulation pattern is shown in Fig. 8.4. If fresh air is admitted downstream, then this is drawn upstream toward the fuel injection region. The use of swirl is a long-established practice with oil and gas firing, but if used alone, is liable to give rather coarse mixing, with some regions overstimulated and others lacking. The basic Lucas combustor (Fig.

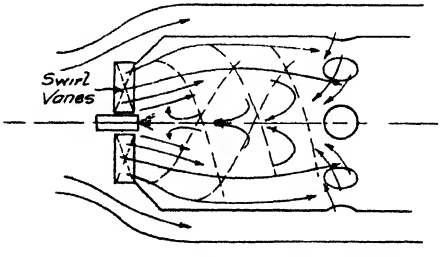

FIG. 8.4. Swirl pattern of stabilization—schematic.

8.5), widely used in British industrial and aircraft gas turbines, combines a small swirler around the fuel injector, with a large number of small holes in the surrounding cone, the latter admitting air in jets, which provide a finer degree of general turbulence. Fig. 8.5 also shows another necessary feature of many combustors, in the flared passage preceding the baffle, which acts as a metering device and flow straightener for the primary air. Only too often, the velocity distribution in the duct from the compressor is highly irregular, which, if uncorrected, would lead to poor mixing, stabilization and temperature distribution in the combustor. Such poor distribution may occur due to separated flow in the diffuser or to a curved passage necessary from the geometry of the components.

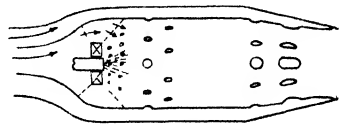

FIG. 8.5. Combustor with small swirler and distributed primary turbulence.

Another simple stabilization pattern, basic to General Electric combustors and others in the U.S.A., is illustrated in Fig. 8.6. Here, the recirculation zone is formed by eddies from a row of holes just downstream of the fuel injection point. This pattern is deceptively simple, in that the location of these primary stabilizing jets, together with the admission of secondary and diluting air further downstream, is critical, and not to be determined without very considerable test work.

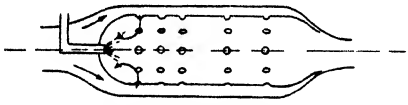

FIG. 8.6. Combustor with simple hole pattern—schematic.

A very different flow pattern is shown in Fig. 8.7, called an

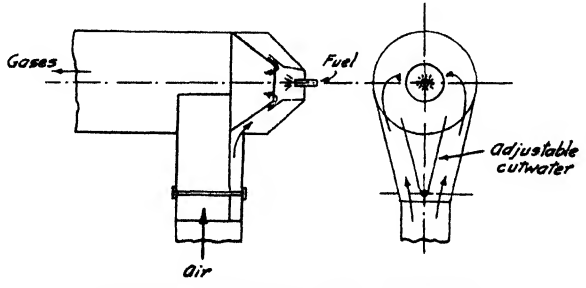

FIG. 8.7. Elbow combustor—shematic.

" elbow " combustor, originally introduced by the Elliott company (Ref. 4) and developed for wide scale use by Ruston and Hornsby (Ref. 5). It makes use of the vortices produced by flow from a duct of smaller diameter perpendicular to a duct of larger diameter

and thus utilizes to good effect the necessary turbulence (and hence loss) produced by a right-angle bend, such a change in flow direction often being necessary in an industrial plant arrangement. The figure shows one basic flow arrangement, but many varieties are possible. One such is shown in section, with a V-shaped " cut-water " which can reverse the secondary air flow pattern and, if made variable, can be used for control.

Very many types of primary zone stabilizing arrangement are possible and the possible variety is so great that one cannot generalize as design information. Those described above are simply among those which have found usage in considerable numbers. These cases, as shown, are all for down-stream fuel injection, but often equally good or better results can be achieved by upstream injection, as shown schematically in Fig. 8.8. The advantage of this is the possibility of improved mixing, as air may be injected directly into the centre of the fuel injection zone. The disadvantage is the possibility of overheating the fuel pipe and injector unless they are adequately cooled, as they are located directly in the reaction zone. Both upstream and downstream injection may be used with gaseous and liquid fuels, sometimes with the same air flow pattern, although usually a gaseous fuel requires less intense turbulence, as the evaporation process is eliminated.

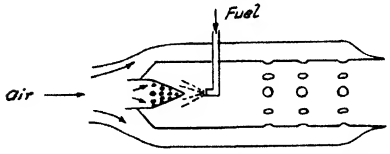

FIG. 8.8. Combustor with up stream fuel injection—schematic.

The easier conditions for gaseous fuel injection lead to the idea of *vaporizing* liquid fuels before combustion is attempted, as in gasoline or kerosense blow-torches and stoves. External vaporization with controlled heating is not attractive due to its complexity and early attempts at vaporizing the liquid fuel alone by passing it through small bore tubes located in the primary zone did not prove satisfactory due to local cracking of the fuel, followed by blockage and burn-out. In the Armstrong-Siddeley aircraft turbine combustor, fuel is injected into " walking sticks " or tubes bent through 180° to give upstream injection (Fig. 8.9). The fuel is not under pressure during vaporization, being mixed with entry air so that vaporization and mixing takes place in the tubes to give a very rich mixture for the primary zone. This mixture is then mixed with more air in turbulent fashion to give

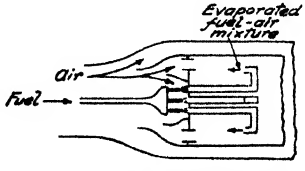

FIG. 8.9. Vaporizing type of combustor—schematic.

the approximately stoichiometric air-fuel ratio for the reaction zone. While equally good results for the equivalent gas turbine performance have been achieved by liquid fuel injection, the vaporizing combustion does not require a high degree of fuel atomization and thus a simpler fuel injector and somewhat lower fuel pressure can be used. The apparent disadvantage of having metal parts suspended in the very hot primary zone, with possible danger of burning out or breaking off, has been successfully overcome in the system shown.

8.5 *Dilution and Mixing*

The problem of adding approximately three-quarters of the total air to the one-quarter of reactant gases is no easy one, because of the necessity for a good temperature distribution with minimum pressure loss. In the typical cylindrical construction discussed, the air is admitted progressively through holes or slots, with usually a small gap being left between the liner and the casing to provide a film of cool air for the final contraction to the nozzle entry (Fig. 8.10). Many more elaborate mixing devices have been tried, consisting basically of ducts projecting into the liner in attempts to provide more even mixing, but most combustors now achieve good results with simple holes. While such ducts are helpful in mixing, the added constructional problem, together with the danger of local overheating and metal failure, present powerful reasons for endeavouring to eliminate them. An excellent method of maintaining the liner walls from excessive temperature is by means of *film cooling*, Fig. 8.11, which consists of making the liner in overlapping sections so that each side has a layer of cool air flowing over it.

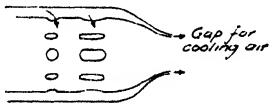

FIG. 8.10. Dilution zone.

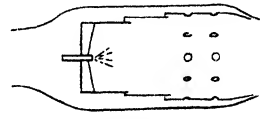

FIG. 8.11. Film-cooled liner—schematic.

The size and number of dilution air holes is a compromise between a large number of small holes to give fine scale mixing and a small number of large holes to give better penetration. It is essential that the mixing air reach well toward the axis of the combustor, as otherwise a core of high temperature gas will persist. A slot with major axis in the flow direction gives good penetration, but tends to weaken the liner. The liner is not subject to a large pressure difference, but may distort owing to local high-temperature gradients. Furthermore, the combustion process is accompanied by vibrations

of high frequency and the whole combustor is subject to a vibration fatigue effect. This is usually most serious in the liner itself, which is at an elevated temperature and care must be taken in reducing to a minimum such stress concentration elements as sharp corners, notches, etc. An account of constructional and metallurgical considerations is given in Ref. 6.

It has been stated that the total air must be divided into primary air and diluent air in a given ratio, but here again a design procedure is to a large extent empirical in nature. The quantity of air flowing through an orifice is governed by the pressure difference and the orifice coefficient. The NACA has published data on discharge coefficients of typical combustor orifices and has made an analysis of pressure loss on the basis of ratio of hole area to liner area and total combustor area, etc. (Ref. 7). Williams (Ref. 8) has also given a method of estimating pressure loss from the hole area and distribution, with good agreement between calculated and measured results. Such methods are useful in laying out a design *ab initio*, although bench testing is necessary to develop the proper combustion performances.

8.6 *Combustor Arrangement*

The typical form of combustor with a cylindrical liner in a surrounding casing may be adapted to a single annular chamber or

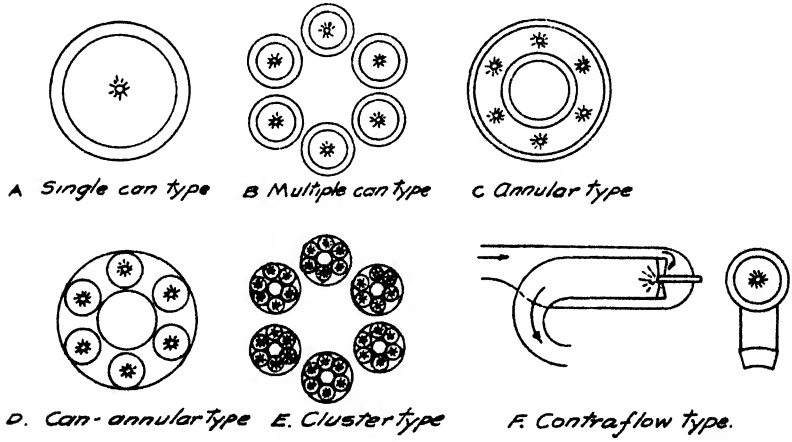

Fig. 8.12. Combustor arrangements.

to a number of liners in a single annular casing. These possible arrangements are shown diagrammatically in Fig. 8.12. Types A and B, with a liner of circular cross-section, are usually called *can* combustors, with the question of having a single unit or a number of

parallel units being largely determined by the application and thus the optimum plant layout. For the industrial plant, the single large combustor is usually favoured owing to its simplicity in manufacture and maintenance. It is not universal, however, and at least one of the large manufacturers (General Electric Co.) prefers to split the air from the compressor and operate several combustors in parallel. For the aircraft gas turbine, where frontal area is all important, an axial or " straight-through " arrangement is most favoured, with the combustor surrounding the shaft between compressor and turbine. With an annular area available for combustion having the outer diameter limited by an overall design requirement and with inner diameter held to some value dependent on mechanical design, the maximum flow area is obtained by a single annular combustor as shown as type C. The use of several separate can combustors arranged in the same annular space is possible, but results in a higher average through-flow velocity and hence higher pressure loss for the same type of internal flow arrangement. The annular arrangement is becoming increasingly popular owing to its making maximum use of the area available, but for many years only the separate can arrangement was considered, owing to the great difficulties of developing a full annular arrangement on a test rig. With, say, eight separate can combustors, a test of one combustor at one-eighth the required engine air supply is a reasonable proposition. A one-eighth sector of an annulus can be used for development, but can lead to differences of behaviour between model and prototypes due to the radial bounding walls. Also the circular fuel distribution from a spray injector is symmetrical with respect to the can type, but is not in the annular arrangement. With the growth of experience in combustion development, there is more confidence in handling such asymmetrical flow patterns. In this connection, the vaporizing type of combustor is especially well suited to the annular type, as the fuel injection pattern is more flexible. A further factor is the exclusive use today of the axial-flow compressor for aircraft turbines, as the discharge is already annular in form, whereas the centrifugal compressor with axial discharge is more suited to a number of separate discharges corresponding to the number of diffuser passages.

With an annular casing it is possible to retain liners of circular cross-section to match the circular pattern of fuel injectors, shown as type D of Fig. 8.12, known as a " cannular " or " can-annular " arrangement. This preserves the total flow area, although limiting that available for primary combustion.

Although the relationship is not necessarily exact for the complex

pattern of a liquid fuel injection combustor, the flame pattern tends to scale in linear dimension. Thus increasing the number of fuel injection points, for a given fixed total fuel rate, will lead to a corresponding reduction in the length of flame from each combustion zone. From this point of view, a large number of separate combustors or a large number of fuel injectors in an annular combustor, tends to reduce the combustor length required. This leads to a possible combustor arrangement consisting of several separate clusters of very small liners in their own individual annular casing with several such assemblies contained in the whole available annular space, shown as type E. A factor which must be considered in this case is the large number of fuel injectors required, each of which must be matched to a given limiting pressure-flow relationship. There is also the stability criterion to be kept in mind, with a small characteristic dimension liable to lead to blow-out at lower pressure levels.

Finally, type F is possible, with reverse flow or " contraflow ". This shortens the shaft length between compressor and turbine and was the arrangement adopted for the original Whittle development. It fell from favour due to the poor flow and constructional difficulties with the 180° discharge bend and to the more widespread use of the axial-flow compressor, which has a mean diameter comparable with that of the turbine, thus making a straight-through flow arrangement logical. Lately, however, it has been reintroduced in the Lycoming T-53 engine, which has a centrifugal stage following an axial-flow compressor.

A very different form of combustor, originated by the French company of Turbomeca, is shown in Fig. 8.13. This is in effect an annular type of chamber, but with fuel injected radially outwards from holes in the hollow shaft. The fuel pressure is generated by centrifugal action and may be very high, thus giving excellent atomization. The air for the downstream side of the primary zone is ducted between the nozzle guide vanes as shown, with dilution air being admitted after the 90° bend of the liner.

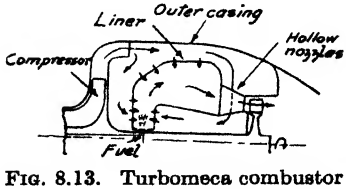

FIG. 8.13. Turbomeca combustor —schematic.

8.7 *Fuel-Injection*

The use of liquid fuel requires that it be injected in a state as finely divided as possible, so that evaporation and mixing may be rapid. This requires the use of a *spray atomizer*, which may have many refinements, but which is basically as shown in Fig. 8.14.

Fuel under pressure is admitted through slots tangentially disposed at the large diameter of a vortex chamber, thus acquiring considerable velocity. It then travels in a thin film at ever-decreasing radius towards the final orifice, from which it is discharged at a high velocity. This velocity has both an axial and a tangential velocity, so that immediately leaving the orifice, the fuel is in the form of a thin conical sheet. In its progression down the sides of the vortex chamber, the velocity is much increased from the value at slot discharge, because the free-vortex principle holds, that is, $V_u r$ is constant. The liquid film in the final orifice is very thin, so that almost immediately on discharge, under the action of surface tension and viscous shearing force, it disintegrates into a magnitude of very small individual drops or a spray. Two points must be realized: (1) that the orifice does not " run full " and that the centre region is a low pressure air core; and (2) that once having left the orifice, an individual fuel particle travels in a straight line unless external forces act on it.

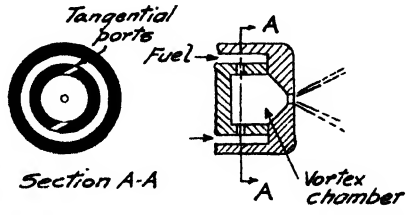

FIG. 8.14. Spray atomizer—pressure type.

This describes the action when the fuel pressure is above a certain limiting value, 10–20 psi for a low viscosity fuel, dependent on the slot and orifice size. At very low pressure, the fuel issues more or less as a twisted solid jet as the tangential velocity component is very small, developing into a tulip-shaped sheet with slightly higher pressure. With further increase of pressure, the sheet disintegrates into drops closer and closer to the orifice until it becomes a " fully-developed " spray, having a definite cone angle. Increasing fuel pressure then not only increases the fuel rate, but improves the atomization, i.e. decreases the mean drop size, albeit at a diminishing rate.

The term " mean drop size " implies that the spray is not uniform and in fact, it consists of a whole range of particle diameters, from less than 10 μ to a few large drops being possibly 500 μ or larger (μ = micron and 25 $\mu \approx$ 0·001 inch), with the majority of particles being in the middle size range. A considerable amount of work has been done on methods of measuring drop size and size distribution, together with methods of rating sprays, that is, expressing spray characteristics by means of distribution laws. One of the simplest and most useful is the *Sauter mean diameter*, defined as the diameter of the particle having the same surface-volume ratio as that of the

whole spray. It is difficult to correlate particle size with combustion performance because of the varying distributions from different types of spray injector and because of the differing reactions of stabilizing zone flow patterns, but reduced average particle size is generally beneficial, and thus Sauter mean diameter is useful as a gauge for purposes of comparison.

A simple pressure atomizer of the above type obeys the usual orifice law approximately, that is, the flow rate is proportional to the square root of the pressure. For an industrial turbine, the required range of fuel flow from idling to full power is not usually so great that the maximum fuel pressure is excessive, but for aircraft turbines, the reduced flow at high altitude entails a much wider range of required operation. Thus with $Q \propto \sqrt{P}$, a range of Q of only 10/1 means a pressure range of 100/1. If the minimum pressure for adequate atomization is taken as 15 psi (and the spray at this pressure is very coarse), then the maximum pressure required is 1500 psi. Although fuel pumps have been developed for continuous flow at this pressure (note that the problem differs from the Diesel injection pump with its discontinuous action capable of realization with reciprocating elements), additional pressure is required for control mechanisms (throttle, governor, etc.), and methods of obtaining better atomization at lower pressures have been required. Many methods have been devised, and only three of particular interest will be outlined here.

The first method is to provide two sets of tangential slots or swirl slots, one set considerably smaller than the other so that only a small quantity of fuel is delivered at a given pressure. By means of automatically controlled valves, fuel is admitted through these small ports at starting, idling or low load conditions, with the larger ports coming into operation at higher loads when the pressure is sufficiently high to give good atomization. A " duplex " injector of this type thus acts as if two separate injectors were used, one for low fuel flows and one for high flows, although it is a single mechanical unit. It is shown diagrammatically in Fig. 8.15 (a).

The second method is that of the " spill-control " type, shown at (b) of the figure, in which a large quantity of fuel is discharged at a reasonably high pressure at all loads through the tangential slots, so that a high velocity is imparted. A large part of this fuel is then removed by a central hole in the back of the vortex chamber and returned to the suction side of the fuel system. The high swirl velocity for a relatively small quantity of fuel delivered to the combustor ensures a thin film in the final orifice, which then breaks up readily into a fine spray. Control is effected by a valve in the

return or spill line and the fuel inlet pressure may be kept constant or relatively so. A disadvantage is that the fuel pump capacity may have to be high, as it has to handle more fuel than that required for combustion.

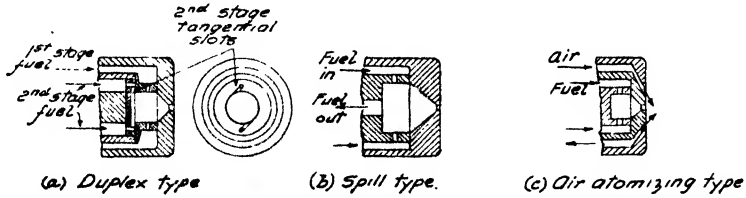

FIG. 8.15. Types of wide-range fuel injectors—schematic.

The third method is that of air atomization, shown at (c), in which a blast of high velocity air is used to break up the liquid sheet. Many variations of the method are possible and the diagram shows only the design principle. Air atomization is particularly desirable, and at times necessary, for heavy fuels, the term heavy implying high viscosity. As fuel viscosity increases, atomization decreases for a given pressure, owing to the lower velocity acquired at the orifice (due to viscous drag in the vortex chamber), with the resulting thicker film disintegrating into drops less readily. Some very heavy fuels require preheating, both to allow reasonable atomization and to enable pumping to be accomplished with reasonable power (sometimes to enable the fuel to be pumped at all). For heavy fuels, the spinning-cup atomizer is possible, in which fuel is admitted at the centre of a hollow metal cone rotating at a fairly high speed, so that a thin film of fuel is thrown off by centrifugal action. This method requires only very low fuel pressure, but necessitates an external drive for the spinning cup.

Except for the vaporizing system, fuel injection is a highly important and critical part of combustor performance, and the injectors and associated equipment are often the most expensive part of the combustor system. Maintenance of good atomization over the flow range has been discussed and a further requirement is that of a suitable cone angle for the air flow pattern and its preservation as pressure changes. The hollow cone of spray must be uniform circumferentially, as otherwise the temperature distribution may be upset. Precision machining for close tolerances and fine surface finishing is necessary in manufacture and, until proved in long-time service, frequent inspection and maintenance is desirable, as a faulty injector can quickly cause trouble due to local overheating of the liner or the turbine nozzle.

8.8 *Fuel Properties*

Of the many properties of fuels, those which have any considerable effect on combustion performance are the viscosity, the distillation range and the chemical composition and structure. Some others which are important, but which do not directly bear on the combustion itself, will be discussed later.

The viscosity of a fuel is important because it affects the quality of atomization. Restricting the discussion to hydrocarbon fuels, the kinematic viscosity in centistokes at ordinary atmospheric temperature varies from about 0·5 for gasoline to possibly 5000 for heavy fuel oil. For distillate fuels such as gasoline, kerosene and light diesel oil, the viscosity causes no great change in atomization qualities, except the initial pressure for a fully-developed spray, and most combustors will handle any such distillate fuel with little change in performance. An exception to this is at very low temperatures, sub-zero values, when the viscosity increases rapidly. At a sufficiently low temperature, the *cloud point* is reached, denoted by separation of solid frozen particles. For industrial applications, such temperatures are seldom approached, but for aircraft gas turbines it is necessary to specify a freezing point of greater than — 70° F, which very definitely restricts the fuel to a gasoline type. Non-distillate or residual fuels have a great viscosity range and many require heating before they can be atomized satisfactorily.

The distillation characteristics of a fuel are given by the initial and final boiling points, preferably with temperatures of 10%, 50% and 90% recovery of the distilled vapour, since this gives some information on the proportion of light and heavy " ends ". A low initial boiling point indicates ready vaporization and, therefore, increased possibility of easy starting at low temperatures. The final boiling point and 90% recovery temperature are indicative of the tendency of the fuel to " crack " before oxidation, that is, to break down into lighter molecules, with the production of free carbon. In the reaction zone, a drop of fuel will receive heat by convection and radiation, with the lighter fraction evaporating and mixing with air, with the heavier fraction more likely to increase in temperature to the cracking point. Most combustors have a yellow flame, indicating glowing carbon particles, some produced directly by cracking of the original fuel and some by the intermediate combustion reactions. With a very high degree of atomization and level of turbulence or with vaporizing combustors under certain conditions, it is possible to get a predominantly blue flame, indicating almost complete evaporation and mixing before reaction. A high boiling

point then indicates a greater possibility of cracking and an increase of the production of free carbon, and thus risk of carbon deposition or smoke.

The chemical composition and structure of the fuel are also important with respect to carbon formation. The carbon-hydrogen, or C/H, ratio varies with the type of hydrocarbon, i.e. paraffin, olefin, aromatic, etc., with in general the lighter fuels having a greater proportion of hydrogen. The C/H ratio is connected with the boiling point range and so they are not independent properties. It appears that aromatic compounds in particular are prone to give rise to carbon formation, and in some fuel specifications for aircraft turbines, a maximum allowable percentage of aromatics is written into such specifications. This is undesirable as it restricts the source of fuel and, as the gas turbine is not dependent on a particular quality such as anti-knock value or spontaneous ignition temperature as a criterion, every effort should be directed to eliminating carbon troubles by combustor flow pattern development rather than by fuel specification.

A very important element of the chemical composition of the non-distillate fuels for industrial turbines is the quantity and nature of the ash content. Such ash content may be quite small, less than $\frac{1}{4}\%$, but over a period of time this may mean a considerable absolute amount. The ash consists of many compounds of a mixed organic and metallic nature, with some being in solution and some in suspension. In the combustion chamber, the ash undergoes chemical change in the high-temperature primary zone, with the resulting compounds having a range of melting points, some above and some below the usual turbine inlet temperature. Some of the ash may deposit on the nozzle vanes and rotor blades, by means of impact or centrifugal action and by means of the action of the boundary layer and separation regions. Some of the ash which is carried through the turbine will be deposited in the heat exchanger, if one is present.

The problem of ash formation is very serious, as in extreme cases the deposition on blade and heat exchanger surfaces may cause, in only a few hours of running, a reduction of efficiency sufficiently great to require shut-down of the plant. In addition to deposition, corrosion of the metal surfaces may occur, that is chemical reaction takes place between metal and ash. Sodium and vanadium compounds appear to be the chief offenders and most attention has been paid to these. The problem is exceedingly complex, as the amount and nature of deposition and corrosion is a function of the chemical nature of the ash, the temperature level, the design of the blade surfaces and the combustion process itself (degree of atomization

and turbulence). Control is possible to some degree by centrifuging the fuel (this removes the insoluble ash only), by combustion control (large fuel drops producing carbon tend to " wrap up " the ash) and by chemical additives. The last method of control would appear to be the ultimate method, but obviously the economic side enters here, as the low cost of residual fuels must not be nullified by the cost of preparation.

A considerable amount of work has been carried out on the ash problem, with some results indicating possible methods of solution. At this time, however, it is unwise to attempt any generalization of the findings, as so often the results of controlled laboratory experiments are not borne out in engine tests. The exact temperature appears to be vital, with quite different results occurring with only small temperature change. It would appear that corrosion does not occur below a temperature of about 1200° F (650° C), with both deposition and corrosion becoming more serious as the turbine inlet temperature is increased.

At the present time, the ash problem is one of the most serious in the continuing development of the gas turbine for industrial use. For many applications, the advantages of the gas turbine, with respect to weight, size, ease of maintenance, independence of auxiliary services and so forth are sufficient to counterbalance the low efficiency and poor part-load performance of the simple cycle, but there are many others in which it is necessary to burn cheap fuel to be competitive and for these, the ash deposition and corrosion problem must be solved.

8.9 *Analysis of Combustor Performance*

The lack of precise design information has been noted, but there are some performance factors which enable combustor performance to be assessed or which may be specified as a target to be reached by development. These factors may be given as (1) combustion efficiency, (2) temperature distribution, (3) pressure loss, and (4) combustion intensity. Although these may be discussed independently, a parameter of combustor performance as it affects the whole gas turbine may include all three. Thus from the point of view of the thermodynamic performance alone, both combustion efficiency and pressure loss affect the cycle efficiency, and because they tend to act in reciprocal fashion, i.e. increase of efficiency may be obtained at the expense of a higher pressure loss, a quantitative answer is really meaningful only for an individual plant. Size enters in indirectly, although it is a very important criterion, in as much as reduced size mitigates against efficiency and increases pressure loss.

Combustion efficiency may be defined logically by either of two methods. The first compares the amount of fuel theoretically required (complete combustion) in order to obtain the actual measured temperature rise, to the amount of fuel actually required, both for the same temperature rise. The second method compares the actual enthalpy rise occurring to the ideal enthalpy rise (complete combustion), both for the same (actual) fuel supplied. Thus for method 1,

$$\eta_{\text{comb}} = \frac{f_{\text{ideal}}}{f_{\text{actual}}} \text{ for the same } \Delta T_{2-3}$$

and for method 2,

$$\eta_{\text{comb}} = \frac{\Delta h_{\text{actual}}}{\Delta h_{\text{ideal}}} = \frac{\Delta h_{\text{actual}}}{f \times LHV} \text{ for the same } f,$$

where f is the fuel-air ratio, h is the enthalpy per lb air and LHV is the lower heating value, Btu per lb fuel. The difference in efficiency by the two methods is small, about 1% at 90% level of efficiency, decreasing to zero at 100% efficiency. The first method is easier to apply, provided that charts are available for obtaining the ideal fuel-air ratio corresponding to the temperature rise. The second method requires an exhaust-gas analysis for computing the actual enthalpy rise and this is seldom available as a routine measurement for all combustor tests. In practice, combustion efficiency is usually expressed as the ratio of actual *temperature* rise for a measured fuel-air ratio to the ideal *temperature* rise for the same fuel-air ratio. This method then neglects differences in unburnt products of combustion and is therefore inexact. It is, however, very convenient for everyday use and as exact efficiencies are very difficult, as well as laborious, to determine, the theoretical error is masked by the experimental error. These difficulties will be discussed later in this section.

At and near the design point of a gas turbine, the efficiency should be 100%, and it usually is for hydrocarbon fuels. As the design point is usually the maximum temperature, because gas turbines are seldom designed for overload service, any part-load operation is at a lower temperature and hence leaner mixture strength. With fixed combustor geometry, the reaction zone mixture strength is lowered and it was seen that this was not conducive to high reaction rate and thus the combustion efficiency may be reduced. This reduction need not be serious, possibly only a very few points over the range of mixture strengths required, but may require some careful development work to ensure. Thus although the design condition may be achieved with optimum conditions

with respect to flame length and carbon formation, it may be necessary to compromise it by reducing the primary air in order to prevent a too-lean condition at part load.

It is conservative practice to assign a value of 98% for the combustion efficiency for plant performance calculations, partly as a margin of caution, and partly because of the uncertainty in measuring efficiency, even under controlled bench conditions. The measurement of the true temperature of the gas at any particular point is difficult at the high temperatures and velocities at nozzle inlet and the temperature and velocity gradients across the discharge area require many such readings to be taken, weighted and averaged. Even then, at any given point in the discharge plane, the measured temperature is not that of a steady state, as the flame is not completely stable in space.

The error in temperature measurement can be obviated by using an exhaust gas analysis as a basis for estimating efficiency, accounting for deficiencies in heat release rate due to the unburnt components, such as carbon monoxide, hydrogen, methane, etc. Here, however, a very precise analysis is necessary, as at the lean overall mixture strengths of the gas turbine (50–120/1), very small fractions of unburnt fuel account for 1% of efficiency. The conventional rapid method based on an Orsat apparatus is quite inadequate for measuring efficiency, although it may be a useful tool for exploring the primary zone. Considerable attention has been paid to methods of analysis, from special chemical methods to the use of infra-red analysers and even the mass spectrograph. For most laboratories, the method developed at the NGTE (Holderness, Ref. 9) appears to be the most suitable with respect to degree of precision and ease of operation. Again, however accurate the sample analysis may be, many such samples are required in order to obtain an average value over the whole discharge area.

The quality of the temperature distribution at nozzle inlet can be expressed as the range of departure from the mean temperature in the form $\Delta T/T_{\text{mean}}$, with ΔT either positive or negative and T_{mean} in degrees absolute. The latter may be that for the whole area or a given radius if a particular temperature profile is being attempted. The value of this factor is arbitrary, but for aircraft engine combustors, where mixing length is limited, a value of $\Delta T/T$ of 10% is usually accepted.

For assessing pressure loss, two factors have found acceptance as simple expressions of performance. The first is the percentage loss of stagnation pressure with respect to the absolute pressure at combustor inlet, i.e. $\Delta P_0/P_2$, which has been seen to be a useful form for

assessing the effect on cycle performance. For industrial gas turbines, a value of 0·02 is a reasonable average, although values ranging from 0·01 to 0·04 have been reported. The factor $\Delta P_0/P$, although convenient, does not express the quality of the combustor with respect to size and throughput, however, and for comparative purposes a *pressure loss factor* (PLF) is used extensively. The PLF is a coefficient λ expressed in terms of loss and dynamic pressure, i.e. $\lambda = \Delta P_0/(\rho V^2/2g_0)$. With ρ the combustor *inlet* density, i.e. $\rho = P_2/RT_2$, and V based on the *maximum* combustor cross-sectional area, i.e. $V = m/\rho_2 A_{\max}$, then λ assesses the pressure loss characteristic in terms of the air flow loading.

It must be recognized that a certain loss of pressure is inevitable in a combustor due to the change of momentum consequent on heating. Taking a combustor of constant area for simplicity, Fig. 8.16, then the idealized process is one of heating at constant area without friction, which for compressible flow is handled by the "Rayleigh line" functions. For the relatively low velocities and small changes of pressure in a gas turbine combustor, the process may be considered as incompressible. Thus for flow between stations a and b, a force-momentum balance gives

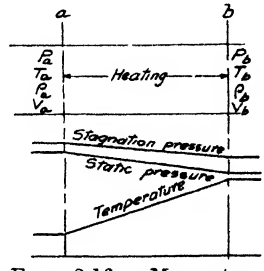

FIG. 8.16. Momentum loss due to heating.

$$P_a A_a + \frac{mV_a}{g_0} = P_b A_b + \frac{mV_b}{g_0}$$

which with $A_a = A_b$ and $m = A\rho V$ reduces to

$$P_a - P_b = \frac{\rho_b V_b^2}{g_0} - \frac{\rho_a V_a^2}{g_0} \tag{8.6}$$

For incompressible flow, the Bernoulli equation for a gas gives

$$P_a + \frac{\rho_a V_a^2}{2g_0} = P_b + \frac{\rho_b V_b^2}{2g_0} + \Delta p_m \tag{8.7}$$

where Δp_m is the loss of stagnation pressure due to heating (not friction). Substitution of (8.6) into (8.7) for elimination of P_a and P_b yields

$$\Delta p_m = \frac{\rho_b V_b^2}{2g_0} - \frac{\rho_a V_a^2}{2g_0}$$

With $\rho_b V_b = \rho_a V_a$,

$$\Delta p_m = \frac{\rho_a V_a^2}{2g_0}\left(\frac{\rho_b}{\rho_a} - 1\right) \tag{8.8}$$

Considering the density change due to pressure negligible compared with that due to temperature, i.e. $\rho \propto 1/T$, then

$$\Delta p_m \approx \frac{\rho_a V_a^2}{2g_0}\left(\frac{T_b}{T_a} - 1\right) \tag{8.9}$$

Thus with T_b/T_a ordinarily about 2–3/1, then the momentum loss is small in comparison with the turbulence loss. For afterburners, however, the loss may be appreciable and a considerable proportion of the total loss. This total loss Δp_0 is the sum of that due to change of momentum Δp_m and that due to friction and turbulence Δp_f, so

$$\Delta p_0 = \Delta p_f + \Delta p_m$$

or expressed in terms of the nominal dynamic pressure $\rho_2 V_m^2/2g_0$,

$$\frac{\Delta p_0}{(\rho_2 V_m^2)/2g_0} = \lambda = \lambda_f + \lambda_m = \lambda_f + (T_3/T_2 - 1) \tag{8.10}$$

The major loss coefficient λ_f may be estimated from a test using air alone, a so-called " cold loss ". This may change somewhat for flow with combustion, as this affects the flow distribution, but usually not markedly, so that air flow tests of models can be used advantageously. Values of λ vary considerably with the turbine application (industrial or aircraft) and with the type of combustor (can, annular, etc.). For industrial combustors, usually of the single or multiple can type, values of 10–20 are realized. For aircraft combustors, values of 15–20 are obtained for annular types, somewhat higher for can types.

Combustion intensity or heat-release rate has been discussed previously in a general manner. Arising out of a comparison with older-established combustion systems, such as furnaces, it is very often expressed as the heat release rate per unit volume per atmosphere and this will be denoted by I_p. The collision rate theory outlined earlier indicates that the pressure exponent might more logically be that of the apparent order of reaction and this intensity will be denoted by I_p^n. A further combustion loading parameter which has some utility is based not on volume, but on combustor cross-sectional area, using unity exponent for the pressure and this will be called I_A. Both volume and area should be referred to the flame tube or liner, that is, exclusive of the region, usually annular, which ducts the air into the liner. Usage is not standardized on this matter, with some of the earlier literature using the whole combustor volume, including air casing.

Maximum values of I_p, usually used only for aircraft turbines where space is at a premium, are of the order of $3{\cdot}5–4 \times 10^6$ Btu/(hr) (ft^3) (atm) or about 2×10^6 Chu/(hr) (ft^3) (atm). For industrial

turbines, values may be only about one quarter of this. Volumetric heat release is not the whole story because it implies a more or less homogeneous reaction throughout the whole space, which is obviously not the case for the typical can combustor with a single liquid fuel injector. Taking a cylinder as model, a given volume may be obtained between extremes of a short, fat cylinder and a long, narrow one, and thus for the practical combustor, shape is a factor. This may be specified by length/diameter ratio, L/D, and values of 2·2–3·0 are representative of current practice. L/D value is implicit in giving a value of I_A, the area intensity parameter in conjunction with I_p, as $I_p/I_A = L/D$ for a simple cylinder. I_A also represents a mass velocity parameter and thus indirectly is a measure of stability, lower values indicating probability of a wider stability range. Corresponding to an L/D of about 2·5, a value of I_A of about 10×10^6 Btu or 5 Chu per (hr) (ft^3) (atm) represents a current limit.

The newer concept of pressure dependence to a power corresponding to the reaction order has not received sufficient acceptance to enable many general values of I_{p^n} to be given. Way (Ref. 10), using the results of bench tests of a simple type of combustor suggests a value of 10×10^6 Btu or $5{\cdot}5 \times 10^6$ Chu/ (hr) (ft^3) (atm)$^{1{\cdot}8}$ as a present upper limit, using $n = 1{\cdot}8$ in line with the overall reaction order of a hydrocarbon flame suggested by most data to date. For a pressure ratio of five, this agrees reasonably well with the limits for I_p given above. The parameter I_{p^n} has particular utility for performance of combustors at the reduced pressures at high altitude, as it is here that the loading problem is acute. It would appear that attention to values of I_{p^n} in initial design would help to obviate the limiting altitude performance with respect to efficiency and blow-out which is sometimes experienced at high altitude with combustors which have a satisfactory performance under the usual ground-level testing conditions.

There have been attempts to relate the interdependence of combustion efficiency and pressure loss as a function of the cycle performance (London, Ref. 11, and Nichols, Ref. 12). Because of the dependence of the efficiency on combustion intensity, then there is a relationship between the latter and the pressure loss. From dimensional analysis, Spalding (Ref. 13) has evolved a "flow criterion", K_f, as

$$K_f \equiv \frac{m^2}{\Delta p \rho_1 d^4 g_0} \tag{8.11}$$

where d is a characteristic dimension. K_f is approximately constant for a given design and high values indicate a good design. If cross-

Considering the density change due to pressure negligible compared with that due to temperature, i.e. $\rho \propto 1/T$, then

$$\Delta p_m \approx \frac{\rho_a V_a^2}{2g_0}\left(\frac{T_b}{T_a} - 1\right) \tag{8.9}$$

Thus with T_b/T_a ordinarily about 2–3/1, then the momentum loss is small in comparison with the turbulence loss. For afterburners, however, the loss may be appreciable and a considerable proportion of the total loss. This total loss Δp_0 is the sum of that due to change of momentum Δp_m and that due to friction and turbulence Δp_f, so

$$\Delta p_0 = \Delta p_f + \Delta p_m$$

or expressed in terms of the nominal dynamic pressure $\rho_2 V_m^2/2g_0$,

$$\frac{\Delta p_0}{(\rho_2 V_m^2)/2g_0} = \lambda = \lambda_f + \lambda_m = \lambda_f + (T_3/T_2 - 1) \tag{8.10}$$

The major loss coefficient λ_f may be estimated from a test using air alone, a so-called " cold loss ". This may change somewhat for flow with combustion, as this affects the flow distribution, but usually not markedly, so that air flow tests of models can be used advantageously. Values of λ vary considerably with the turbine application (industrial or aircraft) and with the type of combustor (can, annular, etc.). For industrial combustors, usually of the single or multiple can type, values of 10–20 are realized. For aircraft combustors, values of 15–20 are obtained for annular types, somewhat higher for can types.

Combustion intensity or heat-release rate has been discussed previously in a general manner. Arising out of a comparison with older-established combustion systems, such as furnaces, it is very often expressed as the heat release rate per unit volume per atmosphere and this will be denoted by I_p. The collision rate theory outlined earlier indicates that the pressure exponent might more logically be that of the apparent order of reaction and this intensity will be denoted by I_p^n. A further combustion loading parameter which has some utility is based not on volume, but on combustor cross-sectional area, using unity exponent for the pressure and this will be called I_A. Both volume and area should be referred to the flame tube or liner, that is, exclusive of the region, usually annular, which ducts the air into the liner. Usage is not standardized on this matter, with some of the earlier literature using the whole combustor volume, including air casing.

Maximum values of I_p, usually used only for aircraft turbines where space is at a premium, are of the order of $3{\cdot}5–4 \times 10^6$ Btu/(hr) (ft^3) (atm) or about 2×10^6 Chu/(hr) (ft^3) (atm). For industrial

turbines, values may be only about one quarter of this. Volumetric heat release is not the whole story because it implies a more or less homogeneous reaction throughout the whole space, which is obviously not the case for the typical can combustor with a single liquid fuel injector. Taking a cylinder as model, a given volume may be obtained between extremes of a short, fat cylinder and a long, narrow one, and thus for the practical combustor, shape is a factor. This may be specified by length/diameter ratio, L/D, and values of 2·2–3·0 are representative of current practice. L/D value is implicit in giving a value of I_A, the area intensity parameter in conjunction with I_p, as $I_p/I_A = L/D$ for a simple cylinder. I_A also represents a mass velocity parameter and thus indirectly is a measure of stability, lower values indicating probability of a wider stability range. Corresponding to an L/D of about 2·5, a value of I_A of about 10×10^6 Btu or 5 Chu per (hr) (ft^3) (atm) represents a current limit.

The newer concept of pressure dependence to a power corresponding to the reaction order has not received sufficient acceptance to enable many general values of I_{p^n} to be given. Way (Ref. 10), using the results of bench tests of a simple type of combustor suggests a value of 10×10^6 Btu or $5{\cdot}5 \times 10^6$ Chu/ (hr) (ft^3) (atm)$^{1{\cdot}8}$ as a present upper limit, using $n = 1{\cdot}8$ in line with the overall reaction order of a hydrocarbon flame suggested by most data to date. For a pressure ratio of five, this agrees reasonably well with the limits for I_p given above. The parameter I_{p^n} has particular utility for performance of combustors at the reduced pressures at high altitude, as it is here that the loading problem is acute. It would appear that attention to values of I_{p^n} in initial design would help to obviate the limiting altitude performance with respect to efficiency and blow-out which is sometimes experienced at high altitude with combustors which have a satisfactory performance under the usual ground-level testing conditions.

There have been attempts to relate the interdependence of combustion efficiency and pressure loss as a function of the cycle performance (London, Ref. 11, and Nichols, Ref. 12). Because of the dependence of the efficiency on combustion intensity, then there is a relationship between the latter and the pressure loss. From dimensional analysis, Spalding (Ref. 13) has evolved a "flow criterion", K_f, as

$$K_f \equiv \frac{m^2}{\Delta p \rho_1 d^4 g_0} \tag{8.11}$$

where d is a characteristic dimension. K_f is approximately constant for a given design and high values indicate a good design. If cross-

sectional area A is a major criterion, then d is taken as the square root of A, giving

$$_AK_f \equiv \frac{m^2}{\Delta p \rho A^2 g_0} \tag{8.12}$$

which can be reduced to the reciprocal of the pressure loss factor λ, i.e.

$$_AK_f = 2/\lambda$$

If volume v is taken as the criterion, then $d = v^{\frac{1}{3}}$ and

$$_vK_f \equiv \frac{m^2}{\Delta p \rho v^{4/3} g_0} \tag{8.13}$$

Introducing the intensity I_p as mfH/pv where f is the fuel-air ratio, and H is the heating value, then

$$_vK_f = \frac{I_p{}^2 pRT_1 v^{2/3}}{\Delta p (fH)^2} \tag{8.14}$$

Eq. (8.14) introduces the intensity, pressure loss, and combustor volume (as a separate factor), the last being a useful feature because simple linear scaling of a combustor introduces difficulties. For example, halving the linear scale throughout for the same initial pressure, temperature and velocity, leads to one quarter of the original fuel flow and one-eighth of the original volume, thus doubling the original intensity. The increase of intensity would indicate a deterioration of performance, but this is not always borne out by the typical can combustor used in gas turbines. The problem of scaling is still a vexed one, as many factors enter in which scale in different ways, notably that of fuel atomization. In addition to the above references, another detailed discussion is given by Stewart (Ref. 14).

REFERENCES

1. Longwell, J. P. and Weiss, M. A. Heat Release Rates in Hydrocarbon Combustion. *Joint Conference on Combustion. I. Mech. E. and A.S.M.E.*, 1955.
2. Spalding, D. B. *Some Fundamentals of Combustion.* Butterworths Scientific Publications, London, 1955.
3. Longwell, J. P., Frost, E. E. and Weiss, M. A. Flame Stability in Bluff Body Recirculation Zones. *Ind. Eng. Chem.*, **45**, 1953, p. 1625.
4. Mayers, M. A. and Carter, W. W. Elbow Combustion Chamber. *Trans. A.S.M.E.*, **68**, 1946, p. 391.
5. Feilden, G. B. R., Thorn, J. D. and Kemper, M. J. Standard Gas Turbine to Burn Variety of Fuels. *Proc. I. Mech. E.*, **170**, 1956.
6. Clarke, J. S. and Lardge, H. E. The Performance and Reliability of Aero-Gas-Turbine Combustion Chambers. *A.S.M.E.* Paper No. 58-GTP-13, 1958.

7. GROBMAN, J. S. and DITTRICH, R. T. Pressure Drop and Air Flow Distribution in Gas-Turbine Combustors. *A.S.M.E.* Paper No. 56-A-208, 1956.
8. WILLIAMS, F. D. M. Gas Turbine Combustion System Design. *Can. Aeron. J.*, **4**, 1958, p. 99.
9. HOLDERNESS, F. H. The η–q Meter. *NGTE* Report No. 194.
10. WAY, S. *Combustion in the Turbojet Engine. Selected Combustion Problems—II.* AGARD, Butterworths Scientific Publications, London, 1956, p. 296.
11. LONDON, A. L. Gas-Turbine Plant Combustion-Chamber Efficiency. *Trans. A.S.M.E.*, **70**, 1948, p. 317.
12. NICHOLS, J. B. An Energy Basis for Comparison of Performance of Combustion Chambers. *Trans. A.S.M.E.*, **75**, 1953.
13. SPALDING, D. B. Performance Criteria of Gas-Turbine Combustion Chambers. *Aircraft Eng.*, **28**, 1956, p. 104, p. 168.
14. STEWART, D. G. *Scaling of Gas Turbine Combustion Systems. Selected Combustion Problems—II.* AGARD, Butterworths Scientific Publications, London, 1956, p. 384.

For analysis of basic combustion phenomena applicable to gas turbine performance, see Ref. 2 and " Basic Considerations in the Combustion of Hydrocarbon Fuels With Air ", *NACA* Report No. 1300, 1957.

CHAPTER 9

HEAT EXCHANGE

HEAT exchange is the broad term covering primarily the heating of the air between compressor and combustion by means of the exhaust gas from turbine discharge and secondarily the cooling of the air between compressor stages. The term regeneration is often used for the former and coincides with thermodynamics usage generally, but here a distinction is made between a *recuperative type* of heat exchanger and a *regenerative type*. The recuperative heat exchanger is exemplified by the common shell-and-tube exchanger, in which heat is transferred across a metal wall separating hot and cold fluids. The regenerative exchanger accomplishes heat transfer by the exposure of a quantity of material of considerable thermal capacity alternately between the hot and cold fluids. At a steady operating state, the fixed transfer surface of the former is at some equilibrium condition with respect to temperature, while the moving transfer medium of the latter has a continuously fluctuating temperature. More attention will be given to the recuperative type, which is also used for the intercooling process, because, although the regenerative type has considerable advantage with respect to size for a given duty, difficulties of sealing against leakage have so far proved next to insoluble for long-life industrial application. For the discussion here it is assumed that the general principles of heat transfer by conduction, convection and radiation are known, with the particular application to gas turbine heat exchangers the subject of any detailed analysis.

Similar to combustion, heat transfer is a well-established technique of long standing, with the difficulties of gas turbine application being those of minimizing size and, with the consequent relatively high velocities necessary, of minimizing pressure loss. The conditions for heat exchange are less arduous than those in many steam superheaters, but the same design methods for the high percentage heat recovery required would lead to such large units that the overall plant size would be quite uneconomic. The importance of minimizing pressure loss, particularly on the low-pressure gas side, has been stressed previously in the cycle analysis.

9.1 *Exchanger Performance—General*

The overall performance of a gas turbine heat exchanger is expressed by the *effectiveness* or thermal ratio, usually in terms of temperature ratio. The effectiveness, denoted by the symbol η_r although it is not a true efficiency, is defined as the ratio of the desired increase or decrease of temperature of the air to the maximum temperature difference available. Thus for the air-gas heat exchanger or " regenerator " (see Sec. 3.5),

$$\eta_r = \frac{T_{2_r} - T_{2'}}{T_{4'} - T_{2'}}$$

and for the intercooler,

$$\eta_i = \frac{T_{i'} - T_{i''}}{T_{i'} - T_w}$$

where T_w is the water inlet temperature.

For the heat exchanger, the mass flow rates of air and gas are the same with negligible error, but the difference in mean specific heats requires that the air temperature rise is slightly more than the gas temperature drop. For the intercooler, which has water one side, the temperature changes on each side are quite different.

Using a heat exchanger as example, a given rate of heat transfer is required, q, Btu/hr or Chu/hr. This rate is given by the product of mass flow rate m, lb/sec, specific heat c_p, Btu/lb F or Chu/lb C, and temperature rise Δt, F or C.

Thus

$$q = m_a c_{p_a} \Delta t_a = m_g c_{p_g} \Delta t_g \tag{9.1}$$

This rate of heat transfer is related to the heat exchanger behaviour by the product of an overall *heat transfer coefficient*, U, Btu/(hr) (ft²) (F) or Chu/(hr) (ft²) (C), the heat transfer surface area, A, ft², and an overall mean temperature difference, θ, F or C, thus

$$q = UA\theta \tag{9.2}$$

The overall coefficient U is a function of the local or surface convection heat transfer coefficients h on each side of the dividing surface and the conduction coefficient across the surface itself. The mean or effective temperature difference θ is a function of the exchanger geometry and can be calculated for standard arrangements. It is desired to minimize the surface area A, as this affects the size and first cost of the exchanger, so that both U and θ should be high. U is primarily a function of flow velocity, hence intimately associated with pressure loss and is the main parameter which requires analysis and test data, but it is also associated with θ for different arrangements so that they must be considered in conjunction.

9.2 *Heat Transfer Process (Recuperative Type)*

Fig. 9.1 represents the generalized condition for heat transfer between gas and air across the metal separating wall. The bulk temperature of the gas is t_g and of the air is t_a, with the wall temperatures being t_{wa} and t_{wg}. The convective film or surface coefficients of heat transfer, expressed in Btu/(hr) (ft²) (F) or Chu/ (hr) (ft²) (C), are denoted by h_a and h_g respectively. These coefficients are invariably for turbulent flow in the recuperative type. Across the metal wall, the process is one of conduction and is thus expressed in terms of the wall thickness b and the thermal conductivity of the material k, Btu/(hr) (ft) (F) or Chu/(hr) (ft) (C). (Note that Btu/F and Chu/C are equivalent, so for these happy but rare occasions giving values of h or k, one value only need be quoted.)

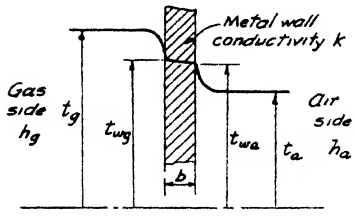

FIG. 9.1. Generalized condition for heat transfer across a metal wall.

For the usual overall adiabatic condition (i.e. no external heat loss), a heat balance gives the rate of transfer q in Btu/hr or Chu/hr,

$$q = U_a A_a(t_g - t_a) = h_g A_g(t_g - t_{w_g}) = \frac{kA_{a_g}}{b}(t_{w_g} - t_{w_a})$$
$$= h_a A_a(t_{w_a} - t_a)$$

where U_a is the overall coefficient based on the *air* side area and A_{a_g} is a function of wall geometry. (The use of U based on air side area is arbitrary and it could equally well be based on the gas side, provided consistency is maintained in the subsequent operations and elsewhere. It is important to remember that U is associated with a given area when the area of each side is different.) Because the conduction coefficient k/b is normally so very much greater than either h_a or h_g, the temperature drop across the wall $(t_{w_g} - t_{w_a})$ is extremely small, so that the *thermal resistance* of the wall is usually neglected and the whole term dropped, with the wall being considered at a uniform temperature t_w. Making this simplification and using $\theta_g = t_g - t_w$, $\theta_a = t_w - t_a$ and $\theta = t_g - t_a$, then

$$q = U_a A_a \theta = h_g A_g \theta_g = h_a A_a \theta_a$$

With $\theta = \theta_g + \theta_a$, then rearrangement yields

$$U_a = \frac{1}{h_a + \frac{A_g}{A_a} h_g} \tag{9.3}$$

Very commonly, the dividing surface is a thin-walled tube, so that $A_a \approx A_g$ and thus

$$U_a \approx \frac{1}{\frac{1}{h_a} + \frac{1}{h_g}} = \frac{h_a h_g}{h_a + h_g} \tag{9.4}$$

The simplified relation (9.4) shows an important feature, namely, that if one coefficient is very much lower than the other, it has a controlling effect. Thus for example, with $h_a = 48$ and $h_g = 12$, then $U_a \approx 9{\cdot}6$. Doubling h_a to 96 with h_g remaining at 12, gives $U_a \approx 10{\cdot}67$, an increase of 11·1%. Doubling h_g to 24, with h_a remaining at 48, gives $U_a \approx 16$, an increase of 66·7%. Thus the air and gas side coefficients should be approximately the same for the best return with respect to overall coefficient, and little is gained by improving a coefficient already high compared with the other. This is particularly true for the intercooler, as the water side coefficient is naturally of the order of 50 to 100 times the air side coefficient and the latter becomes the effective overall coefficient.

The first equation, (9.3), also shows an important relationship if the areas are not necessarily nearly equal, as U_a can be improved by increase in gas side area equally as much as by increased h_g, if this area is all at the same temperature. Even if the area is increased on one side or the other by the use of fins, which are at a lower temperature than the main, or *primary* surface, their use is often advantageous. This will be discussed later as the use of *secondary* surface.

9.3 *Basic Flow Arrangements*

Although the types of heat transfer surface are legion in the sense of the geometry of the passage as circular tubes or the less symmetrical shapes of plate heat exchangers, the general flow directions of air and gas may be described as combinations of a few basic arrangements. The major division may be made into (1) both air and gas flow longitudinal, and (2) air and gas flow normal to one another. The former is subdivided into (1) both air and gas flow in the same direction, so-called " parallel ", unidirectional or co-current flow, and into (2) air and gas flow in opposite directions, called *counterflow*. The case of air and gas perpendicular to one another is called *crossflow*. These are shown diagrammatically in Fig. 9.2.

The different arrangements give rise to different values of *mean temperature difference* (MTD), θ_m, between air and gas from inlet to outlet. The figure shows the variation of temperature of air and

gas along the length of a parallel-flow and a counterflow exchanger, with subscripts h and c for hot and cold fluid respectively.

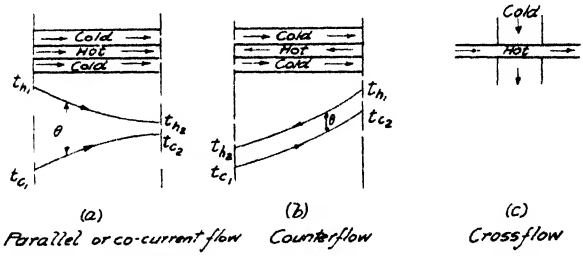

FIG. 9.2. Types of heat exchanger flow arrangement.

For parallel flow, it is seen that the maximum temperature difference is at inlet, decreasing continuously to outlet. The temperature of the cold fluid cannot be raised above that of the hot fluid at discharge, even for an infinitely long exchanger.

For the approximately equal thermal capacity rate of the two fluids in a gas turbine exchanger, then with $\Delta t_c = \Delta t_h$ and $t_{h_2} = t_{c_2}$, the maximum effectiveness η_r is

$$\eta_r = \frac{t_{c_2} - t_{c_1}}{t_{h_1} - t_{c_1}} = \frac{t_{c_2} - t_{c_1}}{(t_{h_1} - t_{h_2}) + (t_{c_2} - t_{c_1})} = \frac{\Delta t_c}{\Delta t_h + \Delta t_c} = 0{\cdot}5$$

Thus normally a parallel-flow arrangement is not used for gas turbines. There is one circumstance, however, when it is useful and that is when the minimum *wall* or metal temperature is required. This temperature lies somewhere between the air and gas temperature. The wall temperature can be estimated by equating the heat transfer rates on the two sides, i.e.

$$q = h_a A_a \theta_a = h_g A_g \theta_g$$

With $\theta_a = t_w - t_a$ and $\theta_g = t_g - t_w$, then

$$\frac{t_w - t_a}{t_w - t_g} = \frac{h_a A_a}{h_g A_g} \tag{9.5}$$

Hence t_w can be controlled by the ratio of the hA products. In the parallel-flow exchanger, the highest gas temperature (at inlet) is associated with the lowest air temperature (also at inlet) and t_w can be kept at a minimum. One application of this occurs in the exhaust-heated cycle, in which the hot gas is the combustion gas and the " cold " air is that from turbine discharge, so that a preliminary parallel-flow unit minimizes the metal temperature.

For counterflow, the air temperature can be raised above that of the discharge gas temperature and for an infinitely long exchanger

theoretically it can reach that of the inlet gas, hence the effectiveness can be unity. Again this would require infinite area and in practice, the area must increase very rapidly as the effectiveness increases. This can be demonstrated in very approximate fashion as follows. The effectiveness is, by definition,

$$\eta_r = \frac{t_{c_2} - t_{c_1}}{t_{h_1} - t_{c_1}} = \frac{\Delta t_c}{t_{h_1} - t_{c_1}}$$

For the counterflow gas turbine exchanger with equal thermal capacity rates on each side, $\Delta t_c = \Delta t_h$ and θ_m is constant along the exchanger, i.e.

$$\theta_m = t_{h_1} - t_{c_2} = t_{h_2} - t_{c_1}$$

Now

$$\begin{aligned} t_{h_1} - t_{c_1} &= (t_{h_1} - t_{h_2}) + (t_{h_2} - t_{c_1}) \\ &= \Delta t_h - \theta_m \end{aligned}$$

Substituting in the expression for effectiveness,

$$\eta_r = \frac{\Delta t_c}{\Delta t_h - \theta_m}$$

and with $\Delta t_c = \Delta t_h$,

$$\frac{\Delta t_c}{\theta_m} = \frac{\eta_r}{1 - \eta_r}$$

From the heat-balance expression, $m_c c_p \Delta t_c = U A_s \theta_m$, then

$$\frac{\Delta t_c}{\theta_m} = \frac{U A_s}{m_c c_p} = \frac{\eta_r}{1 - \eta_r} \tag{9.6}$$

For a given value of overall coefficient U and mass rate of flow, then the surface area is proportional to $\eta_r/(1 - \eta_r)$, which increases very rapidly as η_r increases. Thus if the required surface area is taken as unity for $\eta_r = 0{\cdot}5$, then it is tripled for $\eta_r = 0{\cdot}75$ and is nine times as great for $\eta_r = 0{\cdot}9$. This is the main reason why the effectiveness is usually limited to a value of about 0·75, in spite of the advantages of higher values as demonstrated in the cycle analysis of Chapter 3.

Because the highest gas temperature and highest air temperature are associated in the counterflow arrangement, the maximum wall temperature is higher than in the parallel-flow exchanger and there is likewise a larger temperature gradient from end to end. The wall temperature can be controlled to some extent by the air side coefficient, as shown before in Eq. (9.5.)

In the above analysis, θ_m has been taken to be constant along the exchanger, which is a fair approximation for the gas turbine in which

the thermal capacity rate on each side is about the same, but which nevertheless is not strictly correct. For the general case, it may be shown that the mean temperature difference used for θ_m is a logarithmic function given by

$$\theta_m = \frac{\theta_{max} - \theta_{min}}{\ln \frac{\theta_{max}}{\theta_{min}}} \tag{9.7}$$

where θ_{max} is the maximum temperature difference between hot and cold fluids and θ_{min} is the minimum temperature difference. θ_m is called the *logarithmic mean temperature difference* (LMTD) for counterflow and is used in other exchanger arrangements as a basic value, modified by coefficients pertinent to the geometry of each separate arrangement.

In order to shorten the heat exchanger, a *multi-pass* arrangement may be used, that is, a combination of counterflow and parallel-flow passages. A one shell-pass, two tube-pass arrangement is shown diagrammatically in Fig. 9.3. It is possible to have each fluid make one or more passes, but usually the mechanical arrangement becomes too complicated for many passes. Furthermore, the MTD is reduced below that of the straight counterflow, so that more surface area is needed in return for a gain in overall length. Values of the factor modifying the counterflow MTD for one shell-pass and two, four, etc., tube-passes are given in Fig. 9.4.

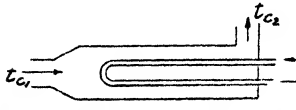

FIG. 9.3. Multi-pass arrangements —one shell-pass, two tube-passes.

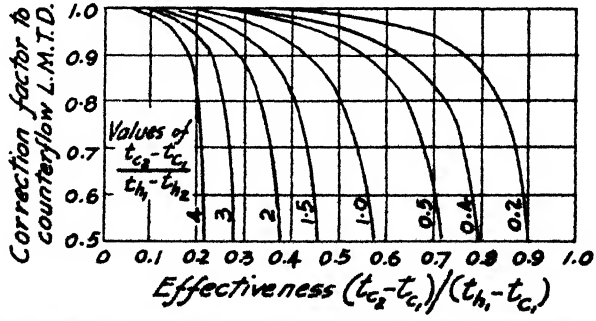

FIG. 9.4. Correction factor to L.M.T.D. for one shell-pass, two-, four-tube passes, counterflow (adapted from Bowman, Mueller and Nagle, ref. 12).

The crossflow arrangement gives rise to a more complex temperature distribution, as the entering fluid encounters a different

temperature of the other fluid in each row. Thus there is both a longitudinal and a transverse temperature gradient. The MTD requires a complex analysis and varies according to whether each fluid is considered as *mixed* or *unmixed* after each infinitesimal temperature change due to thermal contact with the other fluid. If

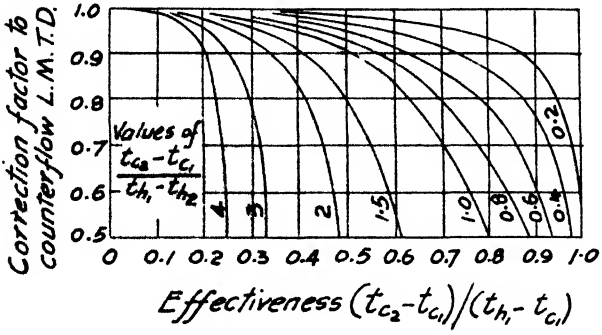

FIG. 9.5. Correction factor to L.M.T.D. for crossflow, single pass, both fluids unmixed (adapted from Bowman, Mueller and Nagle, ref. 12).

both fluids are kept in a multitude of individual longitudinal passages, the fluids are unmixed, a situation which is most closely approached by a practical exchanger. Values of the modifying factor to the calculated counterflow MTD are given in Fig. 9.5 for both fluids unmixed. The crossflow arrangement can also be used for more than one pass.

9.4 *Surface Coefficients*

Surface coefficients of heat transfer, h, are most conveniently given in dimensionless form, the two most common parameters being the *Nusselt* number, $N_u = hd_e/k$ and the *Stanton* number, $S_t = h/Gc_p$, where d_e is the *equivalent diameter* of the flow passage (Sec. 4.9) and $G = \rho V = m/A_c$ is the *mass velocity*, lb/(sec) (ft^2). The equivalent diameter for flow outside and parallel to tubes of a tube bundle is shown in Fig. 9.6. For flow outside and perpendicular to tubes, the equivalent diameter is usually taken as the tube o.d. itself.

The Nusselt number is a more general form for the coefficients of all methods of heat transfer, but the Stanton number is in many ways more useful for the forced convection of gas turbine exchangers. This is because of its similar form to the friction factor f of the pressure loss equation, which can be shown by a form of the original Reynolds analogy between heat transfer and friction. If the ratio

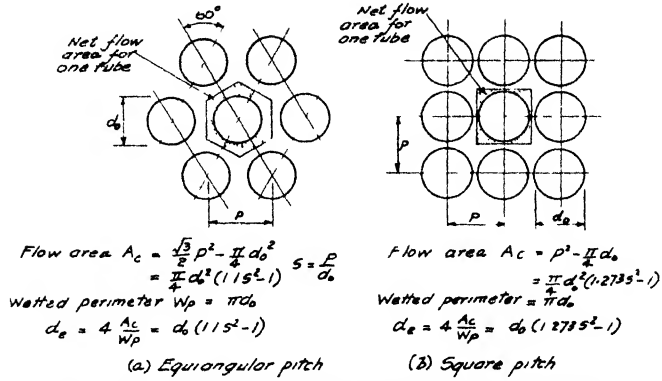

FIG. 9.6. Equivalent diameter for flow outside tubes.

of force corresponding to the actual rate of change of momentum from friction along a tube to the force due to maximum rate of change of momentum (i.e. bringing the fluid to rest) is equated to the ratio of the actual rate of heat transfer to the maximum possible rate (i.e. raising the temperature of all the fluid to that of the wall), there results

$$\frac{f\dfrac{L}{d}\dfrac{\rho V^2}{2g_0}\cdot A_c}{\dfrac{mV}{g_0}} = \frac{hA_s\Delta t}{mc_p\Delta t} \tag{9.8}$$

where A_c is the cross-sectional flow area and A_s is the surface area. For a circular tube of diameter d, $A_c = \pi d^2/4$ and $A_s = \pi dL$ and making the substitution $\rho V = G$, then Eq. (9.8) reduces to

$$\frac{h}{Gc_p} = \frac{f}{8} \tag{9.9}$$

[Note that when the friction factor is defined by the pressure loss equation $\Delta p = 4fL\rho V^2/2g_0 d$, then $S_t = f/2$. This is equivalent to using the hydraulic radius for d rather than the equivalent diameter because $d = 4r_h$ (see Sec. 4.9). This is the original form and is often used.]

The assumptions in Eq. (9.9) include that of assuming that heat transfer is effected by the turbulent core only, which is equivalent to assuming a *Prandtl* number, $P_r = c\mu/k$, of unity. This is not far from the truth for air and gas, for which $P_r \approx 0{\cdot}7$, but is much in error for liquids, for which the Prandtl number is considerably different from unity.

The usefulness of the analogy lies not in any exact quantitative application, but in showing the inter-relationship of heat transfer

and skin friction. Any pressure loss due to flow separation, as distinct from pure friction, is liable to be wasted with respect to heat transfer. Although the ratio of f to S_t is not a complete criterion for the optimum exchanger, as weight, length in relation to frontal area, and plant arrangement have all to be considered, it is an important one to keep in mind.

Some expressions for Nusselt and Stanton numbers will be given, not as exact values, for which the many literature references should be consulted (e.g. 1 and 2), but rather for illustrating certain relationships useful for generalization. For flow inside tubes or for flow outside and parallel to tubes,

$$N_u = 0{\cdot}023\, R_e^{0{\cdot}8}\, P_r^{1/3} \tag{9.10 a}$$

or, spelling out the dimensionless groups,

$$\frac{hd_e}{k} = 0{\cdot}023 \left(\frac{Gd_e}{\mu}\right)^{0{\cdot}8} \left(\frac{c_p\mu}{k}\right)^{1/3} \tag{9.10 b}$$

in which the fluid properties c_p and k are evaluated at the bulk mean fluid temperature and μ at the average temperature of the fluid and the surface. This relationship may be rearranged in the form of the Stanton number thus,

$$S_t\, P_r^{2/3} = \frac{0{\cdot}023}{R_e^{0{\cdot}2}} \tag{9.11 a}$$

or

$$\left(\frac{h}{Gc_p}\right)\left(\frac{c_p\mu}{k}\right)^{2/3} = 0{\cdot}023 \left(\frac{\mu}{Gd_e}\right)^{0{\cdot}2} \tag{9.11 b}$$

This shows at once that the tube size or equivalent diameter d_e should be as small as possible for the highest rate of heat transfer, other factors constant. A reduction of tube diameter from 1 in. to $\frac{1}{2}$ in. increases the heat transfer coefficient by about a third, but there is an even more important reason than this for striving for a small equivalent diameter. Using Eq. (9.6),

$$\frac{UA_s}{mc_p} = \frac{\eta_r}{1 - \eta_r}$$

and substituting $GA_c = m$, where A_c is the cross-sectional flow area, then

$$\frac{UA_s}{GA_cc_p} = \frac{\eta_r}{1 - \eta_r} \tag{9.12 a}$$

For a tubular exchanger of n tubes of diameter d and length L, then $A_s = n\pi dL$ and $A_c = n\pi d^2/4$, when Eq. (9.12 a) becomes

$$\frac{U}{Gc_p} \cdot \frac{4L}{d} = \frac{\eta_r}{1 - \eta_r} \tag{9.12 b}$$

For given values of overall coefficient U and specific flow rate G, then L/d is a function of η_r, a similar function to that of Eq. (9.6). Thus for high effectiveness, L/d must be large and the overall length increases directly with tube diameter.

For crossflow, a very approximate general expression is given by

$$N_u = 0{\cdot}33\, R_e^{0{\cdot}6}\, P_r^{1/3} \tag{9.13 a}$$

or

$$\frac{hd}{k} = 0{\cdot}33 \left(\frac{G_m d}{\mu}\right)^{0{\cdot}6} \left(\frac{c_p \mu}{k}\right)^{1/3} \tag{9.13 b}$$

where d is the outside diameter of the tube and G_m is the *maximum* flow velocity between tubes. The tube arrangement may be *in-line* or *staggered*, Fig. 9.7, and the tube spacing expressed as pitch/

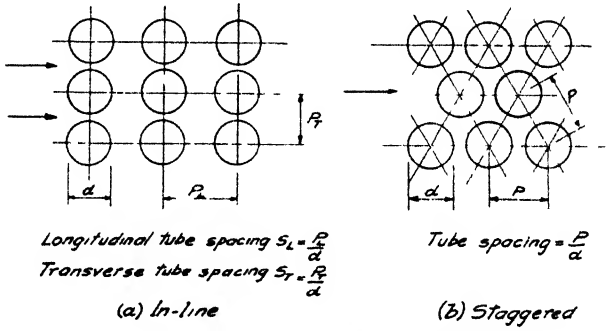

FIG. 9.7. Cross-flow tube arrangements.

diameter, both longitudinal and transverse, may vary widely. For these reasons, Eq. (9.13) is only an average value. Expressed as $N_u = aR_e^b$, then a and b vary for each arrangement and for specific values, Refs. 1 and 2 should be consulted.

Expressed in terms of Stanton number, Eq. (9.13) becomes

$$S_t\, P_r^{2/3} = \frac{0{\cdot}33}{R_e 0{\cdot}4} \tag{9.14}$$

For a given mass velocity and equivalent diameter, the heat transfer coefficient is higher for crossflow than for counterflow and generally results in a more compact exchanger, although comparison at the same Reynolds number is not a sufficient criterion by itself.

9.5 *Pressure Loss*

The pressure loss of an exchanger is of equal importance with that of the heat transfer and it is the interdependence of the two that makes the optimum design a lengthy process. The losses of the heat

exchanger as a whole are composed of four elements: (1) an entrance loss, usually a " sudden contraction "; (2) the loss due to the heat transfer surface itself; (3) an exit loss, usually a " sudden expansion "; and (4) a momentum loss due to heating. The second factor is the most important, but the remainder must be taken into account as a total, though each individually is usually small. Expressing these three losses as $k\rho V^2/2g_0$, where V is the initial velocity immediately preceding the change, then for the contraction, k_c varies from about 0·4 for an area ratio of 0·1 to 0·05 for an area ratio of 0·8. For the expansion, $k_e = (1 - (A_1/A_2))^2$ and for the momentum loss $k_m = (T_2/T_1 - 1)$ (see Sec. 8.9). These losses are mostly outside the control of the designer, and the major loss, that over the surface itself, is the one which is of greatest concern.

For counterflow, the loss is almost wholly due to skin friction along the inside or outside of tubes and may be calculated by the usual equation

$$\Delta p = f \frac{L}{d_e} \frac{\rho V^2}{2g_0} \tag{4.31}$$

with d_e either the i.d. or equivalent diameter, ρ and V the average values from inlet to outlet, and f a function of the Reynolds number. This relationship can be transformed to the more convenient parameter of specific mass flow rate $G = m/A_c = \rho V$, so that

$$\Delta p = f \frac{L}{d_e} \frac{G^2}{2g_0\rho} \tag{9.15}$$

and $R_e = Gd_e/\mu$.

It will be observed that pressure loss is proportional to G^2, while heat transfer is proportional to $G^{0.8}$, so that velocities must be kept low. Because $\Delta p \propto 1/\rho$, the velocity must be lower on the gas side for equal loss, and it has been seen that the loss should be lower on the gas side because of the low pressure level (Sec. 3.6).

For crossflow across rows of tubes, the loss is mostly that due to alternate contractions and expansions, with resulting eddies and turbulence, and the " friction factor " is empirical and varies with each tube arrangement. The loss may be expressed in similar form to that of 9.15, with the number of tube rows N replacing L/d, so that

$$\Delta p = f' N \frac{G^2}{2g_0\rho} \tag{9.16}$$

The factor f' is difficult to generalize in terms of tube arrangement and for individual values the previous references (1 and 2) on crossflow surface coefficients should be consulted. However, a reasonably

close correlation has been given by Jakob (Ref. 3), giving for *in-line* tubes

$$f' = \left[0{\cdot}176 + \frac{0{\cdot}32 S_L}{(S_T - 1)^x}\right] R_e^{-0{\cdot}15} \qquad (9.17\text{ a})$$

where

$$x = 0{\cdot}43 + \frac{1{\cdot}13}{S_L}$$

and for *staggered* tubes

$$f' = \left[1{\cdot}0 + \frac{0{\cdot}47}{(S_T - 1)^{1{\cdot}08}}\right] R_e^{-0{\cdot}16} \qquad (9.17\text{ b})$$

S_L and S_T are respectively the longitudinal and transverse tube pitch/diameter. These expressions are adequate for an initial design to establish the order of dimensions of a heat exchanger. In general, a better heat transfer to pressure loss ratio is given by close pitching, especially in the longitudinal direction.

9.6 *Secondary Surface*

Up to this point, the discussion on heat exchangers has been based mainly on a simple tubular design, which is representative of much existing practice and which is useful for demonstrating some general principles, because of the simple geometry of a circular tube. These principles are still qualitatively valid for the ensuing discussion, which is concerned with more complex geometries.

In the first place, it is possible to obtain increased surface area A_s, even on a tubular type, by the use of *fins* or *extended surface*.

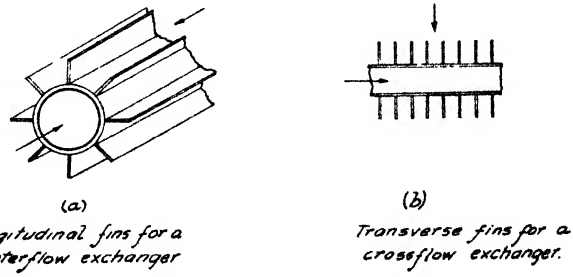

FIG. 9.8. Fins at extended surface.

Such additional material is in thermal contact with one fluid only, transferring heat from the primary surface (e.g. the tube wall) by conduction. The simplest examples are longitudinal fins in a counterflow exchanger or transverse fins on a crossflow exchanger, see Fig. 9.8. Because the conduction path is relatively long, there is a

significant temperature gradient, with the result that the secondary surface temperature is lower than that of the primary surface. This is accounted for by a fin *effectiveness* η_f (sometimes called fin efficiency) defined as the ratio of the actual heat transferred to that which would be transferred if the whole fin were at the temperature of its base. In other words, it is the ratio of the effective temperature of the surface to the base (primary surface) temperature. It is a function of the convection coefficient of heat transfer of the surface, h, the thermal conductivity of the fin material k, the fin height s and the fin thickness b. The effectiveness of fins of simple geometry can be calculated analytically (Ref. 2) but any asymmetrical design is best handled by numerical methods (Ref. 4), relaxation techniques for example. Fin surface can be taken to account by the expression,

$$A_{s_{\text{total}}} = A_{s_{\text{primary}}} + (\eta_f A_{s_{\text{secondary}}})$$

Thus although η_f is less than unity (usually of the order of 0·7–0·9), greatly increased total surface area may be arranged for the same volume of exchanger, as the secondary surface can greatly exceed the primary surface.

Extensive use is made of secondary surface in "plate" heat exchangers, a generic name for other than the tubular type. Great developments have taken place in recent years in the fabrication of sheet-metal exchangers, built of thin material joined by furnace brazing or equivalent methods. This allows a host of different shapes of passage to be designed, of small equivalent diameter and with minimal blockage due to material thickness. The design principle of such a secondary surface heat exchanger is shown in Fig. 9.9. It is essentially adapted for crossflow, as the provision of header plates is difficult for counterflow. Thin sheet-metal construction allows a profusion of surfaces to be used, with slots, holes, dimples, louvres, pins, etc., all of which assist heat transfer in addition to the extra surfaces, by breaking up an otherwise continuous boundary layer which is the main resistance in convective heat transfer. The most complete single work on the performance of secondary surface is that of Kays and London (Ref. 5), which presents Stanton number and friction factor data for a large number of surfaces, including some for conventional plain tubes and finned tubes as well as for the sheet-metal types. No general correlation is possible and, while some of the surfaces appear better than others,

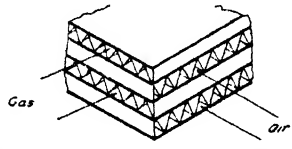

FIG. 9.9. Secondary surface heat exchanger—schematic.

no particular types can be singled out for optimum use, as the individual application may impose particular restrictions on length, frontal area, overall volume, weight, pressure loss, etc.

It should be noted that although the sheet-metal secondary surface type of exchanger offers great advantages in size and weight, due to the fin area and possibility of small passage dimensions (d_e), they are more susceptible to corrosion and do not lend themselves to easy cleaning. Their use therefore demands that there is little chance of fouling due to faulty combustion or (in the present state of the art) the use of heavy fuels.

9.7 *Intercoolers*

Intercoolers, using water, are usually of the shell-and-tube type. With water inside the tubes, then Eq. (9.10) can be used for the heat transfer performance (this is the advantage of the dimensionless representation in terms of Nusselt, Reynolds and Prandtl numbers). The surface coefficient h for water is of the order of 50 times that of air, so that the air side resistance is controlling and profitable use can be made of fins. Since the air is at a relatively high density, the intercooler can be made in reasonably compact form, even though high values of effectiveness are required. Because the thermal capacity rate on the water side can be so much greater than that on the air side, high effectiveness is possible in a single pass with reasonable L/d.

9.8 *Choice of Heat Exchanger Arrangement*

The problem of heat exchanger design for gas turbines rests, not in obtaining the required performance, which it can be said is always possible, but in obtaining the optimum solution for the operating requirements. The fixed given conditions are then likely to be the required effectiveness and maximum permissible performance loss due to pressure drops. If the latter is given as a fraction of the power output, then this can be transplanted to a $\Sigma \Delta p/p$, giving flexibility in the relative values of Δp_a and Δp_g (Sec. 3.6). There may then be one or more limiting criteria, such as maximum length, cross-sectional area, height, etc., dependent on plant layout, or the requirement may be general, such as minimum volume or weight. Perhaps the most difficult requirement to satisfy is that of minimum cost, because although minimum weight of material is a strong index of cost, fabrication cost varies widely with varying types of surface and arrangement. It is also not possible to divorce the heat exchanger design from the other components in the sense, not only of general layout, but of the specific sizes of connecting ducting.

Thus, although the optimum design might develop in the form of a relatively short exchanger of rather large cross-sectional flow area, this might require a diffusing section from compressor outlet which would be of considerable length for good efficiency or occasion a large pressure loss if short. Exclusive of the parallel or unidirectional flow type, which is used only under special circumstances as noted, gas turbine heat exchangers are of the counterflow or crossflow type, usually with a single pass of each fluid, although sometimes a double pass of one fluid is used. The choice is complex, but is to a great extent influenced by the type of construction used and the plant layout. With the conventional shell-and-tube type, a header plate for the tubes is required and then, for counterflow, the outside fluid must enter and leave through transverse ducts in the shell. To distribute the outside fluid, it may be necessary to insert baffles, which must be designed with care to avoid excessive pressure loss. For crossflow, it is easier to arrange for the inlet and outlet ducts. These schemes are shown diagrammatically in Fig. 9.10.

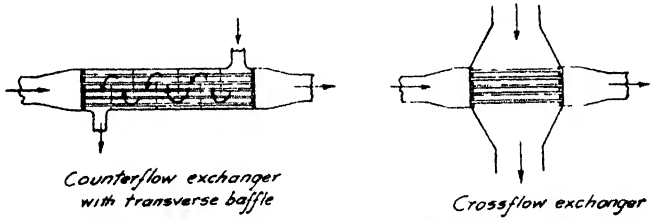

FIG. 9.10. Types of Heat Exchanger.

The choice of tube size has a considerable effect on the choice of arrangement. Although small tube diameter is desirable for heat transfer characteristics (Sec. 9.4), any fouling of the tubes (carbon, tar, ash, etc., from heavy fuels) causes a faster loss of performance in small tubes than in larger ones and furthermore, small tubes are difficult to clean mechanically. A further factor is that for a given specific mass flow rate G, lb/(sec) (ft^2), the number of tubes required is proportional to $1/d^2$, and thus the manufacture of the header plate becomes costly. With large-diameter tubes, however, the length of the exchanger may become excessive for high values of effectiveness, because of the controlling effect of L/d (Sec. 9.4).

There is a continual search for methods of optimizing heat exchanger design. Some of the results, specifically adapted for gas turbine work, are given in references 6, 7, 8 and 9. The last two are the most general, covering most types of surface, whereas the first two are restricted to shell-and-tube counterflow types, but with

the analysis in some detail. Some of the main conclusions, which should be taken only as broad generalizations, are as follows:

1. Shell-and-tube counterflow types give a small frontal area and long length.
2. Shell-and-tube crossflow types give the largest frontal area of any type, because of the blockage area occupied by the tube diameter.
3. Relatively simple relationships can be found for tubular exchangers, resulting in minimum weight or volume designs.
4. Better results are achieved for tubular heat exchangers with the higher pressure fluid (air) inside the tubes. This is also advantageous with respect to the stress, and hence material thickness of the shell, but necessitates adequate insulation to prevent heat loss.
5. Tube diameters of $\frac{1}{4}$ in. or less for tubular exchangers are required for the volume to be competitive with that of the sheet-metal extended surface type.
6. Fins of high-thermal conductivity are worthwhile for the utmost in compactness.
7. There is no one particular type of surface which can be said to be optimal, as so many different criteria arise in the many different applications.

9.9 *Regenerative Heat Exchangers*

The regenerative principle is that of transferring heat by means of a solid medium alternately in contact with the hot and cold streams. It is a method of long standing, as used in connection with blast furnaces, and more recently, in the Ljungstrom type of air preheater for steam generating furnaces. In the former, the action is periodic, with alternate blowing of hot and cold streams through a fixed matrix of checkered brick, while in the latter the metal matrix revolves slowly between fixed fluid streams. For the air preheater, however, the temperature and pressure differences are relatively small, and it is the magnitude of these factors which causes the problems arising for gas turbine use.

The rotating matrix can be basically either a *disc* or a *drum*, these types being shown diagrammatically in Fig. 9.11. As a given small sector of the material passes from the gas side, where it has attained the exhaust-gas temperature, it meets the cold air, which, in passing through the holes or interstices in the disc or cylinder, abstracts the heat in the material, so that ideally the latter has just

been reduced to the air temperature, as it again passes to the gas side. Thus a temperature wave travels through the material in the direction of fluid flow, and ideally the form of the wave is square-topped, although this cannot be realized in practice. High effectiveness can be obtained by being able to heat the matrix up to nearly the full inlet gas temperature, the heat transfer being obtained by laminar flow in passages of very small diameter, of large L/d. Laminar flow causes pressure loss proportional only to the first power of velocity, as opposed to V^2 in turbulent flow, and thus, although low velocities have to be used, and hence large flow areas,

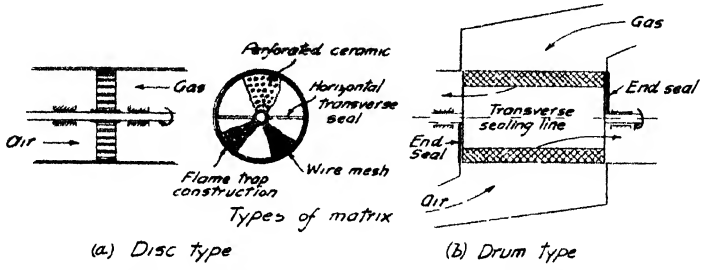

FIG. 9.11. Regenerative heat exchanger—schematic.

the overall loss can be kept to a reasonable value, while obtaining high effectiveness. The matrix material should have a high specific heat, for thermal capacity, and low thermal conductivity, to minimize longitudinal conduction, so shaped that the flow passages are of very small cross-sectional dimensions with very thin walls. Ceramic material appears to be well suited for these requirements, but to date, either layers of wire mesh or plate construction have been used. The latter has often taken the form of a typical flame-trap design, alternate strips of flat thin sheet and crimped thin sheet being wound together in spiral fashion.

The theory of the regenerative heat exchanger is rather complex, because it is an unsteady state phenomenon. It is too lengthy to deal with here and references 10, 11, and 12 should be consulted. The effectiveness is a function of $\Delta t/\theta_m$ as for recuperative types, but also of the matrix thermal capacity and speed of rotation. Defining the latter as C_r = (revolutions/sec) (mass of matrix) (specific heat of matrix), then higher values of C_r result in higher values of η_r for the same $\Delta t/\theta_m$. As $C_r/m_a c_{p_a}$ approaches infinity, the regenerative effectiveness η_{reg} approaches the effectiveness $\eta_{counter}$ of the recuperative counterflow exchanger of the same $\Delta t/\theta_m$.

London (Ref. 11) gives an empirical relationship valid for $C_r/m_a c_{p_a} > 2$ and for $m_a c_{p_a}/m_g c_{p_g} > 0{\cdot}7$ as

$$\eta_{\text{reg}} = \eta_{\text{coun}} \left[1 - \frac{1}{9\left(\frac{C_r}{m_a c_{p_a}}\right)^2} \right] \tag{9.18}$$

from which it is seen that matrix speed has only a very small effect on η. Although the effectiveness of the regenerative type only approaches that of the counterflow recuperative type for the same value of $\Delta t/\theta_m = UA_s/mc_p$, the great advantage lies in the much greater surface area per unit volume of matrix which can be provided. Thus higher values of effectiveness are possible with reasonable volume and weight of exchanger.

The disadvantages of the regenerator are: (1) provision of auxiliary drive for rotation; (2) large inlet and outlet ducts; (3) loss due to leakage and carry-over between high- and low-pressure sides; and (4) distortion due to cyclical thermal loads. The first factor is minimal provided that an electric supply is available, because the rpm is very low and power required is small. The second factor is very variable and depends on the overall design, but may lead to a large diffusing section from the compressor. It is the third and fourth factors which are the most important and they are largely mutually dependent.

The necessity of a running seal between the cold, high-pressure air side and the hot, low-pressure gas side is obvious, whatever the particular type of construction. Any leakage is a serious loss, because it is air which has absorbed compressor work but which then escapes to atmosphere without passing through the turbine. It is more important than pressure loss, as it affects the net work severely. In addition to direct leakage through seals, there is inevitably a " carry-over " or " let-down " loss due to air trapped in the matrix as it passes through to the gas side. Leakage is dependent mainly on pressure ratio and carry-over on matrix rpm. Quantitatively, the effect of a given fractional leakage depends on the values of exchanger effectiveness and cycle pressure ratio. As example, for a cycle with typical temperatures, component efficiencies and regenerator effectiveness of 90%, a leakage of 5% will reduce the net output by about 11%, while a leakage of 10% will reduce it by twice that amount.

A considerable amount of work has been devoted to the seal problem and although progress has been made, there is, at the time of writing, as yet no regenerative exchanger in operational service.

The difficulty appears to be not so much in obtaining initially low leakage, although this requires very careful design work, but in maintaining a close seal over an industrially useful period of time, due either to excessive wear, thermal distortion or both. However, the return in cycle efficiency for a regenerator of high effectiveness is so great that it is to be hoped that perseverance will one day allow a solution to be found. A value of η_r of 90% would make the fuel consumption of a gas turbine of low pressure ratio and medium temperature directly competitive with that of diesel engines.

REFERENCES

1. McAdams, W. H. *Heat Transmission.* 3rd Ed., McGraw-Hill Book Co., Inc., N.Y., 1954.
2. Jacob, M. *Heat Transfer.* J. Wiley and Sons, Inc., N.Y., 1949.
3. Jakob, M. Discussion of "Heat Transfer and Flow Resistance in Cross Flow of Cases over Tube Banks" (*Trans. A.S.M.E.*, **59**, 1937), *Trans. A.S.M.E.*, **60**, 1938, p. 384.
4. Dusinberre, G. *Numerical Analysis of Heat Flow.* McGraw-Hill Book Co., Inc., N.Y., 1949.
5. Kays, W. M. and London, A. L. *Compact Heat Exchangers.* McGraw-Hill Book Co., Inc., N.Y., 1958.
6. Shepherd, D. G. A Design Method for Counterflow Shell-and-Tube Heat Exchangers for Gas Turbines. *A.S.M.E.* Paper No. 47-A-60, 1947.
7. Rohsenow, W. M., Yoos, T. R. Jr., and Brady, J. F. Optimum Design of Gas Turbine Heat Exchangers. *A.S.M.E.* Paper No. 50-A-103, 1950.
8. Aronson, D. Review of Optimum Design of Gas Turbine Regenerators. *Trans. A.S.M.E.*, **74**, 1952, p. 675.
9. London, A. L. Gas Turbine Plant Heat Exchangers. *A.S.M.E.*, 1951.
10. Harper, D. B. and Rohsenow, W. M. Effect of Rotary Regenerator Performance on Gas-Turbine-Plant Performance. *Trans. A.S.M.E.*, **75**, 1953, p. 759.
11. Coppage, J. E. and London, A. L. The Periodic-Flow Regenerator—A Summary of Design Theory. *Trans. A.S.M.E.*, **75**, 1953, p. 779.
12. Bowden, A. T. and Hryniszak, W. The Rotary Regenerative Air Preheater for Gas Turbines. *Trans. A.S.M.E.*, **75**, 1953, p. 767.
13. Bowman, R. N., Mueller, R. C., and Nagle, W. M. Mean Temperature Difference in Design. *Trans. A.S.M.E.*, **62**, 1940, p. 283.

For detailed analysis of heat exchangers for gas turbines, see Ref. 9 above and Hryniszak, W. *Heat Exchangers*, Butterworths Scientific Publications, London, 1957.

CHAPTER 10

PERFORMANCE AND CONTROL

THE previous chapters on components, compressor, turbine, combustor and heat exchanger, have analysed the behaviour and design principles of each as separate units. The discussion of cycle analysis was principally devoted to the design point performance. The object of this chapter is to consider the general performance of a gas turbine over a wide range of operating conditions, both at full and part load, showing the effect of one component on another. The subject is complex and only a limited discussion of some of the main factors will be attempted here.

10.1 *Dimensionless Parameters*

It will be appreciated at this point that there are a very great number of different operating variables covering both individual component performance and the performance of the gas turbine as a whole. When there are so many variables, the method of *dimensional analysis* is extremely useful. It consists of a formal method of combining the individual variables into a number of *dimensionless groups* or π-terms, this number being less than the number of variables, with each group having a physical meaning and giving considerable information on the relationship between variables.

Considerable use has been made previously of dimensionless parameters. Some have been implicit, pressure ratio and efficiency for example, while others have been formed arbitrarily, thus Q/c_pT_1, $\phi = V_a/U$, $\Delta p/\rho V^2$, etc. Dimensionless analysis shows these groupings to be logical and how they may be found by a simple algebraic process, when the variables entering into the physical relationship are known. The method is essentially one of making a relationship dimensionally correct. Thus, to take a familiar and simple example, if the pressure loss Δp in a duct of length L and equivalent diameter d_e is taken to be dependent on the fluid velocity V_1, density ρ and absolute viscosity μ, then dimensional analysis can show that

$$\frac{\Delta p}{\rho V^2} = f\left(\frac{L}{d_e}, \frac{\rho V d_e}{\mu}\right)$$

A total of six variables has been reduced to three groups, each of which is dimensionless (in consistent units). The form of the function is not known without experiment, which actually shows that $\Delta p/\rho V^2$ is directly proportional to L/d_e, inversely proportional to $\rho Vd/\mu$ for laminar flow and with no simple mathematical relationship for turbulent flow. $\rho Vd_e/\mu$ is known as the *Reynolds* number and many groups of wide utility are given names, usually of a proponent or of a distinguished worker in the field, Mach number V/a, Nusselt number hd/k, etc. This is not the place to give methods of dimensional analysis nor of further discussing its implications, for which Ref. 1 should be consulted for a complete and rigorous account or Ref. 2 for a short discussion with particular reference to turbomachines. One point is important, however. That is, that every dimensionless group has a physical significance and is not merely the result of algebraic manipulation. It represents a combination of variables, a given value of which represents a certain physical condition regardless of the values of the individual variables which constitute it. A dimensionless group represents a ratio of two like entities which may be geometric (e.g. L/d_e), kinematic (e.g. V_a/U), or dynamic (forces, energies, etc., e.g. $\Delta p/\rho V^2$). Similar values of all groups representing a physical situation implies complete *similarity* of behaviour. Perhaps the best known example is that of Reynolds number, $\rho Vd/\mu$, which represents the ratio of inertia force to viscous force in a fluid. A given value of $\rho Vd/\mu$, regardless of the size of the apparatus, velocity of the fluid and the fluid properties, then implies a particular flow characteristic, e.g. friction coefficient or drag coefficient. Some appreciation of the meaning of dimensionless groups can be of considerable help when using them for various purposes. Without derivation, some of the most important groups for the gas turbine are given below and their use discussed.

10.2 *Compressor and Turbine Performance*

From the chapters on compressors, it was seen that the delivery pressure P_2 was a function of inlet pressure and temperature, P_1 and T_1, the mass flow rate m, the speed N and the size here denoted by the single linear dimension D. The most useful parameters are $m\sqrt{T_1}/D^2P_1$, P_2/P_1 and $ND/\sqrt{T_1}$, representing dimensionless forms of flow rate, pressure and speed. Their most important use is in correlating the performance of a given compressor at various inlet conditions, P_1 and T_1. For a single compressor, the size dimension is constant and is usually omitted, so that the parameters become $m\sqrt{T_1}/P_1$, P_2/P_1, and $N/\sqrt{T_1}$. The performance is then plotted as

P_2/P_1 against $m\sqrt{T_1}/P_1$, with $N/\sqrt{T_1}$ as parameter, Fig. 10.1, replacing the absolute values with m and N only as given in Chapters 5 and 6. The latter are valid only for one fixed value of inlet density (i.e. P_1 and T_1), while the dimensionless parameters take care of this implicitly. Thus test data plotted in dimensionless form are correlated for any intake conditions, which must inevitably vary continuously. An important point to note is that the true speed is a function of temperature, i.e. the speed as it affects performance is not absolute. Variations of P_1 and T_1 are most acute for aircraft gas turbines, for which dimensionless parameters are a necessity for ease of handling performance characteristics.

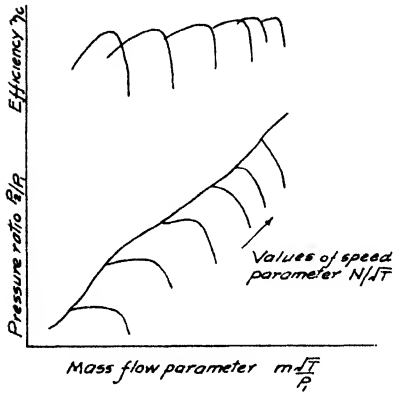

FIG. 10.1. Compressor characteristics plotted in dimensionless form.

The flow parameter $m\sqrt{T_1}/D^2P_1$ can readily be shown to be a form of *fluid* Mach number, reducing to $V/\sqrt{T_1}$ by substituting of $m = \rho_1 V_1 D^2$ and $\rho \propto P_1/T_1$, where D^2 represents flow area. The speed parameter, $ND/\sqrt{T}$ is a form of *rotor* Mach number $U/\sqrt{T_1}$, with $ND \propto U$. Given values of $V/\sqrt{T}$ and $U/\sqrt{T}$ together represent a certain inlet velocity triangle and thus a particular flow condition.

Fig. 10.1 also shows the efficiency, which is a dimensionless parameter by definition. Sometimes other performance variables are useful, such as temperature rise, expressed as $\Delta T/T_1$, and power H expressed in dimensionless form as $H/D^2P_1\sqrt{T_1}$ or $H/P\sqrt{T_1}$.

Although the dimensionless groups are so useful for correlating performance, their numerical values convey very little by themselves and at times it is desirable to present data in the common units, reduced to agreed standard conditions. Dimensional analysis shows how this may be done logically. For similarity, there must be similar values of the performance parameters. Thus for any two conditions a and b, the similarity principle demands that

$$\frac{P_{2_a}}{P_{1_a}} = \frac{P_{2_b}}{P_{1_b}}; \quad \frac{m_a\sqrt{T_a}}{P_a} = \frac{m_b\sqrt{T_b}}{P_b}; \quad \frac{N_a}{\sqrt{T_a}} = \frac{N_b}{\sqrt{T_b}}$$

If now state b is any state at which data are measured, with sub-

script m, and state a is made that of the agreed standard conditions, with subscript s, then

$$P_{2_s} = P_{2_m} \frac{P_{1_s}}{P_{1_m}} = \frac{P_{2_m}}{\delta}$$

with δ the symbol for the ratio of actual ambient pressure to standard ambient pressure, P_{1m}/P_{1s}.

Likewise,

$$N_s = N_m \sqrt{\frac{T_s}{T_m}} = \frac{N_m}{\theta^{\frac{1}{2}}}$$

and

$$m_s = m_m \frac{\theta^{\frac{1}{2}}}{\delta}$$

where

$$\theta = T_m/T_s$$

The standard conditions are taken to be $P_s = 14{\cdot}7$ psia and $T_s = 15°$ C or 59° F (288° K or 518·7° R). The operation of converting measured values to standard values is variously known as " correction ", " reduction " or " standardizing ".

Turbine performance is expressed in similar parameters, that is, using the subscripts 3 and 4 as for cycle performance, P_3/P_4, $m\sqrt{T_3}/P_3$ and $N/\sqrt{T_3}$. There are no standard values of inlet conditions for turbines for obvious reasons, although arbitrary values may be chosen for correlation purposes if desired.

10.3 *Combustor and Heat Exchanger Performance*

Dimensionless parameters for the combustion process as they affect the whole gas turbine performance are seldom used, with the possible exception of the two pressure loss expressions $\Delta p/p$ and $\Delta p/(\rho V^2/2g_0)$. There are two reasons for this, the first being simply that any variation of combustion efficiency does not affect the turbine, which must operate at a certain temperature level regardless of how much fuel is required to accomplish this. The second reason is that, as yet, data on combustors do not exhibit general correlated behaviour with varying pressure, temperature, size, etc., although several tentative schemes have been presented in the literature. The chapter on combustion has indicated the complexity of the problem, due to the large number of variables, and dimensional analysis is almost a necessity in correlating performance. Some of the possible groups have been discussed in Chapter 8, but more data and analysis are needed before a standard form of presentation is generally accepted.

Heat exchangers are in a similar category to combustors with respect to their effect on the operating characteristics of the gas turbine, that is, the pressure losses have a relatively small effect when varying load on a given plant, while the effectiveness, though very important with respect to fuel consumption, does not affect compressor and turbine operation. However, the effectiveness of a heat exchanger, having a certain required value at the design point, *increases* as the mass flow is reduced. This can be estimated approximately in simple fashion from Eq. (9.12 a), which for a given exchanger reduces to $\eta_r/(1-\eta_r) \propto U/G$. For a counterflow exchanger, having $h \propto G^{0\cdot8}$ for both sides, then $U \propto G^{0\cdot8}$, thus $(1-\eta_r)/\eta_r \propto G^{0\cdot8}$ and η_r increases as the mass flow decreases. For a reduction of mass flow by one-half, an effectiveness of 0·75 increases to about 0·776, a seemingly small increase, but having a greater proportionate effect on cycle efficiency.

10.4 *Aircraft Performance*

The installation of a gas-turbine plant in an aircraft introduces the further important variable of forward speed, U_f. This was seen in Sec. 3.22 to affect the inlet temperature and pressure, i.e. the ram effect. The correlating parameter is $U_f/\sqrt{T_a}$, which can be seen in simple fashion to have a logical basis, because the dynamic temperature rise ΔT_a due to forward speed is proportional to U_f^2. $U_f/\sqrt{T_a}$ represents the aircraft *Mach* number, as the velocity of sound is proportional to $\sqrt{T}$. Altitude introduces large variations of inlet temperature and pressure, but these are handled satisfactorily by the dimensionless group $m\sqrt{T_1}/P_1$.

10.5 *Part-load Performance*

All components necessarily " match " at the design point, because each is designed for the required mass flow, speed, pressure and temperature. For any other speed or output, then the individual operating characteristics of each component must be taken into account and the net effect evaluated.

For off-design calculations, the physical arrangement of the plant is highly important in relation to the number of separate compressor and turbine rotors, disposition of combustors and location of the output shaft. This was mentioned in Sec. 3.13, which defined the compound arrangement and hinted at the many possible different arrangements. The varying possibilities may be gauged by considering only the simple cycle, with two compressors and hence a minimum of two turbines, the two compressors being required in order

to achieve a pressure ratio not possible with only one. Considering only the straight-compound arrangement (higher pressure turbine driving H.P. compressor, lower pressure turbine driving the L.P. compressor), then the load may be taken off either turbine or a separate power turbine may be used, which may be located before the H.P. compressor-turbine, after the L.P. compressor-turbine or intermediately. The flow may be split from the combustor with various arrangements of turbine, or may be split from the H.P. compressor into two combustors, each with independent fuel supply, and with the flow from each combustor arranged for several turbine dispositions. Then there is the matter of the load variation, among those most likely being constant output speed (electrical generation), or load varying approximately as the cube of the speed (propeller law). These arrangements can also be made with the cross-compound scheme, so that there are several dozen different layouts for just the simple cycle, with each having different operating characteristics at part load. Most of them may be dismissed as unworkable or requiring a very elaborate control system, but even so there remain several different possible schemes which require investigation. The matter is so complex that little attempt has been made to explore the subject both widely in scope and in detail at the same time. The most inclusive work is that of Mallinson and Lewis (Ref. 3), which explores a wide range of possibilities, while analysis in more detail on a limited range, with examples, is given by Hodge (Ref. 4). In practice, arrangements, with only a few exceptions, have been limited to single-shaft machines, single compressor machines with separate power turbine, and straight-compound machines. Cross-compounding has certain advantages on occasion, but, in general, straight-compounding is simpler in operation. Because a truly valid analysis requires a very detailed computation, plus a close estimate of the actual component characteristics, the discussion here will be limited to some analysis of the general methods of attack and the problems encountered, in order to indicate the type of procedure required for a particular analysis.

The general problem may be broken down into, (1) the behaviour of compressors in series, (2) the behaviour of turbines in series, (3) characteristics of a single shaft machine, (4) effect of a separate turbine, and (5) effect of a heat exchanger.

10.6 *Compressors in Series*

Fig. 10.2 shows the characteristics of each compressor, with subscripts 1 and 2 indicating inlet and outlet of the L.P. compressor, 2 and 3 for the H.P. compressor. The L.P. outlet is the same as the

H.P. inlet, with any loss between the two taken care of by making P_2 the L.P. compressor outlet pressure less losses. The design point is shown at A on both diagrams. Now if the speed is reduced to line 2, it would be desirable for the operating point of the L.P. compressor to be at point B, retaining a high efficiency, which is close to the surge line. Now for the H.P. compressor, which must have the same actual mass flow m, the reduction of the value of the parameter $m\sqrt{T_2}/P_2$ is proportionately much less than that of $m\sqrt{T_1}/P_1$, because P_2 is considerably reduced from its original value. Thus the operating point for the H.P. unit is at B', with reduced efficiency and being closer to choking. At considerable speed reductions, choking is almost inevitable, i.e. operation is impossible. If choking is avoided in the second stage by pushing the first stage change far to the left for the initial speed reduction, further speed reduction is most likely to cause the first stage operating point to move across the surge line, i.e. again operation is impossible.

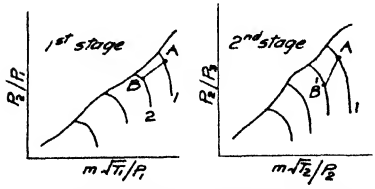

FIG. 10.2. Characteristics of compressors in series.

Help in avoiding the Scylla of choking of the H.P. compressor and of the Charybdis of surging of the L.P. compressor can be obtained by blow-off between stages (cf. Sec. 6.13), but this is tolerable only for starting conditions, reducing the cycle efficiency too much for continued operation. Two methods of relief of real efficacy are possible, (1) splitting the shaft and driving each compressor separately at different speeds, and (2) providing adjustable stator rows on the L.P. compressor. The former is the basis for compounding and is usually adopted for industrial plants where space and weight are not at a premium. It is also used for aircraft turbines but using concentric shafts to shorten the unit. The last arrangement may appear complex and require expensive forms of construction, but many successful turbo-jets and turbo-props are thus designed. The method of using a number of variable stator rows is again mechanically complex, but as many as six such stators are fitted to at least one major turbo-jet unit. It results in a very light compressor, but requires a carefully-designed automatic control system.

With compounding, the separately-driven H.P. compressor is kept at a higher speed, the operating point being at C, for example, as shown in the figure, well away from choking and, in any case, at a better efficiency. With variable stators, new characteristics

are provided for the L.P. compressor, moved bodily over to the left, so that the surge line is not crossed.

10.7 *Turbines in Series*

Turbine characteristics were discussed in Chapter 7 and it was seen that the separate speed characteristics could be condensed into a single line without great error. This fact is the basis for any but the most detailed part-load calculations. A single-stage turbine chokes at the critical pressure ratio $(P_3/P_4 = [(k+1)/2]^{k/k-1})$, but a multi-stage turbine has a typical characteristic as shown in Fig. 10.3. It can be shown that the mass flow-pressure ratio characteristic of a multi-stage reaction turbine may be represented by

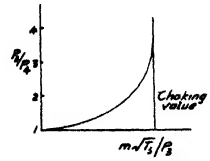

FIG. 10.3. Multi-stage characteristic.

$$m^2 = k f(\phi_i, \eta)\, P_3 \rho_3 [1 - (P_4/P_3)^{2-\eta(k-1)/k}]$$

where k is a constant including the effective flow area, $f(\phi_i, \eta)$ is a function of the ideal velocity ratio, $\phi_i = U/V_3$ and blade efficiency η, with 3 and 4 the turbine inlet and outlet. Assuming constant values of efficiency and $f(\phi_i, \eta)$, then this expression reduces to

$$\frac{m\sqrt{T_3}}{P_3} \propto \left[1 - \left(\frac{P_4}{P_3}\right)^{2-\eta(k-1)/k}\right]^{\frac{1}{2}} \tag{10.1}$$

For $\eta = 0{\cdot}8$ and $k = 1{\cdot}33$, the exponent of P_4/P_3 becomes 1·8. It is often taken as a value of 2, when it is known as the ellipse law, due to Stodola. Eq. (10.1) is in the form of the familiar dimensionless groups and thus the turbine characteristic is readily plotted for any range of pressure ratio. The assumptions used in this simple form should be noted, that is, constant efficiency and $f(\phi_i, \eta)$, which is usually justified over the range of a turbine required for a part-load estimate, but for more accurate calculations when the turbine characteristics are known in some detail, then the latter data should be used directly. What is being demonstrated here is a general method of attack as simply as possible and which is applicable when the detailed data are not available.

Now consider two turbines in series, which, because the characteristics have been made independent of speed, may have different rpm or the same rpm (the latter is equivalent to splitting the stages on a single rotor).

The first turbine characteristic is shown in solid line in Fig. 10.4, operating over a pressure ratio P_3/P_4 and mass flow parameter $m\sqrt{T_3}/P_3$. Immediately below this figure is the characteristic of

the second turbine, with pressure ratio P_x/P_4 and mass flow parameter $m\sqrt{T_x}/P_x$. In broken line on the upper diagram, the characteristic of the first turbine is plotted with the mass-flow parameter in terms of its *outlet* conditions, which are the *inlet* conditions of the second turbine.

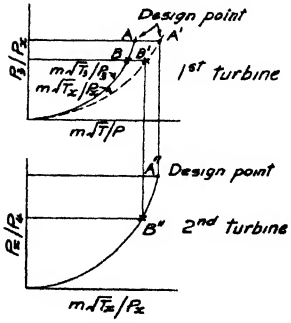

FIG. 10.4. Characteristics of turbines in series.

Point A is the design point, shown on all three characteristics. If the pressure is reduced from the design point to B on the first turbine characteristic, then it will be at B' on the broken line, at the same value of P_3/P_x, but with the appropriate value of $m\sqrt{T_x}/P_x$. Because this last must be the inlet conditions for the second turbine, then vertically below B' must be B'', the operating point of the second turbine. Now the broken line of the upper diagram and the second stage line have the same abscissa, $m\sqrt{T}/P$, but the former has a smaller slope, because it is based on outlet values. Hence a certain reduction of mass flow will cause a correspondingly greater reduction of pressure in the second stage than in the first stage, leaving a smaller pressure ratio across it, i.e. the first stage takes most of the work. This characteristic of turbines in series obviously has an important effect on the various plant arrangements. For example, considering the simple case of compressor-turbine and power turbine, a reduction of load on the latter, effected by a lower pressure ratio, causes correspondingly less drop in the former, which then suffers only a correspondingly small speed reduction.

10.8 *Single Shaft Arrangement*

Consider now a simple gas turbine, with a single compressor and a single turbine, with the load on the same shaft. It is necessary first to know what part-load regulation is required, i.e. constant speed, propeller load, constant turbine temperature, etc. It is not possible to demonstrate the appropriate methods for each case here, but all are essentially similar in assuming one quantity at a part-load condition, then from known performance laws and components characteristics working out the necessary remaining conditions. This usually requires trial-and-error methods or successive approximations, until two calculated values of the same quantity are in agreement. For example, using constant-speed part-load operation,

one has the compressor characteristics (known or assumed) and the turbine characteristic (or ellipse law or equivalent). The design point of the compressor will be close to the surge line and lowered output at constant speed will most likely entail a lower pressure ratio and increased mass flow. Thus one might take the first part-load point to be that of 102% mass flow. From the compressor characteristic, the pressure ratio and temperature rise are read off. Part load at constant speed requires reduction of turbine temperature, so a value of fuel-air ratio slightly lower than the design value is assumed and the turbine mass flow calculated [$m_t = m_c(1 + f)$]. From the compressor pressure ratio and the estimated losses (combustor and exhaust), the available turbine pressure ratio is known, which, with the values of m_t and P_3, yields a value of T_3 from the turbine characteristic (or ellipse law). The combustion temperature rise with this value is then ascertained, yielding a new value of fuel-air ratio. If the latter is not that assumed initially, then it is used to calculate a second value of turbine mass flow and a new value of T_3. This step is repeated until reasonable agreement is obtained. Then all the information is available for calculating turbine work and compressor work, hence net output, from which, with the calculated fuel input necessary for the combustion temperature rise, the efficiency is obtained. It is a somewhat laborious process, but after a few trials are made, very close guesses can usually be made so that the iterative procedure is reduced to a minimum. Other compressor mass flows are then assumed, with the percentage increases being chosen by plotting the part-load results as obtained, so that judiciously spaced points are taken. This type of procedure is representative of any required part-load operation, that is, assumption of a new condition, estimate of unknown quantity and trial-and-error to balance estimate with necessary value from component characteristics. The constant-speed case above ensured that all part-load points were operable, i.e. on the compressor characteristic, but other cases may yield inoperable points, either surging or choking, so that operating limits are obtained.

10.9 *Separate Power Turbine*

In this arrangement, the power turbine is completely independent of the compressor-turbine shaft with respect to speed and, if its characteristics are simplified to the all-speed single line discussed in Sec. 10.7, then its speed may vary with load at will. The governing conditions are that of the distribution of pressure ratio between two turbines in series and that of the relationships of compressor and compressor-turbine on a single shaft. The latter is the heart of

the problem, as the only function of the compressor-turbine is to drive the compressor. Such an arrangement is commonly called a *gas generator*, as its function is only to supply hot, compressed gas to the power turbine.

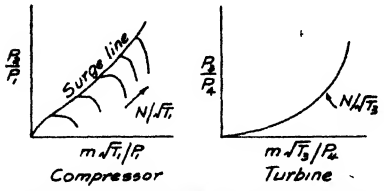

FIG. 10.5. Compressor and turbine performance in terms of pressure ratio.

There are then three conditions which must be satisfied for the gas generator. In the following discussion, use is made of the dimensionless parameters and Fig. 10.5 is shown in these terms, with subscripts 1 and 2 for the compressor, 3 and 4 for the turbine.

The three conditions are:

(1) Compressor speed = turbine speed, N, rpm

(2) Compressor mass flow = turbine mass flow, m, lb/sec

(3) Compressor work = turbine work, W, Btu/sec

The first condition is exact, but the second condition is subject to slight modification as noted previously. The third condition may have to be modified for mechanical efficiency and any auxiliary power take-offs from the shaft. Another simplification required is to make $P_3 = P_2$. This may be accomplished by plotting the compressor characteristic with P_2 including any combustor, heat exchanger or transfer duct loss.

In order to match the compressor and turbine, then for the first condition, equal speed,

$$\frac{N}{\sqrt{T_1}} = \frac{N}{\sqrt{T_3}}\sqrt{\frac{T_3}{T_1}} \tag{10.2}$$

for the second condition, equal flow,

$$\frac{m\sqrt{T_1}}{P_1} = \frac{m\sqrt{T_3}}{P_3}\sqrt{\frac{T_1}{T_3}} \cdot \frac{P_3}{P_1} \tag{10.3}$$

and for the third condition, equal work

$$mc_{p_{12}}\Delta T_{12} = mc_{p_{34}}\Delta T_{34} \tag{10.4}$$

The last may be rearranged in dimensionless form, thus

$$\frac{\Delta T_{12}}{T_1} = \frac{c_{p_{34}}}{c_{p_{12}}}\frac{\Delta T_{34}}{T_3}\frac{T_3}{T_1} \tag{10.5}$$

From this it will be seen that dimensionless temperatue change $\Delta T/T$ is equally useful with that of pressure ratio, although actually

it is immaterial which is used, as one is a function of the other (Sec. 3.3). Thus it is possible to redraw the compressor and turbine characteristics as shown in Fig. 10.6.

From Eqs. (10.2), (10.3), (10.4) and (10.5), it will be seen that the linking parameter common to all three is T_3/T_1, and since, for any given condition, T_1 is fixed, it is T_3, the turbine inlet temperature, which is the control means, i.e., there is only one value of turbine temperature T_3 which will satisfy all the conditions for one particular gas generator state. One method of attack is to select a lower speed of the generator, choose a compressor mass flow and then by a trial-and-error method, find the value of T_3 which will satisfy the equal work condition (10.4) and also the power turbine mass flow-pressure ratio characteristic, with the power turbine pressure ratio being that available after the compressor turbine has taken its required drop. From the conditions thus found at various gas generator speeds, the power turbine output can then be found, with its speed being independent within reasonable limits. A more generalized method of accomplishing the same ends will now be given, essentially similar, but of wider range. The procedure is as follows:

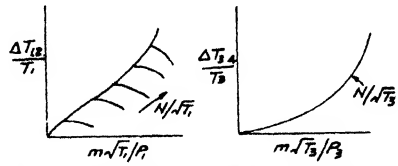

FIG. 10.6. Compressor and turbine performance in terms of $\Delta T/T$.

(1) Take an initial value of T_3/T_1 (lower than design) and assume a value of $N/\sqrt{T_1}$.

(2) Find $N/\sqrt{T_3}$ from Eq. (10.2).

(3) Read off several values of $m\sqrt{T_1}/P_1$ from the compressor map, together with the corresponding value of P_2/P_1 and $\Delta T/T_1$, all at the assumed value of $N/\sqrt{T_1}$.

(4) Calculate $m\sqrt{T_3}/P_3$ from Eq. (10.3) (using $P_3 = P_2$), and find $\Delta T/T_3$ from Eq. (10.5).

(5) Plot these corresponding values on the turbine characteristic with $\Delta T/T_3$ as ordinate.

(6) Join the points in a line and where this cuts the correct $N/\sqrt{T_3}$ line (from step 2), an *equilibrium running* point is located. This is the condition which satisfies the compressor and turbine operating characteristics and the three conditions originally postulated.

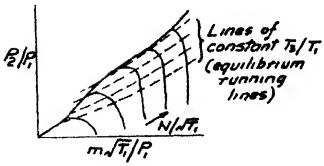

FIG. 10.7. Equilibrium running lines on compressor characteristic.

A succession of T_3/T_1 values, with the procedure repeated, then allows a series of *equilibrium running lines* to be established, which, if superimposed on the compressor characteristic, gives information which can be used for the plant part-load calculations. A typical example is shown in Fig. 10.7.

10.10 *Comparison of Single-Shaft and Free-Turbine Arrangements*

The major advantage of the free- or power-turbine arrangement is the high no-load torque available (Sec. 7.5), as the gas generator can be kept running at a reasonably high speed with the power turbine idling. Immediately load acceleration is required, opening the throttle produces almost instantaneously a flow of hot gas at high pressure from the generator, available for accelerating the power turbine and load. With the single-shaft arrangement, to accelerate from an idling condition requires acceleration of the whole compressor-turbine-load combination on the single shaft all the way through the speed range, a much slower operation.

A comparison of the efficiency-part load relationship, Fig. 10.8, shows that there is some advantage with the free-turbine arrangement with its greater flexibility, slight at the higher loads, but more noticeable below the half-load condition. For the constant speed-single shaft arrangement, load control is effected by reduction of turbine inlet temperature, which reduces the cycle efficiency (cf. Chapter 2), with pressure ratio and flow rate remaining relatively constant. For the power-turbine arrangement, the compressor-turbine inlet temperature may be kept constant, or nearly so, with load reduction, by decrease of mass flow at lower gas generator speeds. However, although T_3 is kept up, the pressure ratio is also reduced, decreasing the cycle efficiency. These basic thermodynamic considerations are, of course, influenced by the varying component efficiencies but the general effects are typified by Fig. 10.8.

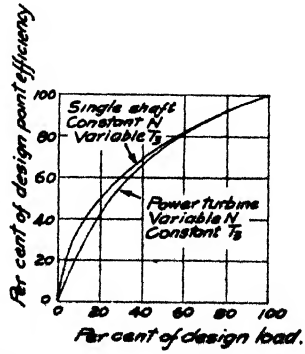

FIG. 10.8. Variation of efficiency with load for single-shaft and free-turbine arrangements—simple cycle.

10.11 *Effect of a Heat Exchanger*

It has been seen previously that the effect of a heat exchanger is almost exclusively on cycle efficiency, with a secondary effect on power output due only to pressure losses. For the single-shaft arrangement, the percentage increase in efficiency brought about by the heat exchanger decreases as the load is reduced, because with decreasing turbine temperature (both inlet and outlet), and constant compressor delivery temperature, the heat exchanger is able to supply less and less of the heat input required, as the temperature difference available ($T_4' - T_2'$) decreases. Eventually, the heat exchanger becomes ineffective, when compressor discharge temperature equals turbine discharge temperature. Added to this effect is that of decreased exchanger effectiveness with the increasing mass flow rate, and that of increasing fractional power loss due to the actual pressure losses in the exchanger.

The effect of a heat exchanger on the part-load characteristics of the power turbine arrangement is considerable, however. In this case, turbine temperature is relatively constant, with the mass flow rate, compressor delivery temperature and pressure ratio being reduced as load decreases. Thermodynamically, the increase of available temperature difference ($T_4' - T_2'$) and the reduced cycle pressure ratio both tend to keep up the overall efficiency. The increase of exchanger effectiveness at reduced flow rate accentuates this effect. Thus the part-load efficiency is kept high and may even be greater than that at full load. It should be noted, however, that in the latter case, it may be necessary to reduce the turbine inlet temperature, because with constant T_4 and lower pressure ratios at reduced generator speeds, the turbine discharge temperature, which is the heat exchanger gas inlet temperature, increases. Hence, with given materials based on the design point values, the exchanger material temperature limit may be exceeded.

For actual operation, it is also necessary to consider the thermal capacity of the exchanger, which may be considerable for high values of effectiveness. Thus, in the operation of reducing from full load to idling for instance, the thermal capacity of the exchanger material limits the rate of load reduction as the fluid flow has to absorb the stored heat. The converse is true for increase of load from idling and, in addition, the effect of sudden temperature changes, or thermal shock, must be taken into account in the mechanical design.

10.12 *Effect on Plant Design*

This brief discussion of part-load performance shows the complexity of the problem, although the analysis should be sufficient

to indicate the line of attack for more complicated situations. It will be appreciated that the choice of gas turbine cycle and arrangement is very dependent on the operating load requirements and that the design point conditions may be compromised by necessity for better performance over a wider range. The flexibility of the gas turbine is helpful in many instances. Thus, it is quite possible to incorporate a heat exchanger only at part load, by-passing it at full load. Again for certain duties, naval vessels for example, one gas turbine with heat exchanger may provide the necessary power at acceptable economy for ordinary cruising conditions, with one or more simple gas turbines in parallel for the maximum power output required for top speed for limited periods.

REFERENCES

1. LANGHAAR, H. L. *Dimensional Analysis and Theory of Models.* J. Wiley & Sons, Inc., N.Y., 1951.
2. SHEPHERD, D. G. *Principles of Turbomachinery.* The Macmillan Co., N.Y., 1956.
3. MALLINSON, P. H. and LEWIS, W. G. E. The Part-Load Performance of Various Gas Turbine Engine Schemes. *Proc. I. Mech. E.*, **159**, 1948; reprinted by *A.S.M.E.*, 1949, " Internal Combustion Engines ".
4. HODGE, J. *Cycle and Performance Estimation.* Butterworths Scientific Publications, London, 1955.

CHAPTER 11

APPLICATIONS OF THE GAS TURBINE

CONSIDERATION of the previous chapters on the thermodynamic and aerodynamic behaviour of the gas turbine, together with some general statements on mechanical aspects, will now allow an assessment to be made of the gas turbine as a power plant.

Perhaps the most outstanding characteristic is that of flexibility of arrangement, with respect to choice of cycle, choice of plant arrangement, type of component and type of fuel. This is borne out by actual developments over the past few years, which have shown gas turbines in power outputs from a few horsepower in portable or auxiliary units, to outputs of over 30,000 hp in straightforward shaft units and of even greater equivalent thrust horsepower in jet engines. Associated with this wide range of output is an equally wide range of duties, many of them unanticipated when the gas turbine was introduced as a prime mover in this era by Brown-Boveri (Stodola 1940, Ref. 1). A gas turbine of extreme simplicity can be made with no manual or automatic control system beyond a fuel throttle, and can be independent of water or electrical supply.

The most outstanding physical characteristics are its small size and low weight per unit of output, much lower than those of other prime movers. Within limits, the gas turbine can burn a wide range of fuels with little modification, and this characteristic is likely to improve in the future. It is possible that in the not-too-distant future, gas turbines will be available which will accept any fuel from a gas to residual oils.

It is these factors above all which have led to the use of the gas turbine as it stands at the present time, because the theoretical analyses have shown that the efficiency, particularly at part load, and the range of satisfactory operation are not very attractive except for the more complex arrangements. There are, however, other features which lead to the choice of the gas turbine when an overall balance sheet is made of the operation and which in some particular applications are over-riding.

11.1 *Assessment of the Gas Turbine*

An attempt is made below to summarize the potentialities of the gas turbine, but it should be recognized that the relative values of

particular characteristics vary with application, advantages in some instances turning to disadvantages in others and vice versa.

(1) High specific output on a weight and volume basis. This is true for all but the most complex cycles or possibly for a heat-exchange cycle with a high effectiveness.

(2) Relatively lower efficiency than comparable prime movers. In the lower output range, diesel and gasoline engines are usually more efficient than the gas turbine, both at the design point and, more particularly, at part load. In the higher output range where the diesel engine becomes unattractive due to size, weight and number of separate units required, the gas turbine has to compete with the steam turbine. The efficiency of the latter is highly variable, depending on the size and on the complexity of its cycle (condensing or non-condensing, reheat, pressure level, etc.), but it is generally comparatively high. A closed-cycle gas turbine plant can compete with all but the largest and most complex steam plants.

(3) Low output per unit flow rate of air, or high air rate. This may pose problems in the air intake and disposal of exhaust gas, particularly for mobile units (automotive and marine). If advantage can be taken of the large volume of exhaust gas at relatively high temperature for use as an auxiliary heating medium (hot water supply or steam raising, for example), then the high air rate is useful and the overall efficiency of the complete thermal power plant is high. No such problem with respect to air and gas ducts occurs in the closed-cycle plant.

(4) Maintenance cost is low and infrequent. Here the gas turbine is comparable to the steam turbine in lubricating oil consumption, and very much superior to the reciprocating type of internal combustion engine. With respect to inspection and repair or replacement of components, the gas turbine is very satisfactory, as it is a much simpler plant, with many fewer accessories than either a steam power unit, a diesel or a gasoline engine. A possible exception to this statement at the present time is the combustor, which may require more frequent inspection or replacement than other components, except when burning a gaseous fuel. It should also be noted that because gas turbine cycle processes are carried out by discrete components, modification is usually easier than in other plants. Thus improved components, such as compressors or turbines, can be introduced with the minimum of disturbance to the rest of the plant.

(5) Freedom from auxiliary services. In the majority of applications, a water supply is unnecessary, often a considerable advantage with respect to location. Although electrical ignition is required, this is necessary for starting only and thus the ignition system is of

maximum simplicity. For aircraft units, the control and electrical systems may be complex, owing to the large variations of ambient conditions. However, this is true of any power plant for an aircraft, and the fuel control system for the gas turbine is no more complicated than the carburettor in its developed form for aero-engines.

(6) Installation costs are low. Because of its high output per unit weight and volume, both the building housing the plant and the actual floor foundation required are much smaller and simpler than for other power plants of similar power. This may be an important point in evaluating the complete economic balance sheet. Furthermore, due to the lack of transmitted vibrations characteristic of turbo-machinery, the carrying structure is simplified and lightened, especially important in aircraft and, to a considerable extent, in marine vessels.

(7) Starting a gas turbine has both favourable and unfavourable aspects. On the favourable side is that except for very large units, it can be started and put on load in a very short time, usually much shorter than the alternative prime mover for the particular application. Turbo-jets of enormous power are ready for aircraft take-off in a matter of seconds. Gas turbines of large output for electrical generation may require minutes of warm-up time, usually much less than the corresponding steam turbine, even assuming steam available at the throttle. This characteristic is due to the light construction, which requires the minimum of large metal masses of great thermal capacity.

On the debit side is the power required from rest to a self-running or idling speed. Not only are component efficiencies very poor at low speed, but the turbine temperature must be limited for the sake of the metal properties and to avoid compressor stalling, so that it is necessary to accelerate the unit after combustion is initiated up to a speed at which it is self-driving at a safe turbine temperature. This speed is usually about one third of design speed.

Thus electric motors of some fair size are needed which will sustain a high current for a relatively long time. Cartridge or " rocket " starters are used successfully for aircraft turbines when self-contained starting means are required, otherwise auxiliary electric generators are needed. Again on the credit side, starting at low ambient temperatures is usually easier than with reciprocating engines, because of the lack of contact resistance.

(8) Sensitivity to variation of ambient conditions also has mixed aspects. The effect of pressure is not serious and comparable to that on reciprocating engines. The effect of temperature is very marked, however, as shown in Chapter 3. The plant must be designed

so that a certain minimum output is maintained at the highest intake temperature, thus probably having excess capacity for the major part of its operation. However, there are many applications when increased output is welcome at low inlet temperatures. Generally speaking, cold weather increases electricity demand, although in some areas, large cities in the U.S. for example, due to the increasing use of air-conditioning systems, extremely hot weather imposes a peak load.

(9) Ability to consume a wide range of fuels. A gas turbine can be designed to utilize gaseous fuels or distillate liquid hydrocarbons with ease. Combustion of the heavier and cheaper fuels is an unsolved problem at the present time, as noted in Chapter 8, at least except for particular units operating on a particular fuel. If the problem of deposit and corrosion due to ash content can be solved, then there is no inherent reason why any liquid fuel cannot be used. This would obviously be a tremendous advantage, obviating the handicap of the relatively high fuel consumption of simple cycle units.

(10) Capital cost. Here quite obviously no generalization can be made, because it is largely numbers of units which determine the first cost and industrial production is not yet sufficiently great to have warranted the standardized and mass-production methods of other prime movers. For small units, the cost of gas turbines is so much greater than that of reciprocating engines, that it must seem improbable for it ever to compete. It is useful, however, to imagine the situation if gas turbines were well-nigh universal and the gasoline engine were the new-comer. Would not the latter, with its forged crankshaft, camshaft, valves, precision-finished cylinders, pistons and piston rings, water-cooling, ignition distribution system, etc., etc., appear to be wholly uneconomic compared with the simple component system of the gas turbine? Wherever performance is superior, production methods will follow in time to allow economic competition.

With these general characteristics in mind, the application of the gas turbine in various major fields will be discussed. In the dozen years or so since the gas turbine has been available for exploitation in other than strictly military areas, a quite astonishing versatility has been demonstrated, with development in some unexpected areas and singularly little progress in other areas which were thought to be very promising some years ago. The discussion will be generalized, with no attempt at listing specific details of plants, because many such compilations are readily available and kept up to date.

11.2 *The Small Gas Turbine*

Before turning to the specific areas of application, it is of interest to note the rather unexpected popularity of the gas turbine in small outputs, say 250 hp and lower. At first sight, this area does not appear promising because of the advanced state of development of gasoline and oil engines of this output, together with their relatively very low capital cost due to mass production for automotive use. For any given cycle, a gas turbine of small size is likely to be less efficient than one of larger size, due to Reynolds number effects and difficulty of maintaining the same relative accuracy of part dimensions and of small clearances. Nevertheless, numerically there are probably many more gas turbines of 200 hp and less in use than those of larger output (exclusive of aircraft engines). It is true that their use is predominantly in the military field, where satisfactory performance over-rides first cost, but their application is in shaft-power units, not for aircraft propulsion, a field in which existing reciprocating engines might be thought to be pre-eminent.

The reason lies mainly in the very high power-weight ratio, enabling easily-transportable units to render otherwise impossible service, together with the high power-volume ratio enabling much higher outputs to be available in existing locations. Thus the Solar 45 hp and the Rover 60 hp units are eminently suitable for use as fire pumps and electrical generators in situations where light weight and immediate mobility are essential. The Boeing unit of approximately 200 hp has found considerable favour for naval vessels, either as direct drive or in auxiliary applications, very largely on the basis of small size for a given output. Efficiencies of these units are low in comparison, but their uses are either where only occasional operation is required or where the power/weight-volume is pre-eminently desirable.

11.3 *Electric Power Generation*

The efficiency of the gas turbine is not high enough to allow it to compete, on this basis alone, with the steam turbine for continuous power generation, but its other characteristics have led to its use in a number of instances. The complex cycle, with intercooling, reheat and heat exchange, allows an efficiency of 30% or better, but the complication and resultant size of unit result in no particular advantage. Also for an open cycle, it is impossible to construct the very large compressors and turbines which are required for the very high outputs which are now usual for central electricity plants. However, the closed cycle is eminently suited and several such plants

are now in operation. They are not of very high output, as they are in the nature of pilot plants, pending the long-term proof of successful operation of the air pre-heater.

Nevertheless, many open cycle plants are being used for electrical generation, a number of them being only simple cycle plants with efficiencies of 17–20%. The reasons are varied, one of the most important being that the location is one where water is either non-existent or very sparse. Thus several are in use in desert areas, notably the Middle East. Many of the installations are in oilfields or at oil refineries, where natural or process gas is either "free" or relatively cheap, thus providing the best possible fuel for trouble-free combustion and compensating for low efficiency. These open-cycle generating plants range in output from about 750 kW to nearly 30,000 kW, with many in the medium power range, 4000–13,000 kW. Some generating units have heat exchangers, thus yielding higher efficiencies. Two Brown–Boveri units (Beznau), with intercooling and heat exchange, yield about 28% efficiency.

Gas turbines are particularly useful for peak-load or stand-by units, as they are self-contained, require no additional steam capacity, can be put on load with the minimum of delay, and occupy less room than other plants for the same capacity. They can also increase the station capacity beyond their own nominal output, because the exhaust gas can be used for air or water preheating, thus raising the existing boiler capacity.

Small gas turbines are also used extensively for electrical generation in connection with aircraft, sometimes for starting power or as a self-contained auxiliary power unit (APU) delivering electricity for a variety of uses. It is usually undesirable or uneconomic to run the main aircraft propulsion engines when the aircraft is on the ground and here the APU takes over for providing the ground services such as lights, etc., as well as providing an emergency supply when in flight, or power for the many auxiliary functions now necessary in aircraft.

11.4 *Gas Pumping*

Gas turbines coupled to centrifugal compressors for pumping natural gas have proved to be one of the most successful uses, an application not immediately anticipated at the advent of gas turbine power. The major pumping application is in cross-country pipelines, in which booster stations are required at frequent intervals. Such locations are often in isolated regions, in which water is difficult to supply. Furthermore, the gas turbine speed is perfectly suited to the centrifugal compressor for the natural gas. The low main-

tenance and low installation cost make it considerably more attractive than a reciprocating gas or oil engine. Again, the available fuel, that in the pipe-line itself, is very suitable and although its cost cannot be written off, it may be deemed inexpensive. The majority of such units are simple cycle, single-shaft units, although for some uses, a free turbine is advantageous, and the addition of a heat exchanger improves the efficiency at the expense of first cost.

A somewhat unusual installation of the pumping application is that in which the oilfield is under water and the pumping operation is one of compressing gas in multi-stage compressors to a high pressure for forcing oil out of the ground, with the whole unit, consisting of batteries of gas turbines and compressors, being floated on a pontoon on the lake surface (Maracaibo, Venezuela). Apart from the reasons given above, the power-weight ratio of the gas turbine is here a prime consideration.

11.5 *Locomotives*

With one outstanding exception, the gas turbine has not to date proved popular for locomotive use, although certain apparent advantages led to earlier predictions that this would indeed be so. In fact, one of the first gas turbines for other than military use was for a locomotive (Brown-Boveri, 1941). Almost any power plant would be an advantage over the reciprocating steam locomotive, but in the U.S.A., the universal replacement has been the diesel engine, and in Britain, where the diesel has not been used extensively due to the oil supply situation, it seems that any transition plant will be obviated by a leap to complete electrification, as the power can be supplied from central stations still based on coal, or, in the future, on nuclear power.

The gas turbine has the advantages of great power in a small volume and of immediate availability. The former is not pre-eminent for Britain, although it is more advantageous in the U.S.A. where loads are many times as great. Availability is met by the diesel engine or electrical power. The major disadvantage is low efficiency, even with a heat exchanger, which cannot be of high effectiveness without requiring a large space. The gas turbine is also not suited to short journeys, owing to its poor part-load efficiency. Thus in Europe, particularly Britain, the gas turbine locomotive does not seem likely to prosper. In the U.S.A. on the other hand, loads are higher and distances are greater. Here again, however, only one railroad, the Union Pacific, uses the gas turbine, in spite of the fact that in this one application it is very successful, judging by repeat orders.

Diesel power requires electrical traction and it is possible for the gas turbine to use a direct mechanical drive, thus eliminating some initial cost and complication. Diesel engines require considerably more costly maintenance than gas turbines and reduction of this item would allow the gas turbine to be viewed very favourably if, at the same time, the fuel cost could be made comparable. Here the solution of the problem of heavy fuel combustion would be important or, alternatively, the introduction of coal burning. The latter has received considerable attention, particularly in North America. In the U.S., development of a direct coal-burning unit has been under way for many years, using pulverized fuel. The major problem is not of combustion, but of the erosive effect on the turbine of the inevitable large quantity of ash. A fair amount of success has been achieved, using ash separators, but no operational unit is in regular use. In Canada, effort has been directed to the exhaust-heated cycle, eliminating the turbine erosion, but requiring a rather large heat exchanger. Here again, considerable progress has been made on a test unit, but no line operation has been reported.

11.6 *Marine Use*

The application of the gas turbine to marine use has likewise been slower than originally anticipated. The slow development in this field is natural perhaps, if one takes into account the low rate of " turnover " of ships, the high capital cost of a single unit and the very great loss involved in breakdown of equipment above and beyond the direct repair cost involved. The relatively high fuel consumption of simple gas turbines, coupled with the difficulties with combustion of the cheaper fuels, has not led to any expectation that great benefit is to be gained in contraverting the conservative viewpoint. Nevertheless, there are apparent advantages and these are gradually being demonstrated in test vessels.

The major advantage is once again in the low weight and compactness of the gas turbine. Engine rooms of all vessels are always crowded, owing to the importance of each ton and cubic foot of capacity for pay load, and the gas turbine can offer either more room or more power in the same space. Also important are the low maintenance costs and the ability to replace individual components with minimum loss of time.

There is a considerable difference in the requirements of mercantile and naval vessels. The former require a power plant which operates at full speed most of the time, reduced speed being necessary only during severe weather and for manœuvring in close quarters. A naval vessel, on the other hand, spends a large portion of its life at

relatively low speed, requiring top speed only in emergency. Because of the operation of the " propeller law ", half speed requires only one-eighth power, for example. Thus part-load efficiency, while highly desirable, is not so important for mercantile as for marine vessels. It would seem that for the former use, a very high degree of reliability might be proved before commitment, while in the latter case, it is high part-load fuel consumption which offsets other advantages.

The gas turbine also has the advantages of almost instant availability and absence of transmitted vibration, the latter being shared with steam turbines, but not by oil engines. The high air rate poses some problems of intake and exhaust ducts, which must be of considerable size for the open cycle. On the other hand, the closed cycle seems very well suited to marine propulsion and it is here that future development may well lie.

Another considerable problem lies in the provision of power for astern movement. It is not possible to utilize a condenser vacuum as does the steam turbine installation and a separate reversing gas turbine leads to windage and disc friction loss. Reversing gear mechanism with torque converter is possible, though difficult for high power, while electrical propulsion, though readily reversible, adds more cost and maintenance. The reversible-pitch propeller is gaining favour, but has not yet been used extensively, particularly for the higher outputs. If the astern power is small, a completely separate auxiliary gas turbine for reversing is a possibility.

For naval gas turbines, one solution for part-load efficiency is the use of the closed cycle, and another is the use of multiple units. For the latter, the long-term low output can be supplied by a relatively small unit of good efficiency, with several other simple cycle units standing by, which can be coupled immediately to the main shaft when required for high speed operation. For small naval craft such as motor torpedo-boats or air rescue boats, the light weight, high-output gas turbine is an excellent plant, because it enables much higher speeds to be attained than would be possible with other types of prime mover. The first marine installation of a gas turbine was in such a craft and has been followed by several others, both in Britain and the U.S.

11.7 *Aircraft Use*

This application is so well known that little comment is necessary. Nearly all military aircraft are powered by turbojets, from trainers to the latest supersonic fighters. The age of the turbojet and turboprop commercial airliner is just beginning as the military use is

passing. The turbojet is satisfactory up to a flight Mach number of possibly 2·5, above which the ram pressure developed leads to diminishing returns. For military use, it would seem that the era of the turbojet has been barely a decade long, with rockets already taking over, leaving even the ramjet stillborn.

The commercial aircraft power plant, including the reciprocating engine, has always been a development of the military unit. It is difficult to foresee any large scale development of the gas turbine for aircraft in the absence of military stimulus, because the numbers of commercial units required is nowhere near that necessary to pay for the prodigious costs involved. Development will undoubtedly continue, but slowly. For example, some two or three dozen engines of a new design are now considered necessary to develop it to the point of production. Unless government assistance is made available, it would not seem likely that design changes will be very radical or very rapid.

11.8 *Automotive Use*

Ever since the gas turbine came to public notice, one of the most often-asked questions has been its adaptability for automotive use. Its apparent advantages are again weight and volume, simplicity (absence of water cooling and simple ignition system), good starting torque characteristics (with a power turbine), and absence of vibration. Against these assets are poor part-load fuel consumption and necessity for a reduction gear of large ratio. The former can be offset by the use of cheap fuel, but here any optimism with respect to technical progress in combustion is dimmed by noting the habit of governments of imposing taxes on any such large-scale revenue-producing sources.

Most of the major automobile manufacturers in Europe and the U.S.A. have engaged in development of suitable gas turbines, from 100 to 300 hp. Some have made major efforts and devoted considerable resources, but so far no real production model has appeared. Unquestionably, the gas turbine can power an automobile with very good results, as demonstrated some time ago by the Rover gas turbine car and followed by comprehensive trials with truck installations in the U.S.A.

For any reasonable efficiency, a heat exchanger is necessary and this is one of the major drawbacks, as with any useful degree of effectiveness, the recuperator type is very bulky and is liable to have considerable thermal inertia. Very great hopes have been placed in the rotating, regenerative type, but it still remains for proof to be given of reliability of adequate sealing over a long period of

time. From the gas turbine point of view, it is unfortunate that the reciprocating engine refuses to lie down and die. In fact, considerable improvements continue to appear, increased compression ratio for example, yielding better fuel consumption, while the introduction of the hydrodynamic transmission has provided the torque characteristics built into the gas turbine.

One disadvantage of the gas turbine not immediately apparent is that of acceleration. Even with a separate power turbine, the moment of inertia of even small turbines is sufficiently large so that the acceleration is slower than that of the reciprocating engine. One remedy is to make the turbine diameter smaller and run it at higher rpm, but this leads to increasing difficulty in bearings and reduction gear.

It would seem that the day of the automotive gas turbine for ordinary use has not yet come. It would have to offer very real advantages to compete with the tremendous investment in the existing facilities for the reciprocating engine, the prime example of mass production being the automobile business.

11.9 *Blast Furnace Use*

A blast furnace requires tremendous quantities of air for steelmaking purposes and produces an even larger quantity of gas (mostly carbon monoxide), which contains both sensible heat and chemical energy. The gas turbine offers a very useful power plant for such operations. The axial-flow compressor is suited to provide a large volume of air at medium pressure and the turbine can burn the blast-furnace gas. The latter is exhausted at a pressure only slightly greater than atmospheric and must be cooled and compressed for injection into the combustor. The cooling process can yield a useful heating effect, but the compression process requires a considerable amount of power, because the gas has a very low heating value (about 10% that of natural gas) and very large quantities are needed. Furthermore, the combustion results in a reduction of volume (2 moles CO + 1 mole $O_2 \rightarrow$ 2 moles CO_2). Nevertheless, these are secondary drawbacks with respect to the overall advantages of the gas turbine plant. Many arrangements are possible, because of the flexibility of the gas turbine, with or without power generation, single or compound layouts, etc. There are many such units being used in Europe and the potentialities are being recognized in the U.S.A.

11.10 *Process Applications*

By process applications is meant those in which the major purpose of the gas turbine is not in supplying shaft power, although some of

the power extraction is possible, but in supplying compressed air or gas for physico-chemical processes. Thus air may be bled off the compressor for some process use, this representing the excess power of the turbine over the compressor. Alternatively, all the compressed air may be passed through a " reactor " of some nature, in which it is required to perform a chemical or physical operation, the air then passing to the turbine, with possibly some fuel being required to raise its temperature sufficiently for an energy balance. In other cases, a normal combustor with outside fuel supply is used in the ordinary way, but the gases are not completely expanded in the turbine, passing to the process at elevated temperature and pressure. This last case is analogous to the turbojet, but with the gases used for a chemical process rather than for propulsion. There are many such different processes in the petrochemical field, catalytic cracking, oxygen production and so forth.

Included in this category are the many different ways of utilizing the gas turbine as an auxiliary component in conjunction with a steam cycle. The possible arrangements are many and will undoubtedly be tried out in the future, although to date they remain largely as schemes and not as hardware. Perhaps one factor which militates against their use in new steam power installations is that the latter are now usually of very large output and of high efficiency, utilizing elevated temperatures and pressures. The latter are now quite often in the supercritical region and represent a considerable advance in technology, so that the inclusion of another new element, the gas turbine, is imprudent at the present time.

11.11 *The Closed-Cycle Plant*

This has been mentioned in connection with some of the types of application discussed above, but deserves a brief mention on its own. It represents a development which may progress considerably, if slowly, in the years to come. Many sets are running in Europe and, perhaps surprisingly, several of them of quite low output. The difficulty has been in the air heater, or indirectly-fired combustor, as the attitude towards the necessary high tube-wall temperatures has been cautious.

A high datum pressure results in very small rotating components, which, because they are not exposed to any erosive or corrosive material nor any depositing solids, should have a life limited only by the ultimate creep of the rotor material. Closed-cycle plants have been proposed on these counts, and others, for use in nuclear reactor plants. In particular they allow the use of a more suitable working medium than either air or steam, as discussed in Chapter 3.

11.12 *Miscellaneous Applications*

The foregoing has sketched some of the major applications, both actual and potential. It by no means exhausts the possibilities and the gas turbine has been used in some bizarre, not to say undignified, applications, such as fog dispersal, smoke laying, and ice and snow melting.

The very wide range of utilization, a characteristic of its all-round flexibility stressed previously, has been a feature of the gas turbine since its practical inception about 20 years ago. It will no doubt continue to find new outlets in the nuclear-space age just ahead.

REFERENCES

1. Stodola, A. Load Tests of a 4000-KW Combustion Turbine Set. *Engineering*, **149**, 1940, p. 1.

For an account of gas-turbine applications, with details of layout and construction, see Welsh, R. J. and Waller, G., *The Gas Turbine Manual*, 2nd Ed., Temple Press, Ltd., London, 1955. For comprehensive bibliographies of applications and summaries of progress in the field, see "Gas Turbine Progress Report—1952", *Trans. A.S.M.E.*, **75**, 1953, and "Gas Turbine Progress Report—1958" (*A.S.M.E.*).

INDEX